How *Plasmodium falciparum* malaria parasites bind to human brain endothelial cells

Antoine Claessens

Thesis submitted for the degree of Doctor of Philosophy to
the University of Edinburgh

August 2010

"*Abracadabra*"*

*This term originated as a spell against semitertian fever recorded by the Roman author Quintus Serenus.

Quintus Serenus, *Liber medicinalis*, 51.932–4, ed. R Pépin, Paris, Presses Universitaires de France, 1950.

Abstract

Cerebral malaria is characterised by an accumulation of infected erythrocytes in the microvasculature of the brain. *Plasmodium falciparum* infected erythrocytes have been shown to bind to a Human Brain Endothelial Cell line (HBEC-5i) *in vitro*. This provides a model for the investigation of interactions between *P. falciparum* and human brain endothelium. Currently neither the parasite adhesion ligands on infected erythrocytes, nor the host endothelial cell receptors necessary for this interaction have been identified. In this work, the identity of the host receptor on brain endothelial cells was addressed by binding assays of selected and unselected parasites on a wide range of malaria-associated host molecules. The identity of the parasite ligand was investigated by microarray analysis of parasites after selection for cytoadherence to HBEC-5i. The hypothesis being tested was that the gene encoding the parasite cytoadherence ligand would show significant upregulation in selected compared to unselected parasites.

The P. f*alciparum* laboratory strains 3D7, HB3 and IT/FCR3 were selected for binding to HBEC-5i using a panning assay.

Compared to unselected parasites, HBEC-5i-selected parasites showed a distinct phenotype with reduced platelet-mediated clumping. There was no significant increase in binding of parasites to any of the known endothelial cytoadherence receptors for *P. falciparum* after selection on HBEC-5i. Binding inhibition assays with various antibodies and soluble receptors did not greatly block the adhesion of parasites to HBEC-5i except for heparin. Altogether, the receptor(s) mediating the interaction with HBEC-5i remains unknown.

In order to carry out transcriptional analysis of selected and unselected parasites from all three parasite strains, it was necessary to update the existing microarray chip which is based on the 3D7 genome. This is because each parasite strain has a unique repertoire of variant surface antigens (VSAs) including *var*, *rif* and *stevor* genes. Therefore, to fully analyse HB3 and IT parasites by microarray, bioinformatic analysis was required to extract the *var, rif* and *stevor* sequences from the HB3 and IT genomes. Unique oligonucleotide

probes were then designed for each new sequence and the 3D7-based microarray chip was updated.

Transcriptional analysis was then carried out on selected and unselected parasites of all strains. Microarray data clearly indicated that the most highly upregulated genes after selection were group A or group A-like *var* genes (*HB3var3*, *3D7_PFD0020c*, *ITvar7* and *ITvar19*), showing 11 to over 100 fold upregulation in selected parasites. The *rif* gene adjacent to the upregulated *var* gene was also highly expressed. To a lesser extent some exported proteins like RESA-1, PfEMP3 or PHIST family members also showed increased transcription in HBEC-selected parasites (2-3 fold upregulation). Reverse transcriptase-PCR confirmed the upregulation of group A *var* genes in selected parasites, suggesting that the group A PfEMP1 variants are major candidate ligands for parasite binding to HBEC-5i. These findings are consistent with previous work showing an association between Group A *var* genes and cerebral malaria.

Declaration

The following contributions were made to my thesis:

1. Dr Ann Hedley (Dr Mark Blaxter group, Edinburgh) wrote the first Perl scripts (Appendix) with me.
2. Dr Guangan Hu (Zbynek Bozdech group, NTU, Singapore) designed the vast majority of the VSA-specific oligos.
3. Sachel Mok and Dr Arshna Gupta programmed the microarray chips printing robot.
4. Ciara Stafford was an undergrad student who performed some of the immunofluorescence assays under my supervision.
5. Dr Monica Arman performed most platelet-mediated clumping assays.

Subject to the above exceptions, I declare that the material presented in this thesis is my own work and has not been submitted to any other university or for any other degree or qualification.

Antoine Claessens

Acknowledgements

Finally, after working for about 1460 days and a dozen nights, using thousands of disposable pipettes, downloading over 1500 papers, fainting twice (blood donations), distributing hundreds of Belgian chocolates at meetings & conferences, I can thank people without whom this thesis would not have happened:

Ladies first, I would like to sincerely thank my supervisor Pr Alex Rowe, for her trust in my work, allowing me to travel the world and always keeping her office door open to answer my questions.

I'm extremely grateful to Dr Zbynek Bozdech who allowed me to work (3 times!) in his lab in Singapore.

Thanks to Ann Hedley and Mark Blaxter for their bioinformatics help at the start of this thesis.

I'm greatly indebted to Sir Henry Wellcome for, indirectly, putting me in his will.

Thanks to every member, past and present, of the Rowe group for making the lab (and the nights out) so enjoyable. Thanks to Ahmed for introducing me to MalariaLand and good sense of humour, to Yvonne/Clare/Monica for last minute corrections, to Ruth & Helen for all the good times and a special thanks to Monica again for endless chats on the usefulness of our work.

Thanks also to all my Trypanosome friends for social activities. Special thanks to Paula and Steph for countless lunch times together. Thanks to the other Ashworthinos for good happy hours; especially Adin, Pedro and Daniel.

Thanks to everyone in ZB's lab for being very welcoming (especially Claudia & Bernardo for introducing me to all canteens). Special thanks to Sachel & Arshna for answering my bombardment of microarray questions.

Thanks to Nico Smargiasso for what was a very fruitful collaboration and probably the most exciting of my projects. Au plaisir du prochain afond!

Thanks to the Montague brewery inhabitants (Aoife, Emma, Sarah, Cian, Eimear, Clare & the mice) for making our flat the best shared accommodation I've lived in.

Merci aux nombreux visiteurs qui sont venus me voir et m'ont apporté un peu de Belgique avec eux, au propre comme au figuré.

Thanks to all my climbing buddies, especially the car owners, for great climbing & drinking times. Merci à Katia (a.k.a. la fille cachée de Desproges) pour les bons moments entre francophones dans ce monde de brutes anglophones.

Thanks to www.WordReference.com for improving my poor English.

Thanks to my family for their continuous love and support. Particulièrement à BP & BM pour m'avoir accueilli lors de la rédaction.

Un grand merci à tous les potes grimpeurs Belges; les séjours-grimpes sont mes plus beaux souvenirs. Et ça ne fait que commencer…

As it is always the most obvious people you forget to thank, if I did not mention you here it means I'm extremely grateful to you.

Last but not least, la plus belle découverte de cette thèse aura été Zabeth, qui est la carotte (crue) me motivant à achever la rédaction.

Abbreviations

°C	Degree Celsius
Ab	Antibody
Ag	Antigen
AMA-1	apical membrane antigen
BBB	Blood brain barrier
BETR	Bayesian estimate of temporal regulation
BSA	Bovine serum albumin
CIDR	Cysteine-rich interdomain region
CLAG	Cytoadherence linked asexual gene
CM	Cerebral malaria
CSA	Chondroitin Sulfate A
CSP	Circumsporozoite protein
DBL	Duffy binding-like
dH_2O	Distilled water
DNA	Deoxyribonucleic acid
EBA	erythrocyte binding antigens
EC	Endothelial Cells
EST	Expressed sequence tag
gDNA	Genomic DNA
HBEC-5i	Human brain (microvascular) endothelial cells
HBMEC	Human brain microvascular endothelial cells
HDMEC	Human dermal microvascular endothelial cells
HMM	Hidden Markov Models
HPMEC	Human pulmonary microvascular endothelial cells
ICAM	Intercellular adhesion molecule
IFA	Immunofluorescence assay
IL	Interleukin
iRBC	*P. falciparum* Infected red blood cells
LT-α	Lymphotoxin-α
MAHRP	Maurer's cleft-associated histidine-rich protein
MeV	Multiexperiments viewer
MHC	Major histocompatibility complex
MSP	Merozoite surface protein
NCAM	Neural cell adhesion molecule
NO	Nitric oxide
o/n	overnight
P.f.	*Plasmodium falciparum*
PBS	Phosphate Buffered Saline
pcv	Packed cell volume
PECAM	Platelet endothelial cell adhesion molecule
PfEMP1	*P. falciparum* erythrocyte membrane protein 1
PfMC-2TM	*P. falciparum* Maurer's cleft two transmembrane protein
PHIST	Plasmodium helical interspersed subtelomeric family
PSA	polysialic acid

RH	Reticulocyte binding protein Homolog
Rif / rifin	repetitive interspersed family
RPMI	Roswell park memorial institute
RT	Room temperature
RT-PCR	Reverse transcription – polymerase chain reaction
SAM	Significance analysis of microarray
SDS	Sodium dodecyl sulfate
SSC	A buffer containing sodium chloride and sodium citrate
STEVOR	Subtelomeric variable open reading frame
SUB	subtilisin-like protease
TGF	transforming growth factor
TNF	Tumor necrosis factor
uRBC	Uninfected red blood cells
VCAM	Vascular cell adhesion molecule
VSA	Variant surface antigens
WHO	World health organisation
ψ	Indicates a pseudogene

TABLE OF CONTENTS

Abstract III
Declaration V
Acknowledgments VI
Abbreviations VIII

1 CHAPTER I: INTRODUCTION 1-1

1.1 General background 1-1
1.1.1 Malaria: the current state of an ancient disease 1-1
1.1.2 Vectors and agents causing malaria 1-2
1.1.3 *P. falciparum* life cycle 1-3
1.1.4 *P. falciparum* malaria pathogenesis 1-6

1.2 Variant Surface Antigens (VSA) 1-8
1.2.1 *Var* genes: 1-8
1.2.1.1 *Var* gene structure 1-9
1.2.1.2 *Var* gene surroundings 1-10
1.2.1.3 From *var* to PfEMP1 1-10
1.2.2 The "neglected" variant surface antigens 1-12
1.2.2.1 Rifin family 1-14
1.2.2.2 Stevor family 1-15
1.2.2.3 Pfmc-2TM family 1-16

1.3 Cytoadherence 1-16
1.3.1 Cytoadherence to endothelial cells 1-18
1.3.1.1 CD36 1-18
1.3.1.2 ICAM1 (intercellular adhesion molecule, CD54) 1-19
1.3.1.3 P-selectin (CD62P) 1-20
1.3.1.4 E-selectin (ELAM1, CD62E) 1-21
1.3.1.5 Thrombospondin 1-21
1.3.1.6 VCAM-1 (CD106) 1-21
1.3.1.7 PECAM1 (CD31) 1-22
1.3.1.8 Heparan sulfate and heparin 1-22
1.3.1.9 Fractalkine/CX3CL1, Integrin αVβ3, Fibronectin, NCAM (CD56) and gC1qR/HABP1 1-23
1.3.2 Rosetting 1-24
1.3.3 Platelet mediated clumping 1-25

1.4 Cerebral malaria 1-26
1.4.1 The sequestration model 1-26
1.4.2 The inflammation model 1-28

1.5 VSA and immunity to cerebral malaria 1-32
1.5.1 Var2CSA adhesion to CSA, rule or exception? 1-34

1.6 Choosing the right model 1-35

1.7 Aims of this thesis 1-36

2 CHAPTER II: MATERIALS AND METHODS 2-39

2.1 General bioinformatics tools 2-39
2.1.1 Genome sequences 2-39
2.1.2 ClustalW 2-39
2.1.3 BLAST 2-40
2.1.4 MEME 2-40
2.1.5 Other software 2-40

2.2 Plasmodium falciparum culture and assays. 2-40
2.2.1 Origins of *P. falciparum* used in this work 2-40
2.2.2 *P. falciparum* routine culturing 2-40
2.2.3 Thawing parasites 2-41
2.2.4 Freezing parasites 2-42
2.2.5 Giemsa smears 2-42
2.2.5.1 Sorbitol synchronization of ring stage parasites 2-42

2.3 Endothelial cells culture and assays 2-43
2.3.1 HBEC-5i thawing 2-43
2.3.2 HBEC-5i passaging 2-43
2.3.3 HBEC-5i freezing 2-44
2.3.4 Primary endothelial cells culture 2-44

2.4 P. falciparum selections and binding assays on endothelial cells 2-44
2.4.1 *P. falciparum* selection by panning on endothelial cells 2-44
2.4.2 *P.falciparum* selection on Chondroitin Sulfate A (CSA) 2-45

2.5 Molecular biology techniques 2-46
2.5.1 RNA extraction 2-46
2.5.2 Agarose gel electrophoresis 2-47
2.5.3 PCR product purification 2-47
2.5.4 Mycoplasma contamination detection 2-48

2.6 Statistical methods 2-48

3 CHAPTER III: *P. FALCIPARUM* SELECTION ON HBEC-5I AND INVESTIGATION OF THE ENDOTHELIAL CELL RECEPTORS 3-49

3.1 Abstract 3-49

3.2 Introduction 3-50

3.3 Aims of this chapter 3-52

3.4 Methods 3-52
3.4.1 Immunofluorescence assay (IFA) of endothelial cells 3-52
3.4.2 *P. falciparum* selections on HBEC-5i 3-55
3.4.3 Assessment of rosette frequency 3-56
3.4.4 Assessment of clumping frequency 3-57
3.4.5 Static binding assay on purified proteins and biomolecules 3-57
3.4.6 Static binding assay on endothelial cells 3-59

3.5 Results 3-61
3.5.1 Receptor expression on HBEC-5i (immunofluorescence assay) 3-61
3.5.2 *P. falciparum* selections on HBEC-5i 3-68

3.5.3 Validation of the selection on HBEC-5i 3-71
3.5.3.1 HB3 selection on HBEC-5i occurs in the presence of human serum. 3-71
3.5.3.2 HB3-HBEC also cytoadheres to primary brain endothelial cells 3-73
3.5.4 Phenotype characterization of HBEC-selected parasites 3-74
3.5.4.1 Selection on HBEC-5i does not increase rosetting frequency 3-74
3.5.4.2 Selection on HBEC-5i significantly reduces platelet-mediated clumping frequency 3-76
3.5.5 HBEC-selected parasites do not show any high increase in binding to any known receptor (static binding assays) 3-78
3.5.6 Binding inhibition assays on HBEC-5i with soluble biomolecules 3-83
3.5.7 Binding inhibition assays on HBEC-5i with specific antibodies 3-85
3.5.8 ICAM1 selected parasites do not bind to HBEC-5i or HBMEC 3-87
3.5.9 Adhesion of HB3-HBEC to HDMEC and HPMEC 3-88
3.5.9.1 Receptors expression on HDMEC (immunofluorescence assay) 3-89
3.5.9.2 Receptors expression on HPMEC (immunofluorescence assay) 3-93
3.5.9.3 HB3-HBEC also cytoadhere to HDMEC and HPMEC 3-98
3.5.10 New heparin-like compounds inhibit binding of HBEC-selected parasites to endothelial cells 3-102
3.5.10.1 CRDS inhibits cytoadhesion to HBEC-5i at therapeutic levels 3-103
3.5.10.2 MS29 & MS31 (heparin-like compounds) strongly block cytoadhesion to HBEC-5i but less to primary endothelial cells 3-105

3.6 Discussion 3-106
3.6.1 Multiple *P. falciparum* strains selected on HBEC-5i 3-106
3.6.2 Not all *P.falciparum* clones are selectable 3-107
3.6.3 HBEC-5i, HDMEC and HPMEC surface proteins and biomolecules characterized by immunofluorescence assay 3-107
3.6.4 Limitations of the *in vitro* brain endothelial cells model 3-108
3.6.5 Endothelial cell adhesion probably involves a different ligand-receptor interaction than rosetting or clumping 3-109
3.6.6 HBEC-selected parasites do not show any high increase in binding to any known receptor (static binding assays) 3-109
3.6.7 Binding inhibition assays do not clearly identify the HBEC-5i receptor 3-110
3.6.8 HB3-HBEC parasites also cytoadhere to HB/D/PMEC 3-112
3.6.9 Future work to identify new endothelial cell receptors 3-112
3.6.10 New heparin-like compounds inhibit cyotadherence to HBEC-5i 3-113

4 CHAPTER IV: BIOINFORMATICS ANALYSIS OF VARIANT SURFACE ANTIGENS 4-115

4.1 Abstract 4-115

4.2 Introduction 4-115

4.3 Methods 4-117
4.3.1 Extracting sequences from a genome 4-117
4.3.2 Designing specific oligos for a microarray chip 4-119

4.4 Results 4-120
4.4.1 VSA sequences extracted from HB3/Dd2/IT genomes 4-120
4.4.1.1 *Var* genes 4-121
4.4.1.2 *Rif* genes 4-122
4.4.1.3 *Stevor* genes 4-123
4.4.1.4 *Pf*mc-2TM genes 4-124
4.4.1.5 *Surfin* genes 4-124
4.4.2 HB3/Dd2/IT VSA specific oligos added to the microarray chip 4-125

4.5 Discussion 4-125

5 CHAPTER V: TRANSCRIPTOME ANALYSIS OF *P. FALCIPARUM* PARASITES SELECTED FOR CYTOADHERENCE TO HUMAN BRAIN ENDOTHELIAL CELLS. 5-128

5.1 Abstract 5-128

5.2 Introduction 5-129

5.3 Aim of this chapter 5-132

5.4 Methods 5-132
5.4.1 Tight synchronization of parasites 5-133
5.4.1.1 Percoll-sorbitol procedure (pilot experiment) 5-133
5.4.1.2 MACS-sorbitol procedure 5-134
5.4.2 Time-course 5-135
5.4.3 Pooling and reverse transcription to cDNA 5-135
5.4.4 Making of microarray chips 5-137
5.4.4.1 Preparing polylysine slides 5-137
5.4.4.2 Printing microarray chips 5-138
5.4.4.3 Post-processing of polylysine slides 5-138
5.4.5 cDNA labelling, microarray hybridization, washing and scanning 5-139
5.4.6 Gridding and normalization 5-140
5.4.7 Microarray data analysis 5-141

5.5 Results 5-145
5.5.1 *P. falciparum* synchronisation and time-course 5-145
5.5.2 RNA extraction, pooling, and cDNA labelling 5-149
5.5.3 Hybridization 5-151
5.5.4 Synchronicity of parasite preparations 5-154
5.5.5 Analysis of variant surface antigen gene expression in selected and unselected parasites 5-158
5.5.5.1 *Var* gene expression in selected and unselected HB3 5-159
5.5.5.2 *Var* gene expression in selected and unselected 3D7 5-163
5.5.5.3 *Var* gene expression in selected and unselected IT 5-164
5.5.5.4 *Rif* and *stevor* gene expression in selected and unselected parasites 5-168
5.5.6 Analysis of non-VSA genes expression in selected and unselected parasites 5-178
5.5.6.1 Approach 1: Differentially regulated genes in common to all 5 selections 5-179
5.5.6.2 Approach 2: Statistical approach 5-188
5.5.6.3 Approach 3: "Area under the curve" 5-199
5.5.6.4 Summary of non-VSA candidates for HBEC-5i cytoadhesion. 5-204

5.6 Discussion 5-206
5.6.1 Parasites were well synchronised. 5-206
5.6.2 Limitations of the microarray approach 5-207
5.6.3 HB3var3 is consistently upregulated in HB3-HBEC1, 2 and TNF. 5-209
5.6.4 *Var* PFD0020c in 3D7-HBEC, ITvar7 and ITvar19 in IT-HBEC. 5-210
5.6.5 Adjacent *rif* genes tend to be upregulated with *var* genes 5-210
5.6.6 Non-VSA genes indirectly involved in cytoadherence to HBEC-5i 5-212
5.6.6.1 MAHRP-1 is essential for cytoadherence (true positive). 5-214
5.6.6.2 PfEMP3 is upregulated but probably not essential for HBEC-5i binding 5-215
5.6.6.3 RESA-1 is upregulated but probably not essential for HBEC-5i binding. 5-216
5.6.6.4 RESA-2 is upregulated in some HBEC-5i selections and in other studies. 5-217
5.6.6.5 PF11_0035 is upregulated but is not necessary for PfEMP1 expression. 5-218
5.6.6.6 Two PHIST members are HBEC-5i ligand candidates. 5-219
5.6.6.7 Other upregulated and exported proteins. 5-220

6 CHAPTER VI: FURTHER ANALYSIS OF THE PUTATIVE *VAR* GENE LIGANDS 6-222

6.1 Abstract 6-222

6.2 Introduction 6-223

6.3 Aims of this chapter 6-225

6.4 Methods 6-225
6.4.1 RNA extraction 6-226
6.4.2 DNase treatment 6-227
6.4.3 cDNA synthesis 6-227
6.4.4 PCR 6-227
6.4.5 Agarose gel electrophoresis 6-228
6.4.6 PCR product purification 6-228
6.4.7 Ligation and cloning 6-228
6.4.8 Mini-prep 6-228
6.4.9 *Eco*RI restriction enzyme digestion 6-229
6.4.10 Sequencing 6-229
6.4.11 Large scale sequencing by GenePool 6-229
6.4.12 Bioinformatics tools and Statistical analysis 6-230

6.5 Results 6-230
6.5.1 DBLα RT-PCR confirms the microarray data for the *var* gene family 6-230
6.5.1.1 *Var* gene expression profile in HB3 selections 6-232
6.5.1.2 Var gene expression profile in 3D7 and IT selections 6-234
6.5.2 Quantitative PCR 6-236
6.5.3 HB3-HBEC-Serum parasites also transcribe *HB3var3* 6-236
6.5.4 HB3 selection on Dermal and Pulmonary cells 6-237
6.5.5 Further analysis of the upregulated *var* genes 6-239
6.5.5.1 Glyosaminoglycans predicted binding motifs are found in most PfEMP1s 6-239
6.5.5.2 CIDR1α1 domain is found in all upregulated *var* genes 6-240
6.5.5.3 Upregulated CIDR1α1 domains are basic 6-242
6.5.5.4 No obvious motif distinguishes CIDR "ligand" to "non-ligand" domains 6-243

6.6 Discussion 6-245
6.6.1 Limitations of the DBLα RT-PCR approach 6-246
6.6.2 HB3var3 is the main ligand candidate binding to HBEC-5i, HDMEC and HPMEC 6-246
6.6.3 The role of group A PfEMP1 and CIDR1α1 in severe malaria 6-247
6.6.3.1 Group A *var* gene expression is associated with cerebral malaria 6-247
6.6.3.2 CIDR1α1 domains are commonly recognized by human semi-immune serum 6-248
6.6.3.3 Future work 6-250

7 CHAPTER VII: CONCLUSION 7-252

7.1 The elusive HBEC-5i receptor 7-253

7.2 Group A or group A-like PfEMP1 are the main ligand candidates 7-256

7.3 HBEC-5i and group A var genes, a model for cerebral malaria? 7-258

7.4 Future work 7-259

7.5 Could the immense sequence diversity of group A PfEMP1 be a vaccine target? 7-261

8 APPENDIX **8-263**

8.1 Perl scripts **8-263**

8.2 Extracted VSA sequences **8-264**
8.2.1 PfEMP1 sequences 8-264
8.2.1.1 HB3 PfEMP1 sequences 8-264
8.2.1.2 Dd2 PfEMP1 sequences 8-265
8.2.1.3 IT PfEMP1 sequences 8-265
8.2.2 Rifin sequences 8-267
8.2.2.1 3D7 Re-annotated Rifin sequences 3D7 8-267
8.2.2.2 HB3 Rifin sequences 8-274
8.2.2.3 Dd2 Rifin sequences 8-275
8.2.2.4 IT Rifin sequences 8-276
8.2.3 Stevor sequences 8-277
8.2.3.1 3D7 re-annotated Stevor sequences 8-277
8.2.3.2 HB3 Stevor sequences 8-279
8.2.3.3 Dd2 Stevor sequences 8-279
8.2.3.4 IT Stevor sequences 8-279
8.2.4 Pfmc-2TM sequences 8-280
8.2.4.1 HB3 Pfmc-2TM sequences 8-280
8.2.4.2 Dd2 Pfmc-2TM sequences 8-280
8.2.4.3 IT Pfmc-2TM sequences 8-280
8.2.5 Surfin sequences 8-280
8.2.5.1 HB3 Surfin sequences 8-280
8.2.5.2 Dd2 Surfin sequences 8-280
8.2.5.3 IT Surfin sequences 8-280

8.3 VSA oligo sequences for microarray **8-281**

8.4 Microarray data **8-281**

8.5 Publication **8-281**

References **8-282**

1 Chapter I: Introduction

1.1 General background

1.1.1 Malaria: the current state of an ancient disease

Homo sapiens has probably suffered from malaria since the appearance of our species. The disease would have arisen in our primate ancestors in Africa and evolved with humans, spreading with human migrations throughout the world (Cox, 2002). Even in England, the marshlands had high levels of malaria mortality until the nineteenth century (Dobson, 1994). The high burden of the disease has left an impact on the human genome by selecting genes conferring resistance. Sickle-cell disease, thalassaemias, and glucose-6-phosphate dehydrogenase deficiency were already present in Mediterranean populations 2000 years ago during the Roman era (Sallares, et al., 2004). Malaria is also the only biological weapon that has ever been used in Europe, as the Nazis tried to halt the advance of Allied troops in Italy by flooding marshes and unleashing millions of *Anopheline* larvae (Snowden, 2006).

Today, although the disease is in decline in some places (O'Meara, et al., 2008), it is still estimated that malaria causes about 450 million clinical cases annually (Hay, et al., 2010), of which 863 000 are fatal (WHO, 2009). The vast majority of fatal cases are children under 5 years old in Sub-Saharan Africa (Figure 1-1).

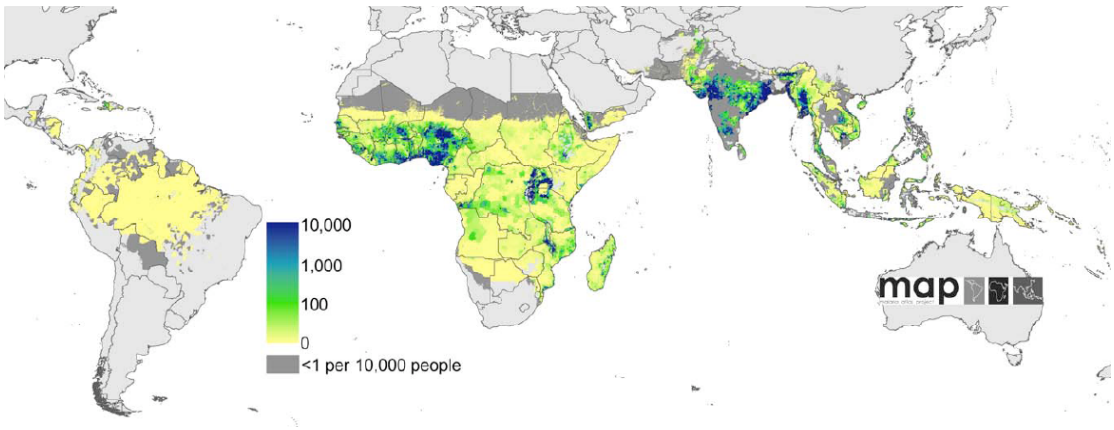


Figure 1-1. Global clinical burden of *P. falciparum* malaria in 2007. Bayesian geostatistical estimates of the number of clinical cases per 5x5 km pixel displayed on a logarithmic colour scale between 0 and 10,000 cases. Taken directly from (Hay, et al., 2010).

1.1.2 Vectors and agents causing malaria

Although the pharaoh Cleopatra already used a mosquito net (Lindsay and Gibson, 1988), it is not until 1897 that Ronald Ross proved that *Anopheline* mosquitoes are the vector of malaria. Within this genus of mosquitoes 30 to 40 species can transmit human malaria parasites (reviewed in (Cohuet, et al., 2010)).

The third worse infectious disease, in terms of worldwide deaths, is caused by the protozoan apicomplexan parasites of the genus *Plasmodium*. Five species are known to infect human:

- *P. falciparum:* causing the vast majority of the mortality.
- *P. vivax:* the most common malaria parasite in Asia.
- *P. malariae*: less common.
- *P. knowlesi*: normally infects macaques, only rarely humans.
- *P. ovale:* probably comprises two nonrecombining species (Sutherland, et al., 2010).

Cerebral malaria, a complication of the disease causing the patient to fall into unrousable coma, is almost entirely due to *P. falciparum*. This thesis is therefore focused entirely on that parasite.

1.1.3 *P. falciparum* life cycle

P. falciparum parasites enter the human body via a mosquito bite (Figure 1-2). Tens to hundreds of sporozoites travel in the blood circulation and rapidly invade hepatocytes via Kupffer cells (reviewed in (Prudencio, et al., 2006)). Sporozoite adhesion is mediated by the parasite circumsporozoite protein (CSP) and thrombospondin related adhesive protein (TRAP) binding to host cell heparan sulfate proteoglycans (Frevert, et al., 1993). Following sporozoite invasion, differentiation and intensive mitotic replication occur; these processes take approximately 6 days.

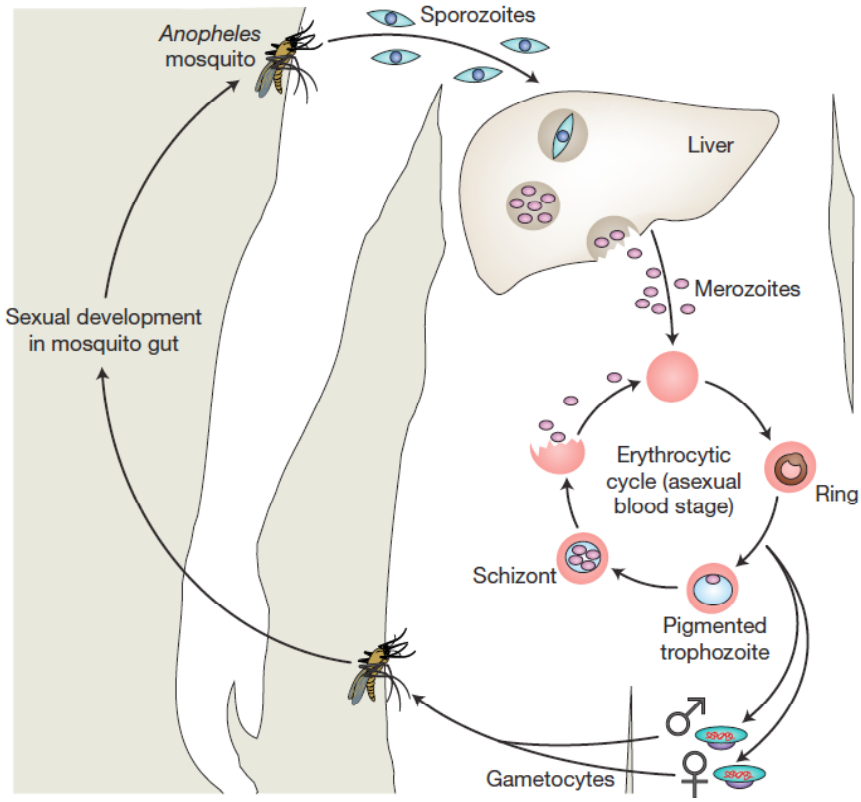


Figure 1-2. *Plasmodium falciparum* life cycle. See text for details. Figure courtesy of Monica Arman.

Parasites, now called merozoites, burst out of the hepatocyte and start the asexual erythrocytic cycle. The merozoite, covered with merozoite surface protein (MSP-1), sticks to a red blood cell (RBC). It then reorients so that it is attached by its apical end to the RBC, using apical membrane antigen 1 (AMA-1)

(reviewed in (Persson, 2010)). Invasion is a complex process involving various parasite ligands (including the MSP and EBA (erythrocyte binding antigens) families) and RBC receptors (glycophorin A, glycophorin C and sialic acid). During invasion a deep membrane pit, the parasitophorous vacuole is formed that eventually contains the parasite within the erythrocyte (Figure 1-3). The parasite flattens into a thin disc that when stained with Giemsa and viewed under microscope, appears as a ring.

The infected red blood cell (iRBC) is subject to massive modifications induced by the developing parasite. Nucleosides and amino acids are imported to the parasite by a network of tubovesicular membranes. Haemoglobin from the erythrocyte is also digested which releases free haem, a toxic waste product that the parasite converts into non-toxic haemozoin (Egan, 2002). The rigidity of the erythrocyte is increased (Suwanarusk, et al., 2004). Some parasite proteins, mostly the ones bearing a PEXEL/VTS motif (see section 0 and chapter 5), are exported to the erythrocyte cytosol via the translocon (PTEX) and Maurer's Cleft (de Koning-Ward, et al., 2009). As the parasite matures into pigmented-trophozoite stages, "knobs" start to appear on the surface of the iRBC, 16-18 hours post invasion (Figure 1-3). The knob structures contain parasite ligands, including *P. falciparum* erythrocyte membrane protein 1 (PfEMP1). These ligands are thought to mediate cytoadherence to endothelial cells, other uninfected RBC (uRBC) or platelets. Note that cytoadherence is specific to pigmented-trophozoite and schizont stages. This allows sequestration of mature parasites within the microvasculature of the human body. Schizonts encase about 16-32 new merozoites within the parasitophorous vacuole. Schizont ruptures occurs roughly 48 hours after invasion, releasing merozoites which will reinvade a fresh uRBC within seconds (Glushakova, et al., 2005).

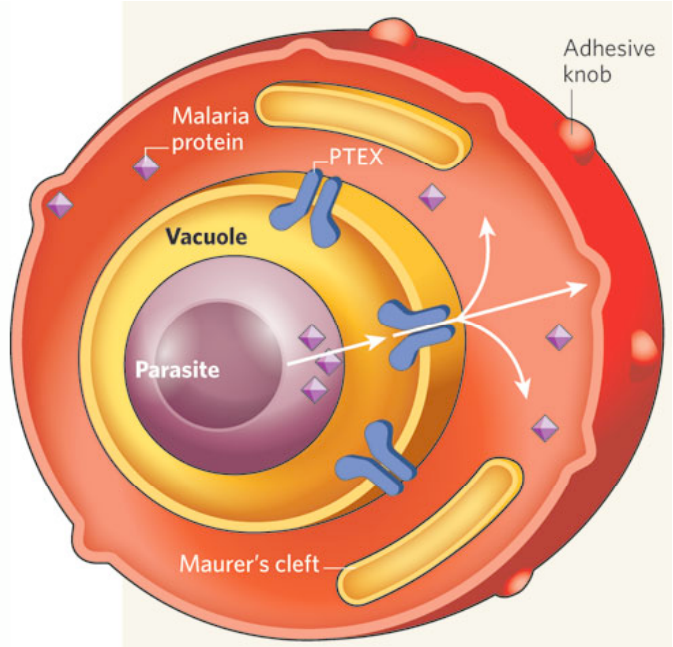


Figure 1-3. *Plasmodium falciparum* parasitizes red blood cells (RBC) and resides in a specialized vacuole formed during host-cell invasion. PTEX allows proteins bearing a Pexel motif to be exported to the host cytoplasm. Maurer's clefts and knob structures are also parasite derived. Figure taken directly from (Reiff and Striepen, 2009).

To complete the life cycle, *P. falciparum* must undergo a number of developmental stages in a mosquito. For this purpose, a few merozoites differentiate into male or female gametocytes (Kuehn and Pradel, 2010). Early gametocytes express PfEMP1 and are able to sequester like asexual parasites. Late stage gametocytes however are released into peripheral blood in order to enter the mosquito blood meal.

Once in the mosquito's midgut, male gametocytes exflagellate to produce eight motile gametes. After fertilisation of a female gamete, the resulting motile ookinete migrates from the lumen of the midgut to the basal lamina where it forms an oocyst. A large amount of replication occurs to produce about 2000-8000 haploid nuclei. The oocyst then bursts, releasing sporozoites that migrate to the mosquito salivary gland, ready for injection into another human host (Vlachou, et al., 2006).

1.1.4 *P. falciparum* malaria pathogenesis

P. falciparum infection is associated with a wide spectrum of consequences, from asymptomatic through to fatal (Crawley, et al., 2010). A wide variety of factors can influence the outcome: virulence of the parasite, host immune status, host age, geographic and social factors (Crawley, et al., 2010). Malaria patients are classified in two categories "mild malaria" (also called "uncomplicated malaria") or "severe malaria" according to the symptoms listed below.

The intraerythrocytic cycle is responsible for the disease pathology of malaria. Thus, symptoms appear at the earliest about a week after an infectious mosquito bite. Fever generally coincides with the rupture of erythrocytes by mature schizont-stage parasites. Other symptoms are listed in Figure 1-4.

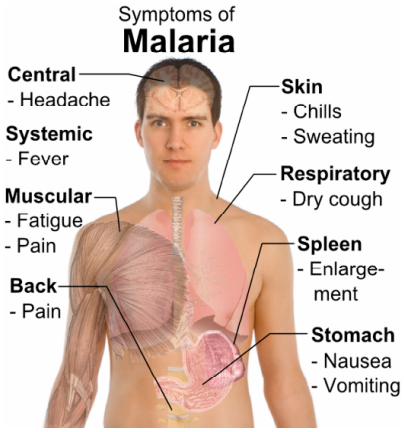


Figure 1-4. Symptoms of malaria. Figure obtained from Wikimedia Commons.

In relatively few cases (<0.5% of infections per year are fatal (Rowe, et al., 2006)), malaria progresses to severe disease with symptoms including anaemia, acidosis, respiratory distress, hypoglycaemia, prostration and coma (Haldar, et al., 2007).

Acidosis results from metabolic, circulatory and renal dysfunction (Idro, et al., 2005) (see also section 1.4.2). It is commonly associated with hyperlactaemia in malaria patients (Day, et al., 2000, Maitland, 2006). Acidosis multiplies the odds of death by 7 fold in Asia (Dondorp, et al., 2008b).

Respiratory distress, defined as a combination of a high respiratory rate (132 breaths/min for adults and 140 breaths/min for children aged <5 years)

and increased work of breathing, is a risk factor for death in all ages (Dondorp, et al., 2008b, Marsh, et al., 1995). In Asia, about 20% of malaria patients with respiratory distress do not survive (Dondorp, et al., 2008b). Autopsies revealed parasite sequestration in the alveolar-capillary (reviewed in (Haldar, et al., 2007)).

Severe malarial anaemia, defined as haemoglobin concentration of < 5 g/dL, causes approximately a third of all malaria related deaths. Removal of iRBC and uRBC, decreased erythrocyte production and suppression of the erythropoietic response all lead to severe anaemia (Haldar and Mohandas, 2009). However, it was recently shown the co-infections with hookworms, HIV or bacteria, which are common in some areas, also contribute to severe anaemia (Calis, et al., 2008).

Cerebral malaria is defined as an unrousable coma (Blantyre score ≤ 2) associated with iRBC appearing in blood smear but without any other cause of encephalopathy (WHO, 2000). Even with this strict definition, a post-mortem study found that 23% of Malawian children had died from other causes, illustrating the difficulty of diagnosis of the disease (Taylor, et al., 2004). In sub-saharan Africa, young children are most at risk, with a mortality rate of 7 to 19% (Newton and Krishna, 1998). Swollen brain (in children), hypoglycaemia, seizures and malarial retinopathy are also commonly reported in cerebral malaria cases (Idro, et al., 2005). Retinopathy is in fact a very good indicator of malaria induced coma (Beare, et al., 2006). A meta-analysis has reported a 10.9% incidence of neurological sequelae in African children (Newton and Krishna, 1998). There is no treatment specific to cerebral malaria other than standard anti-malarial drugs and supportive therapies such as fluid replacement (Mishra and Wiese, 2009). Most fatal cases died within 24h of admission to hospital (Newton and Krishna, 1998).

The hallmark of cerebral malaria is the sequestration of *P. falciparum* iRBC within the brain microvasculature. This adhesion to endothelial cells is thought to be mediated by the parasite variant surface antigens (VSA), in particular the PfEMP1 family. The identification of the ligand(s) and receptor(s) involved in this interaction are the focus of this thesis, as such, extensive

background is given later in this chapter. First the molecular candidates are described (sections 1.2 and 1.3) before an explanation of how they would interact in the context of cerebral malaria (sections 1.4 and 1.5).

1.2 Variant Surface Antigens (VSA)

The main way the parasite escapes the immune system is by "hiding" within erythrocytes. These anucleated cells lack the MHC (major histocompatibility complex) molecules and a mechanism for antigen presentation. It may thus be surprising that *P. falciparum* betrays its presence by exporting VSA to the surface of the RBC. The risk of exposing itself is however counterbalanced by a gain: the ability to sequester within microvessels. This would be necessary for pigmented trophozoite stages parasites to avoid being cleared by the spleen (Buffet, et al., 2009). The parasite ligand proteins mediating cytoadherence of the iRBC are thought to be VSA. Furthermore, parasites have evolved hypervariability within the VSA gene sequences. This results in a population of iRBC expressing a multitude of different surface antigens. Moreover, each strain of parasite bears an almost entirely unique set of VSA sequences (Barry, et al., 2007, Kraemer, et al., 2007). In other words, each infected mosquito bite brings new antigens to the immune system. This may explain why sterile immunity against malaria is virtually never achieved.

By definition, VSA are exported to the surface of the iRBC, show some hypervariability in part of their sequence and are the target of the immune system. In *P. falciparum*, the *var*, *rif*, *stevor* and *Pfmc-2TM* gene families fit these criteria and are detailed here under.

1.2.1 *Var* genes:

The PfEMP1 family were the first discovered VSA family and are still the most studied today (Tembo and Montgomery, 2010). They are encoded by about 50 to 60 *var* genes and are specific to *P. falciparum*.

1.2.1.1 *Var* gene structure

Although it is the most variable gene family in *P. falciparum*, *var* genes share a similar structure. All genes have 2 exons separated by a 0.8-1.2kb intron (Figure 1-5). Exon 1 (4-10kb) starts with an N-terminal segment (NTS) and is followed by a succession of Duffy Binding Like (DBL) and cysteine rich interdomain regions (CIDR) domains. The DBL domains are subdivided into 5 categories: α, β, γ, δ and ε. DBLα domains can even be further subdivided into α_0 and α_1. The CIDR domains fall into 4 categories: α, α1, β and γ. All domains are categorised by conservation of just a few residues, the rest of the sequence being highly polymorphic (Smith, et al., 2000b). The order of these different domains is not random as almost all genes start with a DBL1α followed by a CIDR1 and DBL2 (the number indicates the position of the domain within the gene sequence, e.g. "DBL3" would be the third DBL domain in a particular *var* gene). Var2csa and "type 3" *var* genes are exceptions to this rule as they do not have a CIDR as their second domain (see section 1.5.1). Exon 2 is semi-conserved and encodes a trans-membrane domain (TM) followed by a conserved acidic terminal segment (ATS).

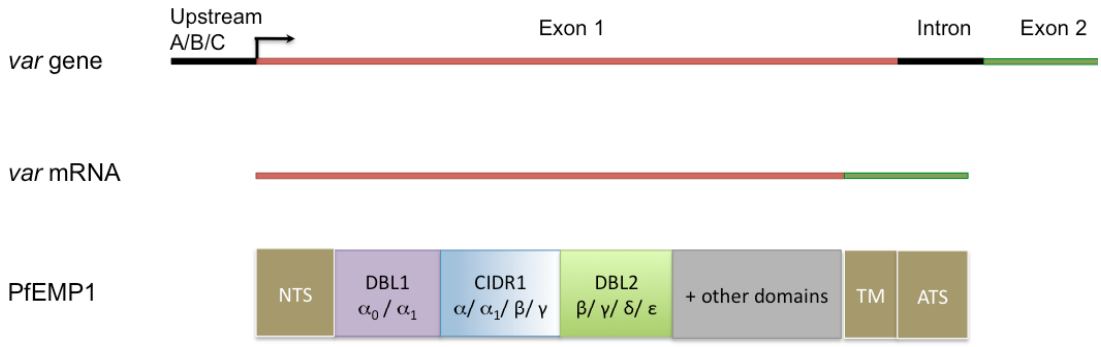


Figure 1-5. Proto-typical *var* gene encoding a *P. falciparum* erythrocyte membrane protein 1 (PfEMP1). The gene is composed of two exons and one intron. The main types of upstream sequences and domains are indicated. DBL = Duffy binding like; CIDR = cysteine-rich interdomain regions; NTS = N-terminal segment; ATS = A-terminal segment; TM = transmembrane domain.

1.2.1.2 *Var* gene surroundings

Var genes can be described according to their sequence but also according to their upstream regions and chromosomal localization. The vast majority of upstream sequences are classified according to phylogenetic analysis into three groups: A, B or C (Lavstsen, et al., 2003a). They are sometimes subdivided further by adding a number, for example *var1csa* shows an "A2" upstream sequence. *Var2csa* is again an exception with an upstream "E" sequence. Importantly, this A/B/C grouping of *var* is conserved in all lab and field isolates investigated to date (Falk, et al., 2009, Kalmbach, et al., 2010, Kraemer, et al., 2007). The latest *var* classification also indicates whether the gene is found near the centromeres (C) or the telomeres (T). All group A *var* genes are located near the telomeres, all group C near the centromeres and group B can be found in either location. In summary, a gene classified as "A1T" will have an upstream region "A1" and is located in the subtelomeres, while a "B3C" shows a "B3" upstream region and is found centromerically.

Very interestingly, there is a link between the *var* gene domain types and its surrounding sequence. Group A *var* genes all show a DBLα1 domain, as opposed to group C and almost all group B genes that show a DBLα0. Group A tend have more domains thus resulting in a larger PfEMP1.

There is evidence to suggest that the *var* gene structure and classification is associated with the pathogenesis of the parasite (see section 1.5).

1.2.1.3 From *var* to PfEMP1

Despite their high copy number (50 to 60 per genome), *var* genes are thought to undergo mutually exclusive expression. The current hypothesis is that in each parasite a single *var* is transcribed in ring stages, with a peak transcript abundance around 8 – 20 hours post invasion that leads to a single type of PfEMP1 molecule found at the surface of the iRBC from young pigmented trophozoite to schizont stages (Horrocks, et al., 2004, Kyes, et al., 2000, Kyes, et al., 2003). However, some authors argue for transcription of multiple *var* genes in a single parasite only one of which is translated into a functional PfEMP1 (Chen, et al., 1998b, Duffy, et al., 2002, Noviyanti, et al., 2001). All these studies

were performed with laboratory *P. falciparum* strains; transcription timing in field isolates may differ. Blomqvist and colleagues suggest that *var* genes may be highly transcribed 22-26h post-invasion in patient isolates (Blomqvist, et al., 2009). The paradigm of mutually exclusive expression is also affected by recent experiments showing that two PfEMP1 variants can be found at the surface of an iRBC (David Arnot oral communication). This was however an artificial selection and could be an exception rather than the rule.

Only a few pieces of the *var* expression regulation mechanism jigsaw are known. Their expression is regulated at the level of transcription initiation (Kyes, et al., 2007). Many mechanisms have been shown to be involved in the silencing of the non-transcribed *var* genes: *var* intron sequences (Dzikowski, et al., 2006a) ; SPE and CPE motifs located in respectively upsB and upsC sequences (Voss, et al., 2003, Voss, et al., 2007); the histone deacetylase PfSir2 and heterochromatin protein 1 (PfHP1) are required for chromatin silencing in subtelomeres (Duraisingh, et al., 2005, Flueck, et al., 2009); histone methylation in the 5' region of *var2csa* can regulate its transcription (Lopez-Rubio, et al., 2007) and a *var*-specific subnuclear expression site has been proposed (Dzikowski, et al., 2007). Finally, in collaboration with De Pauw group (University of Liège, Belgium), we identified "G-quadruplex" (guanine-rich sequences capable of forming a four-stranded structure) upstream of many group B *var* genes that might have a role in their silencing (Smargiasso, et al., 2009) (publication attached as an appendix). How these pieces fit together remains unclear and other mechanisms are likely to be discovered before we can get the full picture.

The rate of antigenic variation is still a matter of debate but it likely varies between strains and between *var* genes (Horrocks, et al., 2004). Centromerically located genes switch at a rate of 0.3% while genes in subtelomeric loci show a 2.7% rate per cycle (Frank, et al., 2007). When human volunteers were infected with the lab strain 3D7, it switched *var* expression at a much higher 16% rate (Peters, et al., 2002).

1.2.2 The "neglected" variant surface antigens

Rifins, Stevor and Pfmc-2TM are *P. falciparum* gene families that share many characteristics with PfEMP1 (Table 1-1). However, the possibility that these gene families may represent cytoadherence ligands has hardly been investigated. As of the end of 2010, a PubMed search revealed over 400 peer-reviewed publications with the keywords 'PfEMP1' or 'var' while only about 50 with the keyword 'Rif' or 'Stevor'. Thus this thesis will focus on the analysis of all putative parasite ligand proteins, not just PfEMP1.

Despite showing distinct sequences, *rif*, *stevor* and *Pfmc-2TM* have many characteristics in common. They bear an N-terminal signal sequence (SS) that is responsible for translocation of their protein products into the endoplasmic reticulum (Figure 1-6). A Pexel (or VTS) motif is encoded at the start of exon 2 and allows the protein to be trafficked into the RBC cytoplasm (Hiller, et al., 2004, Marti, et al., 2004). All genes of these 3 families have 2 predicted transmembrane (TM) domains that flank a hypervariable loop. This structure suggests that these proteins are anchored in the membrane by the two TM with their hypervariable loop exposed on the iRBC surface (Lavazec, et al., 2006). The immune system would select for this variability by eliminating parasites with conserved surface molecules. Moreover, most of these putative VSAs are located in the subtelomeric regions of each chromosome where *var* genes are also found (Table 1-1).

	Var (PfEMP1)	Rifin	Stevor	Pfmc-2TM
Gene copies	~60	~150	~30	~12
Size (kDa)	200 to 400	30 to 45	30 to 40	30 to 40
Gene location	Subtelomeric or centromeric	Mainly subtelomeric	Mainly subtelomeric	Subtelomeric
Mutually exclusive expression	Only one gene per cell is expressed	Restricted subset of genes transcribed	Restricted subset of genes transcribed	?
Pexel motif	Non-classical	Yes	Yes	Yes
Transmembrane domains	1	1 or 2	2 (?)	2
Hypervariable domain	yes	yes	yes	yes
Confirmed protein expression	Sporozoite, merozoite, trophozoite, gametocyte	Sporozoite, merozoite, trophozoite, gametocyte	Sporozoite, merozoite, trophozoite, gametocyte	Trophozoite
Peak of transcription in the asexual cycle	6-20 hours	18-23h	22-32h	
Protein location in the iRBC	Surface of the iRBC	Surface of the iRBC	Maurer's cleft, Surface of the iRBC	Maurer's cleft, iRBC membrane?
Immunogenic	Yes	Yes	Yes	?
Function	Immune evasion, Cytoadherence, Rosetting,…	Antigenic variation + ?	Antigenic variation + ?	?

Table 1-1. Summary table of putative variant surface antigens.

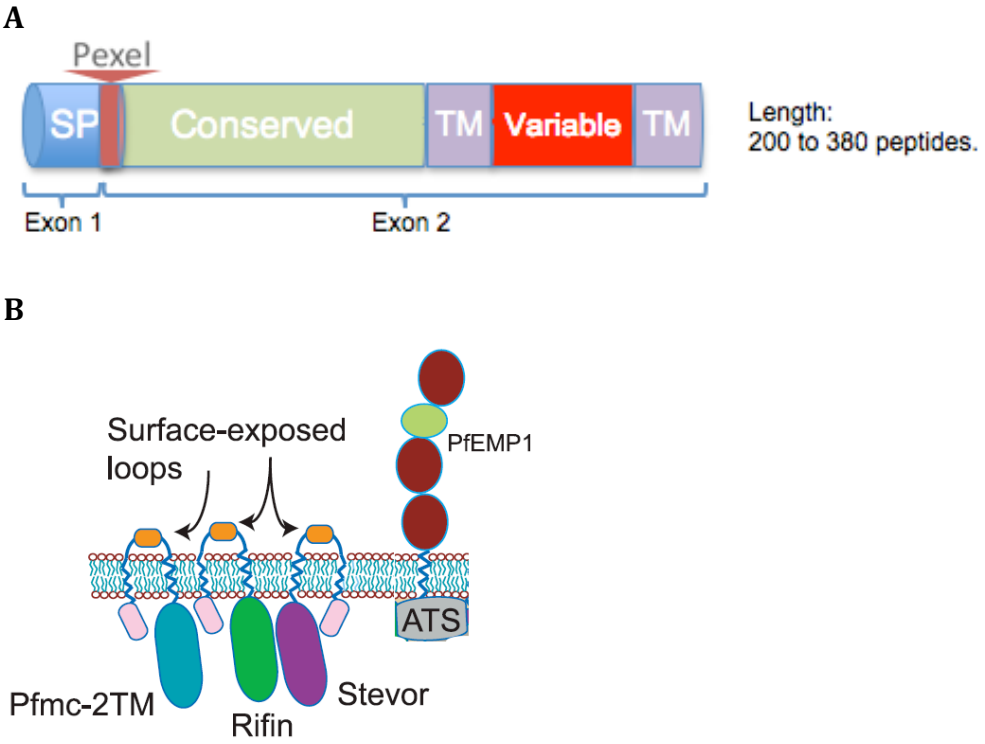


Figure 1-6. General structure of Rifin, Stevor and PfMC-2TM. (A) Although their sequences are distinct, *rif*, *stevor* and *pfmc-2TM* genes share the same general structure. SP = Signal peptide; TM = Transmembrane. (B) Hypothesis about how VSA could be inserted into the iRBC membrane (Adapted from (Lavazec, et al., 2006).

1.2.2.1 Rifin family

The *rif* gene family represents the largest multi-copy gene family in *P. falciparum.* They have recently been subdivided in two major groups, RifA and RifB, based on a 25 amino acids insert found in the RifA family only (Joannin, et al., 2008). The upstream sequences also reflect the RifA/B subdivision (Petter, et al., 2008). Importantly, this sequence-based classification correlates with the final localization of these proteins: RifAs are exported to the surface of the iRBC via the Maurer's Cleft while RifBs accumulate within the parasite cytosol. This pattern of expression is also found in gametocytes (Petter, et al., 2008). A detailed bioinformatic analysis found RifAs to lack a signal peptide and contain a single transmembrane (TM) domain (Bultrini, et al., 2009). RifBs however show a couple of TM domains surrounding the hypervariable loop.

Experimental validation is thus needed to validate the TM domain predictions. Some RifAs harbour particular features: RifA1s are relatively similar to each other (84% between strains) and each of them is found head to head with a group A *var* gene (Wang, et al., 2009b). RifA2 has both a different sequence and upstream sequence from other RifAs that is conserved in all tested *P. falciparum* strains (see also chapter 3). It also appears to be constitutively expressed in many 3D7 subclones (Cabral and Wunderlich, 2009). Finally RifA3s are head to head with type 3 *var* genes.

In a series of studies of individuals exposed to *P. falciparum* infections, Abdel-latif and colleagues showed that naturally induced anti-Rifin antibodies are commonly found in semi-immune and immune people (Abdel-Latif, et al., 2004, Abdel-Latif, et al., 2003, Abdel-Latif, et al., 2002). Whether the antibodies actually provide protection against the disease has yet to be determined.

To date, no function for the Rifin family has been demonstrated yet, although an "Armadillo-like" structure has been predicted for RifA, which may indicate a protein-protein interaction (Bultrini, et al., 2009).

1.2.2.2 Stevor family

Stevor is a family of about 30 copies encoding 30-40kDa proteins. Although a single parasite can transcribe more than one s*tevor* at a given time, this is restricted to a small subset of *stevors* and it is clonally variant (Niang, et al., 2009). *stevor* transcription occurs 22 to 32 hours post invasion (Kaviratne, et al., 2002). The protein is trafficked via the Maurer's cleft until it reaches the membrane of schizonts or the apical tip of merozoites (Blythe, et al., 2009, Blythe, et al., 2008, McRobert, et al., 2004). The most recent evidence points towards a surface expression of Stevors (Niang, et al., 2009). However this expression is mostly found in field isolates as unselected lab strains hardly express *stevor* genes (Blythe, et al., 2008, Daily, et al., 2005). This issue applies to all VSA families as the obvious lack of immune pressure in a culture flask is highly likely to influence their expression.

1.2.2.3 Pfmc-2TM family

This relatively small VSA family (~10 members) was first identified through a library of antibodies against *P. falciparum* using coimmunoprecipitation and shotgun proteomics (Sam-Yellowe, et al., 2004). As indicated by their name, they localize to the Maurer's cleft. There is also evidence that they reach the iRBC membrane although this has yet to be confirmed (Lavazec, et al., 2006).
The hypervariable loop, albeit shorter than for *rif* or *stevor*, indicates that they are under immune pressure. Whether malaria-exposed people naturally develop antibodies against PfMC-2TM remains to be tested.

The possibility that these 'neglected' VSA families could mediate cytoadherence has hardly ever been investigated. Virtually all studies that have tried to identify parasite ligands for a cytoadhesion phenotype have focused on the PfEMP1 family. The fact that VSA families like Rifin and Stevor are clonally variant, immunogenic and located at the surface of the iRBC make them candidates as mediators of cytoadherence.

1.3 Cytoadherence

P. falciparum pigmented-trophozoites are known to undergo three main types of cytoadherence: adhesion to the endothelium, to other uninfected red blood cells (rosettes) and to platelets (clumping) (reviewed in (Rowe, et al., 2009a)).

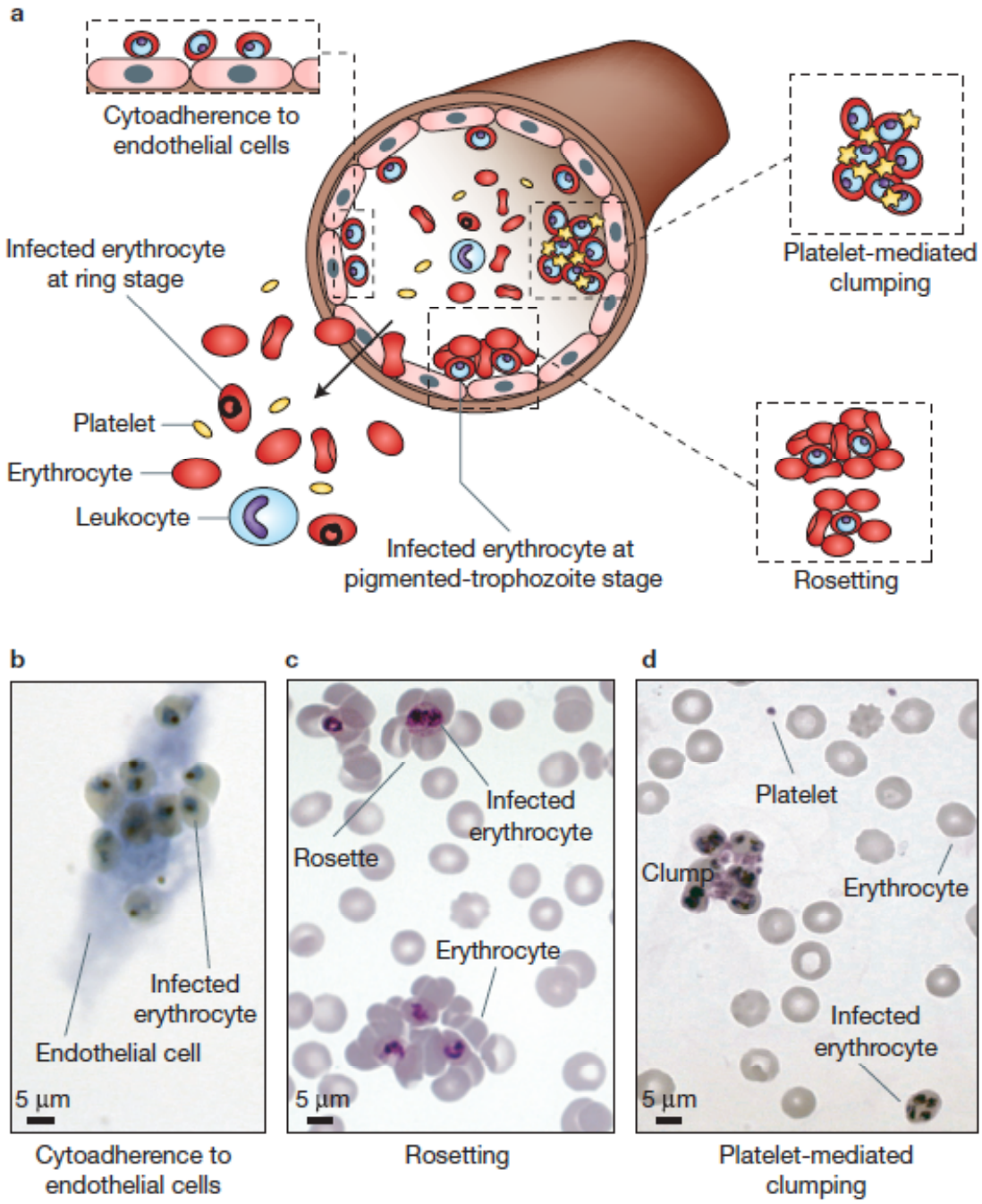


Figure 1-7. The three types of *P. falciparum* iRBC mediated cytoadherence. (a) schematic representation of putative cytoadhesion mechanisms occurring in a blood vessel. (b, c, d) Giemsa stain of *in vitro* culture of endothelial cells (HBEC-5i) and *P. falciparum* parasites in human group O blood. Courtesy of Monica Arman.

1.3.1 Cytoadherence to endothelial cells

Sequestration of *P. falciparum* iRBC within the microvasculature was documented over 100 years ago (Marchiafava, 1894). Since then many key players have been identified, both on the side of the parasite and of the host. However, much work remains to be done as most of the identified endothelial cell receptors are poorly characterized. Here under is the current knowledge on 14 host molecules that have been postulated to mediate cytoadherence to endothelial cells. The consequences of this attachment will be discussed in the next section. Adhesion to hyaluronic acid and chondroitin sulfate A (CSA), which are thought to be involved in the special case of pregnancy-associated malaria only, are discussed in section 1.5.1.

1.3.1.1 CD36

The scavenger receptor CD36 is a well-known, well studied receptor for iRBC yet 20 years after its discovery (Barnwell, et al., 1989, Oquendo, et al., 1989), its role in the pathogenesis of malaria remains controversial (Serghides, et al., 2003).

The ligands binding to CD36 *in vitro* are clear: PfEMP1 proteins harbouring a CIDR1α domain (Miller, et al., 2002, Robinson, et al., 2003). The structure of the CIDR1α binding portion is a bundle of three α-helices that are connected by a loop and three additional helices (Klein, et al., 2008). On the other hand, mammalian cells transfected with CIDR1α1, β and γ do not bind to CD36 (Robinson, et al., 2003). Interestingly, PfEMP1 with a CIDR1α domain tend to be part of the group B or C family and not group A. Hence one current hypothesis is that parasites expressing group B and C PfEMP1 bind to CD36 while the ones expressing group A do not. In any case, considering the immense variability between each PfEMP1 sequence, it is highly remarkable that so many of them share the same ability to adhere to CD36.

It is generally acknowledged that most parasites isolates are able to adhere to CD36 (Newbold, et al., 1997). However, there is apparently no difference in adhesion to CD36 between isolates from severe (or cerebral) and uncomplicated malaria in Africa (Heddini, et al., 2001b, Newbold, et al., 1997,

Rogerson, et al., 1999). Note that the brain microvasculature lacks CD36 expression (Silamut, et al., 1999, Turner, et al., 1994). Hence this receptor cannot be the molecule mediating the sequestration seen in all cerebral malaria cases (MacPherson, et al., 1985, Seydel, et al., 2006). Whether CD36 adhesion is detrimental is uncertain as macrophages also require it for non-opsonic phagocytosis of iRBC (McGilvray, et al., 2000, Serghides and Kain, 2001). In rodents, macrophages lacking CD36 are significantly less efficient at phagocytosing iRBC (Patel, et al., 2004). Thus, in terms of cytoadherence-based therapy (i.e. preventing or removing sequestered parasites), it is unclear whether acting on CD36 would be beneficial for the patient. Blocking the ability of iRBC to sequester via CD36 might favour the switching to different and perhaps more virulent *var* gene expression (Serghides, et al., 2003).

1.3.1.2 ICAM1 (intercellular adhesion molecule, CD54)

ICAM1 has also received much attention since the discovery of *P. falciparum* iRBC adhering to COS cells transfected with ICAM1 (Berendt, et al., 1989). iRBC can also bind to ICAM1 under flow conditions (reviewed in (Chakravorty and Craig, 2005)). This effect is enhanced by CD36 as parasites bind in synergy to these receptors (McCormick, et al., 1997, Yipp, et al., 2007). However, it has been reported that some iRBC bind exclusively to ICAM1 and not CD36 (Chattopadhyay, et al., 2004). iRBC bind to ICAM1 on the opposite side to the natural ligand LFA-1 (Ockenhouse, et al., 1992, Tse, et al., 2004).

The parasite antigen PfEMP1 connects to ICAM1 via its DBLβ-C2 domain (Chattopadhyay, et al., 2004, Smith, et al., 2000a, Springer, et al., 2004). Not all DBLβ-C2 domains bind to the receptor however and the difference in sequences between binder and non-binder domains is unclear (Howell, et al., 2008). In the IT/FCR3 strain, the ability to bind to ICAM1 is limited to some group B and C but not group A PfEMP1.

Postmortem and *in vitro* studies have shown that the high level of TNF cytokine found in severe malaria patients can activate brain endothelium which in turn increases the amount of surface ICAM1 (Silamut, et al., 1999, Tripathi, et al., 2006, Turner, et al., 1994, Wassmer, et al., 2005) (see also section 1.4.2).

Furthermore, sequestered parasites can co-localize with ICAM1 (Turner, et al., 1994).

Considering these facts, it would seem possible that ICAM1 is the receptor for iRBC sequestered in cerebral malaria. If this were the case, one would expect field isolates from cerebral malaria patients to bind significantly better to ICAM1 than isolates from non-cerebral malaria patients. Also, ICAM1 polymorphisms preventing adhesion from iRBC should protect against cerebral malaria. However, African field-isolate studies found no statistically significant association between ICAM1 binding and severe malaria (Heddini, et al., 2001b, Newbold, et al., 1997, Rogerson, et al., 1999). There is an ICAM1 polymorphism named "ICAM1-Kilifi" which is common in the African population (Fernandez-Reyes, et al., 1997) and reduces binding to ICAM1 under flow conditions (Craig, et al., 2000). However, multiple human genetic studies failed to link this polymorphism with a protection against cerebral malaria (Amodu, et al., 2005, Bellamy, et al., 1998, Fernandez-Reyes, et al., 1997, Fry, et al., 2008, Ndiaye, et al., 2005). Altogether, the precise function that ICAM1 may play in cerebral malaria remains uncertain. The ICAM1-iRBC interaction on its own is unlikely to be the full story explaining the difference between a mild and a cerebral case of malaria.

1.3.1.3 P-selectin (CD62P)

P-selectin is a glycoprotein of the cell adhesion molecule (CAM) family expressed by activated platelets and endothelial cells. It initiates the tethering of leukocytes to endothelium (Alon, et al., 1995). A similar behaviour has been observed with iRBC: under flow conditions, P-selectin, as an immobilized soluble protein or expressed in transfected cells, mediates the tether and rolling of most field isolates (Ho and White, 1999, Udomsangpetch, et al., 1997). This interaction is Ca^{2+}-dependent and requires sialic acid residues on the iRBC membrane. The ligand is probably PfEMP1, as when the latter is isolated, it can bind to the lectin domain of P-selectin *in vitro* (Senczuk, et al., 2001). Although this tethering and rolling does not lead to static binding, this interaction may have some relevance *in vivo*. In fact, when P-selectin is knocked-out in

endothelial cells in mice, they do not develop experimental cerebral malaria (see section 1.6 for description of the mouse model) (Combes, et al., 2004). The role of this receptor in human severe malaria is however untested.

1.3.1.4 E-selectin (ELAM1, CD62E)

Despite various studies on this cell adhesion molecule, *P. falciparum* field isolates show no binding or tethering and rolling on E-selectin under flow conditions (Udomsangpetch, et al., 1996a, Udomsangpetch, et al., 1997). However a monoclonal E-selectin antibody slightly inhibits binding on lung endothelial cells (Traore, et al., 2000). The role of E-selectin in cytoadherence is thus probably minor, if any.

1.3.1.5 Thrombospondin

Thrombospondin (TSP) is an adhesive glycoprotein released in response to platelet activation by alpha-thrombin. Historically the first molecule to be identified as a cytoadherence receptor (Roberts, et al., 1985), iRBC have been shown to bind to soluble TSP in static assay (Heddini, et al., 2001c) and under flow conditions to vascular cells (Rock, et al., 1988). It is also able to stimulate E-selectin, VCAM1 and ICAM1 expression on endothelium (Narizhneva, et al., 2005) and to trigger endothelial apoptosis via CD36 activation (Jimenez, et al., 2000).

PfEMP1, but also the RBC exposed phosphatidylserine (a membrane phospholipid) and band 3 protein may mediate adherence to TSP (Baruch, et al., 1996, Eda, et al., 1999, Eda and Sherman, 2002). Although most field isolates from Kenya adhere to TSP in a static assay, there is no correlation with severity of the disease (Heddini, et al., 2001c). Moreover, TSP plasma levels are not significantly elevated in cerebral malaria (Larkin, et al., 2009).

1.3.1.6 VCAM-1 (CD106)

VCAM1 is a member of the Ig superfamily and encodes a cell surface sialoglycoprotein expressed by cytokine-activated endothelium. It promotes the adhesion of lymphocytes, monocytes, eosinophils, and basophils.

Elevated serum levels of VCAM1 have been reported in the febrile phase of falciparum malaria but there is no correlation with parasitaemia or severity of the disease (Ohnishi and Kimura, 2001). VCAM1 cytoadhesion has been tested in different studies under flow conditions: field isolates tether and roll on VCAM1 but do not bind (Udomsangpetch, et al., 1997).

1.3.1.7 PECAM1 (CD31)

Platelet endothelial cell adhesion molecule 1 (PECAM1) is found on endothelial cells and platelets (among other cell types). Both the DBL2δ and CIDRα domains belonging to one PfEMP1 variant show some PECAM1 binding activity (Chen, et al., 2000). Although about half field isolates from Kenya adhere to PECAM1 in a static assay, there is no correlation with severity of the disease (Heddini, et al., 2001a, Heddini, et al., 2001c). PECAM1 polymorphisms do not protect against severe malaria in Papua New Guinea or Kenya (Casals-Pascual, et al., 2001). Another polymorphism increased the risk of cerebral malaria in Thailand (Kikuchi, et al., 2001). Altogether, PECAM1 is unlikely to be critical to microvasculature sequestration.

1.3.1.8 Heparan sulfate and heparin

Heparan sulfate is a linear polysaccharide found as a proteoglycan in all animal tissues. Heparin, produced by mast cells, is simply a highly sulphated form of heparan sulfate. The DBLα domain of one PfEMP1 variant is able to bind to heparin (Barragan, et al., 2000, Chen, et al., 2000, Vogt, et al., 2003). This interaction is dependent on N-sulphation and requires a minimal heparin fragment size of 10- or 12-mers (Barragan, et al., 2000). Heddini *et al* found Kenyan field isolates to bind to soluble heparin (Heddini, et al., 2001c). Interestingly, the binding was significantly increased when parasites were isolated from severe malaria patients compared to mild malaria patients. More experiments are needed to determine the importance of heparan sulfate and its derivatives in cerebral malaria.

1.3.1.9 Fractalkine/CX3CL1, Integrin αVβ3, Fibronectin, NCAM (CD56) and gC1qR/HABP1

The role of Fractalkine/CX3CL1, Integrin αVβ3 and Fibronectin, NCAM (Neural Cell Adhesion Molecule) and gC1qR as iRBC receptors has only been reported once. Field isolates bind to some extent to Fractalkine, Integrin αVβ3 and gC1qR through an unknown ligand (Biswas, et al., 2007, Hatabu, et al., 2003b, Siano, et al., 1998). The host protein modified band 3 has been suggested to bind to the RGD motif of Fibronectin (Eda and Sherman, 2004). Antibodies against NCAM can only slightly inhibit the binding to CHO-745 cells that naturally express NCAM (Pouvelle, et al., 2007).
Whether the binding to any of these 5 receptors can be associated with severity of malaria has not been investigated yet.

It is striking how few of these putative receptors have been thoroughly investigated. Moreover, it has to be noted that a systematic, high-throughput investigation of all endothelial cell surface proteins has not been performed to date. Thus it is likely that more receptors remain to be discovered.

Endothelial cell receptor	***P. falciparum* Ligand**	**Binding associated with severe malaria?**	**Main reference/Review**
CD36	CIDR1α domain (group B and C PfEMP1)	No	(Serghides, et al., 2003)
ICAM1 (CD54)	DBLβ-C2 domain (group B and C PfEMP1)	No	(Chakravorty and Craig, 2005)
P-Selectin (CD62P)	PfEMP1	No	(Senczuk, et al., 2001)
E-Selectin (CD62E)	ND (probably minor role)	No	(Udomsangpetch , et al., 1996b)
Thrombospondin	PfEMP1? Phosphatidylserine? Band 3?	No	(Heddini, et al., 2001b)
VCAM1	?	No	(Ohnishi and Kimura, 2001)
PECAM1	DBL2δ and CIDRα domains of PfEMP1	No	(Heddini, et al., 2001b)

Heparan Sulfate (Heparin)	DBLα domain of PfEMP1	Yes	(Heddini, et al., 2001b, Vogt, et al., 2003)
Fractalkine	?	No	(Hatabu, et al., 2003a)
Integrin αVβ3	?	No	(Siano, et al., 1998)
Fibronectin	Band 3?	No	(Eda and Sherman, 2004)
NCAM	?	No	(Pouvelle, et al., 2007)
gC1qR/HABP1	?	No	(Biswas, et al., 2007)

Table 1-2. Summary of known endothelial cell receptors and *P. falciparum* ligands interactions. For an exhaustive list of references, see (Rowe, et al., 2009a).

1.3.2 Rosetting

A rosette is an iRBC attached to two or more uRBC (Figure 1-7C). Only pigmented-trophozoite stages parasites form rosettes *in vitro*, thus rosettes cannot be directly observed *in vivo* as these stages are sequestered and are not seen in a blood smear (reviewed in (Mercereau-Puijalon, et al., 2008)). When field isolates are cultured for a few hours, rosettes spontaneously start to form. The rosetting frequency can be estimated by counting the number of iRBC forming a rosette compared to the total number of iRBC. Interestingly, a high rosetting frequency is constantly found in isolates extracted from all forms of severe malaria patients in Africa (Doumbo, et al., 2009, Rowe, et al., 1995, Rowe, et al., 2009a, Rowe, et al., 2007) (see (Rowe, et al., 2009a) for full list of references). This association is however not found in Asia, due to unknown reasons (Chotivanich, et al., 2004, Ho, et al., 1991). In principle, the combination of rosetting and sequestration could cause the obstruction of microvasculature and ultimately lead to coma (Kaul, et al., 1991). This would explain the link between rosetting and severe malaria in Africa.

PfEMP1 is the major parasite ligand for rosetting (Rowe, et al., 1997). Other molecules may be involved as other Plasmodia infecting are able to rosettes even in the absence of *var* genes in their genome (Jemmely, et al., 2010). Interestingly, *P. falciparum* parasites selected for rosetting mostly express group A *var* genes (Rowe, et al., 1997, Vigan-Womas, et al., 2008) and

Rowe group, unpublished data). However, whether the same group A PfEMP1 can bind to uRBC and endothelial cells has not been investigated yet.

The best characterized receptor for rosetting is complement receptor 1 (CR1) which binds to the PfEMP1 DBLα1 domain from the rosetting R29 strain (Mayor, et al., 2005, Rowe, et al., 1997, Rowe, et al., 2000). Other receptors include heparan sulfate-like molecules (Barragan, et al., 2000, Chen, et al., 1998a) and the A and B blood group antigens. The latter are particularly interesting as human genetic studies support a direct role for A and B antigen mediated rosetting in the pathogenesis of severe malaria (Rowe, et al., 2009b). On the other hand, blood group O confers significant protection against the severe form of the disease (Rowe, et al., 2007).

1.3.3 Platelet mediated clumping

Platelet-mediated clumping, the adhesion of many iRBC and platelets together, has only been discovered recently (Pain, et al., 2001). The propensity of binding to platelets is strain dependent and parasites can be selected for or against this phenotype (Monica Arman, unpublished data). Although it remains to be tested, clumps of iRBC and platelets could contribute to microvascular obstruction *in vivo*. Three studies have found an association between high clumping frequency and severe malaria (Chotivanich, et al., 2004, Pain, et al., 2001, Wassmer, et al., 2008) whereas a fourth one did not (Arman, et al., 2007). However each study used different experimental methods which has got a profound impact on the outcome of the assay (Arman and Rowe, 2008). Thus the link between severe malaria and platelet-mediated clumping remains to be appropriately investigated.

The parasite ligand mediating the platelet binding is currently under investigation and is probably a member of the PfEMP1 family (Monica Arman, unpublished data). Three putative platelet receptors have been identified: CD36, gC1qR and P-selectin (Biswas, et al., 2007, Pain, et al., 2001, Wassmer, et al., 2008). CD36 is probably the main platelet receptor, however field isolates adhering to CD36 do not necessarily form clumps (Pain, et al., 2001).

Moreover, it has been shown that platelets can bind to iRBC and endothelial cells (Wassmer, et al., 2004). Therefore they could act as a "bridge" which would increase parasite sequestration. This would be of particular interest in the brain, as it would allow CD36 binding parasites to cytoadhere via platelet to endothelial cells lacking this receptor. In other words, *P. falciparum* iRBC expressing a group B or C PfEMP1 could bind to CD36 on a platelet, which in turn could bind to an activated brain microvascular endothelial cell.

1.4 Cerebral malaria

The molecular mechanisms that kill cerebral malaria patients, mostly young children in Sub-Saharan Africa, are still poorly understood. The two current hypotheses are the "sequestration model" and the" inflammatory model". Note that a combination of both models may also occur (van der Heyde, et al., 2006).

1.4.1 The sequestration model

Probably the only feature consistent in all cerebral malaria cases is the sequestration of iRBC within the brain microvasculature (Figure 1-8). However iRBC cytoadherence to brain endothelial cells probably occurs to some extent in all malaria patients. The sequestration is also found in other organs, mainly the skin, intestine and lungs (Table 1-3). Thus *P. falciparum* sequestration is necessary but not sufficient to cause cerebral malaria and is not specific to the brain microvasculature (Pongponratn, et al., 2003).

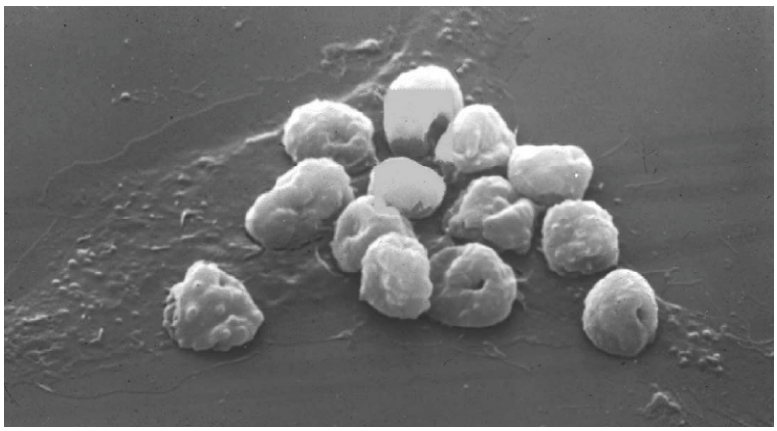


Figure 1-8. Electron micrograph of *P. falciparum* iRBC adhering to endothelial cell monolayer. (Chakravorty and Craig, 2005)

Reference	Postmortem study description	Location of sequestered parasites
(MacPherson, et al., 1985)	7 CM cases versus 6 NCM cases in Thailand.	Brain > heart > lung, liver kidney
(Pongponratn, et al., 1991)	24 CM cases versus 15 NCM cases in Thailand.	Brain > intestine, heart, lungs
(Nakazawa, et al., 1995)	Single CM case finding a correlation between sequestration in subcutaneous tissue and CM.	Brain and subcutaneous tissue
(Wilairatana, et al., 2000)	Skin biopsies of 10 SM and 10 UM cases in Thailand.	Subcutaneous tissues >> dermis
(Pongponratn, et al., 2003)	37 CM cases versus 28 NCM cases in Thailand.	Brain >>> kidney Within the brain: Cerebellum > Cerebrum >Medulla
(Montgomery, et al., 2006)	Clonality of *P.f.* parasites within differents body parts (19 children).	Brain, spleen > liver, heart, lung > gut, muscles, kidney
(Seydel, et al., 2006)	43 CM versus 17 NMCD cases (African children). Sequestration determined by pLDH concentration.	Brain, intestine, skin > lungs, liver > kidney.
(Genrich, et al., 2007)	Five travellers. pLDH and other antigens.	Brain, heart, lung > other organs

Table 1-3. List of postmortem cerebral malaria studies that investigated sequestration in other organs. A ">" sign indicates the relative abundance of sequestered parasites while a "," indicates similar level of sequestration. Note that estimating and comparing the burden of sequestration between different tissues is complex because of the extensive heterogeneity in the intensity of parasitisation, even within very small areas. The Seydel *et al.* report measures the concentration of the parasite-derived lactate dehydrogenase (pLDH) enzyme in order to estimate

the parasite burden within each tissue. (N)CM = (non) cerebral malaria; UM = Uncomplicated Malaria; NMCD = assumed cerebral malaria with nonmalaria causes of death.

It is acknowledged that sequestration can have a deleterious effect on the host, causing obstruction of blood flow and localised hypoxia (Dondorp, et al., 2008a). Sequestration has also been reported to lead to haemorrhage into the surrounding brain parenchyma (reviewed in (Medana and Turner, 2006)). iRBC and uRBC become less deformable during the infection creating a "plug" within the capillaries, which is associated with poor outcome (Dondorp, et al., 2000). Another key element of this model is the high-blood lactacte level, which is significantly associated with the development of cerebral malaria (Marsh, et al., 1995). Lactic acidosis is an indication that tissues are respiring anaerobically. Yet other explanations have been proposed, including altered redox state or mitochondrial dysfunction (Maitland and Newton, 2005).

However, there are important factors that cannot be explained by this "mechanical model" alone. Firstly, there is no clear evidence for irreversible hypoxic damage to neurones in fatal cerebral malaria (Medana, et al., 2001), second, the fact that iRBC can be found sequestered in asymptomatic people (Pongponratn, et al., 1991). Furhtermore, the human parasite *P. vivax,* which does not sequester, can on rare occasion cause fatal cerebral malaria (Rogerson and Carter, 2008).

1.4.2 The inflammation model

Brain capillaries form a unique structure of tight junctions between endothelial cells called the blood-brain barrier. Its function is to separate the circulating blood and potentially harmful pathogens from the brain parenchyma. These brain endothelial cells are activated during cerebral malaria although whether this always leads to disruption of the blood-brain barrier is controversial (Combes, et al., 2010, Newton and Warrell, 1998). The main molecules involved in this process are detailed here under; Figure 1-9 summarizes the pathogenesis of cerebral malaria.

As soon as the first schizont ruptures, parasite toxins are freed into the blood. Monocytes and neutrophils are activated via Toll-like Receptors resulting in secretion of proinflammatory cytokines including TNF (Tumour Necrosis Factor), IFNγ (Interferon), IL-1 (Interleukin), IL-6, NO (nitric oxide) and LT-α (Lymphotoxin) (Gazzinelli and Denkers, 2006). IL-1β, IL-6 and IL8 are raised in patients with malaria and correlate with disease severity (Day, et al., 1999, Lyke, et al., 2004). These cytokines in turn recruit other immune cells such as CD4+ and CD8+ T cells (Martins, et al., 2009). These events make up the first inflammatory response that has the beneficial effects of diminishing parasite growth and removing toxins like free heme. However, the release of cytokines also activates endothelial cells.

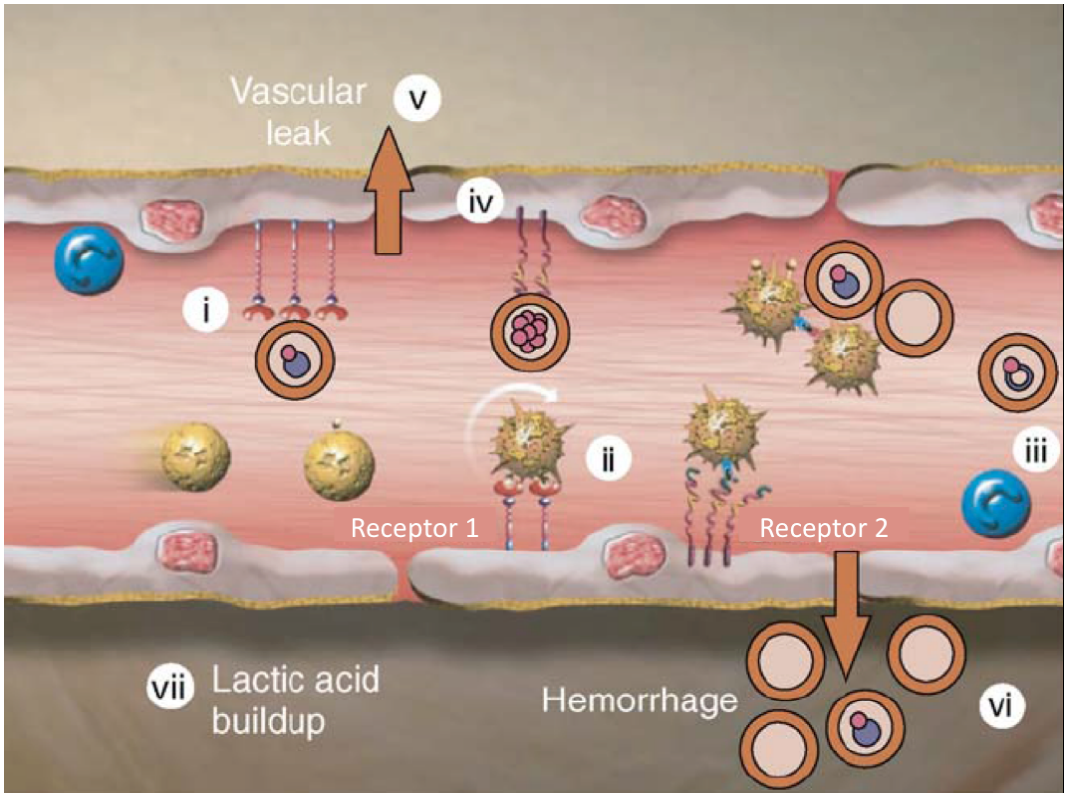


Figure 1-9. Molecular and cellular mechanisms leading to cerebral malaria. This hypothetical model of pathogenesis suggests a role for both sequestration and inflammation. (i) Basal expression of various receptors at the surface of microvascular endothelial cells would mediate cytoadhesion of the first iRBC. This would act as a signal in conjunction with platelets and cytokines (especially TNF) to activate endothelial cells to increase their expression of surface receptors, including

ICAM1, leading to the adhesion of additional iRBC and platelets. These platelets would act as bridges for iRBC to adhere to the brain endothelium (ii). The formation of rosettes around these adherent iRBCs is another process that could contribute to disruption of blood flow. Sequestration and vasoactive molecules would then disrupt endothelial tight junctions (v). Endothelial cell apoptosis could also be involved (vi). The resulting plugging of capillaries leads to an increase of lactic acid in the tissue (vii). Figure modified from (van der Heyde, et al., 2006).

Endothelial cell activation

Endothelial cells can be activated by platelets, iRBC adhesion or cytokines; it is unclear which of these events occurs first or is most important.

TNF is a major endothelial cell activation molecule that greatly upregulates surface receptors such as ICAM1 and VCAM1 (Wassmer, et al., 2005, Wassmer, et al., 2006c). The *in vitro* cytoadherence of iRBC is significantly increased on endothelial cells when activated with TNF (Wassmer, et al., 2005). Further evidence for the crucial role of TNF is that plasma levels (Grau, et al., 1989) and brain levels (Porta, et al., 1993) are elevated in cerebral malaria. iRBC themselves can activate endothelial cells but it is unclear whether direct contact of iRBC is needed for this effect (Viebig, et al., 2005, Wilson, et al., 2008). Also, it was recently shown that metabolic acidosis induced by iRBC can induce permeability of endothelial cells and ultimately disrupt the blood-brain barrier *in vitro* (Zougbede, et al., 2010).

This potentially harmful proinflammatory response to malaria antigens might be counteracted by the anti-inflammatory cytokines IL-10 and TGF-β (transforming growth factor) (Crawley, et al., 2010). Another probably beneficial molecule is nitric oxide (NO) (Weinberg, et al., 2008). NO is a potent inhibitor of TNF production (Iuvone, et al., 1996); importantly it reduces cytoadherence under flow conditions by inhibiting receptor expression (e.g. ICAM1 and VCAM) (Serirom, et al., 2003).

The role of platelets in cerebral malaria

Thrombocytopenia (platelet count < 150 x 10^9/L) is typically found in acute *P. falciparum* infections. Platelets have been shown to bind to iRBC and endothelial cells *in vitro* (the consequences for sequestration were discussed in section 1.3.3). Activated platelets release CD40 ligand (CD40L) that binds to CD40, a receptor constitutively expressed on endothelium. Endothelial cells in turn release chemoattractants (monocyte chemoattractant protein 1 and IL-8) and enhance their expression of E-selectin, ICAM1, and VCAM1 (Henn, et al., 1998, Slupsky, et al., 1998). Platelets also secrete chemotactic factors that can contribute to inflammation including IL-1β, transforming growth factor-β1 (TGF-β1), Thrombospondin, RANTES, platelet factor 4 (PF4) and β-thromboglobulin (β-TG). IL-1β and TGF-β1 are upregulated in the brains of cerebral malaria patients (Brown, et al., 1999, Prakash, et al., 2006). IL-1β can cause neuronal cell damage (Rothwell and Luheshi, 2000) but also increases the endothelium expression of Integrin $\alpha_V\beta_3$ (see section 1.3.1.9) *in vitro.* TGF-β1 seems to have a protective effect in the mouse model by slowing down parasite growth (Omer and Riley, 1998). Its effect in humans remains to be tested. PF4 and β-TG are significantly elevated in acute *P. falciparum* infection (Essien and Ebhota, 1983). Mice deficient for PF4 showed less severe experimental cerebral malaria (Srivastava, et al., 2008). The same effect is seen in RANTES null mice (Belnoue, et al., 2003). The RANTES cytokine is thought to have a deleterious effect when released by sequestered platelets during cerebral malaria (Faille, et al., 2009b).

Microparticles

Many recent publications have focused on the roles of microparticles, derived from endothelial cells or platelets, in cerebral malaria (reviewed in (Combes, et al., 2010). These submicrometer vesicles are characterized by the presence of functional adhesive receptors derived from the plasma membrane of the cell of origin (Faille, et al., 2009b). Platelet microparticles were shown to bind specifically to iRBC and increase their adhesion to brain endothelial cells (Faille, et al., 2009a). Platelet microparticles also adhere to these endothelial

cells, conferring some new surface proteins such as PECAM and GPIV (Faille, et al., 2009a).

Although it is clear from the evidence described above, that inflammation contributes to the pathogenesis of cerebral malaria it is not sufficient to explain everything. For example, *P. vivax* malaria also generates high levels of inflammatory cytokines, yet it does not usually lead to cerebral malaria (Anstey, et al., 2009). Also, anti-inflammatory agents and antibodies against TNF have failed to ameliorate symptoms to date (van Hensbroek, et al., 1996). A consequence both of sequestration and the pro-inflammatory response seen in cerebral malaria is disturbed haemostasis. Patients with *falciparum* malaria show prolonged bleeding time, petechial haemorrhage is observed at autopsy and retinal haemorrhage indicates poor prognosis (Beare, et al., 2004). Overall, a procoagulant state is seen in patients, which might contribute to the pathogenesis of cerebral malaria. Altogether, sequestration, cytokines and alterations in haemostasis are likely to play a role in this complex disease (Figure 1-9). The parasite antigens involved in the pathogenesis of cerebral malaria are detailed here under.

1.5 VSA and immunity to cerebral malaria

Despite the incredible diversity of parasite VSA sequences such that each new infection brings large set of new antigens, immunity to cerebral and severe malaria in general is acquired relatively quickly, in comparison to the lack of acquisition of sterilising immunity (reviewed in (Hviid and Staalsoe, 2004)). Cases of individuals developing cerebral malaria a second time are indeed an exception, indicating some level of acquired immunity (Gupta, et al., 1999b). However, the key antigens targeted by the immune system in order to confer this protection remain unclear.

Antibody recognition experiments demonstrate that parasites infecting young children express a restricted set of VSA that are associated with severity of malaria and age of the patient (Bull, et al., 2000, Bull, et al., 1998, Nielsen, et al., 2002). This subset is defined as VSA_{SM} (i.e. VSA associated with severe

malaria) while VSAs expressed by parasites from patients with uncomplicated malaria are called VSA_{UM}. With repeated infection, immunity against VSA_{SM} is acquired and parasites mostly express VSA responsible for uncomplicated malaria (VSA_{UM}) in older children (Hviid and Staalsoe, 2004). These previous studies (Bull, et al., 2000, Bull, et al., 1998, Nielsen, et al., 2002) showed that in endemic areas, most children acquire antibodies to VSA_{SM} by the age of approximately 5 years, whereas broadly reactive antibody responses to VSA_{UM} are not acquired until adolescence or adult life. A pool of semi-immune sera from children in the 5-10 year age group therefore provides a reagent that preferentially recognises VSA_{SM} over VSA_{UM}, and such sera can be used to select parasites expressing a VSA_{SM} -like phenotype (Jensen, et al., 2004a, Staalsoe, et al., 2003).

The major VSA family is thought to be PfEMP1. An *in vitro* study showed the first link between *var* gene classification and severity of the disease: laboratory clone *P. falciparum* 3D7 was selected using semi-immune serum to express VSA_{SM}, the selected parasites were found to upregulate expression of group A *var* genes (Jensen, et al., 2004b). Field studies reveal results that may seem conflicting: studies in Papua New Guinea and Tanzania found group B *var* genes to be associated with severe malaria while parasite isolates from Brazilian adults with severe malaria and Malian children with cerebral malaria predominantly transcribe group A *var* genes (Joergensen, et al., 2007, Kaestli, et al., 2006, Kirchgatter and Portillo Hdel, 2002, Kyriacou, et al., 2006, Rottmann, et al., 2006). It has to be noted that the latter field study in Mali focuses on three well-defined group of patients (uncomplicated malaria, cerebral malaria or hyperparasitaemia) while the other studies grouped their patients as “severe malaria” which may represent very different symptoms. More recently, a large Kenyan study found group A *var* gene expression to be independently associated to these 3 factors: young host age, low PfEMP1 antibody levels and disease severity (Warimwe, et al., 2009). Another publication in Gabon however found group B and C *var* gene expression to be more common in children suffering from cerebral malaria (Kalmbach, et al., 2010).

Together, these results suggest that substantial and systematic differences in *var* gene expression exist between different clinical presentations. It is also possible that the current *var* gene classification into group A, B and C does not represent the actual pathogenic effect of these antigens.

1.5.1 Var2CSA adhesion to CSA, rule or exception?

It is now well established that the PfEMP1 variant "Var2CSA" is crucial for mediating adhesion to Chondroitin sulfate A (CSA) in the placenta (Tuikue Ndam and Deloron, 2008). Although this glycan is found at the surface of endothelial cells of other tissues, parasites only express *var2csa* and bind to CSA when they are located in the placenta. This *var* gene is an exception as its sequence is very similar in each parasite, i.e. it is a strain-transcending *var* gene. Some clones, like *P. falciparum* HB3, have two copies in their genomes (Kraemer, et al., 2007).

Infected pregnant women develop antibodies against Var2CSA which can explain the much reduced prevalence of malaria in multigravida women (Tuikue Ndam and Deloron, 2008). Thus the hypothesis is that parasites in a primigravida woman express *var2csa* and bind to CSA in the placenta. The immune system develops antibodies against this new antigen, which will prevent severe symptoms in case of re-infection in a subsequent pregnancy.
Could a similar hypothesis explain why children in endemic areas usually never suffer from cerebral malaria more than once (Snow, et al., 1993)? Is there a parasite ligand and a brain endothelial cell receptor that would be at the origin of the disease? So far, some studies have linked group A PfEMP1 with cerebral malaria symptoms (Kyriacou, et al., 2006, Warimwe, et al., 2009). In endemic areas, antibodies against recombinant domains are first acquired against group A PfEMP1 (Cham, et al., 2009). Although group A *var* genes share some common features like the DBL1α1 domains, their sequences show much higher variability compared to *var2csa*. However, most group B and C PfEMP1 are able to bind to the CD36 receptor on endothelial cells in spite of their very different amino acid sequences (Robinson, et al., 2003). This may indicate that the ligand structures are conserved despite the variable sequences, and that this shape is

sufficient to confer adhesion to CD36. Whether VSA involved in the sequestration of an unknown receptor in the brain microvasculature share common features (e.g. a conserved motif) remains to be tested.

1.6 Choosing the right model

As with any human disease involving the central nervous system, investigating cerebral malaria is challenging. Three main approaches are currently being undertaken: postmortem studies of cerebral malaria cases, *in vitro* culture of human brain endothelial cells and parasites, and the mouse model (also called "experimental cerebral malaria"). Each model has its pros and cons, very briefly discussed here under.

Postmortem studies

Autopsies allow direct study of the interaction between *P. falciparum* and its host. Studies usually compare fatal cerebral malaria cases with non-cerebral malaria cases. However, this approach only shows a static endpoint of the disease and the comparison is not to a healthy persons brain, but one who has died of some other cause. It is virtually impossible to study the onset and the development of cerebral malaria. The difficulties in obtaining samples for obvious social and ethical reasons are another significant drawback. In fact, this is the least common way of studying cerebral malaria.

Mouse model

The malaria mouse model offers many advantages, mainly being able to monitor the parasite development from infection to transmission but also to study the effect of host genetic variation. However, *P. falciparum* is specific to *Homo sapiens* and is therefore unable to infect rodents. Therefore rodent malaria parasites such as *P. chabaudi*, *berghei* or *yoelii* are typically used. One of the fundamental discrepancies between mouse and human malaria pathogenesis is in the sequestration: it is mainly mediated by iRBC in human cerebral malaria but by leukocytes in experimental malaria (Martins, et al., 2009). The debate on how the mouse model can contribute to our knowledge of human malaria is still heated (Carvalho, 2010, Renia, et al., 2010, Stevenson, et al., 2010, White, et al., 2010).

In vitro endothelial cell culture

Although most studies have used cell lines such as COS (simian fibroblast), CHO (Chinese ovary hamster) or HUVEC (human umbilical vein endothelial cell), more relevant endothelial cells from a wide range of human tissue are now available. Assuming these cultured cells grow the same way they would *in vivo*, they provide a convenient way of investigating their interaction with iRBC. The main drawback of this system is the impossibility of studying the influence of the immune system on the sequestration phenomenon.

For this particular thesis, the aim was to identify the brain endothelial receptor and its *P. falciparum* ligand. This interaction is thought to be mediated by the parasite VSA. As neither the *var*, *rif* or *stevor* gene families are present in any other genome than *P. falciparum*, it was immediately clear that the *in vitro* model had to be used to answer this particular question.

This background chapter exposed a number of gaps in the knowledge of cerebral malaria, particularly about the molecules involved in the interaction between the iRBC and endothelial cells. In recent years, an *in vitro* culture of human brain microvascular endothelial cells (HBEC-5i) has been developed to study cytoadherence of iRBC and its effects. This model is used in this thesis to identify the molecules involved in sequestration.

1.7 Aims of this thesis

The main question driving this research is: what are the *Plasmodium falciparum* ligand(s) and the human brain endothelial cell receptor(s) mediating sequestration? (Figure 1-10). An *in vitro* model was developed to address this query.

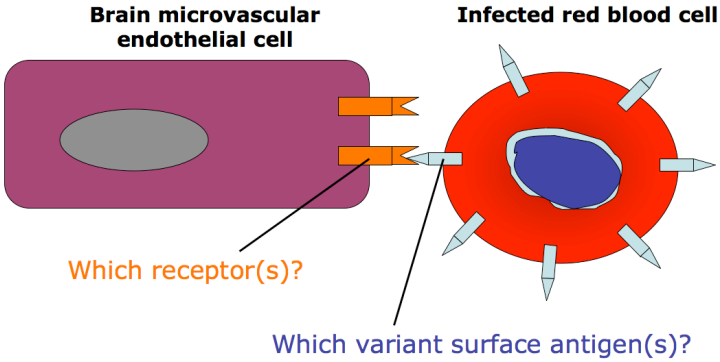


Figure 1-10. This thesis aims to identify the host cell receptor (the list of putative candidates can be found in Table 1-2) and the parasite ligand (postulated to be part of the VSA family).

Investigation of the endothelial cell receptor:

- **Chapter 2**: General materials and methods
- **Chapter 3**: Investigation of the endothelial cell receptor by:
    - Characterization of surface receptors of a human brain microvascular endothelial cell line (HBEC-5i).
    - Selection of various *P. falciparum* strains for binding to HBEC-5i.
    - Static binding assays with selected parasites on soluble immobilised receptors.
    - Binding inhibition assays with antibodies and soluble receptors to inhibit cytoadhesion to HBEC-5i.
    - Also, new drugs are tested for their anti-cytoadhesion properties.

Investigation of the parasite ligand:

- **Chapter 4**: Bioinformatic approach to extract VSA sequences from various *P. falciparum* genomes. These sequences were used to develop specific oligonucleotides for use in microarrays.
- **Chapter 5**: Parasites were synchronised to allow comparison of the transcriptome of selected and unselected parasites by microarray. The

data analysis was particularly focused on VSA (*var, rif, stevor*) but also included proteins predicted to be exported from the parasite.

- **Chapter 6**: Verification of the *var* gene microarray data by RT-PCR. The specificity of the *var* ligand was also tested by selection on dermal and pulmonary endothelial cells followed by RT-PCR of the selected parasites.
- **Chapter 7**: Conclusion.

2 Chapter II: Materials and methods

This chapter describes the bioinformatics and cell culture methods used in this thesis. Methods specific to a single chapter can be found at the start of that chapter.

2.1 General bioinformatics tools

2.1.1 Genome sequences

The following genome sequences were used:

Genome	**Source**	**Web address**
P.f. 3D7	PlasmoDB	www.plasmodb.org
P.f. HB3	Broad Institute	http://www.broadinstitute.org/annotation/genome/plasmodium_falciparum_spp/MultiDownloads.html
P.f. Dd2	Broad Institute	http://www.broadinstitute.org/annotation/genome/plasmodium_falciparum_spp/MultiDownloads.html
P.f. IT	Sanger centre	ftp://ftp.sanger.ac.uk/pub/pathogens/Plasmodium/falciparum/IT_strain/
P.f. Ghanian field isolate	Sanger centre	ftp://ftp.sanger.ac.uk/pub/pathogens/Plasmodium/falciparum/Ghanaian_Isolate/
Neurospora crassa	Broad Institute	http://www.broadinstitute.org/annotation/genome/neurospora/MultiHome.html
All other sequences	GenBank	http://www.ncbi.nlm.nih.gov/Genbank/

2.1.2 ClustalW

ClustaW is an algorithm used for alignment of sequences (http://www.ebi.ac.uk/Tools/clustalw2/index.html). JalView was used to visualize and manually modify these alignments.

2.1.3 BLAST

BLAST finds regions of local similarity between sequences. It was used locally or on PlasmoDB or on the NCBI website (http://blast.ncbi.nlm.nih.gov/Blast.cgi).

2.1.4 MEME

MEME (http://meme.sdsc.edu/meme4_3_0/cgi-bin/meme.cgi) was used to look for conserved motifs within a subset of protein sequences.

2.1.5 Other software

- TranSeq (http://www.ebi.ac.uk/Tools/emboss/transeq/index.html) was used to translate DNA into protein sequences.
- ReverseComplement (http://www.bioinformatics.org/sms2/rev_comp.html) was used to convert a DNA sequence into its reverse-complement counterpart.
- ProtParam Tool (http://www.expasy.org/tools/protparam.html) was used to compute various physical and chemical parameters for a given protein.
- PlasmoDB (http://www.plasmodb.org) was used to retrieve 3D7 gene sequences and various information.

2.2 Plasmodium falciparum *culture and assays.*

2.2.1 Origins of *P. falciparum* used in this work

Parasite	Origin	Reference
HB3	Honduras	(Bhasin and Trager, 1984)
3D7	Cloned from NF54, probably of African origin	(Walliker, et al., 1987)
Dd2	Indochina	(Wellems, et al, 1988)
IT/FCR3	IT and FCR3 lineages probably got mixed during laboratory culture	(Trager, 1993)

2.2.2 *P. falciparum* routine culturing

Any work involving live *P. falciparum* parasites was carried out in a category 3

laboratory, under a class II microbiological safety cabinet.

P. falciparum parasites were grown in sterile flasks of various sizes (25, 75 and 150 cm2, Iwaki). The culture medium used was RPMI 1640 medium (Invitrogen) supplemented with 25 mM Hepes (Lonza), 2 mM glutamine (Invitrogen), 25mM glucose (Sigma), 25 μg/ml gentamicin (BioWhittaker), adjusted with 1M NaOH (Sigma) to pH 7.2 to 7.4 (this is now referred as 'incomplete RPMI') with 10% pooled normal human serum (Scottish National Blood Transfusion service, Edinburgh, UK), now referred as 'complete medium'. Flasks were gassed with 96% N_2, 3% CO_2, 1% O_2 and incubated at 37°C.

Human red blood cells (RBC) (Scottish National Blood Transfusion service, Edinburgh) were separated from whole blood (blood group: O+) by passage through a leukocyte depletion filter. RBC were washed twice with 10 ml of incomplete RPMI and centrifuged at 3500rpm for 10 minutes. RBC were kept for a week at 4°C in incomplete medium at 50% haematocrit.

The complete medium of each flask was changed daily by spinning down the culture suspension at 2000rpm for 4 minutes. The old medium was aspirated and parasites were resuspended at 2% haematocrit with complete medium. Fresh uRBC were added every other day in order to keep the parasitaemia between 5 to 10%.

2.2.3 Thawing parasites

Parasites are kept in liquid nitrogen (-196°C) for long-term storage. They were thawed in a water bath at 37°C. RBC were transferred to a 50ml Falcon tube. For a 1ml packed cell volume (pcv), 200μl of a 12% NaCl in water sterile solution was added drop by drop while mixing. RBC were allowed to equilibrate for 5 min before the addition of 5ml of a 1.8% NaCl solution drop wise. Finally 5ml of a 1.8% NaCl, 0.9% glucose solution was added. RBC were washed once with incomplete medium before being resuspended with complete medium. This was poured into a flask, gassed and kept at 37°C.

2.2.4 Freezing parasites

RBC were spun down and the medium aspirated out. Glycerolyte (42.25% glycerol, 0.1M sodium lactate, 4mM KCl, 0.1M NaH_2PO_4, pH 6.8) was added drop by drop at a ratio of 5 volumes of glycerolyte to 3 volumes of packed cells. After the first volume was added, the cells were allowed to equilibrate for 5min. RBC were aliquoted in cryovials (Nunc) and stored at -80°C overnight, then -196°C for longer storage.

2.2.5 Giemsa smears

A small aliquot was taken every day from each flask. It was spun down, resuspended to about 40% haematocrit, spread on a glass slide, air dried, fixed with methanol and finally stained with filtered 10% Giemsa stain (0.67M Na_2HPO_4 and 0.67M $NaH_2PO_4H_2O$) in Giemsa buffer (phosphate buffer tablets in distilled water pH 7.2, Merck Cat. No. 1.09468) for about 15 min. Slides were then rinsed with water, air-dried and observed under a light microscope (100x objective, with a drop of immersion oil). Parasitaemia was determined after counting at least 500 RBC. Photographs of Giemsa smears were taken using a Leica DMLB2 microscope with attached DFC300FX digital camera.

2.2.5.1 Sorbitol synchronization of ring stage parasites

For other purposes than microarray, where tight synchronization is not crucial, parasites were sorbitol treated once a week. Parasites older than 20 hours post invasion are susceptible to osmotic lysis by sorbitol treatment, leaving rings and uninfected erythrocytes intact (Lambros and Vanderberg, 1979).

To sorbitol synchronise, the culture was spun down and medium aspirated. At least 10 times the volume of 5% D-sorbitol (Sigma) in dH_2O was mixed with the parasites. After incubating at 37ºC for 20min, parasites were washed twice with incomplete RPMI. Cultures were then supplemented with complete medium, transferred to a flask and gassed and incubated as usual. A blood smear was taken to verify that only ring and no pigmented-trophozoite stage parasites were left.

2.3 Endothelial cells culture and assays

Human Brain Endothelial Cells (HBEC-5i) were derived from small fragments of human cerebral cortex by Dorovini-Zis and colleagues(Dorovini-Zis, et al., 1991). They were provided by Dr George Grau (Wassmer, et al., 2006b). They were cultured in DMEM/F-12 medium (Sigma D6421) supplemented with 2mM L-glutamine (Invitrogen), 1U/ml Penicillin/streptomycin (ScienCell 0503), 1μg/ml Streptomycin (ScienCell 0513), (this is now referred as 'incomplete DMEM'), 10% foetal bovine serum, 30μg/ml endothelial cell growth supplement (ScienCell 1052), and the pH adjusted to 7.4 with 1M NaOH (now referred to 'complete DMEM').

Cells were regularly checked for mycoplasma contamination using a PCR detection kit (see section 2.5.4).

2.3.1 HBEC-5i thawing

HBEC-5i were kept in liquid nitrogen for long-term storage. An aliquot was thawed in a 37°C water bath then resuspended with 10ml complete DMEM in a Falcon tube. The tube was spun down (4 minutes at 2000rpm) and the supernatant removed. Cells were well-resuspended with 5ml complete medium before being plated in a 25cm^2 flask (Iwaki) with a filter cap incubated at 37°C with 5% CO_2.

2.3.2 HBEC-5i passaging

Before cells reached 100% confluency they were passaged and diluted into a new flask. Cells were washed twice with sterile PBS or incomplete DMEM. 1ml of trypsin/EDTA (0.25% Trypsin, 0.1% EDTA, in Hank's Balanced Salt Solution, ScienCell 0103) was added and incubated for 2-3 minutes 37°C until almost all cells detached from the bottom of the flask. 9ml of complete medium was added to block further protease activity, and the cells were resuspended and transferred to a 15ml Falcon tube. The tube was spun down and the supernatant removed. Cells were diluted 1 in 10 and plated in a new flask with complete DMEM.

2.3.3 HBEC-5i freezing

Cells were cultured in a 75 or 150 cm^2 flask (Iwaki) and passaged as described in the section above, with an extra wash with complete DMEM at the end. The cell density was counted on a haemocytometer. Cells were frozen at approximately 1 x 10^6 cells/ml in cell-freezing mixture-DMSO (Sigma C6164).

2.3.4 Primary endothelial cells culture

Human Brain Microvascular Endothelial Cells (HBMEC), Human Dermal Microvascular Endothelial Cells (HDMEC), Human Pulmonary Microvascular Endothelial Cells (HPMEC) were ordered from ScienCell (Cat. No 1000, 2000 and 3000, respectively). According to the suppliers (ScienCell website) "The primary cell lines were isolated from the named tissue and frozen immediately after purification. They are characterized by an immunofluorescent method with antibodies to vWF/Factor VIII and CD31 (PECAM), by uptake of DiI-Ac-LDL and [in the case of HBMEC only] by the formation of microtubular structures *in vitro*". The primary cell lines were cultured as HBEC-5i with a few exceptions:

- Complete medium: Endothelial cell medium (ScienCell 1001), 5% foetal bovine serum (ScienCell 0025), 30μg/ml endothelial cell growth supplement (ScienCell 1052), 1U/ml Penicillin/streptomycin (ScienCell 0503).
- All flasks and Petri dishes were coated with human Fibronectin (50μg/ml) in PBS for about 20min before adding cells.
- The lifetime of these primary cell lines is limited and cells used were not older than 4 passages (~3 weeks).

2.4 P. falciparum selections and binding assays on endothelial cells

2.4.1 *P. falciparum* selection by panning on endothelial cells

Usually 2 days prior to the assay, endothelial cells were plated on 60mm tissue culture treated Petri dishes (BD 351005). Beforehand dishes had been incubated for 20min with 50 μg/ml human Fibronectin (Millipore, FC010) in PBS. This is to ensure endothelial cells detach during the washes. Ideally, the

confluency will have reached about 90% on the day of the assay. The dish is then washed twice with freshly made incomplete DMEM. Assays were carried out with parasites at pigmented trophozoite stage at 7 to 15% parasitaemia. Cultures were washed twice with incomplete medium. 1.5 ml of 2% haematocrit parasites were incubated on endothelial cells for 75min at 37°C with a resuspension halfway through (gentle rocking in the 4 directions, on a tray to ensure similar resuspension of all dishes). After incubation, dishes were washed 5 times with binding medium by aspirating medium, adding 3 ml fresh medium with a plastic Pasteur pipette, and gentle rocking. Dishes were checked under an inverted microscope with a 40X objective. If many uRBC were still visible, the dishes were washed a couple more times. Extra care was taken to keep parasites in sterile conditions. To ensure parasites were kept warm, the washes were carried out on a heated block made from a 150cm^2 flask filled with water at 37°C. After washing to remove non-adherent cells, the dish was replenished with 3ml of warm complete medium and 30µl pcv of uRBC. The dish was placed in an airtight incubating chamber, gassed for 2min and left in the incubator at 37°C overnight.

24 hours later, parasites will have reinvaded fresh RBC. These younger ring stage parasites do not cytoadhere. The content of the dish was transferred into a 15ml Falcon tube. The dish was further washed 3 to 5 times with incomplete medium and all liquid put into the same Falcon tube. The dish was checked under inverted microscope to verify no RBC were left. The tube was spun down and the pellet resuspended with complete medium and cultured as usual.

This selection process was repeated as soon as as soon as the parasites grew back to a parasitaemia of at least 7%. This could take days or weeks following the first round of selection, but occurred more rapidly in subsequent rounds. At least 4 rounds of selection were carried out before parasites were considered as adequately "selected".

2.4.2 *P.falciparum* selection on Chondroitin Sulfate A (CSA)

The day prior the assay, 4ml of 50 µg/ml CSA (Sigma) in PBS was plated on a 100mm dish (BD 351029) and incubated overnight at 4°C in a moist chamber.

The next day, the selection with parasites was performed as in section 2.4.1. Briefly, CSA was removed and the dish was blocked for 2 hours at 37°C with 2% BSA and 0.05% Na Azide in PBS. It was then rinsed with binding medium. Mature pigmented trophozoite parasites (~10% parasitaemia) were washed twice with binding medium and added to the dish at 2% haematocrit in a total volume of 4.5ml. After one hour of incubation, unbound parasites were washed away. 100 μl pcv fresh RBC was added with 4.5ml complete RPMI to the dish and left overnight in the incubating chamber at 37°C. The next day parasites were harvested from the dish and cultured as described previously.

2.5 Molecular biology techniques

2.5.1 RNA extraction

All following steps were carried out in areas cleaned with ethanol using fresh, high quality chemicals to avoid RNAase contamination. Gloves were worn at all times and only autoclaved filtered tips were used when handling RNA.

For analysis of *var* gene transcriptional profiles by reverse-transcirptase PCR, RNA was extracted from synchronised parasites harvested at late ring to early trophozoite stages at around 10% parasitaemia.

Cultures were spun down and the supernatant aspirated off. RBC were lysed with the addition of 10 times the packed cell volume of Trizol reagent (Invitrogen). The solution was thoroughly mixed before being incubated at RT for 5min, then kept in a 15ml Falcon tube at -80°C.

The tube with Trizol solution was thawed on ice. Two volumes chloroform (Sigma) were added per volume packed cells. After mixing, the tube was incubated on ice for 5min then centrifuged at 3600g for 40min at 4°C without brakes. The supernatant (aqueous layer) was carefully transferred into a fresh tube without disturbing the pellet. The same volume of icecold isopropanol (Sigma) was added and the tube was incubated at 4°C overnight. The next day, the tube was centrifuged at 3600g for 60 min at 4°C. The supernatant was discarded and the pellet was resuspended and washed with ice-cold 70% ethanol (Sigma). After another centrifugation at the same speed at 4°C for 10min, the supernatant was

completely but carefully removed using a fine Pasteur pipette. The tube was left upside down to air dry for 15 to 60min until no liquid was visible. The dried pellet was resuspended with 25µl of warm DEPC-H_2O then placed on ice. DEPC-H_20 was prepared by addition of 0.1% DEPC (diethyl pyrocarbonate) to high grade Millipore water overnight at 37˚C then autoclaved to destroy the DEPC. The quality of the RNA was assessed by spectrometric measurement of the absorbance at 260 nm and 280 nm. An A_{260}-A_{280} ratio of > 1.8 was considered indications of good quality RNA that was used for hybridizations or RT-PCR. If RNA was not used immediately, it was stored at -80°C.

2.5.2 Agarose gel electrophoresis

All PCR products were run on an agarose gel.

1.5% agarose gel was prepared using 1.5 g electrophoresis grade agarose (Invitrogen), 10 ml UltraPure 10xTBE (1M Tris, 0.9 M Boric acid and 0.01M EDTA, Invitrogen) and 90 ml distilled water. This mixture was warmed in a microwave oven until all agarose had dissolved. This liquid was then poured in a cast and left to cool down. 5µl of PCR products were loaded with 1µl of dye buffer (60 mM Tris-HCl, pH 7.5; 60 mM EDTA, pH 8.0; 0.36% Xylene Cyanol FF ; 2.4% Orange G; 30% glycerol). 100 bp DNA ladder (Invitrogen) was also loaded. Gels were run at 80 V for 45-60 min. Half-way through the running time the gel was removed and stained in 0.5 µg/ml Ethidium Bromide (EtBr) for 3 min, before replacing the gel in the tray. DNA products were visualised under UV.

For RT-PCR, “RT control” samples were a negative control thus a band in that lane would have indicated a gDNA contamination.

2.5.3 PCR product purification

PCR products and cDNA samples were purified using the QIAquick PCR Purification Kit (Qiagen 28006). 5 volumes buffer PB (contains guanidine hydrochloride and isopropanol) was added to the products in a column and spun down. All centrifugations for this protocol were at 13000rpm for 1min in a bench-top centrifuge. 750µl wash buffer PE (confidential composition) was added to the column and spun again. The flow-through was discarded and the

column spun one more time to remove any residual ethanol. Products were then collected in a fresh tube after addition of 10µl elution buffer (10 mM Tris-Cl, pH 8.5) to the column and a final spin.

2.5.4 Mycoplasma contamination detection

Parasite and cell cultures were discarded as soon as any obvious yeast/bacteria/fungi contamination was seen. Mycoplasma are not visible on Giemsa smears thus a PCR detection kit was used to regularly check for possible contamination (Minerva Biolabs VenorGeM- Mycoplasma Detection Kit). 100 µl aliquots of medium were heated at 100°C for 5 min then briefly centrifuged. In a clean PCR tube was mixed: 2µl heated conditioned medium, 15.3µl dH2O, 2.5µl primer-nucleotide mix, 2.5µl 10x buffer (100mM Tris-HCl pH 8.5, 500 nM KCl, 30 mM $MgCl_2$), 2.5µl internal control, 0.2µl hot-start Taq DNA polymerase. PCR Program: 2 min at 94°C, 40 x (30 sec at 94°C, 30s at 55ºC, 30s at 72°C), 4°C forever. A positive control DNA sample and a negative control (H_2O) were used. PCR products were run on an agarose gel as explained in section 6.4.5. A successful PCR was indicated with a 350bp product, whereas positive cultures also had an additional band at 280bp.

2.6 Statistical methods

Data manipulation was carried out using Microsoft Excel. Statistical analysis for all chapters except chapter 5 (microarray) was performed using GraphPad Prism version 5.00 for Mac OS X, GraphPad Software, San Diego California USA. T-tests were performed when the mean between two groups needed to be compared (e.g. binding inhibition assay with or without drug). Chi-squared tests were used to compare distribution of observed data compared to a null hypothesis (e.g. the frequency of CIDR1α1 domains expressed by selected parasites).

3 Chapter III: *P. falciparum* selection on HBEC-5i and investigation of the endothelial cell receptors

3.1 Abstract

Cerebral malaria is characterised by an accumulation of infected erythrocytes in the microvasculature of the brain. *P. falciparum* infected red blood cells (iRBC) have been shown to bind to a Human Brain Endothelial Cell line (HBEC-5i) *in vitro*. This provides a model for the investigation of interactions between *P. falciparum* and human brain endothelium. The main aims of this chapter were to select *P. falciparum* strains for HBEC-5i binding and investigate the endothelial cell receptor(s) for parasites on HBEC-5i mediating the binding of iRBC. The expression of 14 putative receptors was characterized by immunofluorescence assay. *P. falciparum* HB3, 3D7 and IT parasites were successfully selected on HBEC-5i. HB3 was also selected on TNF activated cells. The selection did not increase the rosetting frequency of any parasite population and the platelet-mediated clumping frequency was greatly reduced after selection. Static binding assays and binding inhibition assays with putative receptors and their specific antibodies were performed but no definite HBEC-5i receptor was identified. Although more experiments are needed, these results suggest that a surface molecule not previously associated with malaria may be responsible for the cytoadherence of iRBC. Finally, preliminary experiments show that curdlan sulfate, an anti-adhesion drug candidate, as well as other heparin-like compounds greatly inhibit binding of selected parasites to HBEC-5i. Our data support further research with these compounds as anti-adhesion drugs to treat severe malaria.

3.2 Introduction

Sequestration of infected red blood cells (iRBC) within the brain microvaculature is the hallmark of cerebral malaria. This cytoadhesion of parasites to endothelial cells is not limited to the brain however and can be found in various organs of the body (chapter 1, Table 1-3). The parasite ligands mediating the interaction are thought to be part of the PfEMP1 family (see chapter 5 and 6). As the *var* genes coding for these proteins are not found in the rodent malaria parasite genomes, the mouse model cannot address the question of the *P. falciparum* iRBC – endothelial cell interaction. The alternative model is to culture human endothelial cells *in vitro* and characterize the cytoadhesion of lab or field isolate *P. falciparum* parasites.

HBEC-5i is an immortalized cell line originally derived from adult human brain microvessels isolated from cortical fragments at autopsy (Dorovini-Zis, et al., 1991). The endothelial nature of the cells was confirmed by the expression of von Willebrand factor (vWF) antigen and by the capacity of cultured cells to bind *Ulex europaeus* type I (UEA1). These cultured cells form a tight junctional complex, just like the blood-brain barrier. This was proven by horseradish peroxidase being impeded from penetration into the inter-endothelial spaces (Dorovini-Zis, et al., 1991). Primary HBEC-5i cells in their fifth passage from isolation were transfected using a plasmid coding for SV40 large T antigen, to produce a stable and immortalized cell line (Edwin W. Ades, unpublished and (Wassmer, et al., 2006b)).

Immortalized HBEC-5i cells show characteristics typical of endothelial cells: the presence of Weibel-Palade bodies (storage granules), a high number of tight junctions, high transendothelial electrical resistance, expression of ICAM1, Integrin aVb3 and VCAM-1 (see also Table 3-6 in section 3.5.9.2 for an exhaustive list of known surface receptors) (Wassmer, et al., 2005, Wassmer, et al., 2006b, Wassmer, et al., 2006c, Xiao, et al., 1996). The blood-brain barrier origin of HBEC-5i is demonstrated by its high transendothelial electrical resistance, which is lowered after TNF activation (Wassmer, et al., 2006b). These features allow the use of HBEC-5i as a model for the blood brain barrier

including for the discovery of anti-cytoadherence drugs (Wassmer, et al., 2006a).

An important element that distinguishes brain endothelial cells (and HBEC-5i) from other microvascular endothelia is the lack of CD36 expression (Silamut, et al., 1999). The interaction of iRBC with this receptor has been widely studied as most field isolates adhere to CD36 *in vitro* (Newbold, et al., 1997). Thus, in the brain microvasculature, iRBC must adhere to a different surface receptor. ICAM1 is regularly cited as the protein responsible for this interaction as some iRBC adhere to the receptor under flow conditions (ICAM1 was reviewed in (Chakravorty and Craig, 2005)). However, field-isolate studies showed no statistically significant association between ICAM1 binding and severe malaria in Africa (Heddini, et al., 2001a, Newbold, et al., 1997, Rogerson, et al., 1999). In fact, of all 15 receptors that could potentially be involved with iRBC sequestration (see chapter 1), none has yet been associated with increased binding to isolates from cerebral malaria cases.

Although selection of *Plasmodium falciparum* on human brain microvascular endothelial cells (HBMEC) has been reported in the literature (Tripathi, et al., 2007, Xiao, et al., 1996), the parasite ligands and the endothelial receptors mediating this interaction have not been investigated. The *P. falciparum* clone 3D7 is a commonly used parasite for *in vitro* culture and its genome has been fully sequenced (Gardner, et al., 2002). However, 3D7 is poorly cytoadherent and unable to form rosettes (JA Rowe, unpublished data). Thus, in the first instance, we decided to focus our work on *P. falciparum* HB3, a clone that shows a range of adhesion phenotypes and has recently been sequenced. IT/FCR3, 3D7 and Dd2 clones were also used at a later stage. The transcriptome of these parasites before and after selection on HBEC-5i is examined in chapter 5.

3.3 Aims of this chapter

This chapter will aim:

1. To characterize the surface proteins of HBEC-5i, HDMEC and HPMEC.
2. To select *P. falciparum* HB3, 3D7, IT and Dd2 for their cytoadherence property on HBEC-5i. HB3 parasites will also be selected on HBEC-5i activated with the TNF cytokine.
3. To characterize the phenotype of these selected parasites in terms of their rosetting and platelet mediated clumping frequency.
4. To identify the HBEC-5i receptor(s) mediating the interaction with HB3 selected parasites using three approaches:
    a. Binding assays on soluble proteins and biomolecules.
    b. Binding inhibition assays with soluble proteins.
    c. Binding inhibition assays with antibodies.
5. To test the specificity of HBEC-5i-selected parasites by binding assay on HDMEC and HPMEC.
6. To test new compounds (curdland sulfate and others) for their anti-cytoadherence property.

3.4 Methods

Routine culture of *P. falciparum* parasites and endothelial cells were described in chapter 2.

3.4.1 Immunofluorescence assay (IFA) of endothelial cells

Immunofluorescence assay (IFA) involves the labelling of antigens using a first specific antibody and a secondary antibody linked to a fluorescent dye.
The list of antibodies used is shown below. All of them are against human antigens.

Antigen	Clone	Supplier/order number	Isotype	Clonality	BIA*	Reference BIA*
CD36	Smphage	Sigma: AV48129	Mo. IgM	Monoclonal	/	
CD36	FA6-152	Beckman Coulter: IM2279U	Mo. IgG1	Monoclonal	10 µg/ml	(Andrews, et al., 2005)
ICAM1 (CD54)	15.8	Alistair Craig	Mo. IgG1	Monoclonal	20 µg/ml	
ICAM1 (CD54)	15.2	AbD Serotec: MCA1615XZ	Mo. IgG1	Monoclonal	20 µg/ml	(McCormick, et al., 1997)
Heparan sulfate	T320.11	Chemicon: MAB2040	Mo. IgG1	Monoclonal	10 µg/ml	
CSA	CS56	Sigma: C8035	Mo. IgM	Monoclonal	/	
CR1 (CD35)	E11	Serotec: MCA554	Mo. IgG1	Monoclonal	/	
Blood group Ag A	?	Diagnostics Scotland	Mo. IgG1	?	/	
Blood group Ag B	?	Diagnostics Scotland	Mo. IgG1	?	/	
VCAM (CD106)	1G11	Immunotech: 1244	Mo. IgG1	Monoclonal	/	
Integrin αV (CD51)	AMF7	Immunotech: 07701855	Mo. IgG1	Monoclonal	10 µg/ml	
Integrin αV (CD51)	468255	Abcam: AB55991-100	Rabbit IgG	Polyclonal	10 µg/ml	
Fractalkine (CX3CL1)	AXV02	R&D Systems: AF365	Goat IgG	?	10 µg/ml	(Hatabu, et al., 2003a)
NCAM (CD56)	LV1378368	Chemicon: AB5032	Rabbit	Polyclonal	20 µg/ml	(Pouvelle, et al., 2007)

PECAM (CD31)	WM59	bioLegend: 303113	Mo. IgG1	Monoclonal	10 µg/ml	
E-selectin (CD62E)	P2H3	ABcam: ab24723	Mo. IgG1	Monoclonal	10 µg/ml	
P-selectin (CD62P)	AK6	Beckman Coulter IM1315	Mo. IgG1	Monoclonal	10 µg/ml	
Thrombospondin	A6.1	Invitrogen: 39-9300	Mo. IgG1	Monoclonal	/	
gC1qR/HABP1	ab37851	ABcam	Chick. IgY	Polyclonal	25 µg/ml	(Biswas, et al., 2007)
Control Mouse IgG1	MOPC-31c	Sigma	Mo. IgG1	Monoclonal	/	
Control Mouse IgM	MOPC104E	Sigma	Mo. IgM	Monoclonal	/	

*BIA = concentration used for binding inhibition assays. Reference is mentioned when that particular antibody has been shown to block cytoadherence.

Secondary antibodies	Supplier/order number	Stock concentration
Goat anti-mouse IgG	Invitrogen: A11029	2 mg/ml
Goat anti-mouse IgM	Invitrogen: A21042	2 mg/ml
Chicken anti-goat IgG	Invitrogen: A21467	2 mg/ml
Goat anti-chicken	Invitrogen: A11039	2 mg/ml
Goat anti-rabbit	Invitrogen: A11039	2 mg/ml

Concentrations of antibodies used for IFA are indicated within the results section.

Method: After passaging, endothelial cells (EC) were plated on glass coverslips (10mm diameter) contained in a 6-well plate (5 coverslips per well). Once cells reached at least 50% confluency, coverslips were rinsed twice with PBS then fixed with 2% paraformaldehyde for 15min. Coverslips were washed with PBS again three times. 40 µl drops of antibodies diluted in PBS with 1%BSA were prepared on parafilm. Using a pair of tweezers, each coverslip was put cells-side down on a drop of antibodies and incubated in a moist chamber at RT for one hour. Coverslips were then washed in a bath of PBS with 1% BSA for 10min. From here, all steps were carried out in the dark. 40 µl drops of secondary conjugated antibodies diluted in PBS with 1%BSA were prepared on parafilm. Coverslips were added cells-side down on the appropriate secondary antibody drop and incubated at RT for 30min. Coverslips were again washed in a bath of PBS with 1% BSA for 10min. They were finally mounted on a glass slide with a drop of Fluoromount (SouthernBioTech 0100-01). Slides were kept in the fridge overnight.

Coverslips were visualized using a fluorescence microscope (Leica DMLB2) with a 20x or 40x objective. All pictures were taken using a DFC300FX digital camera with the same exposure and camera settings for the negative controls and test samples (Exposure: 1.7 s).

3.4.2 *P. falciparum* selections on HBEC-5i

The methods for the selections of *P. falciparum* iRBC on HBEC-5i and other endothelial cell lines were described in chapter 2. Figure 3-1 schematizes the selection process.

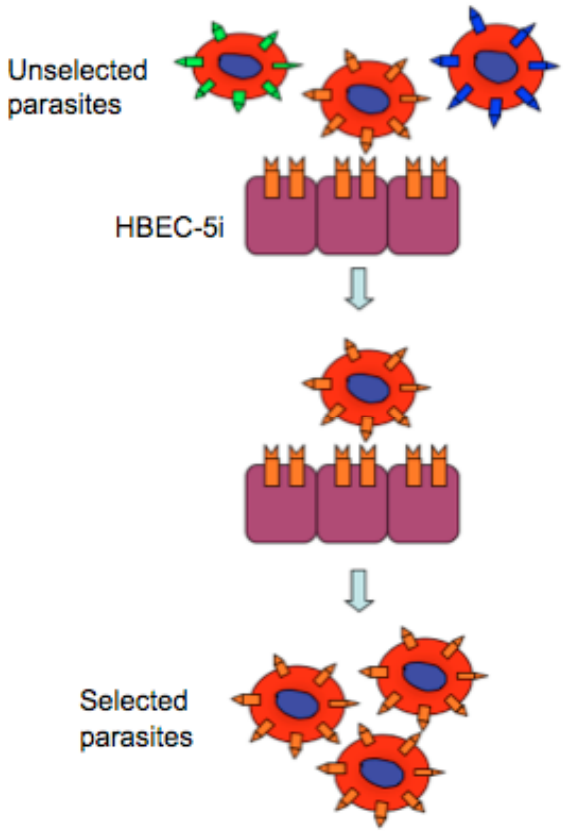


Figure 3-1. Schematic representation of the parasites selection on HBEC-5i. The unselected population of parasites is postulated to express a wide repertoire of variant surface antigens (VSA), here represented by spikes of various colours. They are selected by incubation on a layer of live human brain microvascular endothelial cells (HBEC-5i). After washing to get rid of unspecific binding, bound parasites are cultured with fresh RBC until the next cycle of selection.

3.4.3 Assessment of rosette frequency

A parasite is considered to be "rosetting" if it is bound to at least two uRBC.

A 10 µl aliquot of the parasite culture was incubated with ethidium bromide (20 µg/ml) for 10min at 37°C. The wet culture preparation was placed on a microscopic slide and visualized with bright and fluorescence light. At least 200 iRBC were counted to assess rosette frequency, which is defined as the percentage of pigmented trophozoites forming a rosette.

3.4.4 Assessment of clumping frequency

A clump consists of three or more iRBC bound together via platelets.

Platelet-rich plasma (PRP) was prepared prior to the assay by centrifugation of whole blood for 10min at 250g (Arman and Rowe, 2008). Mature pigmented-trophoizite stage parasites were first stained with 25 µg/ml of ethidium bromide for 5min at 37°C. PRP was added to a 0.5ml sample of the parasite culture at 10% haematocrit and 1% parasitaemia in binding medium in a 1.5ml tube. The aliquot is mixed on a rotating wheel for 30 or 60min at room temperature. Three wet-preparations are taken for counting. For each wet-preparation, a 10 µl aliquot of culture suspension was placed on a microscope slide, covered with a coverslip and the edges sealed with nail polish to avoid drying out. For each slide, at least 500 iRBC were counted and scored for clumping under on a fluorescence microscope (400× magnification). The propensity of parasites to clump is measured as the number of iRBC forming clumps with platelets compared to the total number of iRBC ("clumping frequency").

3.4.5 Static binding assay on purified proteins and biomolecules

The list of molecules tested in static adhesion assays with iRBC is shown below. All proteins are human unless otherwise stated.

Protein/molecule	Supplier/order number	Type	Diluted in	Concentra-tion used BA	BIA
ICAM1 (CD54)	R&D Systems: 720-IC	Recombinant	PBS	50 µg/ml	20 µg/ml
CD36	R&D Systems: 1955-CD	Recombinant	PBS	25 µg/ml	
Fractalkine/CX3CL1	R&D Systems: 365-FR	Recombinant	PBS	50 µg/ml	5 µg/ml
PECAM-1 (CD31)	R&D Systems: ADP6	Recombinant	PBS	50 µg/ml	
P-Selectin (CD62P)	R&D Systems: 137-PS	Recombinant	PBS	40 µg/ml	
E-selectin (CD62E)	R&D Systems: 724-ES	Recombinant	PBS	40 µg/ml	
VCAM-1 (CD106)	R&D Systems: 862-VC	Recombinant	PBS	50 µg/ml	
Integrin αV β1	Chemicon : CC1092	Purified	PBS	25 µg/ml	
Integrin αV β3 (CD51)	Chemicon : CC1020	Purified	PBS	25 µg/ml	15 µg/ml
Thrombospondin	Calbiochem: 605225	Purified	50mM Tris	50 µg/ml	15 µg/ml
Fibronectin	BD: 354008	Human plasma	BTC[1]	200 µg/ml	100 µg/ml
Fibronectin	Sigma: F1141	Bovine plasma	BTC[1]	200 µg/ml	
NCAM (CD56)	Chemicon: AG265	Embryonic chicken brain	PBS	10 µg/ml	10 µg/ml
Heparan Sulfate Proteoglycan	Sigma: H4777	Isolated the basement membrane of Engelbreth-Holm-Swarm mouse sarcoma	PBS	100 µg/ml	
Heparin sodium salt	Sigma: H4784	Porcine intestinal mucosa	50mM Tris	50 µg/ml	50 µg/ml
Chondroitin sulfate A (CSA)	Sigma: C8919	Bovine trachea	PBS	100 µg/ml	100 µg/ml
Hyaluronic acid	Sigma: H1504	Human umbilical cord	2mM $CaCl_2$	100 µg/ml	
gC1qR/HABP1	R&D Systems: 4529-HB	Mouse	PBS	40 µg/ml	15 µg/ml

[1]BTC = 50mM Bis-Tris, 100mM NaCl, 25 mM Calcium lactate, 1 mM $MnCl_2$, pH7.4. BIA = Binding inhibition assay.

These receptors were diluted to various concentrations as specified later in this chapter and 3µl of the solution was spotted on an untreated Petri dish (BD Falcon 351007) in a radial fashion at an equal distance from the centre. This equalizes the shearing forces generated during resuspensions and washes. For each experiment, at least 2 spots per dish and 2 dishes were used for each receptor tested. Dishes were incubated overnight at 4°C in a moist box. NCAM receptor was incubated for 2 hours at 37°C with 1U/ml Neuraminidase (Sigma N3001) to digest polysialic acid (PSA) (Pouvelle, et al., 2007). Drops of protein were aspirated off and the plate was blocked for 2 hours at 37°C with 2% BSA and 0.05% Na Azide in PBS. It was then rinsed with RPMI binding medium (RPMI-powder [Invitrogen 13018-031] containing L-Glutamine and 25mM Hepes, adjusted to pH = 7.1. Unlike RPMI-1640 for the parasite culture, this binding medium does not contain sodium bicarbonate). Assays were carried out with parasites at pigmented trophozoite stage at 5 to 10% parasitaemia. When different lines were compared, parasitaemia were matched before the assay. Cultures were washed twice with binding medium. 1.5 ml of 2% haematocrit culture in binding medium with 1% BSA was added to each dish. Dishes were incubated at 37°C for 1 hour, with resuspension every 12 minutes (gentle rocking in the 4 directions, on a tray to ensure similar resuspension of all dishes). They were then washed 5 times with binding medium by aspirating medium, adding 3 ml fresh medium with a plastic Pasteur pipette, and gentle rocking. Dishes were checked under an inverted microscope with a 40X objective. If many uRBC were still visible, the dishes were washed two more times. Adherent cells were fixed with 1% glutaraldehyde (Sigma G6257) for at least 1 hour, and stained with 5% Giemsa for 20 minutes.
Adherent cells were counted with a light microscope using the 100X objective.
At least 5 fields were counted for each spot.

3.4.6 Static binding assay on endothelial cells

Binding assays were carried to measure the amount of iRBC cytoadhering to endothelial cells under static conditions. Various antibodies, soluble molecules

and drugs were tested for their anti-cytoadherence effect. The assay is then called a "Binding Inhibition Assay" (BIA).

Method: The day prior to the assay, endothelial cells were plated on Fibronectin precoated 8-well chamber slides (BD BioCoat 354628, unspecified Fibronectin concentration) at about 10^4 cells per well. Ideally, the confluency will have reached about 30% by the next day. As the amount of binding will be counted as parasites bound per isolated endothelial cell (EC), it is important for EC not to be too confluent on the day of the assay. For each assay, at least 2 wells (replicate) per slide were used. 24 hours later, iRBC and plates were prepared and washed as described in section 3.4.5.

For binding inhibition assay (BIA) with antibodies, EC were pre-incubated with antibodies for 20min at 37°C with 2 resuspensions (see section 3.4.1 for concentrations used). For BIA with soluble proteins, serum or drugs, parasite culture suspensions were pre-incubated with proteins/serum/drugs for 20min at 37°C with 2 resuspensions (see section 3.4.5 for concentrations used). 200 μl of parasites at 2% haematocrit in fresh incomplete DMEM with 1% BSA was added per well. The slide was incubated for 75min at 37°C with a resuspension halfway through. The chamber was then removed according to manufacturer's instructions. The slide was washed in a 100mm Petri dish (BD 351029) filled with incomplete DMEM. The slide was held still using tweezers and the dish gently rocked. This step was repeated 4 times in a new dish with fresh medium. The slide was checked under inverted microscope to ensure there were no or few uRBC left. It was then fixed and stained as described in section 3.4.5.

For "re-binding" assays, after the washing step, bound parasites were detached by vigorous shaking and flushing with incomplete DMEM using a Pasteur pipette at least 10 times until most of them came detached. iRBC were placed in a 15ml tube and centrifuged at 300g for 5min. They were resuspended with 200 μl of incomplete DMEM per well, then re-incubated on endothelial cells as described above.

Parasites bound to at least 100 isolated cells (i.e. EC that do not touch any other cell) were counted by light microscopy using 40X or 100X objectives.

Endothelial cells very close to the edges of the well were not counted because background binding could sometimes be seen near the edges. Results were expressed as the average number of iRBC bound per isolated EC. Pictures were taken using a DFC300FX digital camera.

3.5 Results

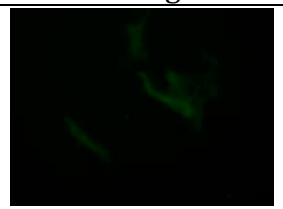
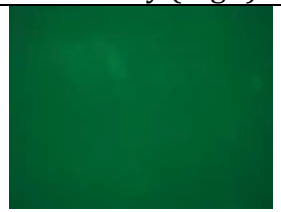
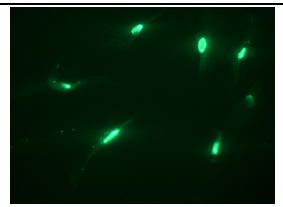
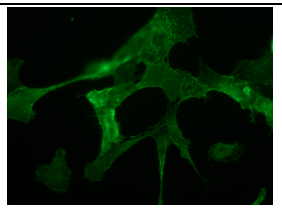
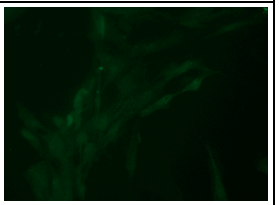
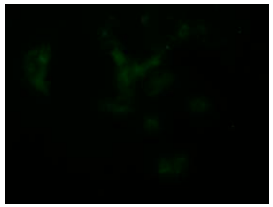
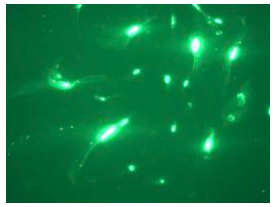
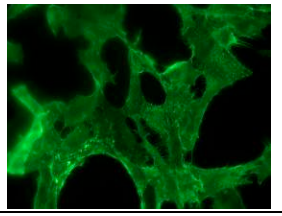
3.5.1 Receptor expression on HBEC-5i (immunofluorescence assay)

HBEC-5i proteins that could act as receptors for iRBC cytoadherence were characterised by immunofluorescence assay (IFA). Experiments were performed on "resting" as well as "activated" HBEC-5i with TNF (tumour necrosis factor, added a day prior to the assay). This cytokine is found at high level in cerebral malaria patients and has been show to induce the expression of many surface proteins (reviewed in (Chakravorty, et al., 2008)). In the first instance, antibodies against molecules thought to be involved in *P. falciparum* sequestration were tested (Rowe, et al., 2009a). A nonspecific isotype matched antibody was used as a control (e.g. IFA with IgG1 mouse VCAM antibody was performed in parallel with a nonspecific mouse IgG1 antibody as a negative control). A second antibody linked to a fluorescent dye and specific to the isotype of the first antibody was then used to visualize the protein expression. The amount of fluorescent signal was estimated by eye and given a score from "-" (no signal) to "++++" (very bright signal) (Table 3-1). As a second negative control, the secondary antibody was incubated on its own on HBEC-5i. The absence or very limited amount of signal indicates there is no unspecific binding of the secondary antibody on HBEC-5i. Representative pictures are shown in Figure 3-2. All pictures were taken with the same exposure and camera settings for the negative controls and test samples.

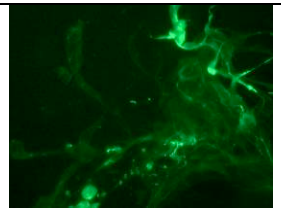
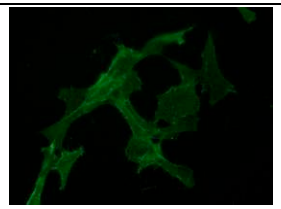
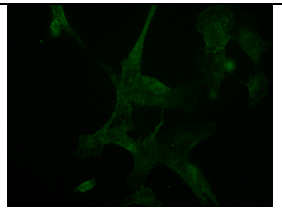
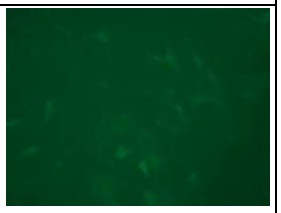
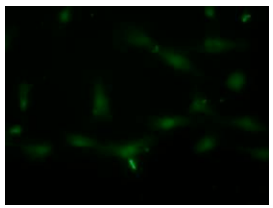
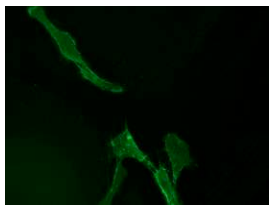
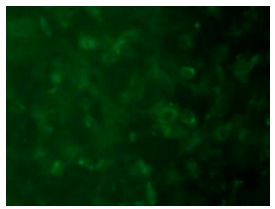
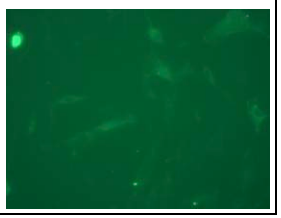
1st Antibody	1st Ab Isotype	Concen-tration	2nd Ab	Dilution	Fluorescence score	
					HBEC-5i	TNF-HBEC-5i
Control Mo. IgG1	Mo. IgG1	20µg/ml	Go α-Mo IgG	1/800	-	-
Control Mo. IgM	Mo. IgM	20µg/ml	Go α-Mo IgM	1/800	-	+/-
Control IgY Ab	Chick. IgY	20µg/ml	α-IgY	1/10000	+/-	-
Control: 2nd Ab only	/	/	Go α-Mo IgG	1/800	+/-	-
Control: 2nd Ab only	/	/	Go α-Mo IgM	1/800	+/-	-
Control: 2nd Ab only	/	/	Go α-Rab.	1/2000	+/-	-
Control: 2nd Ab only	/	/	α-IgY	1/5000	+/-	-
Control: 2nd Ab only	/	/	α-Go.	1/2000	+/-	NP
ICAM1 15.2	Mo. IgG1	20µg/ml	Go α-Mo IgG	1/2000	++	++++
Integrin AMF7	Mo. IgG1	20µg/ml	Go α-Mo IgG	1/2000	++	+++
Integrin 468255	Rab. IgG	20µg/ml	Go α-Rab.	1/2000	++	NP
VCAM	Mo. IgG1	10µg/ml	Go α-Mo IgG	1/800	+/-	++
Thrombospondin	Mo. IgG1	20µg/ml	Go α-Mo IgG	1/2000	++	+
CR1	Mo. IgG1	10µg/ml	Go α-Mo IgG	1/800	+/-	+/-
CD36 Smphage	Mo. IgM	10µg/ml	Go α-IgM	1/800	-	+/-
CD36 FA6-152	Mo. IgG1	20µg/ml	Go α-Mo IgG	1/2000	+/-	NP
Fractalkine	Go. IgG	10µg/ml	α-Go IgG	1/2000	++++	NP
gC1qR	Chick. IgY	20µg/ml	α-IgY	1/10000	+/-	+/-
NCAM	Rabbit	20µg/ml	Go α-Rab.	1/2000	+++	NP
PECAM	Mo. IgG1	10µg/ml	Go α-Mo IgG	1/4000	+	NP
P-selectin	Mo. IgG1	10µg/ml	Go α-Mo IgG	1/4000	+/-	NP
E-selectin	Mo. IgG1	10µg/ml	Go α-Mo IgG	1/4000	+/-	NP
Heparan Sulfate	Mo. IgG1	10µg/ml	Go α-Mo IgG	1/800	+++*	+++*
CSA	Mo. IgM	1/300	Go α-Mo IgM	1/800	+++	+++
Blood group A Ag	IgG	1/100	Go α-Mo IgG	1/800	-	NP
Blood group B Ag	IgG	1/100	Go α-Mo IgG	1/800	-	NP

Table 3-1. Immunofluorescence assay (IFA) on HBEC-5i. The amount of fluorescent signal was estimated by eye and given a score from "-" (no signal) to "++++" (very bright signal). Bolded receptor names are considered to be positive (note that VCAM is only expressed on TNF activated cells). If the stock concentration of the first antibody is unknown, the dilution used is indicated. If different dilutions of secondary antibody were used, the "secondary antibody only" control was always the highest concentration. All IFA were repeated twice independently and each experiment is done in duplicate. See Figure 3-2 for representative pictures of these IFA. *The anti-heparan sulfate antibody seem to label the nucleus rather than the surface of the cells. Abbreviations used: TNF-HBEC-5i = HBEC-5i cells activated with TNF a day prior the assay; Ab = Antibody; Ag = antigen; Mo = mouse; Go = goat; Rab = rabbit ; chick = chicken; α = anti; NP = experiment not performed or result discarded due to technical issue.

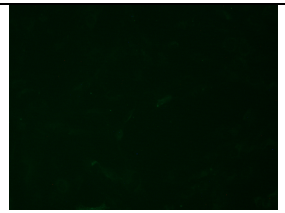
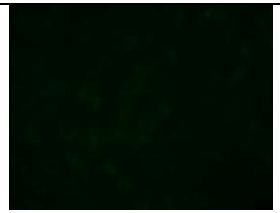
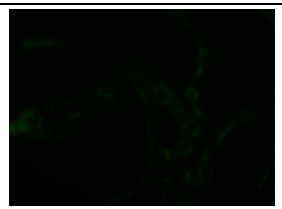
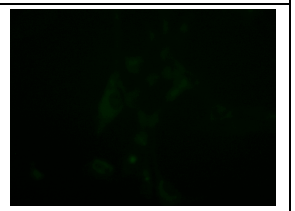
A

Mouse IgG1	**Control** Mouse IgG1	**Control** 2nd Ab only (αIgG)	**Heparan Sulfate**	**ICAM1** 15.2	**CD36** FA6-152
HBEC-5i					
TNF activated HBEC-5i					NP

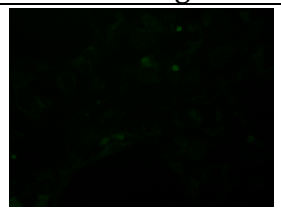
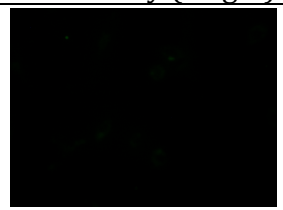
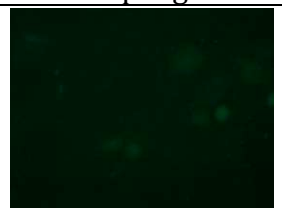
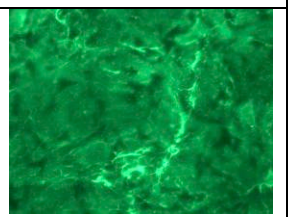
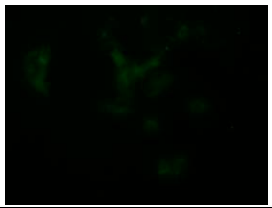
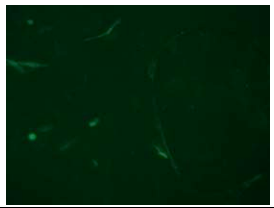
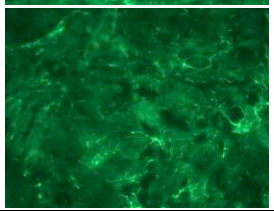
A (continued)

Mouse IgG1	**Thrombospondin**	**Integrin αV** AMF7	**VCAM**	**PECAM**	**CR1**
HBEC-5i					
TNF activated HBEC-5i				NP	

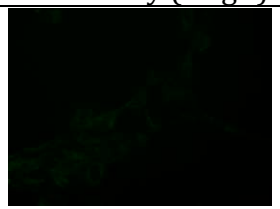
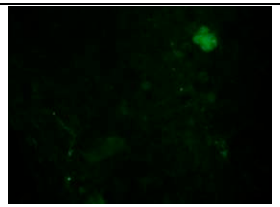
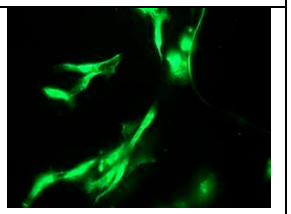
A
(continued)

Mouse IgG1	**Blood group A Ag**	**Blood group B Ag**	**P-selectin**	**E-selectin**
HBEC-5i				
TNF activated HBEC-5i	NP	NP	NP	NP

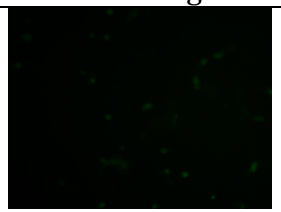
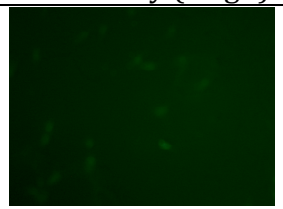
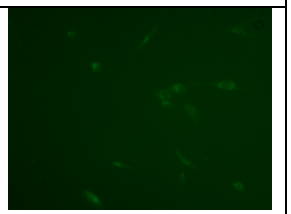
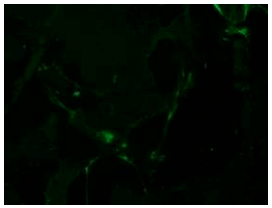
B

Mouse IgM	**Control** Mouse IgM	**Control** 2nd Ab only (α-IgM)	**CD36** Smphage	**CSA**
HBEC-5i				
TNF activated HBEC-5i				

C

Rabbit IgG	**Control** 2nd Ab only (α-IgG)	**Integrin αV** 468255	**NCAM**
HBEC-5i			
TNF activated HBEC-5i		NP	NP

D

Chicken IgY	**Control** Chicken IgY	**Control** 2nd Ab only (α-IgY)	**gC1qR**
HBEC-5i			
TNF activated HBEC-5i			

E

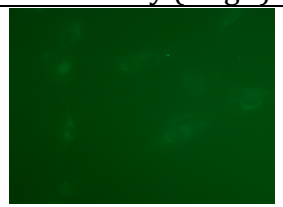
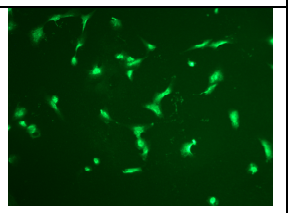
Goat IgG	**Control** 2nd Ab only (α-IgG)	**Fractalkine**
HBEC-5i		
TNF activated HBEC-5i	NP	NP

Figure 3-2. Immunofluorescence assay (IFA) on HBEC-5i. Antibodies are grouped together according to their isotype. The first 2 columns of each group are controls: a non-specific antibody of the same isotype, and the secondary antibody only. All pictures were taken at 200X magnification, except for NCAM, PECAM, Heparan Sulfate, ICAM1, Integrin αV and Thrombospondin at 400X magnification.

Note that a goat IgG and a rabbit IgG isotypes controls are missing for Fractalkine and NCAM antibodies, respectively. Ab = Antibody; Ag = Antigen; NP = experiment not performed or result discarded due to technical issue. All IFA were repeated twice independently and each experiment is done in duplicate. See Table 3-1 for fluorescence score and other information.

ICAM1, a receptor well-studied for its implication in malaria (Chakravorty and Craig, 2005), is also expressed by HBEC-5i and is clearly upregulated after TNF activation. The cytokine also led to the expression of VCAM, which showed no signal on resting cells (Figure 3-2A). This had been previously reported (Wassmer, et al., 2006a, Wassmer, et al., 2006b, Xiao, et al., 1996). Other molecules showing positive signal are Chondroitin Sulfate A (CSA), thrombospondin, Integrin αV (with the AMF7 monoclonal antibody only, the 468255 polyclonal antibody did not show any signal), NCAM and Fractalkine. PECAM seems only weakly expressed on HBEC-5i, as previously reported (Wassmer, et al., 2006b). The strong signal seen with the anti-heparan sulfate antibody seems to indicate the nucleus rather than the surface (Figure 3-2A). Repeating the experiment on live cells instead of fixed with paraformaldehyde may settle the issue.

As previously reported, HBEC-5i does not express CD36 (Wassmer, et al., 2005, Wassmer, et al., 2006b, Xiao, et al., 1996), a receptor binding to most parasite isolates (reviewed in (Serghides, et al., 2003)). This lack of expression is in line with what has been observed in post-mortem studies since CD36 is scarcely detected in the brain microvasculature (Silamut, et al., 1999). Expression of P-selectin and E-selectin was also negative. The signal with the anti-gC1qR antibody is very faint, probably negative. Neither anti blood group antigens antibodies showed any immunofluorescence, however a positive control to show that these antibodies are effective on fixed cells was not performed. This also applies to the Complement Receptor 1 (CR1) antibody. Note that this antibody had been shown to bind to fixed or unfixed cells before (Paccaud, et al., 1988).

All receptors identified on HBEC-5i by IFA are in agreement with the literature (see Table 3-6 in section 3.5.8).

3.5.2 *P. falciparum* selections on HBEC-5i

To study the molecular interaction between HBEC-5i receptor(s) and *P. falciparum* ligand(s), parasites were selected on HBEC-5i cells to enrich the number of binding parasites in the population.

Unselected parasites of all tested strains (HB3, Dd2, 3D7 or IT/FCR3) showed only a very limited amount of binding to HBEC-5i (see Figure 3-3 as an example with HB3). With HB3 and IT strains, a high level of binding was reached after 4 rounds of selection on HBEC5i (Figure 3-3 and Table 3-2) and they have been renamed "HB3-HBEC1" and "IT-HBEC", respectively. An extra round of selection was performed during the synchronisation for microarray purposes (chapter 5). With 3D7 however, it took 6 rounds for parasites to become selected ("3D7-HBEC"). With Dd2, even after 5 rounds of selection, there was no more binding than with unselected Dd2. As all these strains were selected in parallel, a technical mistake with the Dd2 selection process is unlikely. Furthermore, Dd2 are mostly knobless parasites, which impedes cytoadhesion (Herricks, et al., 2009, Nakamura, et al., 1992). Thus Dd2 parasites were not used further.

Although the binding ability was not specifically recorded over time, it was clear that parasites were starting to lose their cytoadherence phenotype after a few weeks of culturing without any selection. As most experiments were performed with the HB3 strain, the selected line was regularly reselected on HBEC-5i (up to 9 rounds). It will be referred as "HB3-HBEC" in this chapter.

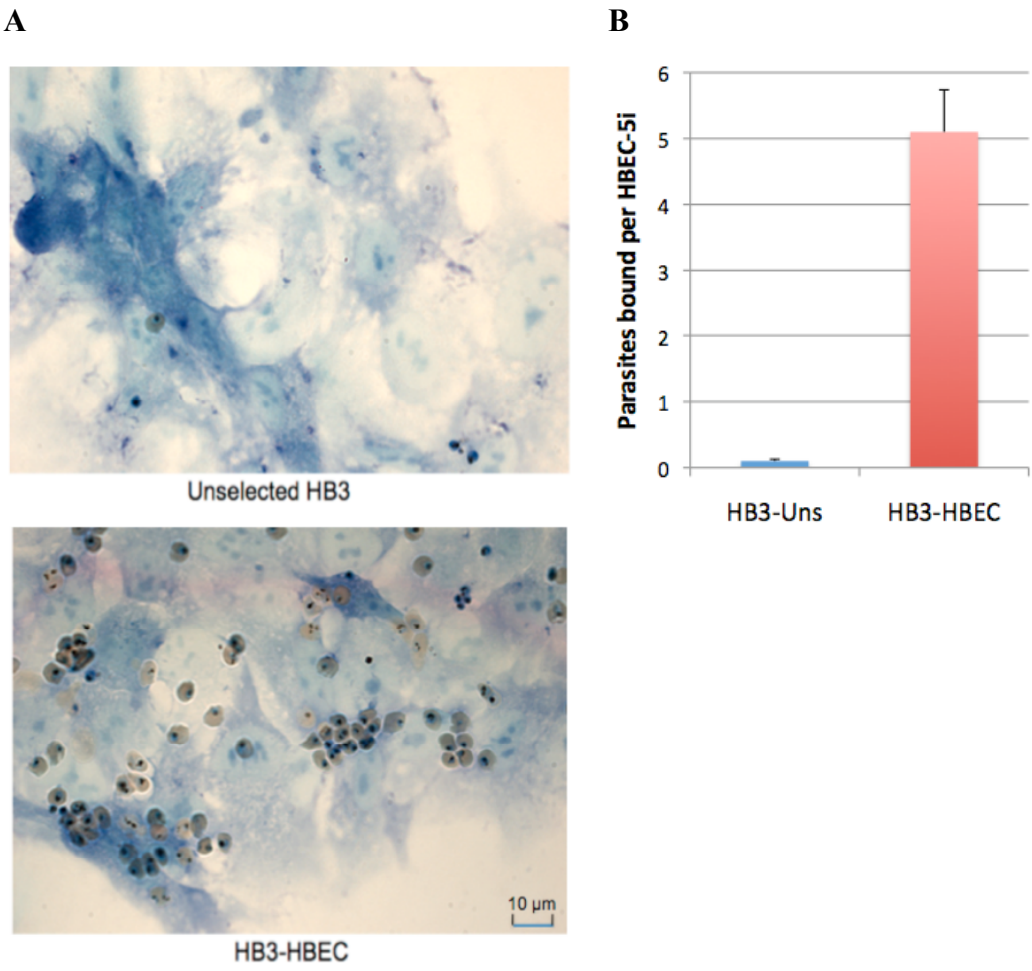


Figure 3-3. Typical example of parasites binding to HBEC-5i. (A) The blue layer is HBEC-5i fixed with glutaraldehyde and stained with Giemsa, visualized under microscope at 1000X magnification. Pictures were taken after uRBC and unbound iRBC were washed away. The upper panel shows a single *P. falciparum* HB3 (unselected) parasite bound to HBEC-5i. In the lower panel the HB3-HBEC parasites had been selected for 5 rounds. (B) Data represents the average of two independent experiments, each performed in duplicate. The number of parasites bound per endothelial cell was counted.

Unselected parasite lines (control)	Rounds of selections	HBEC-5i selected parasite lines
HB3-Uns1	5	HB3-HBEC1
HB3-Uns2	5	HB3-HBEC2
HB3-Uns2	6	HB3-HBEC-TNF*
HB3-Uns3	5	HB3-HBEC-Serum
Dd2-Uns	*5*	*no binding*
3D7-Uns	7	3D7-HBEC
IT-Uns	6	IT-HBEC

Table 3-2. Summary of all HBEC-5i selected lines. * HB3-HBEC-TNF is HB3 parasite population selected on HBEC-5i activated with TNF the day prior each assay. HB3 parasites selected on HBEC-5i in the presence of 10% pooled human serum. The Dd2 strain did not increase its binding ability even after 5 rounds of selection on HBEC-5i.

The selection with HB3 was repeated a second time, starting again from unselected HB3. This replicate will be used in chapter 5 (microarray analysis) to verify whether two independent selections of the same strain result in the upregulation of the same genes. The second selected HB3 strain is called "HB3-HBEC2" (Table 3-2).

HB3 was also selected on HBEC-5i previously activated with 50µg/ml TNF. As shown in section 3.5.2, this cytokine induces the expression of many surface receptors, including known *P. falciparum* cytoadherence receptors such as ICAM1 (Wassmer, et al., 2005). Thus, it was hypothesized that different genes might be upregulated after selection on TNF activated HBEC-5i compared to resting HBEC-5i. This selected strain is now referred as "HB3-HBEC-TNF".

3.5.3 Validation of the selection on HBEC-5i

3.5.3.1 HB3 selection on HBEC-5i occurs in the presence of human serum.

In this work, all parasite selections on endothelial cells were performed in serum-free medium. Many studies performed *P.falciparum* binding assays (Berendt, et al., 1989, Marsh, et al., 1988, Siano, et al., 1997, Traore, et al., 2000, Wassmer, et al., 2005, Wassmer, et al., 2006b) or selection (Tripathi, et al.,

2007) on endothelial cells without serum during the incubation. The addition of human serum is however more physiologically relevant and has been performed in this way by other groups (Sharling, 2004, Sharling, et al., 2004, Xiao, et al., 1996). Furthermore, it was later noticed that human serum could to some extent inhibit the binding of selected iRBC on HBEC-5i (Figure 3-4). Thus it was important to determine whether parasites could be selected on HBEC-5i in the presence of human serum.

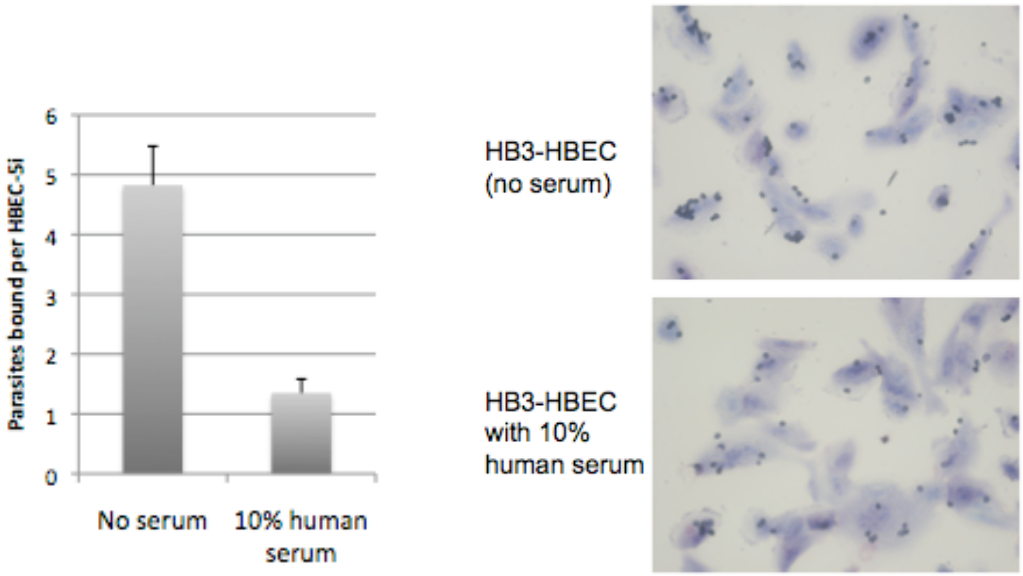


Figure 3-4. HB3-HBEC selected parasites show reduced binding to HBEC-5i when human serum is added. The pooled human serum was added to HBEC-5i 15min prior to HB3-HBEC for incubation. 10% is the concentration that is normally used for culturing parasites. Data shown is the average of three independent experiments, each performed in duplicate. Pictures were taken at 400X magnification.

HB3 parasites were selected in the exact same way on HBEC-5i (section 3.4.2) apart from the addition of 10% human pooled serum during the incubation of each selection round. After 4 rounds of selection, HB3-HBEC-Serum parasites bound well to HBEC-5i in the presence of serum (Table 3-2). Therefore human serum does not prevent the selection of HB3 iRBC on endothelial cells. The *var* gene transcription pattern of HB3-HBEC-Serum parasites is characterized in chapter 6.

3.5.3.2 HB3-HBEC also cytoadheres to primary brain endothelial cells

HBEC-5i was isolated from the human brain microvasculature (Dorovini-Zis, et al., 1991) and immortalized with SV40 large T antigen at passage 5 (Edwin W. Ades, unpublished). Discrepancies in phenotypes and cell surface proteins between primary and immortalized cell lines has been reported. For example, the first extraction and culture of human dermal microvascular endothelial cells (HDMEC) showed von Willebrand factor (vWF) and CD36 expression (Swerlick, et al., 1992a). The initial immortalization of the cell line did not seem to affect this expression (Ades, et al., 1992). However, a later analysis of the immortalized HDMEC found a lack of vWF and CD36 expression compared to the primary cell line (Xu, et al., 1994). Therefore, in order to make our brain endothelial cells model as physiologically relevant as possible, it was important to test whether HBEC-5i selected parasites also bind to primary human brain microvascular endothelial cells (HBMEC, commercially available from ScienCell).

HB3-HBEC parasites, selected on immortalized HBEC-5i, were tested for their cytoadherence to HBMEC (primary cells) by binding assay. Parasites were incubated on endothelial cells, unbound parasites were washed away and the slides were visualised by microscopy after fixation (Figure 3-5). HB3-HBEC, but not HB3-Uns, showed good binding to both HBEC-5i and the primary HBMEC line. The number of parasites binding to HBEC-5i and HBMEC cannot be directly compared as HBEC tend to be bigger than HBEC-5i (Figure 3-5), hence more parasites are likely to cytoadhere. However it can safely be concluded that the selection of HB3 parasites to HBEC-5i led to a population also cytoadhering to primary HBMEC.

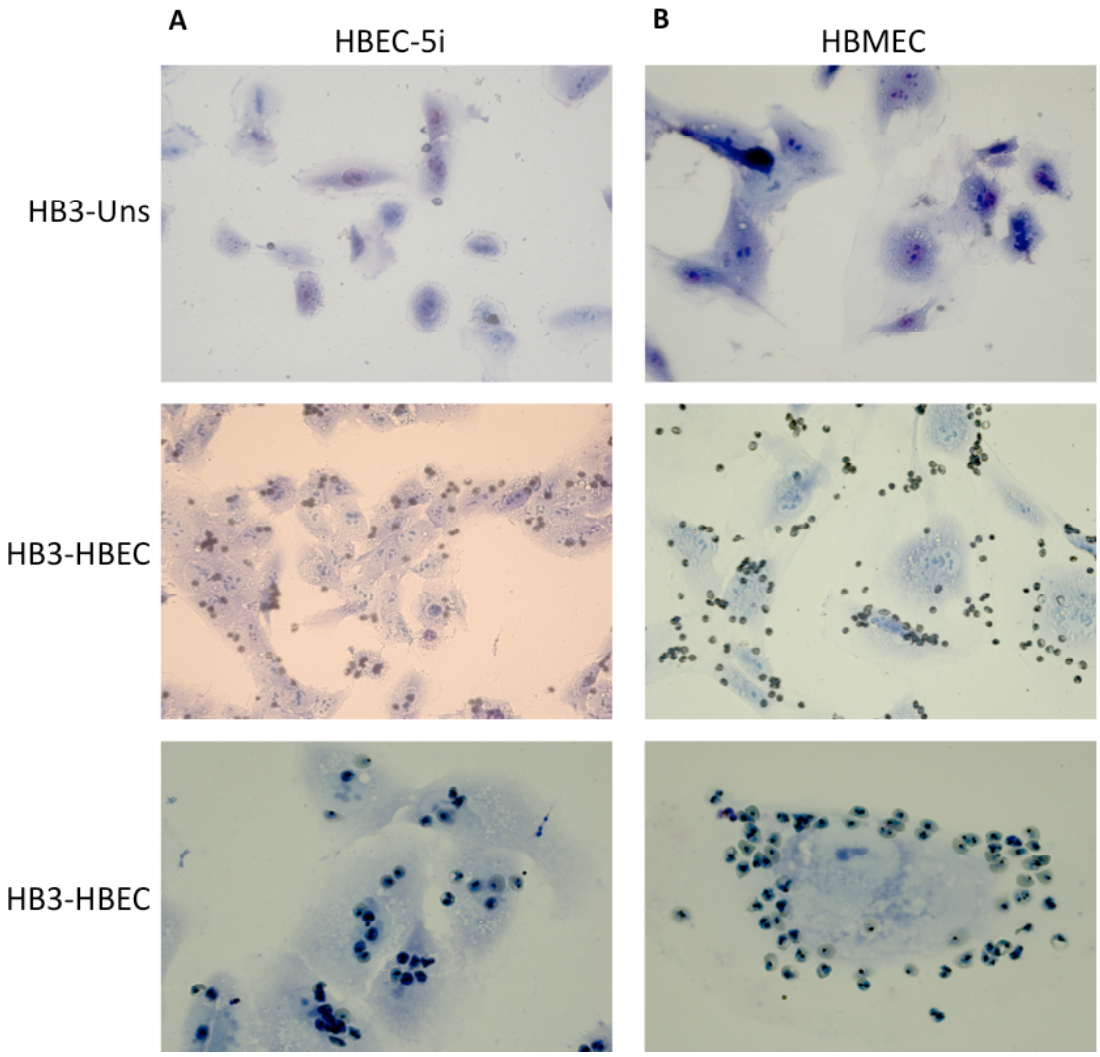


Figure 3-5. HB3-HBEC parasites adhere to HBEC-5i (A) and HBMEC (B). Upper and middle panels were taken at 400X and lower panels at 1000X magnification.

3.5.4 Phenotype characterization of HBEC-selected parasites

3.5.4.1 Selection on HBEC-5i does not increase rosetting frequency

Infected red blood cells (iRBC) can attach to two or more uninfected RBC (uRBC), a phenomenon called rosetting (reviewed in (Rowe, et al., 2009a)). Interestingly, rosette formation has been repeatedly associated with severe malaria in African children (Carlson, et al., 1990, Doumbo, et al., 2009, Rowe, et al., 1995), including in cerebral malaria cases (Kyriacou, et al., 2006). It was thus tested whether the selection of parasites on HBEC-5i would modify the rosette frequency of these parasites.

A wet-prep was prepared and at least 200 iRBC were counted for each strain. Very few rosettes were found, both in unselected and selected populations, in any strain (Table 3-3).

Unselected parasites	Rosetting frequency	HBEC-selected parasites	Rosetting frequency
HB3-Uns	<1%	HB3-HBEC	<1%
HB3-Uns2	<1%	HB3-HBEC-TNF	<1%
3D7-Uns	<1%	3D7-HBEC	<1%
IT-Uns	<1%	IT-HBEC	<1%

Table 3-3. Rosette frequency of unselected and HBEC-selected parasites. The rosetting frequency is expressed as the percentage of rosetting parasite (i.e. at least two uRBC bound to an iRBC) in the total population of iRBC. The experiment was performed twice for HB3-Uns and HB3-HBEC, once for all other strains. A rosetting count with a rosetting selected strain was also performed in parallel as a positive control.

Reciprocally, rosetting parasites were tested for their adhesion to HBEC-5i. Three strains (R29+, PAR+, TM284+) selected for their high rosetting frequency were assessed by binding assay on HBEC-5i. Virtually no parasites were bound to the endothelial cells (Figure 3-6). It is possible however that the uRBC surrounding the rosetting parasites prevented the adhesion to the endothelial cells.

Altogether, the lack of rosettes in the HBEC-selected populations and the lack of binding of rosetting parasites on HBEC-5i tend to indicate that cytoadhesion to uRBC (rosettes) and HBEC-5i are two separate mechanisms.

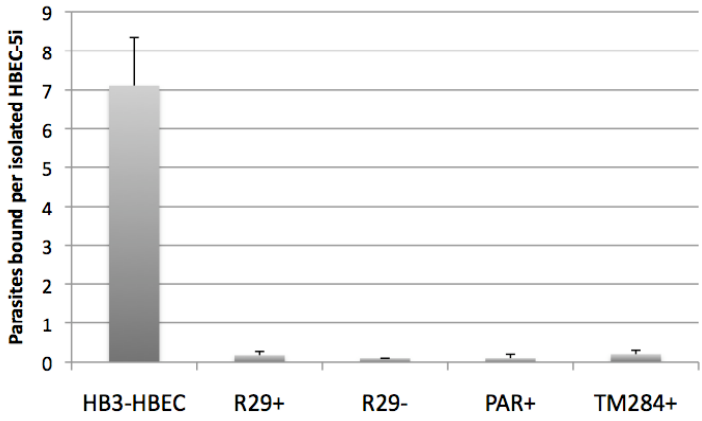


Figure 3-6. Rosetting parasites do not bind to HBEC-5i. R29+, PAR+ and TM284+ are parasites selected for rosetting, at a frequency of 74%, 60% and 67%, respectively, on the day of the assay. R29- is a control selected against rosetting (frequency < 2%). Data is the average of 3 to 5 wells (replicates within the same experiment). Rosetting parasites were cultured by Ahmed Raza and Ashfaq Ghumra.

3.5.4.2 Selection on HBEC-5i significantly reduces platelet-mediated clumping frequency

Another cytoadherence ability of *P. falciparum* is "platelet-mediated clumping" where iRBC bind to platelets to form aggregates that can reach hundreds of iRBC and platelets *in vitro* (Arman and Rowe, 2008). The propensity of parasites to clump is measured as the number of iRBC forming clumps with platelets compared to the total number of iRBC ("clumping frequency"). Parasites can also be selected for or against clumping (Monica Arman, unpublished data).

Interestingly, it has been shown that platelets may act as a bridge between endothelial cells and parasites (Wassmer, et al., 2004). Some of the proteins found at the surface of endothelial cells (CD36, gC1qR and P-selectin) are also thought to act as receptors on platelets (Rowe, et al., 2009a). Therefore we investigated whether the selection of parasites on HBEC-5i would influence their platelet-mediated clumping frequency.

Unselected and selected HB3, 3D7 and IT strains were assayed for the clumping ability with platelets (Figure 3-7). In all cases, the clumping frequency was greatly reduced with the HBEC-selected lines. Clearly, the selection of

parasites on HBEC-5i results in much lower platelet-mediated clumping frequency of these parasites.

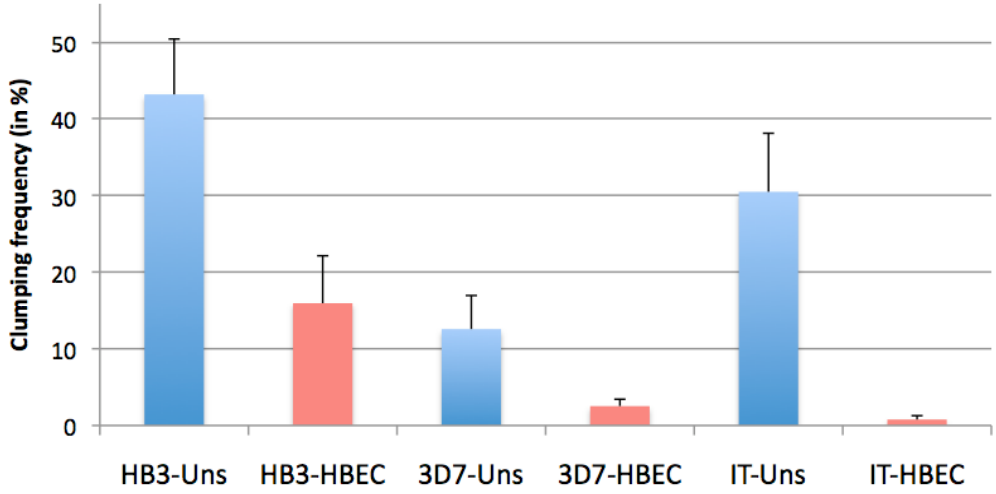


Figure 3-7. Platelet-mediated clumping frequency in unselected and HBEC-selected IT and 3D7 strains. The percentage indicates the proportion of iRBC binding to platelets. Data is the average of three separate experiments, each of them counted after 30min and 60min incubation with platelets. A positive control with a clumping selected strain was performed in parallel with each assay. Monica Arman carried out experiments of this figure. All differences in clumping frequency between unselected and HBEC-selected strains are statistically significant (paired t-test, $P < 0.01$).

Conversely, it was hypothesized that parasites selected for clumping would not increase their binding frequency to endothelial cells. A binding assay was performed on HBEC-5i and also on HDMEC with HB3 parasites selected for binding to platelets ("HB3 Clumping") and selected against platelet binding ("HB3 No clumping"). On both types of endothelial cells, the HB3 Clumping population cytoadhered to the same extent as the "HB3 No clumping" population and HB3-Uns (Figure 3-8).

Altogether, these results strongly suggest that HBEC-5i cytoadherence and adhesion to platelets are two separate phenomenon probably involving different receptors and ligands.

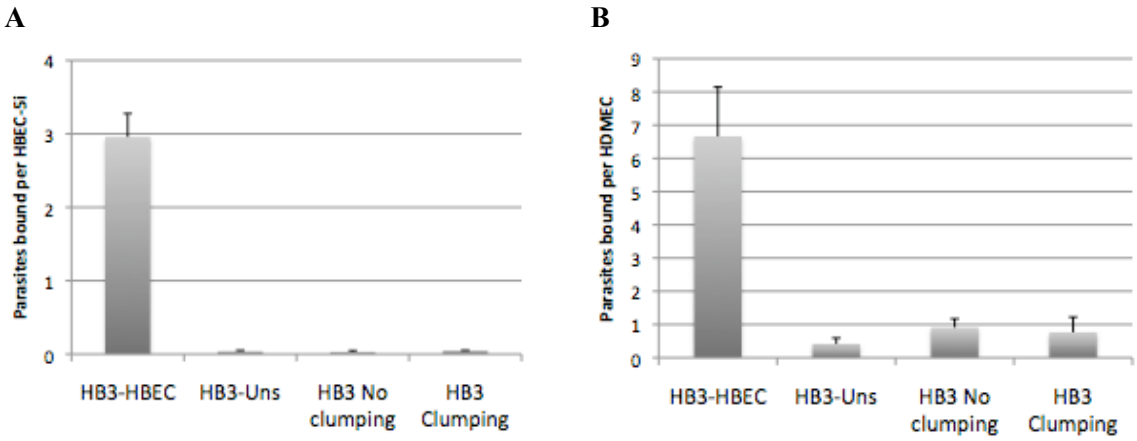


Figure 3-8. Cytoadhesion on HBEC-5i (A) and HDMEC (B) of HB3 parasites selected for platelet-mediated clumping. Monica Arman selected HB3 parasites for and against binding to platelets ("HB3 clumping" and "HB3 No clumping", respectively). On the day of the binding assay on HBEC-5i/HDMEC, "HB3 No clumping" showed a clumping frequency of 1% and "HB3 Clumping" of 59%. Note that, as for all binding assays, no platelets were added. Data is the average of one experiment performed in duplicate.

3.5.5 HBEC-selected parasites do not show any high increase in binding to any known receptor (static binding assays)

In order to further characterize the phenotype of HBEC-selected parasites, static binding assays on 15 putative receptors as described in section 3.4.5 were performed. A higher amount of bound HBEC-selected parasites to a particular receptor compared to the unselected population would indicate that the receptor was potentially involved in the HBEC-5i-parasite interaction.

HB3 unselected parasites only bound to recombinant human CD36 and not to any other receptors tested (Figure 3-9). HB3-HBEC parasites also showed high level binding to CD36 (Figure 3-9). Although the amount of bound parasites is almost identical with the HB3-Uns and HB3-HBEC populations, this does not necessarily mean that the percentage of CD36-binding parasites in the two populations is the same. Indeed, the protocol uses a saturating amount of iRBC in the Petri dish. Thus, even if the HBEC-5i binding parasites were unable to bind to CD36, due to heterogeneity in the

culture, there could still be some CD36-binding parasites in the HB3-HBEC population.

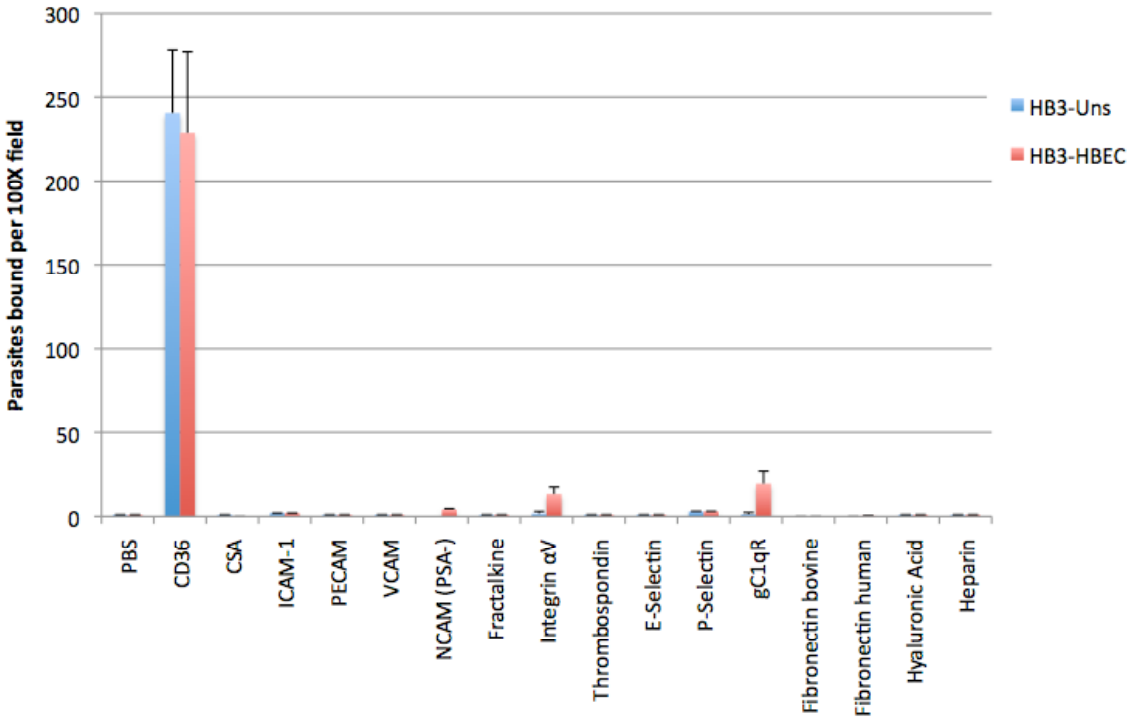


Figure 3-9. Adhesion of HBEC-5i selected parasites on 15 soluble receptors. For all binding assays, parasites were incubated for 1 hour on soluble receptors. After washing unbound parasites and fixation, parasites bound to each receptor were counted. PBS was always used as a negative control, CD36 as a positive control. The binding assay shown is the average of three independent experiments for CD36, CSA, Integrin αV, ICAM1 and gC1qR, or a single experiment performed in quadruplicates for all other receptors (2 dishes with 2 receptor spots per dish). Concentrations used are indicated in section 3.4.5.

The only change in cytoadhesion between HB3 unselected and selected parasites was a slight increase in binding to gC1qR/HABP1 and Integrin αV (Figure 3-9). This was examined further by repeating the binding assay to gC1qR and Integrin αV three times (Figure 3-10 and Figure 3-11). A consistent and significant binding with the HB3-HBEC parasites was observed. A preliminary experiment was performed with IT-HBEC and the same trend was seen: HBEC-5i selected IT parasites bind significantly better to gC1qR and Intgerin αV than IT-Uns (Figure 3-12). However, the amount of parasites bound

to these two receptors is still relatively low compared to CD36 binding (Figure 3-9). Note that gC1qR is a mouse recombinant protein with a sequence 90% identical to the human protein. It is possible that parasites would bind better to the human protein.

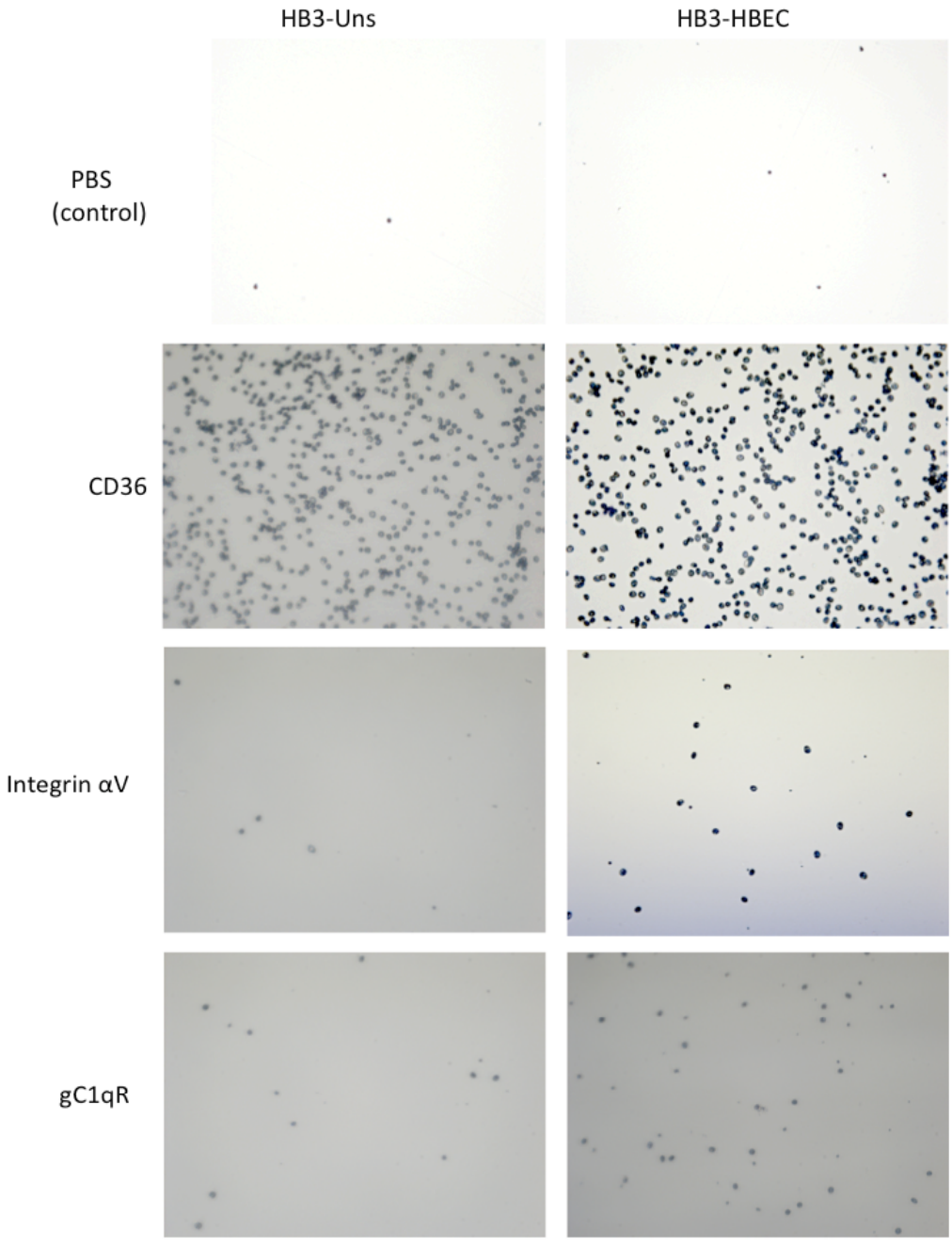


Figure 3-10. HB3-Uns and HB3-HBEC binding to CD36, Integrin αV and gC1qR. Pictures were taken at 400X magnification.

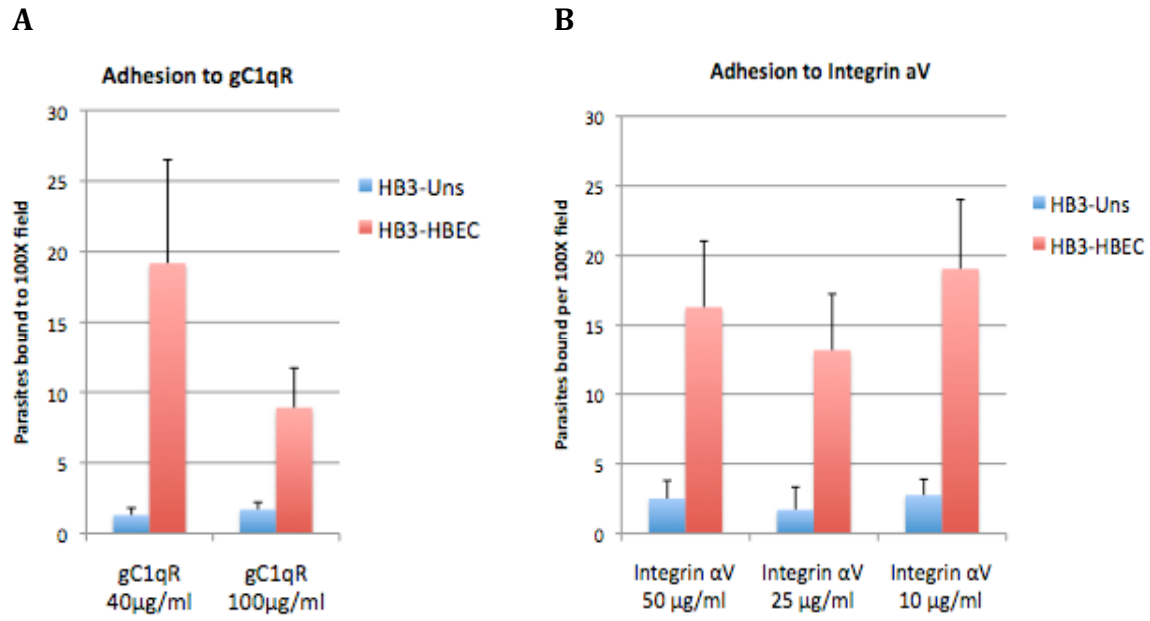


Figure 3-11. HB3-Uns and HB3-HBEC adhesion to gC1qR and Integrin αV. Data for gC1qR 40ug/ml and Integrin αV 25ug/ml is the average of three independent experiments, other concentrations used is the average of a single experiment performed in quadruplicates.

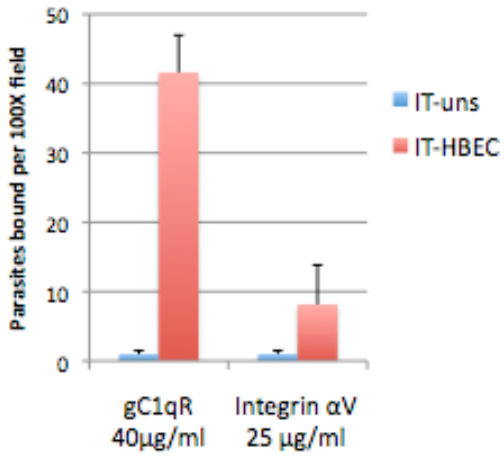


Figure 3-12. Adhesion of IT-Uns and IT-HBEC on gC1qR and Integrin αV. Data is a single experiment performed in quadruplicates.

Five receptors were not from human but from animal origin (gC1qR, CSA, Heparin, bovine Fibronection and NCAM). Fibronectin extracted from bovine was used as it was the protein tested by the first and only publication on the

subject (Eda and Sherman, 2004). Human Fibronectin was also tested, as it is obviously more relevant. No binding of parasites was seen on either of them (Figure 3-9). Prior to the binding assay on the NCAM protein, the polysialic acid (PSA) moiety was digested by neuraminidase as the PSA- form is the one predominating in post-natal tissues (Pouvelle, et al., 2007). Note that this NCAM is of embryonic chicken brain origin, as used by (Pouvelle, et al., 2007), thus more binding might be seen with the human protein (not commercially available).

One problem with this binding assay approach is the lack of a positive control for most receptors. For example, as the majority of receptors are poorly characterised in terms of their interactions with *P. falciparum*, the conditions used (pH, concentration, buffer…) for the binding assays may not be optimal. Also many receptors were only tested once. Ideally, for all receptors a positive control should be carried out to prove that these soluble receptors are indeed able to attach to *P. falciparum* iRBC. This was done for CSA (Figure 3-13A) and ICAM1 (Figure 3-13B). HB3 parasites were panned on CSA for 5 five rounds to obtain a population of high affinity to CSA (called HB3-CSA, see chapter 2). Avril and colleagues used these HB3-CSA parasites to show that, as expected, they express the *var2csa* genes (2 copies in the HB3 genome) (Avril, et al., 2008). HB3-CSA parasites do bind to CSA while HB3-HBEC or IT-HBEC do not (Figure 3-13A). A4 is an IT/FCR3 derived strain selected for ICAM1 binding (provided by Chris Newbold group). Here it was used as a positive control for cytoadhesion to soluble ICAM1 (Figure 3-13B). HB3-HBEC showed almost no binding to this receptor. Thus the selection of parasites on HBEC-5i did not lead to an increase of binding on CSA or ICAM1.

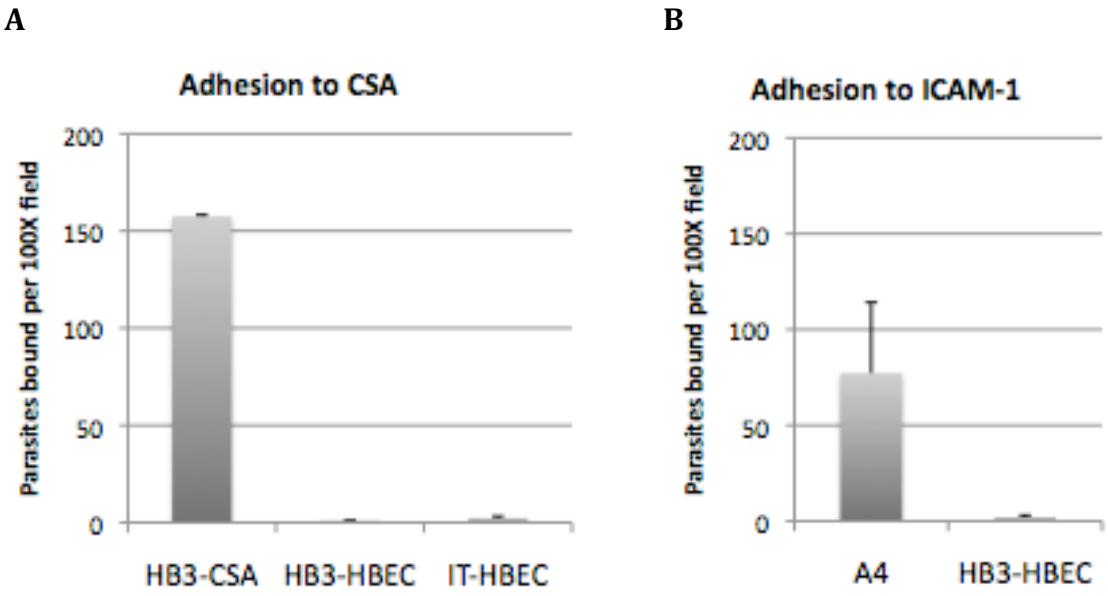


Figure 3-13. Adhesion to CSA and ICAM1. (A) HB3-CSA was selected for binding to CSA. (B) A4 is an IT-derived line that had been selected for ICAM1 binding. Experiments performed twice in quadruplicates.

To sum up this section, HBEC-5i selected parasites only showed a slight increase in binding to gC1qR and Integrin αV, but none to ICAM1 or CSA. Nothing definitive can be concluded about other receptors due to lack of positive controls.

3.5.6 Binding inhibition assays on HBEC-5i with soluble biomolecules

In an alternative approach to identify the HBEC-5i receptor(s) that the HB3-HBEC parasites may be binding to, the main known malaria cytoadherence receptors were tested in a binding inhibition assay. The same soluble proteins and glycosaminoglycan molecules tested in the binding assay approach (section 3.5.5) were pre-incubated with HB3-HBEC before incubation on HBEC-5i. If one of these molecules inhibits the adhesion to the endothelial cells, it would indicate that the parasites might be binding to that particular receptor.

Soluble Integrin αV, gC1qR, Fractalkine, Fibronectin (human), thrombospondin and CSA hardly inhibited any binding of HB3-HBEC to HBEC-5i (Figure 3-14). Note however that most of these experiments were performed only once and thus need repeats before drawing any firm conclusions. The same

experiment performed on an immortalized HDMEC line with soluble thrombospondin, CSA and hyaluronic acid did not inhibit binding of selected parasites either (Xiao, et al., 1996). The binding inhibition assay was not performed with the soluble CD36 protein because this receptor is not found on HBEC-5i (Table 3-1).

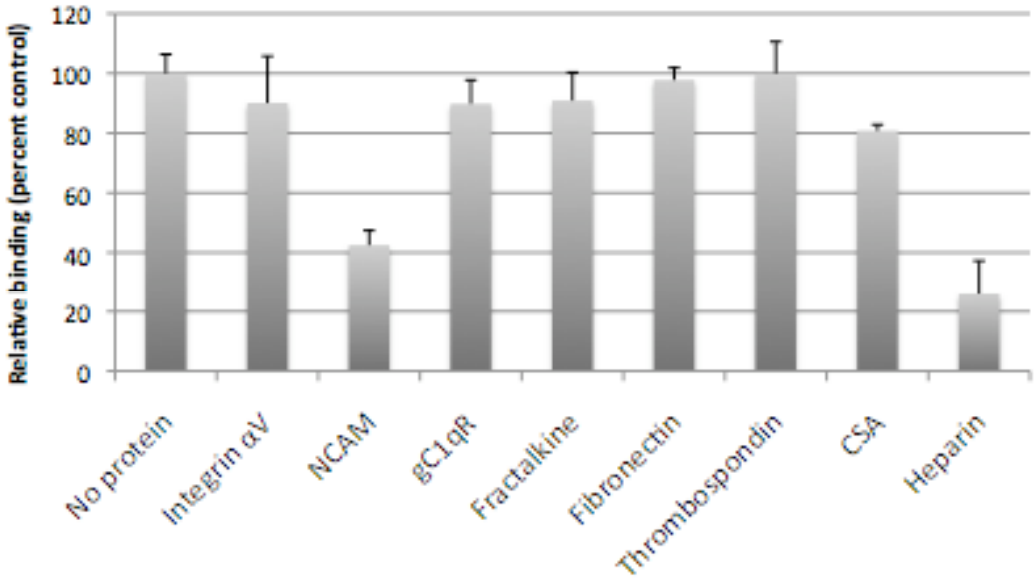


Figure 3-14. Binding inhibition assay of HB3-HBEC on HBEC-5i with various molecules. Data with the ICAM1 protein could not be used due to technical issues. Each receptor was tested in a single experiment in duplicate.

NCAM and Heparin were the only molecules showing a significant binding inhibition (unpaired t-test, $P < 0.01$) (Figure 3-14). However in the assay performed with NCAM, the protein had not been treated with neuraminidase beforehand. Thus it is possible that the reduction in binding with this receptor is due to the PSA, which is highly negatively charged. A repeat of the experiment could not be used due to very low amount of binding of the control.

Heparin, a highly sulphated form of heparan sulfate, is only found in mast cells, not on endothelial cells. However it has been previously reported to inhibit cytoadherence presumably by binding to the DBL1 domain of PfEMP1 (Vogt, et al., 2003). The binding inhibition assay was repeated with various concentrations of heparin and again a large decrease in parasites binding was

seen (Figure 3-15). Interestingly, heparin has the highest negative charge density of any known biological molecule (Alter, et al., 1987). This might indicate that HB3-HBEC parasites are binding to a negatively charged receptor.

These preliminary experiments are inconclusive in terms of the HBEC-5i receptor identification.

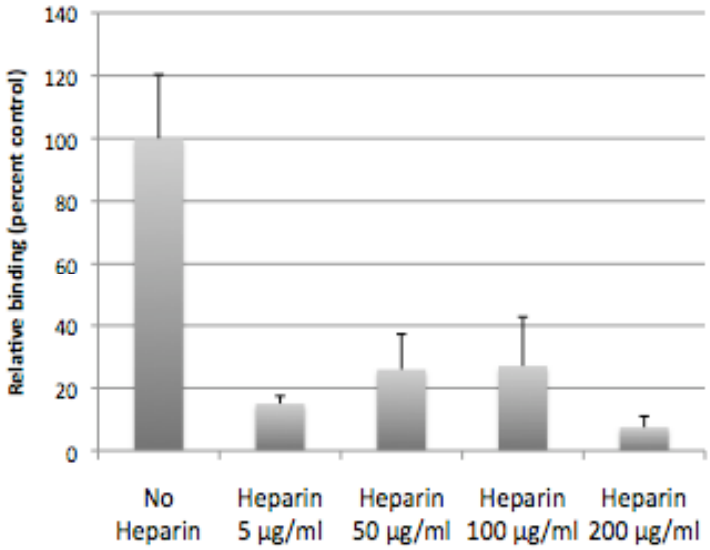


Figure 3-15. Heparin added to HB3-HBEC partially inhibited the binding of parasites onto HBEC-5i. Data is the average of two independent experiments, each performed in duplicate.

3.5.7 Binding inhibition assays on HBEC-5i with specific antibodies

This approach is very similar to the previous binding inhibition assay experiments (section 3.5.6) except that antibodies, rather than soluble molecules, are used to block the cytoadhesion. Each antibody was pre-incubated with HBEC-5i prior to the addition of HBEC-selected parasites. Concentrations used were based on previously published data when available (see methods).

All HB3-HBEC binding inhibition assays on HBEC-5i with antibodies used are summarized in Figure 3-16. Neither of the α-ICAM1 antibody altered the cytoadhesion, which correlates with the fact that HB3-HBEC does not bind to soluble ICAM1 (Figure 3-9). The monoclonal AMF7 Integrin antibody blocked almost half the cytoadhesion, indicating that HB3-HBEC

might be binding to Integrin αV. The anti-Integrin polyclonal 468255 did not show this trend, however it did not stain HBEC-5i on IFA either (Figure 3-2C). The other antibody that reduced the binding of HB3-HBEC was α-NCAM, although a mixture of anti-Integrin-NCAM-gC1qR failed to reproduce that effect. The α-CD36 antibody did not show any reduction in binding as expected.

Again, these experiments require a positive control showing that these antibodies are actually capable of blocking parasite cytoadhesion to their receptors. The results with the Integrin and NCAM antibodies are potentially interesting, however more experiments are needed before any definite conclusion on the binding inhibition assays can be drawn.

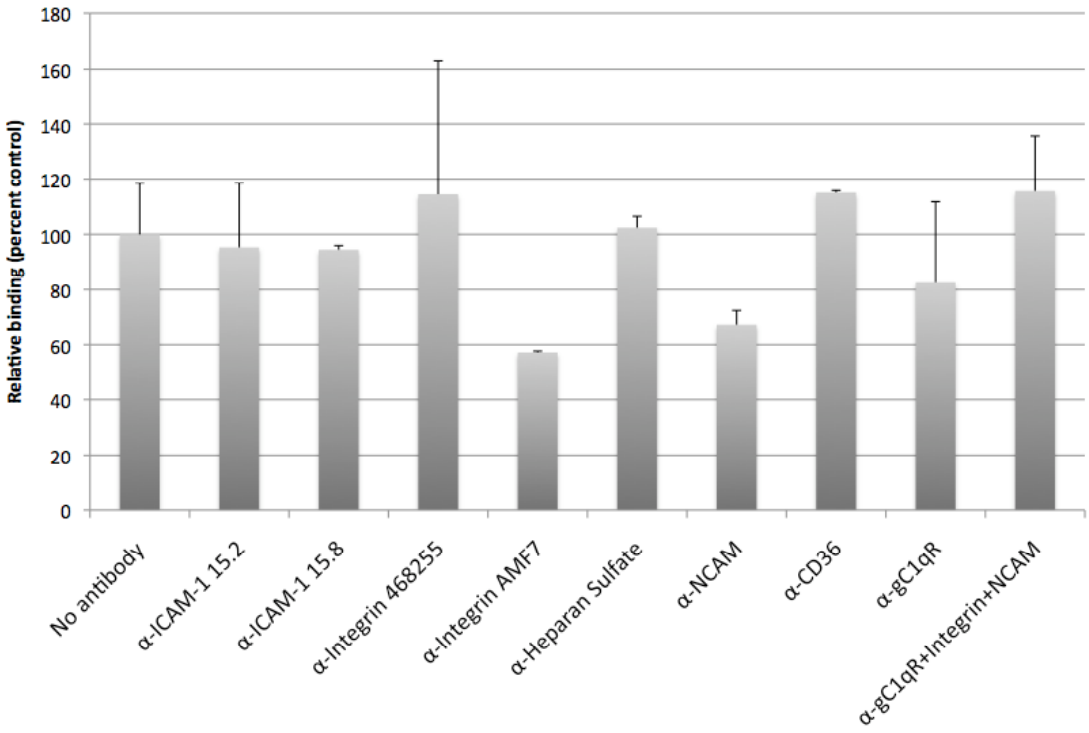
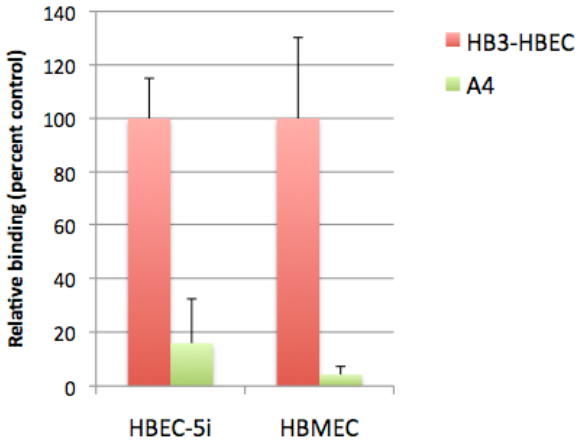


Figure 3-16. Binding inhibition assay of HB3-HBEC on HBEC-5i with various antibodies. Data shown is the average two independent experiments (ICAM 15.2, Integrin 468255, NCAM and gC1qR) or a single experiment (ICAM 15.8, Integrin AMF7, heparan sulfate, CD36 and a mix of gC1qR-Integrin 468255-NCAM) or 9 experiments ("No antibody", control). All experiments were performed in duplicate.

3.5.8 ICAM1 selected parasites do not bind to HBEC-5i or HBMEC

A4 is a *P. falciparum* IT/FCR3 derived strain selected for its affinity to ICAM1 (Adams, et al., 2000). As ICAM1 has been postulated to mediate cytoadherence in cerebral malaria, the strain was expected to adhere to HBEC-5i. However, a binding assay performed with A4 on HBEC-5i and the primary culture HBMEC showed virtually no binding to any endothelial cell (Figure 3-17). A4 does bind well to recombinant ICAM1 (Figure 3-13B) thus it may mean that the ICAM1 on endothelial cells surface is not "available" for cytoadherence, i.e. for example carbohydrate molecules could prevent binding of the parasites.
In any case, this indicates that ICAM1 is unlikely to be the receptor for the HB3-HBEC parasites.

A



B

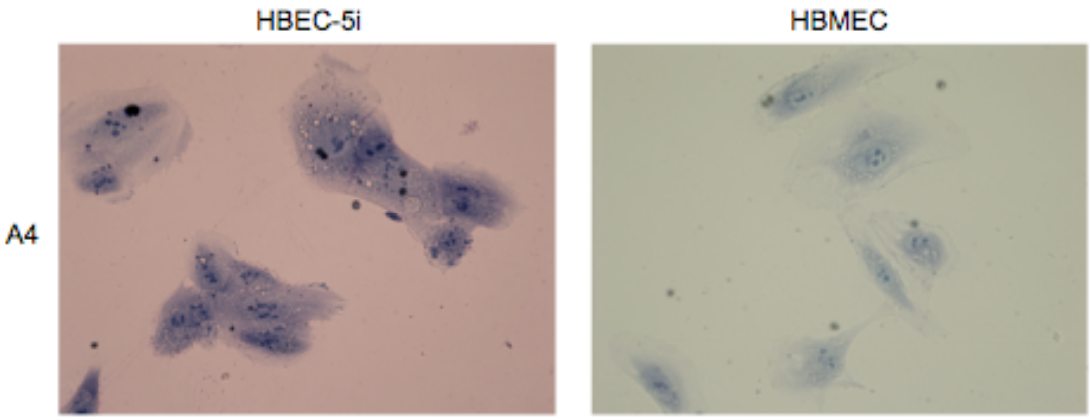


Figure 3-17. ICAM1 selected strain A4 does not bind to HBEC-5i or HBMEC. Experiment was performed twice in duplicate. Pictures taken at 400X magnification.

3.5.9 Adhesion of HB3-HBEC to HDMEC and HPMEC

In cerebral malaria cases, parasites sequestration is not restricted to the brain microvasculature. In fact, all post-mortem cerebral malaria studies that autopsied the rest of the body found sequestration in other organs (Genrich, et al., 2007, MacPherson, et al., 1985, Montgomery, et al., 2006, Nakazawa, et al., 1995, Pongponratn, et al., 1991, Pongponratn, et al., 2003, Seydel, et al., 2006, Wilairatana, et al., 2000). Therefore this section investigates whether the selection of *P. falciparum* on HBEC-5i would result in a change in cytoadherence phenotype to other microvascular endothelial cells. Two primary cell lines were

chosen: human dermal endothelial cells (HDMEC) for its expression of CD36 (Swerlick, et al., 1992a) and human pulmonary endothelial cells (HPMEC) as parasites often sequester in this tissue (Montgomery, et al., 2006). Both lines were ordered from ScienCell. They isolated the cells from human dermal/lung tissue and characterised them with antibodies to vWF/Factor VIII and CD31 (P-CAM) and by uptake of DiI-Ac-LDL.

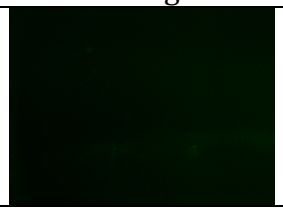
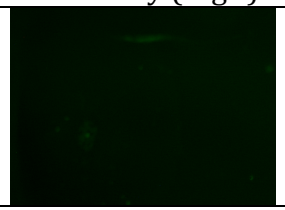
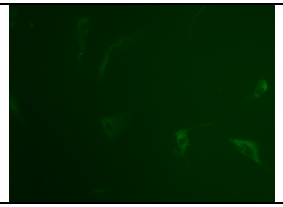
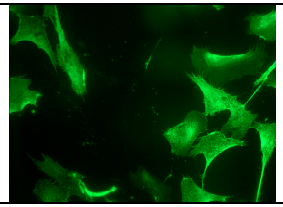
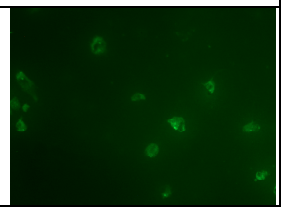
3.5.9.1 Receptors expression on HDMEC (immunofluorescence assay)

In order to test whether HDMEC surface proteins expression differ from HBEC-5i, immunofluorescence assays were performed using the same antibodies and the same protocol as in section 3.5.1. As with HBEC-5i cells, α-ICAM1, α-Integrin aV, α-Fractalkine, α-NCAM antibodies showed strong positive signals (Table 3-4 and Figure 3-18). α-VCAM, α-Thrombospondin and α-heparan sulafte gave weak signal. The immunofluorescence with the heparan sulfate antibody was low. At the time the assay was carried out, the same antibody also showed very weak signal on HBEC-5i (unlike what was seen in Figure 3-2) thus it might have degraded. Although this experiment is inconclusive and should be repeated, heparan sulfate has previously been reported on the surface of HDMEC (Gupta, et al., 1999a). The only major difference in the expression profile of tested proteins is CD36, which is expressed on HDMEC (Figure 3-18A) but not on HBEC-5i. This is particularly interesting as most *P. falciparum* isolates bind to this receptor (Serghides, et al., 2003). The α-CD36 immunofluorescence signal on HDMEC is however weaker than many other receptors (Table 3-4). No binding assay was performed with activated HDMEC so the surface expression profile after TNF activation was not tested.

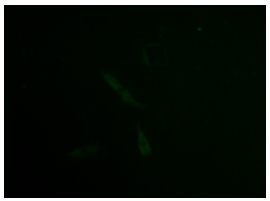
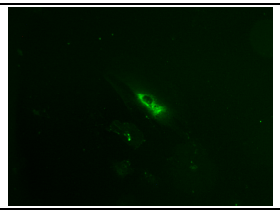
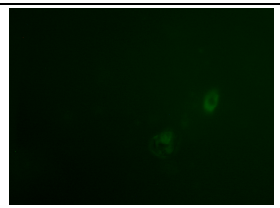
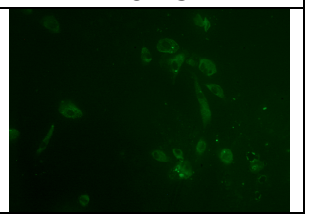
1st Antibody	1st Ab Isotype	Concentration	2nd Ab	Dilution	Fluores. score
Control Mo. IgG1	Mo. IgG1	10µg/ml	Go α-Mo IgG	1/4000	-
Control Mo. IgM	Mo. IgM	10µg/ml	Go α-Mo IgM	1/4000	-
Control: 2nd Ab only	/	/	Go α-Mo IgG	1/4000	-
Control: 2nd Ab only	/	/	Go α-Mo IgM	1/2000	-
Control: 2nd Ab only	/	/	Go α-Rab.	1/2000	+/-
Control: 2nd Ab only	/	/	α-Go.	1/4000	+/-
ICAM1 15.2	Mo. IgG1	10µg/ml	Go α-Mo IgG	1/4000	++++
ICAM1 15.8	Mo. IgG1	10µg/ml	Go α-Mo IgG	1/4000	++
Integrin AMF7	Mo. IgG1	10µg/ml	Go α-Mo IgG	1/4000	+ (weak)
Integrin 468255	Rab. IgG	10µg/ml	Go α-Rab.	1/4000	++
VCAM	Mo. IgG1	10µg/ml	Go α-Mo IgG	1/4000	+ (weak)
Thrombospondin	Mo. IgG1	10µg/ml	Go α-Mo IgG	1/4000	+ (weak)
CD36 Smphage	Mo. IgM	10µg/ml	Go α-Mo IgM	1/2000	++
CD36 FA6-152	Mo. IgG1	10µg/ml	Go α-Mo IgG	1/4000	++
Fractalkine	Go. IgG	10µg/ml	α-Go IgG	1/4000	+++
NCAM	Rabbit	20µg/ml	Go α-Rab.	1/2000	+++
Heparan Sulfate	Mo. IgG1	10µg/ml	Go α-Mo IgG	1/4000	+ (weak)

Table 3-4. **Immunofluorescence assay (IFA) on HDMEC**. The amount of fluorescent signal was estimated by eye and given a score from "-" (no signal) to "++++" (very bright signal). Bolded receptor names are considered to be positive. Heparan Sulfate and Thrombospondin IFAs and their associated controls were performed twice, each time in duplicate. All other IFAs were performed once in duplicate. See Figure 3-18 for representative pictures of these IFA. CR1, blood group A&B antigens, PECAM, CSA and gC1qR antibodies were not tested on HDMEC. Abbreviations used: Ab = Antibody; Ag = antigen; Mo = mouse; Go = goat; Rab = rabbit ; chick = chicken; α = anti; NP = experiment not performed or result discarded due to technical issue.

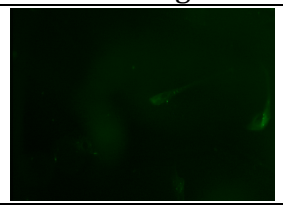
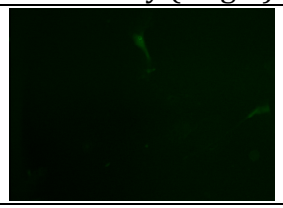
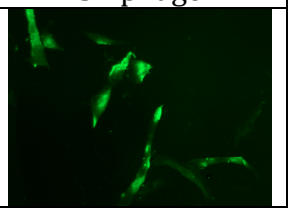
A

Mouse IgG1	**Control** Mouse IgG1	**Control** 2nd Ab only (αIgG)	**Heparan Sulfate**	**ICAM1** 15.2	**ICAM1** 15.8
HDMEC					

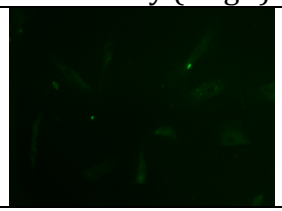
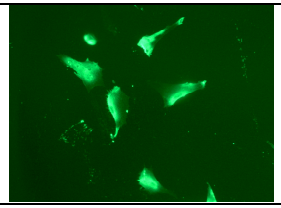
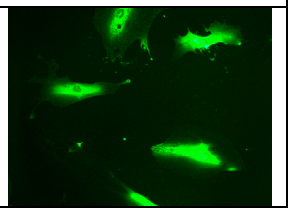
A (continued)

Mouse IgG1	**VCAM**	**Thrombospondin** A6.1	**Integrin αV** AMF7	**CD36** FA6-152
HDMEC				

B

Mouse IgM	**Control** Mouse IgM	**Control** 2nd Ab only (α-IgM)	**CD36** Smphage
HDMEC			

C

Rabbit IgG	**Control** 2nd Ab only (α-IgG)	**Integrin αV** 468255	**NCAM**
HDMEC			

D

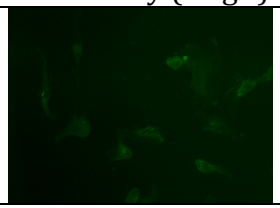
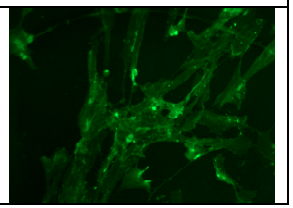
Goat IgG	**Control** 2nd Ab only (α-IgG)	**Fractalkine**
HDMEC		

Figure 3-18. Immunofluorescence assay (IFA) on HDMEC. Antibodies are grouped together according to their isotype. The first 2 columns of each group are controls: a non-specific antibody of the same isotype, and the secondary antibody only. All pictures were taken at 200X magnification, apart from ICAM1 15.2, NCAM and Integrin 468255 at 400X. Note that a goat IgG and a rabbit IgG isotypes controls are missing for Fractalkine and NCAM antibodies, respectively. Ab = Antibody; Ag = Antigen; NP = experiment not performed or result discarded due to technical issue. See Table 3-4 for fluorescence score and other information.

3.5.9.2 Receptors expression on HPMEC (immunofluorescence assay)

In order to test whether HPMEC surface proteins expression differ from HBEC-5i and HDMEC, immunofluorescence assays were performed using the same antibodies protocol as in section 3.5.1. The expression profile of the tested receptors was virtually identical to HDMEC (Table 3-5). The scavenger receptor CD36 also seems to be expressed, although at a low level (Figure 3-18A).

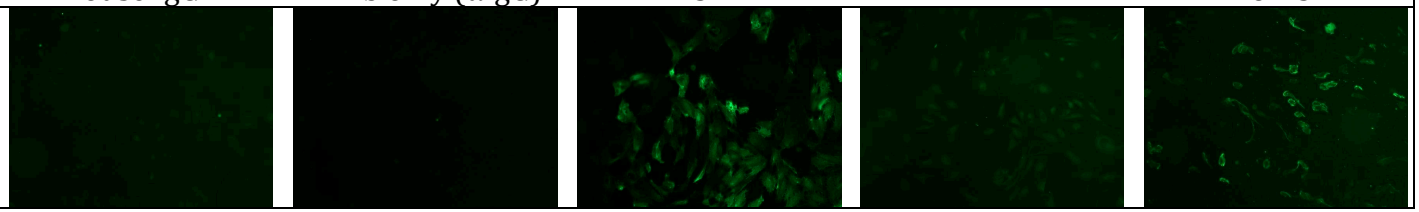
Altogether, HBEC-5i, HDMEC and HPMEC showed very similar receptor expression pattern with the antibodies tested here. The only difference resides in the expression of CD36. Reports from the literature are all in agreement with our findings (Table 3-6). It is of course possible that other unknown surface receptors may be differentially expressed between these 3 endothelial cell lines.

1st Antibody	1st Ab Isotype	Concentration	2nd Ab	Dilution	Fluores. score
Control Mo. IgG1	Mo. IgG1	10µg/ml	Go α-Mo IgG	1/4000	-
Control Mo. IgM	Mo. IgM	10µg/ml	Go α-Mo IgM	1/4000	+/-
Control: 2nd Ab only	/	/	Go α-Mo IgG	1/4000	-
Control: 2nd Ab only	/	/	Go α-Mo IgM	1/4000	-
Control: 2nd Ab only	/	/	Go α-Rab.	1/4000	+/-
Control: 2nd Ab only	/	/	α-IgY	1/5000	+/-
Control: 2nd Ab only	/	/	α-Go.	1/4000	-
ICAM1 15.2	Mo. IgG1	10µg/ml	Go α-Mo IgG	1/4000	++++
Integrin 468255	Rab. IgG	10µg/ml	Go α-Rab.	1/4000	++++
VCAM	Mo. IgG1	10µg/ml	Go α-Mo IgG	1/4000	+ (weak)
Thrombospondin	Mo. IgG1	10µg/ml	Go α-Mo IgG	1/4000	+++
CR1	Mo. IgG1	10µg/ml	Go α-Mo IgG	1/4000	-
CD36 Smphage	Mo. IgM	10µg/ml	Go α-Mo IgM	1/4000	+/-
CD36 FA6-152	Mo. IgG1	10µg/ml	Go α-Mo IgG	1/4000	+
Fractalkine	Go. IgG	10µg/ml	α-Go IgG	1/4000	++
gC1qR	Chick IgY	10µg/ml	α-IgY	1/5000	+++
NCAM	Rabbit	20µg/ml	Go α-Rab.	1/4000	+++

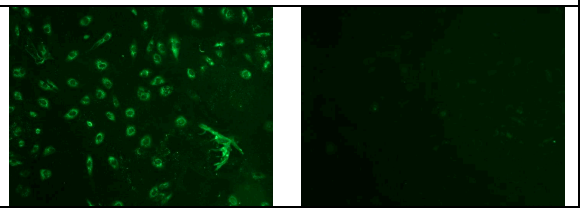
Table 3-5. Immunofluorescence assay (IFA) on HPMEC. The amount of fluorescent signal was estimated by eye and given a score from "-" (no signal) to "++++" (very bright signal). Bolded receptor names are considered to be positive. All IFA were performed once in duplicate. See Figure 3-19 for representative pictures of these IFA. CSA, heparan sulfate, blood group A&B antigens and PECAM antibodies were not used

on HPMEC. Abbreviations used: Ab = Antibody; Ag = antigen; Mo = mouse; Go = goat; Rab = rabbit ; chick = chicken; α = anti; NP = experiment not performed or result discarded due to technical issue.

A

Mouse IgG1	**Control** Mouse IgG1	**Control** 2nd Ab only (αIgG)	**ICAM1** 15.2	**VCAM**	**CD36** FA6-152
HPMEC					

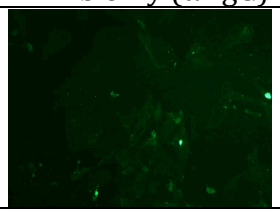
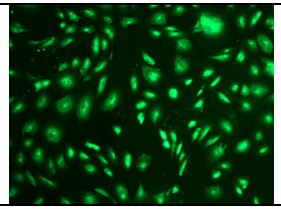
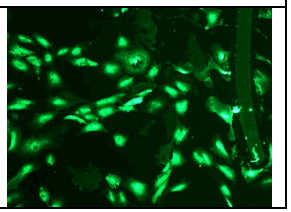
A (continued)

Mouse IgG1	**Thrombospondin** A6.1	**CR1**
HPMEC		

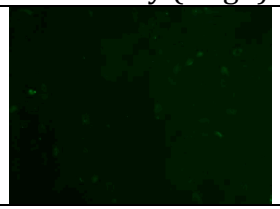
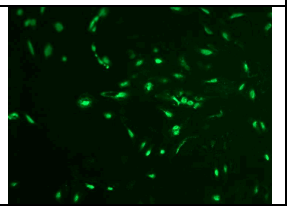
B

Mouse IgM	**Control** Mouse IgM	**Control** 2nd Ab only (α-IgM)	**CD36** Smphage
HPMEC			

C

Rabbit IgG	**Control** 2nd Ab only (α-IgG)	**Integrin** 468255	**NCAM**
HPMEC			

D

Chicken IgY	**Control** 2nd Ab only (α-IgY)	**gC1qR**
HPMEC		

E

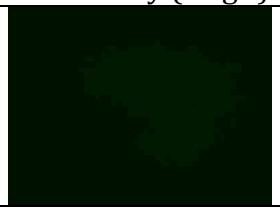
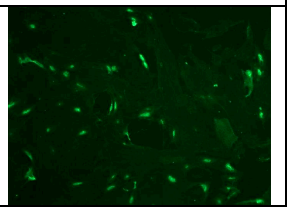
Goat IgG	**Control** 2nd Ab only (α-IgG)	**Fractalkine**
HPMEC		

Figure 3-19. Immunofluorescence assay (IFA) on HPMEC. Antibodies are grouped together according to their isotype. The first 2 columns of each group are controls: a non-specific antibody of the same isotype, and the secondary antibody only. All pictures were taken at 200X magnification. Note that a goat IgG, a chicken IgY and a rabbit IgG isotypes controls are missing for Fractalkine, gC1qR, Integrin 468255 and NCAM antibodies, respectively. Ab = Antibody; Ag = Antigen; NP = experiment not performed or result discarded due to technical issue. See Table 3-5 for fluorescence score and other information.

		HBEC-5i	TNF activated HBEC-5i	HDMEC	HPMEC
CD36	This study	✗	✗	✔	✔
	Literature	✗1, 2, 3	✗1, 2, 3	✔4, 9	✔14, 18
ICAM1	This study	✔	✔✔	✔	✔
	Literature	✔1, 2, 3	✔✔1, 2, 3	✔1	✔12, 14
Integrin αV	This study	✔	✔	✔	✔
	Literature	✔3	✔3	✔10	NA
Throm-bospondin	This study	✔	✔	✔weak	✔
	Literature	✔1	✔1	✔1, 4	NA
VCAM	This study	✗	✔	✔weak	✔weak
	Literature	✔1, 2, 3weak	✔1, 2, 3	✗4	✔14, 18
PECAM	This study	✔weak	NP	NP	NP
	Literature	✗3, 19	✗3	✔8, 4	✔12, 14
gC1qR	This study	✗v. weak	✗v. weak	NP	✔
	Literature	NA	NA	NA	NA
Fractalkine	This study	✔	NP	✔	✔
	Literature	NA	NA	NA	NA
NCAM	This study	✔	NP	✔	✔
	Literature	NA	NA	✔4	NA
E-selectin	This study	✗	NP	NP	NP
	Literature	✗1, 2	✗1, 2	✗8	✗14
P-selectin	This study	✗	NP	NP	NP
	Literature	NA	NA	✔8	✗15 ✔14
CR-1	This study	✗	NP	NP	✗
	Literature	NA	NA	NA	NA
Heparan Sulfate	This study	✔	✔	✔weak	NP
	Literature	NA	NA	✔12, 16	✔17
CSA	This study	✔	✔	NP	NP
	Literature	✔3	✔3	✔16	✔18

Table 3-6. Summary of endothelial cell lines receptors expression. For each receptor, the first line indicates the expression or lack of according to my IFA, the second line indicates data from other published studies. A double tick mark indicates the expression of that receptor is increased after TNF induction. NP = not performed. NA = data not available in the literature. References: 1 = (Xiao, et al., 1996); 2 = (Wassmer, et al., 2005); 3 = (Wassmer, et al., 2006b); 4 = (Xu, et al., 1994); 5 = (Biswas, et al., 2007); 6 = ScienCell company ; 7 = (Gingras, et al., 1995); 8 = (Kraling and Bischoff, 1998); 9 = (Swerlick, et al., 1992b); 10 = (Siano, et al., 1998); 11 = (Stins, et al., 1997); 12 = (Gupta, et al., 1999a); 13 = (Krump-Konvalinkova, et al., 2001); 14 =

(Muanza, et al., 1996); 15 = (Ocana-Macchi, et al., 2009); 16 = (Luo, et al., 2001); 17 = (Vogt, et al., 2003); 18 = (Andrews, et al., 2003); 19 = (Faille, et al., 2009a) (note that HBEC-5i can acquire PECAM via platelet microparticles; * = HBMEC derived from children do not express E-Selectin (ELAM) while other commercial HBMEC do (Stins, et al., 1997). ♪ = When activated with Histamine or Thrombin.

3.5.9.3 HB3-HBEC also cytoadhere to HDMEC and HPMEC

A binding assay with unselected HB3 parasites on HDMEC and HPMEC revealed a very low amount of binding (Figure 3-20 and Figure 3-21). This was somewhat unexpected considering that HB3-Uns binds well to purified CD36 (Figure 3-9 in section 3.5.5) and that the latter receptor is found on HDMEC and HPMEC (Table 3-6).

HB3-HBEC however shows a more than 10 fold increase in binding to HDMEC and HPMEC compared to HB3-Uns (Figure 3-20). Note that the number of iRBC binding to HBEC-5i or to the primary endothelial cells cannot be compared directly as HDMEC and HPMEC tend to be bigger in size (Figure 3-21). Nevertheless, it is clear that the selection of HB3 on HBEC-5i also leads to a large increase in binding to HDMEC and HPMEC.

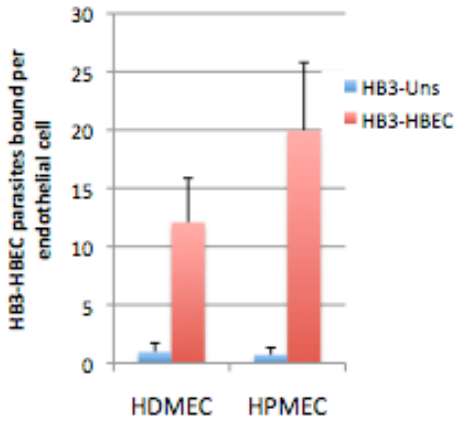


Figure 3-20. HB3-HBEC, but not HB3-Uns, bind to HDMEC and HPMEC. Data is the average of two experiments, each performed in duplicate.

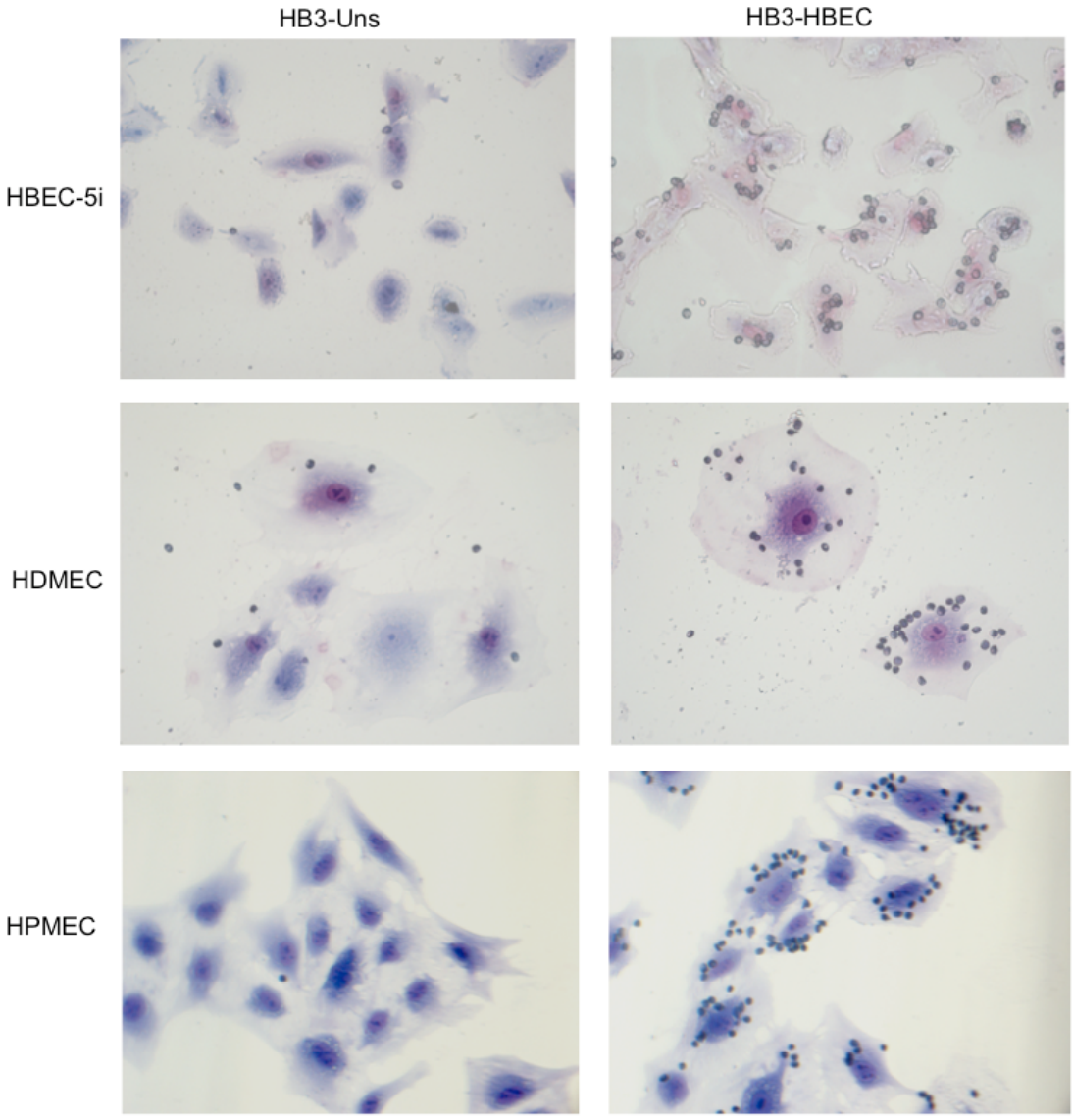


Figure 3-21. HB3-HBEC parasites also cytoadhere to HDMEC and HPMEC. Pictures taken at 400X magnification.

To determine whether the same iRBC are able to bind to both HBEC-5i and HD/PMEC, I developed a "re-binding" assay. HB3-HBEC parasites were first incubated on HBEC-5i as for a regular binding assay. After the washings to get rid of any unbound RBC, the dishes were vigorously shaken and the cells flushed with medium from a pipette many times in order to detach most iRBC. These iRBC were then re-incubated on HDMEC or HPMEC, or on HBEC-5i again as a control. The number of iRBC bound per endothelial cell was counted as usual at the end of this second "re-binding" assay.

The HB3-HBEC parasites detached from HBEC-5i clearly bound well to both HDMEC and HPMEC (Figure 3-22 and Figure 3-23). The numbers of bound parasites in a normal or a "re-binding" assay cannot be compared as the haematocrit and parasitaemia (almost 100% in a "re-binding" assay) are different between the two assays. However, it can confidently be concluded that a parasite selected for cytoadherence to an immortalized brain microvascular cell (HBEC-5i) is also able to bind to a primary endothelial cell derived from skin or lung tissues.

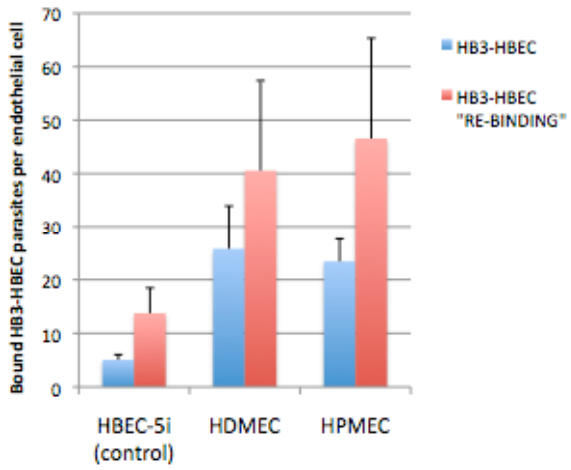


Figure 3-22. "Re-binding" assay: HB3-HBEC parasites bound to HBEC-5i were detached then added to HDMEC or HPMEC or HBEC-5i (control). Note that the haematocrit and parasitaemia for a normal or "re-binding" assay are different. The purpose of this figure is to illustrate that the exact same parasites binding to HBEC-5i are able to bind to HDMEC and HPMEC. Data is the average of two experiments, each performed in duplicate (HPMEC) or a single experiment performed in quadruplicate (HBEC-5i and HDMEC).

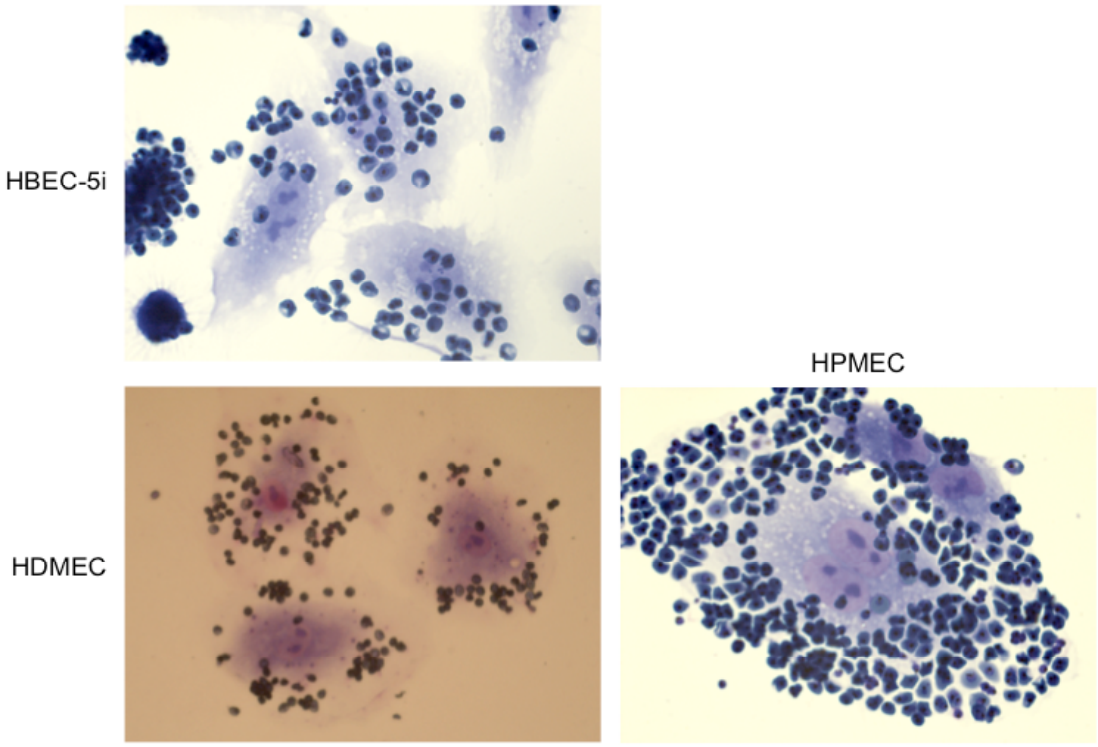


Figure 3-23. "Re-binding" assay of HB3-HBEC on HBEC-5i, HDMEC and HPMEC. HB3-HBEC parasites were incubated on HBEC-5i, washed, then detached and re-incubated on HBEC-5i (control) or HDMEC or HPMEC. Thus parasites seen on these pictures were previously binding to HBEC-5i. Pictures taken at 400X magnification for HDMEC, 1000X for others.

The cytoadherence property of HB3-HBEC parasites on multiple cell lines (HDMEC, HPMEC and also HBMEC) prompted the question of how specific the interaction between the selected parasite and the HBEC-5i cell was. A binding assay was carried out on COS-7, an unrelated cell line derived from simian kidney (Figure 3-24). Neither unselected nor selected HB3 showed binding above background level on these COS-7 cells. Thus so far HB3-HBEC parasites have been shown to bind to human endothelial cell lines only. More experiments on a wider range of cell lines are needed to characterize the binding specificity of HB3-HBEC.

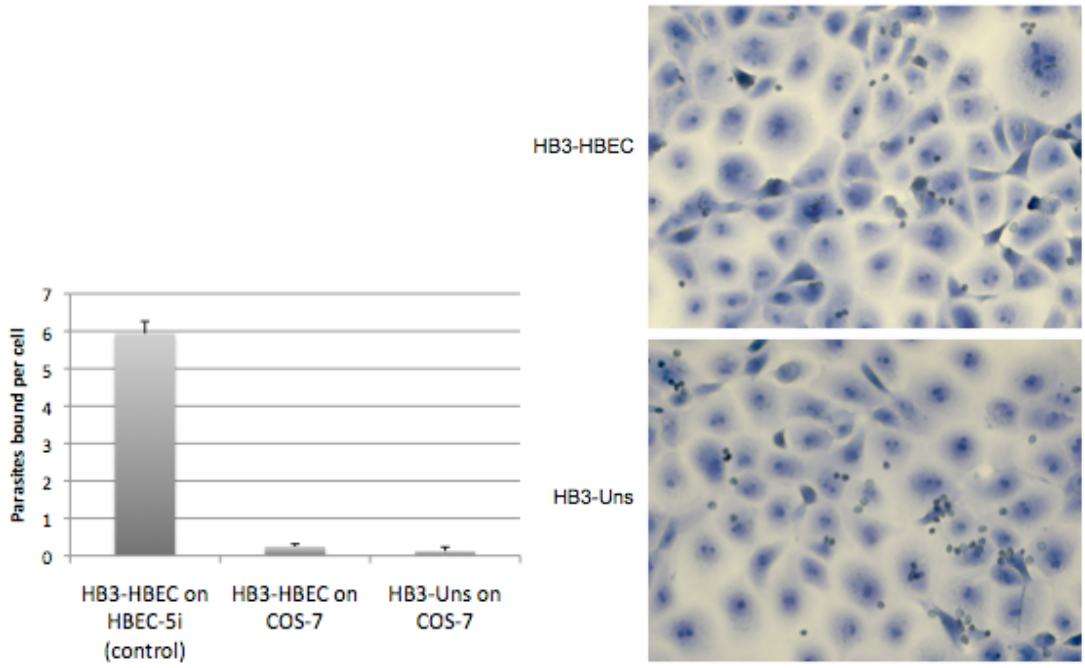


Figure 3-24. HB3-HBEC does not cytoadhere to COS-7 cells (immortalized cell line derived from simian kidney). Pictures were taken at 400X magnification. The experiment was performed once in duplicate.

3.5.10 New heparin-like compounds inhibit binding of HBEC-selected parasites to endothelial cells

The different approaches used to attempt to identify the HBEC-5i receptor(s) were mostly unsuccessful. The only compound that greatly blocked parasites binding to endothelial cells was heparin (Figure 3-15). Heparin is a highly sulphated glycosaminoglycan widely used as an injectable anticoagulant. It is able to disrupt rosettes (Carlson, et al., 1992), probably via interaction with the DBLα domain of PfEMP1 (Barragan, et al., 2000). Heparin binding is also more frequent with iRBC from severe malaria than from uncomplicated malaria cases (Heddini, et al., 2001a). The strong anticoagulant effect however prevents this compound from being used for malaria treatment (WHO, 2000).

Nevertheless, a chemical named curdlan sulfate (CRDS), chemically similar to heparin, has been tested for its anti-adhesion effects. It inhibits *P. falciparum* invasion (Havlik, et al., 1994) and rosetting formation *in vitro* (Kyriacou, et al., 2007). Interestingly, its 10 fold lower anticoagulant effect than

heparin (Kaneko, et al., 1990) means it is a better drug candidate (Havlik, et al., 2005). In fact, it has already been shown to be safe and well tolerated in clinical trials for human immunodeficiency virus and malaria (Gordon, et al., 1995, Havlik, et al., 2005).

A new range of heparin-like compounds has also recently been synthesized (M. Skidmore and E. Yates, Liverpool university). Their effect on rosetting is currently under investigation (Clare Sweenie, Alex Rowe, ongoing experiments). Two of them, MS29 & MS31 showed particularly encouraging results with rosette blocking activity in the micromolar range of concentration.

Thus the heparin effect on cytoadherence to HBEC-5i prompted us to test CRDS and other heparin-like compounds as new drugs to block cytoadhesion to human endothelial cells.

3.5.10.1 CRDS inhibits cytoadhesion to HBEC-5i at therapeutic levels

At therapeutic doses (4 mg/kg), the plasma level of CRDS is estimated to be approximately 50 to 60 µg/ml (Havlik, et al., 2005, Kyriacou, et al., 2007). Thus binding inhibition assays with heparin-like compounds were performed around that concentration range. Fucoidan, a sulphated polysaccharide, was used as a positive control as it has been shown to inhibit rosetting (Rowe, et al., 1994) but also binding to the receptor P-selectin (Berteau and Mulloy, 2003). In the first instance, CRDS or Fucoidan were pre-incubated with iRBC in a similar way as the binding inhibition assays with soluble proteins. This led to large decrease in binding of HB3-HBEC to HBEC-5i, whether at 100, 50 or 10 µg/ml (Figure 3-25, all p-values < 0.05, unpaired t-test). Even when CRDS was added to HBEC-5i at the same time as HB3-HBEC, the blocking of cytoadherence by CRDS was significant (p-value < 0.05, unpaired t-test) (Figure 3-25B). The same effect was seen with IT-HBEC parasites (Figure 3-26, p-value <0.01, unpaired t-test). 3D7-HBEC parasites have not been tested yet.

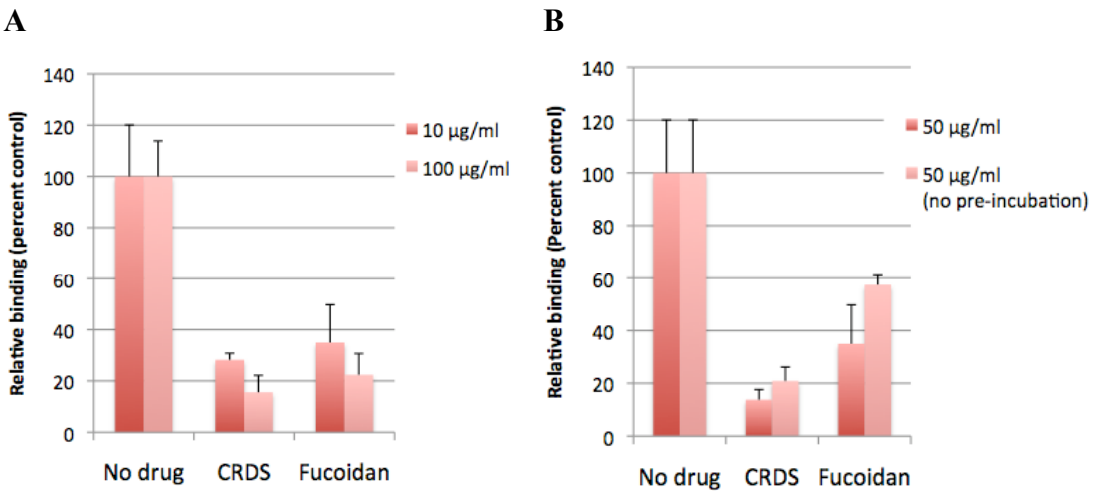


Figure 3-25. Inhibition of HB3-HBEC cytoadherence to HBEC-5i by CRDS. (A) Fucoidan or CRDS were pre-incubated with iRBC for 20min, (B) CRDS and Fucoidan were added with or without pre-incubation. Data is the average of a single experiment performed in triplicate. The control (no drug) showed an average of 5.7 iRBC per endothelial cell.

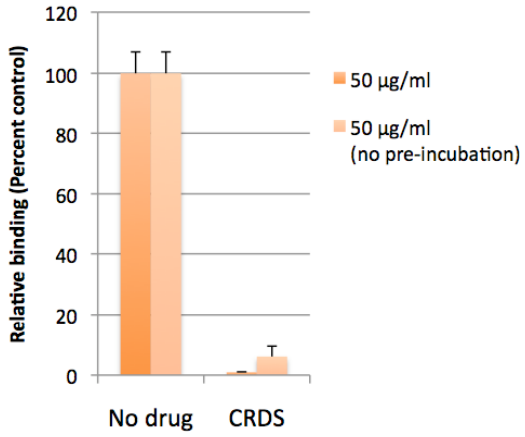


Figure 3-26. Inhibition of IT-HBEC cytoadherence on HBEC-5i with CRDS. CRDS was added with or without pre-incubation. Data is the average of a single experiment performed in quadruplicate. The control (no drug) showed an average of 6.6 iRBC per endothelial cell

Thus these preliminary experiments indicate that curdlan sulfate at physiologically relevant concentration is able to prevent most, but not all, cytoadhesion of selected parasites onto HBEC-5i.

3.5.10.2 MS29 & MS31 (heparin-like compounds) strongly block cytoadhesion to HBEC-5i but less to primary endothelial cells

MS29 and MS31 are two out of many newly synthesized compounds that have been tested for anti-rosetting activity. MS29 and MS31 block rosettes formation at about 1 µg/ml. Their cytoadhesion blocking efficiency was tested by binding inhibition assay without any pre-incubation. Even with concentrations as low as 1 µg/ml, the binding of HB3-HBEC to HBEC-5i was greatly inhibited (Figure 3-27). The blocking was in fact stronger than what was observed with CRDS (Figure 3-25).

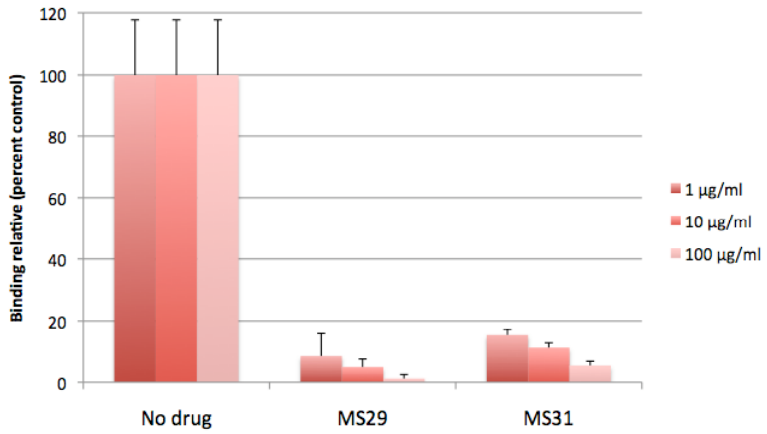


Figure 3-27. Inhibition of HB3-HBEC cytoadherence on HBEC-5i with MS29 and MS31 compounds. The drugs were added at the same time as HB3-HBEC on HBEC-5i (no pre-incubation). Data shown is a single experiment performed in triplicate.

The activity of MS29 was also tested on the primary endothelial cells HDMEC and HPMEC. MS31 was tested on HPMEC only. At 10 µg/ml of MS29 or MS31, the adhesion of HB3-HBEC parasites was inhibited to a lower extent than on HBEC-5i (Figure 3-28). The only significant blocking was obtained with MS29 on HPMEC (unpaired t-test, $p < 0.01$).

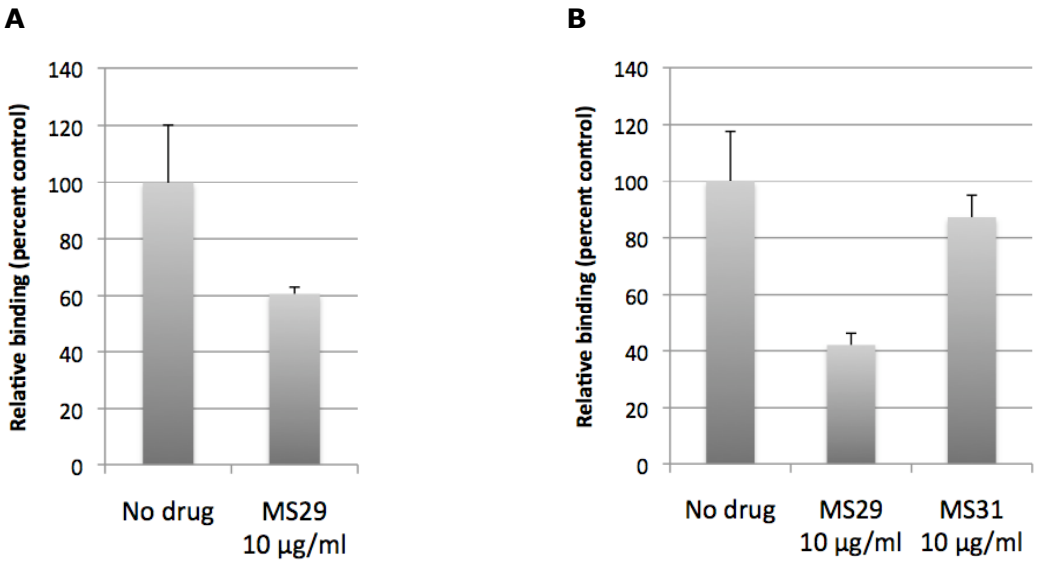


Figure 3-28. Slight inhibition of cytoadherence to HDMEC (A) and HPMEC (B) by MS29 and MS31 (no pre-incubation). Data is a single experiment performed in duplicate.

This may indicate that the interaction parasites – H(D/P)MEC is stronger than the interaction parasites-HBEC-5i. It could denote, for example, that the receptor(s) involved in the interaction with iRBC are more abundant on primary endothelial cell lines or that different or additional receptors are used on the primary lines compared to HBEC-5i.

3.6 Discussion

3.6.1 Multiple *P. falciparum* strains selected on HBEC-5i

The first aim of this chapter was successfully reached: HB3, 3D7 and IT parasites were selected for cytoadherence to HBEC-5i. There was a considerable increase in the amount of bound iRBC after selection. Unselected parasites bound poorly to HBEC-5i (<0.5 iRBC per endothelial cell) but after 5-6 rounds of selection this increased to over 5 iRBC per endothelial cell. This difference in phenotype between unselected and selected parasites implies a change in the proteome of *P. falciparum*, hence most likely a change in the transcriptome of these parasites. This will be analysed in the following chapters.

It was found that the number of bound parasites per HBEC-5i tended to diminish after a few weeks of culturing without selection. This may indicate that the *P. falciparum* ligand for HBEC-5i binding is part of a variant surface antigen family which undergoes switching of expression from one variant to the other in long-term culture.

3.6.2 Not all *P.falciparum* clones are selectable

Unlike the other *P. falciparum* clones, Dd2 showed no sign of cytoadherence to HBEC-5i even after 5 rounds of selection. Many hypotheses, not mutually exclusive, could explain this fact:

1. Dd2 does not possess the appropriate variant surface antigen (VSA) gene that could mediate the binding to HBEC-5i.
2. Dd2 VSA gene expression switches too quickly. It is plausible that after a round of selection, by the time a sufficient amount of parasites is reached for the next round (about 3 weeks), all parasites have already switched back to a non-binding-VSA variant.
3. It is possible that PfEMP1, which are thought to be the main cytoadherence ligands, is not or poorly trafficked to the surface of the Dd2 iRBC. This would prevent binding to HBEC-5i.
4. Finally, Dd2 parasites have been reported to be knobless, which deeply impedes the cytoadherence (Herricks, et al., 2009, Nakamura, et al., 1992).

As parasites tended to bind better to primary endothelial cell lines (section 3.5.3.2) it would be interesting to test whether Dd2 could be selected on primary cells.

3.6.3 HBEC-5i, HDMEC and HPMEC surface proteins and biomolecules characterized by immunofluorescence assay

In order to hypothesize what the selected parasites might be binding onto, the surface molecules of HBEC-5i, HDMEC and HPMEC were characterized by immunofluorescence assay. Antibodies used were against receptors that are thought to be involved with iRBC sequestration. The only major discrepancy

noticed between the different cell lines was the expression of CD36 that was not detected on HBEC-5i. This is consistent with previous publications arguing that the human brain microvascular endothelium, unlike other endothelia, shows little or no CD36 expression (Silamut, et al., 1999, Xiao, et al., 1996). This is a crucial distinction as most of the cytoadherence in a human body is thought to be CD36 mediated (Serghides, et al., 2003). This makes it highly unlikely that CD36 is the receptor on HBEC-5i for HBEC-selected parasites. Consistent with this, α-CD36 antibodies that are known to block *P. falciparum* cytoadherence did not reduce binding to HBEC-5i (Figure 3-16).

HB3 parasites were also selected on HBEC-5i activated with the cytokine TNF. Immunofluorescence assays had showed that at least ICAM1 and VCAM were expressed at higher level after the cells were incubated with TNF (**Table 3-6**). Probably many other surface receptors were differentially regulated after TNF activation. This may result in a different *P. falciparum* ligand being expressed in the HB3-HBEC-TNF population compared to the HB3-HBEC. This will be analysed in chapter 5.

3.6.4 Limitations of the *in vitro* brain endothelial cells model

Although the culture of HBEC-5i and other HBMEC strains are becoming widely used, these *in vitro* cultured cells have limitations as a model for endothelium. Endothelial cells removed from their native microenvironment are uncoupled from critical extracellular cues and undergo phenotypic drift (Aird, 2007). A proteomic study in rats comparing living endothelium *in vivo* and cultured endothelial cells showed that 41% of proteins were not detected in the *in vitro* culture (Durr, et al., 2004). Thus there is a risk that the receptors on brain microvascular endothelium that are important *in vivo* are not expressed by HBEC-5i or HBMEC. As any *in vitro* study, the purpose of our data is to generate hypotheses that will have to be validated in humans.

3.6.5 Endothelial cell adhesion probably involves a different ligand-receptor interaction than rosetting or clumping

To date, three main types of *P. falciparum* cytoadherence have been described: rosetting, platelet-mediated clumping and adhesion to endothelial cells. Surprisingly, the three cytoadherence phenotypes have yet to be studied together, whether using lab or field isolates. For example, there is currently no study characterising the cytoadhesion to endothelial cells, platelets and uRBC (rosetting) of the same field isolates. It would be of great interest to correlate these phenotypes with the various manifestations and seriousness of the disease.

Here we showed that all parasite strains selected for HBEC-5i cytoadhesion do not form rosettes and significantly decrease their platelet-mediated clumping frequency. Furthermore, rosetting selected and platelet selected parasites only marginally bind to HBEC-5i. Note that the binding assay with rosetting parasites should be repeated with uRBC detached from their iRBC. Altogether, these results suggest that endothelial cell cytoadhesion involves different ligand(s) and receptor(s) than rosetting and clumping.

To further study the rosetting and endothelial cell adhesion phenotypes, one could to start a selection on HBEC-5i with a highly rosetting parasite line, and record the rosetting frequency as well as *var* genes expression after each round of selection.

3.6.6 HBEC-selected parasites do not show any high increase in binding to any known receptor (static binding assays)

Binding assays on static recombinant CD36 showed no change in binding from HB3-uns or HB3-HBEC. This does not necessarily imply that HB3-HBEC parasites are able to bind to CD36. The adhesion seen could result from unselected parasites within the HB3-HBEC population. A “re-binding” assay is necessary to test whether HB3-HBEC parasites are able to bind to CD36 (i.e. to detach parasites from HBEC-5i and incubate them on CD36). Alternatively, in order to estimate the CD36 binding/non-binding ratio in a population, one

could use a saturating amount of CD36-covered beads and count the number of bound and unbound parasites.

The increase of binding to gC1qR and Integrin αV does not definitely mean that they are involved in the HBEC-5i-parasite interaction. It could simply reflect the fact that the HB3-HBEC parasites are expressing a different ligand molecule from HB3-Uns that would be able to bind to some extent to gC1qR and Integrin αV. For example, gC1qR and Integrin αV with a pI of 4.74 and 5.45 respectively are predicted to be highly negatively charged at neutral pH. On the other hand, ICAM1 and CD36 would be positively charged with pI of 7.8 and 9.24, respectively. Thus it may indicate that HB3-HBEC, but not HB3-uns, parasites are expressing a positively charged ligand that would bind non-specifically to gC1qR and Integrin αV.

Finally, as previously mentioned (section 3.5.5), the static binding assay approach is missing a positive control for most receptors. Ideally, parasites should be selected on each receptor to be used as a control. They could also be utilized to work out the optimal conditions for adhesion to each receptor (pH, concentration, buffer).

3.6.7 Binding inhibition assays do not clearly identify the HBEC-5i receptor

Various proteins and antibodies were tested for their binding inhibition capabilities. Only heparin seems to consistently reduce the cytoadhesion, while the Integrin αV and NCAM antibodies showed some partial inhibition. α-NCAM was tested twice and α-Integrin once thus these experiments are worth being repeated. A similar experiment performed with HB3 on an immortalized HDMEC line with α-ICAM1 15.2, α-CD36 and α-thrombospondin did not inhibit binding either (Xiao, et al., 1996). On the other hand, another group using the same strain and endothelial cells, succeeded to inhibit binding with α-Integrin αV (by 45%), with α-ICAM and α-CD36 (by 65% each) (Siano, et al., 1998). The amount of parasites adhering to HDMEC was however very low, even without any antibody.

Note that, as for the binding assay approach, a positive control is crucially missing for most assays. Also, these experiments analyze each putative receptor

individually. It is possible that cooperation between two or more molecules produce the binding of iRBC. This synergetic effect has been shown between CD36 and ICAM1 proteins (McCormick, et al., 1997).

Heparin is the most highly negatively charged biological molecule. Its anti-cytoadherence activity may due to a charge effect. One would therefore predict that the *P. falciparum* ligand is positively charged.

The binding inhibition induced by heparin may point towards a glycosaminoglycan (GAG) being the receptor for cytoadherence. GAGs are long unbranched polysaccharides consisting of a repeating disaccharide unit. They are usually attached to a core protein to form the proteoglycan. Proteoglycans act as receptors to numerous pathogens (Bartlett and Park, 2010). This includes *P. falciparum* as iRBC are able to adhere to CSA in the placenta. Heparan sulfate from lung endoethelial cells has also been shown to bind to iRBC via PfEMP1 (Vogt, et al., 2003). We tried to remove heparan sulfate from HBEC-5i using Heparinase III and hyaluronic acid using hyaluronidase before doing a binding assay with HB3-HBEC parasites. The results were inconclusive due to technical issues. This experiment should be repeated as a priority, as it may give a good indication whether GAG are the receptors. Also, Chondroitinase ABC should be tested as it cleaves a wider range of sugar moieties, exposing the proteoglycan part (for example (Andrews, et al., 2005)).

ICAM1 is frequently postulated as the receptor for sequestration of iRBC in cerebral malaria cases. However no polymorphism in the gene sequence has yet been shown to confer protection from malaria, and field isolates from cerebral malaria cases are not statistically associated with ICAM1 binding (reviewed in (Rowe, et al., 2009a)). Our data show that HB3-HBEC do not bind to recombinant ICAM1 under static conditions and that α-ICAM1 antibodies do not reduce cytoadhesion to HBEC-5i. The positive control A4 however binds well to ICAM1 on a Petri dish and does not bind to HBEC-5i. Therefore ICAM1 is not the HBEC-5i receptor for HB3-HBEC selected parasites.

3.6.8 HB3-HBEC parasites also cytoadhere to HB/D/PMEC

Perhaps surprisingly, unselected parasites, which bind to CD36 in a Petri dish, only slightly cytoadhere to CD36 expressing lines like HDMEC and HPMEC. However, the concentration of soluble CD36 in the static binding assay is probably much higher than what is found at the surface of these endothelial cells. Equally important, the CD36 on endothelial cells may not be "available" for the parasites to bind to, for example if cells are covered with various carbohydrates.

Interestingly, HB3 parasites selected for HBEC-5i adhesion also adhere to HBMEC, HDMEC and HPMEC. Xiao and colleagues observed similar results after selecting HB3 on HDMEC or C32 cells: the selected parasites were able to bind to many cell lines, including HBEC-5i (Xiao, et al., 1996). This is in line with post-mortem data showing sequestration in various locations of the body. The most likely hypothesis from this *in vitro* model is that the same *P. falciparum* ligand is binding to a receptor found on all endothelial cells. Whether this is the case *in vivo* remains to be tested.

3.6.9 Future work to identify new endothelial cell receptors

It is striking how, apart from CD36, ICAM1 and CSA, putative receptors have been poorly investigated, often by a single publication. If any of these "neglected" surface proteins (Integrin, gC1qR, Fractalkine, NCAM) were found to be critical for cerebral malaria, they could be a potential drug or vaccine target. Moreover, it has to be noted that a systematic, high-throughput investigation of all endothelial cell surface receptors binding to iRBC has not been performed to date. Thus it is likely that more receptors remain to be discovered. A pilot experiment using yeast 2-hybrid screening has attempted to fulfil this gap (Vignali, et al., 2008). *P. falciparum* fragment proteins were tested against human liver and cerebellum libraries. Various technical issues induced a large number of false positive interactions therefore the results are inconclusive. A library of all 2200 human secreted proteins has recently been reported (Lin, et al., 2008) hence this type of approach could be applied using *P. falciparum* ligand(s) as probe(s).

An easier receptor identification approach, yet comprehensive and unbiased, has been described using HBMEC (Zou, et al., 2006). Zou and colleagues discovered the HBMEC receptor mediating the binding with the *E. coli* protein IbeA. The HBMEC were biotinylated to purify all surface proteins. These were resolved by SDS-PAGE and transferred to a PVDF membrane. A GST-tagged IbeA protein was incubated with the membrane protein lysate, assuming the ligand IbeA would bind to its receptor. Finally, a mass spectrometry analysis identified vimentin as the receptor for IbeA. The same method could be applied to HBEC-5i, using the *P. falciparum* ligand(s) as the probe. The recombinant ligand, or at least the domain from that protein mediating the cytoadherence, could be tagged with GST to identify the HBEC-5i receptor on a gel.

Once a few putative receptor candidates are identified, one could relatively easily suppress the receptor expression using RNAi technology. Kits with short hairpin RNA specific to a particular gene are now commercially available (Sigma). This has allowed, for example, the transfection of HBMEC to silence the CD44 transcript (Jong, et al., 2008).

The new receptor identification technique (Zou, et al., 2006) and the RNAi transfection (Jong, et al., 2008) were both successfully performed with HBMEC, thus they could very likely be applied to HBEC-5i or the HBMEC used in this study.

3.6.10 New heparin-like compounds inhibit cyotadherence to HBEC-5i

CRDS is already an anti-adhesion drug candidate thanks to its activity as *P. falciparum* invasion and rosetting inhibition (Havlik, et al., 1994, Kyriacou, et al., 2007). It is also safe to use in adult patients with malaria (Havlik, et al., 2005). Our data shows that it can also prevent most of cytoadhesion to HBEC-5i. Whether CRDS can reverse cytoadhesion (i.e. to detach already bound iRBC) remains to be tested. This should ideally be done under flow conditions. LMP-420 is another drug inhibiting cytoadhesion to HBEC-5i *in vitro* (Wassmer, et al., 2005). It would be interesting to compare LMP-420 and CRDS in the same set of experiments.

MS29 and MS31, two new heparin-like compounds, also merit further investigations. Preliminary data suggest a high anti-cytoadhesion activity when HBEC-5i are used. This effect is however weaker with HDMEC or HPMEC. The anticoagulant property of these heparin derivatives will be an essential feature to test.

As 85% of malaria-related deaths in hospitalised patients occur within 24-hour post admission (Marsh, et al., 1995), it is of great importance to develop a drug acting quickly on sequestration. CRDS, MS29 and MS31 are worth further investigations for their potentiality to be used as reversal cytoadherence drugs.

However, the effect of such a drug should also be taken into considerations. It is not known how the human body would coop with iRBC being released from the microvasculature all at once. The consequences of this burden on the spleen for example are unknown, although in saimiri monkeys sequestration was reversed without any damaging effect to the animals (David, et al., 1983).

All in all, this chapter achieved its first goal of selecting many *P. falciparum* strains (HB3, 3D7, IT, HB3 with 10% serum and HB3 on TNF activated cells) for cytoadhesion to HBEC-5i. Other phenotypes were also observed as a result from the selection, such as a significant reduction in platelet-mediated clumping. HB3-HBEC also binds to HDMEC and HPMEC, indicating that the binding is not specific to HBEC-5i only. It has not been possible to identify the HBEC-5i receptor, although gC1qR and Integrin αV may have a role in the cytoadhesion process.

4 Chapter IV: Bioinformatics analysis of variant surface antigens

4.1 Abstract

Various *P. falciparum* strains were selected for their binding ability to brain endothelial cells (chapter 3). Cytoadhesion is thought to be mediated by the parasite variant surface antigens (VSA). These genes carry at least one hypervariable domain of which the unique sequence is not found in any other parasite clone. The current microarray chip is based on the 3D7 genome, i.e. the array contains oligos specific to the 3D7 VSA only. Thus, in order to analyse the VSA transcription from other strains (HB3, Dd2, IT), it was necessary to supplement the existing 3D7-based microarray chip with new oligos specific to each VSA.

The HB3, Dd2 and IT genomes have been sequenced but not yet annotated. All VSA (*var, rif, stevor, Pfmc-2TM*) were extracted from these genomes using an HMMer approach with Perl scripts. Oligos specific to these VSA were designed with OligoRankPick. This updated microarray chip will be used in chapter 5.

4.2 Introduction

The main *Plasmodium falciparum* parasite ligand molecules mediating sequestration are thought to be PfEMP1 variants, encoded by *var* genes. Different PfEMP1 variants have been shown to bind *in vitro* to CD36, ICAM-1, PECAM-1, P-selectin, heparan sulfate and possibly thrombospondin (See introduction chapter for further details). All these studies focused on the interaction between PfEMP1 (or PfEMP1 domains) with a particular receptor, but none has considered whether other variant surface antigen (VSA) families could also be involved.

As mentioned in the introduction chapter, other VSA families show characteristics that make them, in principle, suitable cytoadherence ligands.

Surfin, *Pfmc-2TM*, *rif* and *stevor* multigenic families all encode proteins predicted to be exported ("Pexel" motif) with at least one transmembrane (TM) domain (Templeton, 2009). Pfmc-2TM, Rifin and Stevor share a similar sequence structure with a hypervariable loop. This hypervariability is thought to be driven by the host immune pressure and this would indicate the presence of these proteins at the membrane surface (Lavazec, et al., 2006). In fact immunofluorescence assays indicate that Rifin subgroup A (RifA) and Stevor proteins are located at the surface of infected red blood cells (iRBC) (Niang, et al., 2009, Petter, et al., 2007). Rifins localization had already been shown by surface-iodination, trypsinisation and immunoprocipitation (Kyes, et al., 1999). Moreover, these two VSA families naturally elicit antibodies production by the host immune system (Abdel-Latif, et al., 2004, Abdel-Latif, et al., 2003, Abdel-Latif, et al., 2002, Schreiber, et al., 2008).

Despite these interesting features rendering Surfin, Pfmc-2TM, Stevor and Rifin proteins cytoadherence ligand candidates, this possibility has hardly ever been explored. Apart from the special case of the adhesion to chondroitin sulfate A (CSA), only one study has investigated whether VSA other than PfEMP1s are involved in cytoadherence (Mok, et al., 2007). In that publication, CD36 and rosetting selected 3D7 parasites showed high upregulation of particular *var* genes but also some *rif* and *PHIST* genes. Therefore, in order to identify the parasite ligand(s) binding to HBEC-5i, an unbiased approach taking into account the entire genome of *P. falciparum* was needed.

Microarray technology was one of the very first techniques to allow the analysis of a whole transcriptome at the same time, as opposed to individual gene techniques like Northern blotting or reverse transcriptase-PCR (RT-PCR). First developed in the late nineties, microarrays are now performed with cDNA from all model organisms, including humans. The basic principle is the complementarity between a transcribed gene and its specific probe (a short oligonucleotide). Preceding hybridization, transcribed genes are reverse transcribed to cDNA and labelled with a fluorescent dye. Once bound to the probe (oligo), the amount of light emitted by the probe is proportional to the amount of mRNA present in the transcriptome.

Microarray applications are thus limited to organisms with sequenced genomes. For *P. falciparum*, the current microarray chip is made of oligos specific to clone 3D7, the first and only clone fully sequenced, assembled and annotated to date (Gardner, et al., 2002). In *P. falciparum*, the vast majority of genes have virtually identical sequences from one strain to the other. The divergence is limited to a few single nucleotide polymorphisms (SNP) that have no or little effect for microarray hybridizations (Llinas, et al., 2006). In fact, the very first microarray experiment was performed with the HB3 clone on the 3D7-based microarray chip (Bozdech, et al., 2003). However, by definition, the sequences of the variant surface antigens (VSA) are unique to each strain. Therefore these genes require strain-specific oligos for microarray purposes.

At the start of this PhD, the strains HB3, Dd2 and to a lesser extent IT had just been sequenced but not yet annotated. Thus the aim of this chapter is to extract all VSA sequences from the above-mentioned genomes and design specific oligos for updating the microarray chip.

4.3 Methods

4.3.1 Extracting sequences from a genome

The entire method used for extracting VSA sequences is outlined in Figure 4-1.
HMMer is an implementation of profile Hidden Markov Model (HMM) software for protein sequence analysis (Eddy, 1995). HMM is a statistical model used to determine the hidden parameters from the observable parameters (Eddy04).
In this case, HMMer is used to search for VSA homologues in the HB3/Dd2/IT genomes using an "HMMer profile" based on an alignment of 3D7 sequences. In other words, the program uses conserved motifs within a given protein family and finds similar motifs in a new genome.

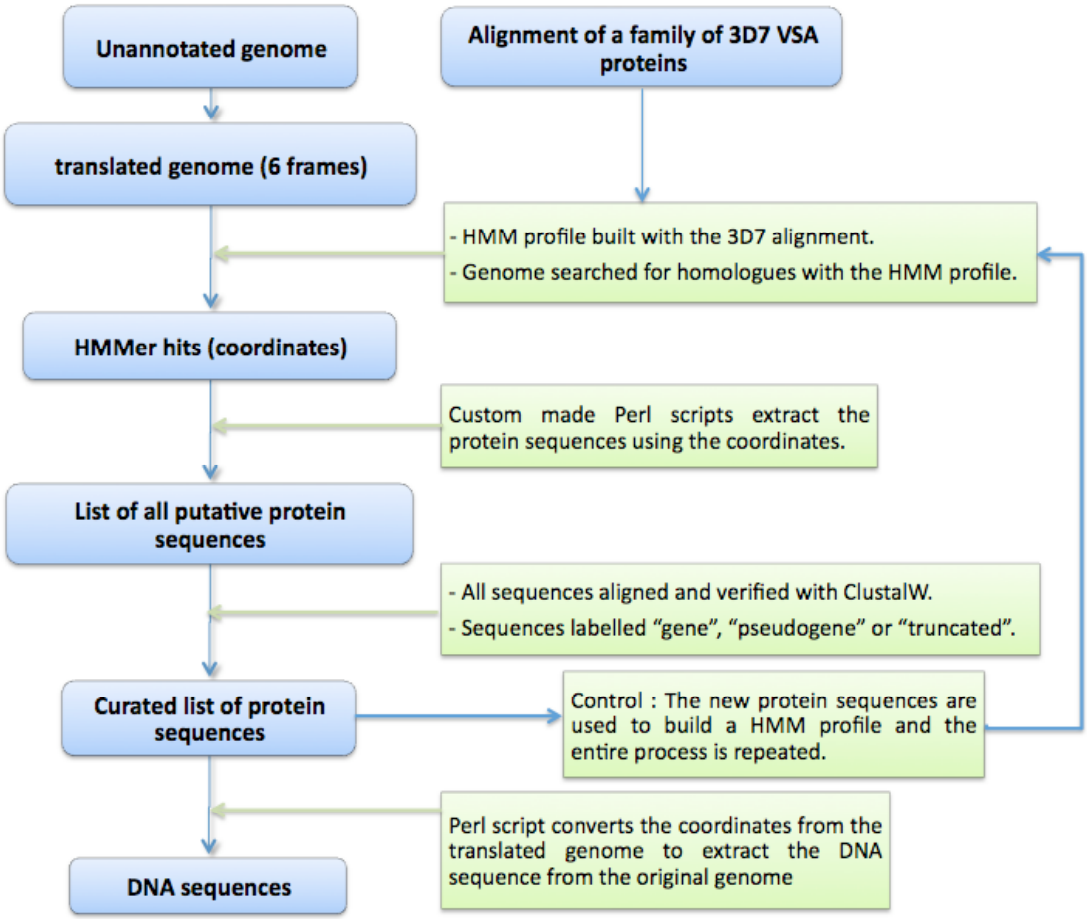


Figure 4-1. Flowchart of the process used for extracting VSA sequences from a genome.

To establish the HMMer profile, each translated exon of each VSA family (*var*, *rif*, *stevor*, *Pfmc-2TM*, *Surfin*) of the well-annotated 3D7 genome was aligned separately with ClustalW. Each resulting file was used to build a profile HMM specific to that exon. These profiles were used to search for homologues in the 6 frames of the translated HB3, Dd2 and IT genomes, as well as the *Neurospora crassa* (negative control, genome of similar size) and 3D7 genomes (positive control). The HMMer output file only shows the coordinates of the hits, thus Perl scripts (see Appendix) were used to retrieve the actual amino acid sequences from the coordinates. All hits, even with relatively poor E-values, were aligned with the original 3D7 exons and visualized with ClustalW-JalView. This arbitrary non-stringent cut-off was used to make sure no sequence was

missed (see Table 4-1 in section 4.4.1). Alignments were verified by eye and hits that were obviously not part of the expected protein family were deleted. Sequences with stop codon(s) and/or frameshift were annotated as "pseudogene" while shorter sequences with missing amino acids were annotated as "truncated". Other Perl scripts (appendix) were used to concatenate translated exon1 with the appropriate translated exon2. DNA sequences were also retrieved using the coordinates from the HMMer output file. As a last control, each group of newly found VSA sequences were used to build a HMM profile and searched against their original genomes. If a comprehensive set of VSAs had been extracted in the initial procedure, then no new sequences would be expected in the repeated search.

For the subgrouping annotation of *var* genes, 500bp upstream of the start codon were extracted and aligned (ClustalW) with known upstream sequences from 3D7.

4.3.2 Designing specific oligos for a microarray chip

70-mer long oligonucleotide probes ("oligos") specific to the extracted VSA sequences were designed using OligoRankPick (Hu, et al., 2007). This Perl-written software selects one or more optimal oligo sequences for each VSA gene based on four parameters: (1) uniqueness of the sequence to avoid possible cross-hybridizations with other targets in the genome, (2) sequence complexity which evaluates the presence of short nucleotide repeats, (3) GC content which influences the melting temperature, (4) the reverse Smith-Waterman score which evaluates the possibility of self-binding (internal secondary structures). Note that oligo sequences only need to be unique within a single genome, not across clones. This is because the two populations hybridized together are always derived from the same clone (e.g. 3D7 cDNA is never hybridized with HB3 cDNA so it would not matter if HB3 oligos cross-hybridize with 3D7 VSA sequences).

The vast majority of oligos were designed by Dr Guangan Hu (Zbynek Bozdech group, NTU, Singapore). As explained later in this chapter, an updated version of

the IT genome was released during the course of this PhD. Oligos specific to the "new" IT *var* genes were designed by myself using OligoRankPick.
Oligos were synthesized by Invitrogen.

4.4 Results

4.4.1 VSA sequences extracted from HB3/Dd2/IT genomes

The software HMMer was used to extract all VSA sequences from HB3, IT and Dd2 genomes in order to design oligos for microarray analysis. For each gene family, the number of hits returned from HMMer was compared to 3D7 (positive control) and *N. crassa* (negative control) (see Table 4-1 as an example). The coordinates of all extracted sequences are given in the appendix. Some genes or truncated genes were found on 2 different supercontigs. More exactly a full-length VSA gene on a long supercontig sometimes showed 100% identity with a shorter sequence on a short supercontig. These short sequences were labelled "duplicated" and not used further.

E-value cutoff	**3D7 hits**	**HB3 hits**	**Dd2 hits**	**IT hits**	***N. crassa* hits**
E-150	154	96	86	84	0
E-100	171	114	108	111	0
E-50	174	127	124	121	0
E-20	177	131	133	129	0
E-10	179	143	143	138	0
E-06	179	146	152	142	0
0.1	179	148	159	144	1

Table 4-1. Number of HMMer hits with 3D7 Rifins exon2 as a profile. Aligned 3D7 Rifins exon2 were used as a HMMer profile and searched against HB3, Dd2 and IT translated genomes. This table indicates the numbers of hits (amino acid sequences) that pass a given E-value threshold. 3D7 is shown as a positive control and *N. crassa* as a negative control. Note that because HMMer uses only peptide sequences, pseudogenes containing frameshift mutations may appear as two or three hits (one hit per frame). Similar tables were generated for each exon of each VSA family.

Since this bioinformatics work was carried out, other groups have published some of the data. When this is the case, the published gene names or annotation is used here (Joannin, et al., 2008, Kraemer, et al., 2007, Schreiber, et al., 2008, Wang, et al., 2009a). Also, I updated the annotation of the 3D7 *rif* and *stevor* gene families (see appendix). These modifications will be published as part of the PlasmoDB reannotation effort.

4.4.1.1 *Var* genes

The total number of *var* genes and pseudogenes detected in the four parasite strains is indicated in Table 4-2. Kraemer *et al* published the annotation of HB3 and IT *var* genes (Kraemer, et al., 2007) hence their nomenclature will be used here. However, at the time of publication of that study, the IT genome was not sequenced as extensively as it is today. Thus I repeated my HMMer approach in September 2009 and identified an additional 8 "new" *var* genes as well as completing full-length genes for 7 sequences that were previously described as "truncated". The upstream sequences of all IT *var* genes were also extracted in order to identify the subgrouping of 14 genes (see Appendix section "IT PfEMP1 sequences").

The annotation of the Dd2 *var* gene repertoire has not yet been published. Altogether 50 *var* genes were extracted; including 8 truncated genes (due to incomplete genome sequencing) and excluding 6 duplicated sequences. I identified a copy of *var1csa*, which is probably a pseudogene, a copy of *var2csa* (while HB3 has got 2 copies, 3D7 & IT a single copy) and no "Type3" *var* genes. 43 genes could be subgrouped according to their upstream sequences: 11 Ups A (including *var1csa*), 21 Ups B, 10 Ups C and 1 Ups E (*var2csa*). The rest were truncated genes where the upstream sequence was not available.

	3D7	HB3	Dd2	IT
var genes	62	38	39	49
Pseudogenes	1	6	4	3
Truncated genes	0	6	7	4
Total	**63**	**50**	**50**	**56**

Table 4-2. Summary of all extracted *var*/PfEMP1 sequences. Pseudogene = sequence containing at least one stop codon and/or a frameshift. Truncated = sequence partly missing due to incomplete sequencing. These numbers do not take into account duplicates (i.e. a sequence identical but shorter than another sequence of the same strain).

4.4.1.2 *Rif* genes

The total number of *rif* genes and pseudogenes detected in the four parasite strains is indicated in **Table 4-3**. The coordinates of each extracted sequence are given in the appendix. Considering that HB3, Dd2 and IT have been sequenced to roughly the same extent, it is interesting to note that the number *rif* genes is similar in these three strains (about 125-130). The 3D7 clone however has got about 180 *rif* genes.

After ClustalW alignment of all Rifins of all 4 strains, I noticed that about one third of sequences have the same "gap" of about 25 amino acids (aa) in the middle of the conserved region. This gap includes two cysteine residues, which could involve a different conformation (Figure 4-2). Interestingly, this ratio of "gapped" Rifins is the same in all 4 strains. Recently, Joannin *et al* made the same discovery and renamed the gapped Rifins "RifB" while other Rifins are named "RifA"(Joannin, et al., 2008). Importantly, the subgrouping has been linked to Rifin localization within the iRBC: RifAs are exported towards the iRBC membrane via the Maurer's Cleft while RifBs seem to reside within the parasite (Petter, et al., 2007). Neither of these studies however has extracted the full repertoire of *rif* and *stevor* genes of any strain.

	3D7	HB3	Dd2	IT
rif genes	153	100	99	102
Pseudogenes	28	21	21	15
Truncated	3	4	13	8
Total	**184**	**125**	**132**	**125**

Table 4-3. Summary of all extracted *rif*/Rifin sequences. Pseudogene = sequence containing at least one stop codon and/or a frameshift. Truncated = sequence partly missing due to incomplete sequencing. These numbers do not take into account duplicates (i.e. a sequence identical but shorter than another sequence of the same strain).

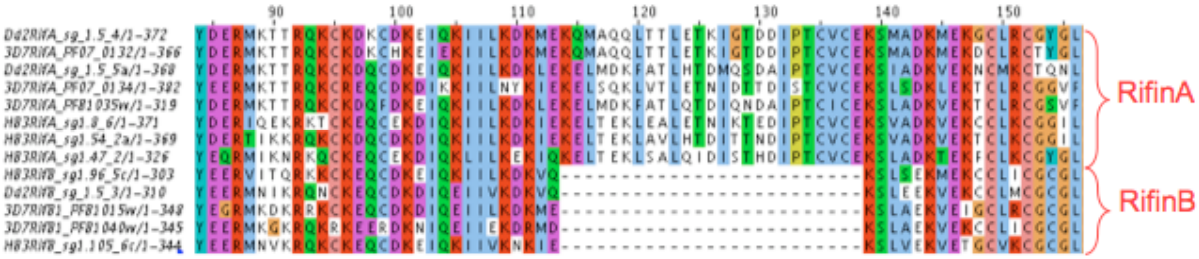


Figure 4-2. **Alignment of 13 Rifins from 3 strains.** RifinA subgroup is defined by the 25 extra amino acids found in the conserved domain of Rifins. This region is absent in RifinB subgroup.

4.4.1.3 *Stevor* genes

The total number of *stevor* genes and pseudogenes detected in the four parasite strains is indicated in Table 4-4. The coordinates of each extracted sequence is given in the appendix.

Alignment of all *Stevor* also revealed two subgroups that Schreiber *et al* named Stevor A and Stevor B (Schreiber, et al., 2008). Whether this subdivision represents any difference in localization or function is still unknown. HB3, Dd2 and IT Stevors can also be divided in Stevors As and Bs (see appendix).

	3D7	HB3	Dd2	IT
stevor genes	30	17	24	25
Pseudogenes	7	9	7	8
Truncated	0	0	0	0
Total	**37**	**26**	**31**	**33**

Table 4-4. Summary of all extracted *stevor*/Stevor sequences. Pseudogene = sequence containing at least one stop codon and/or a frameshift. Truncated = sequence partly missing due to incomplete sequencing. These numbers do not take into account duplicates (i.e. a sequence identical but shorter than another sequence of the same strain).

4.4.1.4 *Pf*mc-2TM genes

The total number of *Pfmc-2TM* genes and pseudogenes detected in the four parasite strains is indicated in Table 4-5. The coordinates of each extracted sequence is given in the appendix. The hypervariable loop of *Pfmc-2TM* is only about 50 nucleotides long on average (Lavazec, et al., 2006). Oligos for the microarray chip need to cover a unique stretch of 70 nucleotides. So the variability within the *Pfmc-2TM* gene family is too little to design specific oligos for each gene.

	3D7	HB3	Dd2	IT
Pfmc-2TM genes	10	7	2	6
Pseudogenes	3	1	0	2
Truncated	0	0	1	0
Total	**13**	**8**	**3**	**8**

Table 4-5. Summary of all extracted *pfmc-2TM*/Pfmc-2TM sequences. Pseudogene = sequence containing at least one stop codon and/or a frameshift. Truncated = sequence partly missing due to incomplete sequencing. These numbers do not take into account duplicates (i.e. a sequence identical but shorter than another sequence of the same strain).

4.4.1.5 *Surfin* genes

Based on *surfin* genes from 3D7 only, this family was first described as VSA (Winter, et al., 2005). However, ClustalW alignments with HB3 and Dd2 *surfins*

indicate that each ortholog is very well conserved from one clone to the other (Figure 4-1). In other words, although *surfin* paralogs within one strain show variability between each other, there is no variability between strains (Templeton, 2009). Thus unlike previously reported by Winter et al (Winter, et al., 2005), this is not a VSA family. For microarray purposes, there is no need to design new oligos for this gene family.

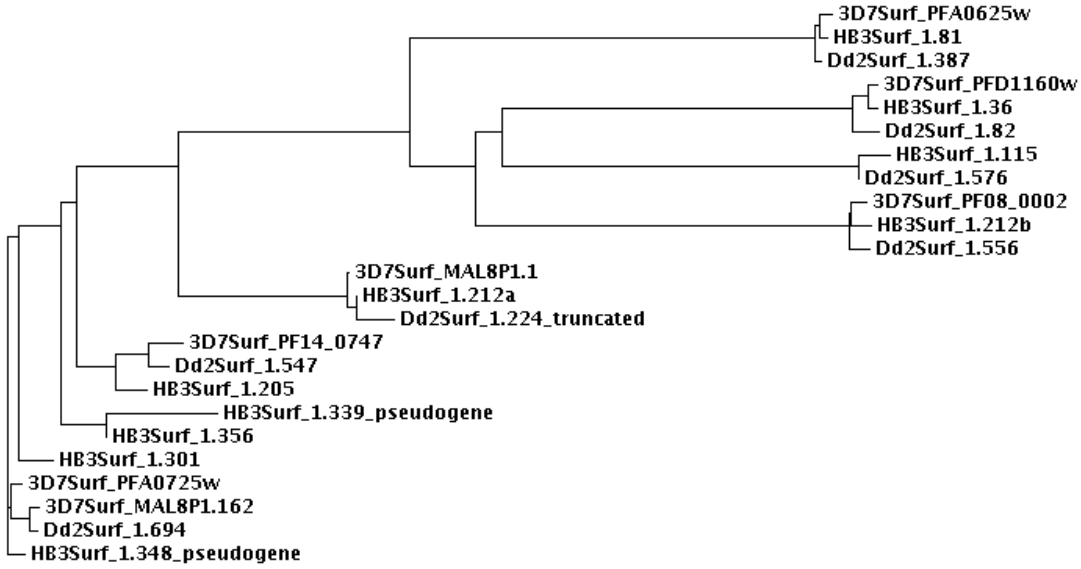


Figure 4-3. Phylogenetic tree of Surfin proteins from 3D7, HB3 and Dd2. Note how, as opposed to other VSA families, orthologs are very easily identified.

4.4.2 HB3/Dd2/IT VSA specific oligos added to the microarray chip

A total of 990 70-mer oligos corresponding to the *var*, *rif* and *stevor* gene families of HB3, Dd2 and IT were added to the 10166 existing oligos on the *P. falciparum* microarray chip (Hu, et al., 2007). The sequences of the new oligos are shown in the appendix.

4.5 Discussion

VSA sequences from HB3, Dd2 and IT genomes were extracted using HMMer and Perl scripts. The multiple controls carried out using HMMer (repeating the approach with the output sequences and extraction of the original 3D7 VSAs)

give confidence that no VSA sequences were missed. Some VSA sequences were, however, truncated due to the incomplete assembly of the HB3, Dd2 and IT genomes. Although these parasite strains have been sequenced at a relatively high coverage (≥ 8X), the assembly resulted in 1189, 2837 and 2185 supercontigs for HB3, Dd2 and IT, respectively. This resulted in a few sequences located near the ends of the contigs being truncated, especially for the *var* family due to the length of its genes.

It is possible that some VSA genes are missing altogether from these incompletely sequenced genomes and would therefore not be represented on the microarray chip. RT-PCR with DBLα universal primers allows identifying transcribed *var* genes (see chapter 6). We found no *var* tag that did not exist in the sequenced HB3/Dd2/IT genome (chapter 6 and Rowe group unpublished data), thus indicating that the number of missing *var* genes would be small, if any.

Kraemer *et al* published the annotation of HB3 and IT *var* genes (Kraemer, et al., 2007). They used a different approach based on the DBLα motif with BLAST and Artemis tools. Their results are virtually identical to mine. However they do not indicate that *HB3var43p, 44p,* and *45p* are short duplicated sequences and thus likely to be assembly errors. As stated above, the HB3 genome is currently assembled as 1189 supercontigs (a complete assembly would result in 14 supercontigs corresponding to the 14 chromosomes, as is the case with 3D7). Some of the smallest supercontigs are almost completely identical to parts of larger supercontigs. These short supercontigs could correspond to genuine genome duplications but more likely are redundant sequences that have not been assembled yet. *HB3var43p, 44p,* and *45p* happen to be on these short supercontigs (Kraemer, et al., 2007). Also, because Kraemer *et al* based their search on the DBLα domain only, they missed out a couple of short duplicated sequences that do not show a DBLα domain due to truncation. In all cases, whether these "duplicated" VSA are genuine or not is irrelevant for microarray purposes, as 2 identical genes would be represented by the same oligo(s).

New sequencing technologies now allow the sequencing of genomes at unprecedented scales and new sequenced lab strains and field isolates are to be expected in the near future (Dominic Kwiatowski communication). The method presented here, sequences extraction with HMMer and oligo design with OligoRankPick, is fairly quick and straightforward and could be applied to any new *Plasmodium* genome. This handy tool will be of great use in order to analyze a wide range of *P. falciparum* strains by microarray. Note however that in the longer term the future of transcriptome analysis probably lies in Illumina-based massively parallel sequencing (RNA-seq) (Otto, et al., 2010), which directly sequences the cDNA. This new technique avoids the need to design oligos and leads to the identification of gene boundaries and alternative splicing events which microarray does not allow.

5 Chapter V: Transcriptome analysis of *P. falciparum* parasites selected for cytoadherence to human brain endothelial cells.

5.1 Abstract

Cerebral malaria is characterised by an accumulation of infected erythrocytes in the microvasculature of the brain. This process can be studied *in vitro* using Human Brain Endothelial Cell line (HBEC-5i). *P. falciparum* infected erythrocytes have been shown to bind to HBEC-5i, however, the parasite adhesion ligands necessary to anchor the infected erythrocytes onto HBEC-5i have not been identified. This chapter aims to identify parasite variant surface antigens (VSA) and other genes that are differentially transcribed after selection for cytoadherence to HBEC-5i.

In chapter 3, the *P. falciparum* laboratory strains HB3, 3D7 and IT/FCR3 were selected using a panning assay for binding to HBEC-5i. This led to a distinct phenotype between the selected cytoadherent parasites and the unselected non-binding parasites. In this chapter RNA samples from selected and unselected populations were extracted in a time-course study. The entire transcriptomes were characterized and compared using microarray technology. The data indicates a massive upregulation of *HB3var3*, *var_PFD0020c*, *ITvar7* and *ITvar19* by 17 to 100 fold in HB3, 3D7 and IT selected parasites, respectively. Activation of HBEC-5i with TNF, a cytokine found at high level in cerebral malaria patients, did not change the *var* gene expression pattern. The only other genes to be highly upregulated (15-18 fold) in HB3 and 3D7 selected parasites were the *rif* genes chromosomally located "head to head" to the upregulated *var* gene. Different analyses of the non-VSA genes point towards other candidates that could be directly or indirectly involved in cytoadhesion, although none were upregulated more than 3 fold in selected parasites. They include: MAHRP-1, a PHISTc, a PHISTa and other exported proteins. PfEMP3

and RESA-1 are also upregulated in all selections. In conclusion, the specific PfEMP1 variants encoded by the highly upregulated *var* genes and their associated upregulated head-to head *rif* are the strongest candidates for the parasite ligands binding to HBEC-5i. Whether these PfEMP1 variants and other possible candidates are actively involved in cytoadherence remains to be tested.

5.2 Introduction

Sequestration, resulting from the binding of *Plasmodium falciparum* infected red blood cells (iRBC) on the walls of microvessels, is one of the key features that distinguish *P. falciparum* infection from other human malarias. This is thought to be a way for pigmented trophozoites to avoid spleen clearance (Buffet, et al., 2009). Sequestration is also the hallmark of cerebral malaria (reviewed in (Combes, et al., 2006)) as iRBC can be seen in the brain microvasculature of all cerebral malaria patients (Seydel, et al., 2006). The binding of an iRBC to an endothelial cell must involve at least two molecules: a ligand (parasite protein located at the surface of the iRBC) and a receptor (host protein located at the surface of the endothelial cell, see chapter 3). The ligand is postulated to be a member of the *Plasmodium falciparum* Erythrocyte Membrane Protein 1 (PfEMP1) family as they have been shown to bind to many receptors, including some found at the surface of brain endothelial cells (reviewed in (Rowe, et al., 2009a)). These proteins are encoded by *var* genes and are fully described in chapter 1 and 6. However, a direct proof that a PfEMP1 variant binds to a brain endothelial cell has not been shown yet. Research to solve this question is impeded by the absence of *var* genes in any rodent malaria parasite genome (Hall, et al., 2005). Therefore, only *P. falciparum* species can be used to investigate the mechanism of iRBC sequestration in microvessels.

A new *in vitro* model for cerebral malaria has recently been developed. By extracting endothelial cells from human brain tissue and immortalizing the cells *in vitro* (Dorovini-Zis, et al., 1991), it is possible to study the direct interaction between these cells and *P. falciparum* iRBCs (Wassmer, et al., 2005,

Wassmer, et al., 2006a, Xiao, et al., 1996). Until now these studies have mostly focused on the endothelial cell response after iRBC cytoadherence (Tripathi, et al., 2007(Wassmer, et al., 2006b)). To our knowledge, the identification of parasite ligands binding to human brain microvascular endothelial cells (HBEC-5i) has never been investigated.

Moreover, the vast majority of cytoadherence related publications have considered only PfEMP1 as putative ligands (Rowe, et al., 2009a). As detailed in chapter 1 and 4, other variant surface antigens (VSA), like Rifins and Stevors, could in theory be involved in cytoadhesion. A comprehensive and unbiased approach is needed to explore the possibility that any of the ~5500 *Plasmodium falciparum* genes may play a role in binding to HBEC-5i.

Microarray technology was one of the very first techniques to allow the analysis of a whole transcriptome at the same time, as opposed to individual gene techniques like Northern blotting or reverse transcriptase-PCR (RT-PCR). First developed in the late nineties, microarrays are now performed with cDNA from all model organisms, including humans. The basic principle is the complementarity between a transcribed gene and its specific probe (a short oligonucleotide) (Leung and Cavalieri, 2003). Preceding hybridization, transcribed genes are reverse transcribed to cDNA and labelled with a fluorescent dye. Once bound to the probe (oligo), the amount of light emitted by the hybridized product is proportional to the amount of mRNA present in the transcriptome. Microarray is thus suited for measuring changes in gene expression in parasites selected for binding to HBEC-5i.

VSA are the best ligand candidates due to their localization at the surface of the iRBC and the fact they naturally elicit antibody production by the host immune system (Jemmely, et al., 2010). They are also characterized by hypervariability in part of their sequences, hence the need to design specific oligos for every parasite strain to be used in a microarray analysis (chapter 4). The possibility that Rifins and Stevors may be involved in cytoadherence has only been examined once, in a transcriptome comparison between CD36-binding and rosetting 3D7 parasites (Mok, et al., 2007). Two *rif* variants, among

other non-VSA genes, were found to be linked with cytoadherence, but no direct evidence that Rifins mediated cytoadherence has yet been shown.

Non-VSA genes may also be necessary for binding to HBEC-5i, at least indirectly (i.e. indispensable for cytoadherence without being the actual molecule mediating the binding to the receptor). In the last few years, non-VSA proteins harbouring a Pexel motif have been intensively studied (Maier, et al., 2009). The Pexel motif (RxLxQ/E) allows these proteins to be exported into the iRBC cytosol (Marti, et al., 2004). The translocon trafficking these proteins has recently been discovered (de Koning-Ward, et al., 2009). Interestingly, at least 11 Pexel proteins are necessary for PfEMP1 surface expression as well as cytoadherence (Maier, et al., 2008) (see also Table 5-17 in the discussion section). However none has yet been shown to function as a direct cytoadherence ligand.

In an *in vitro* environment, *P. falciparum* iRBC show little cytoadherence to HBEC-5i (chapter 3). After many rounds of selection for parasites binding to these cells, a large proportion of parasites do attach to HBEC-5i. We hypothesize that this major change of phenotype can be explained by a change in the transcriptome, which can be measured by microarray analysis, before and after selection. If the parasite ligands are VSAs, it would be expected that unselected parasites would transcribe a wide range of VSA while the selected populations of parasites would express a more restricted repertoire of VSA. The "up-regulation of expression of specific VSA variants" should be read here as "enrichment of VSA expression at the population level rather than in individual parasite cells". In other words, the selection would enrich the population for parasites expressing the "right" VSA, i.e. the gene(s) encoding the ligand(s) binding to HBEC-5i. If the parasite ligands are non-VSAs, it would be expected that the transcription of the relevant gene(s) would be highly upregulated after selection. VSA, but also exported proteins, will be particularly scrutinized in the microarray data analysis.

5.3 Aim of this chapter

The main aim is to identify the parasite ligand(s) mediating the interaction of *P. falciparum* infected erythrocytes with human brain endothelial cells. The hypothesis is that by selecting parasite cultures for binding to HBEC5i, we will enrich for parasites expressing the appropriate ligand. This enrichment will be assessed by microarray. A gene found to be substantially more expressed in the selected than in the unselected parasite population will be considered as a candidate for HBEC-5i cytoadherence.

5.4 Methods

An outline of the methods from parasite cultures synchronization to microarray data analysis is shown in Figure 5-1. Methods not specific to this chapter (*P. falciparum* culture, HBEC-5i selections…) were described in chapter 2.

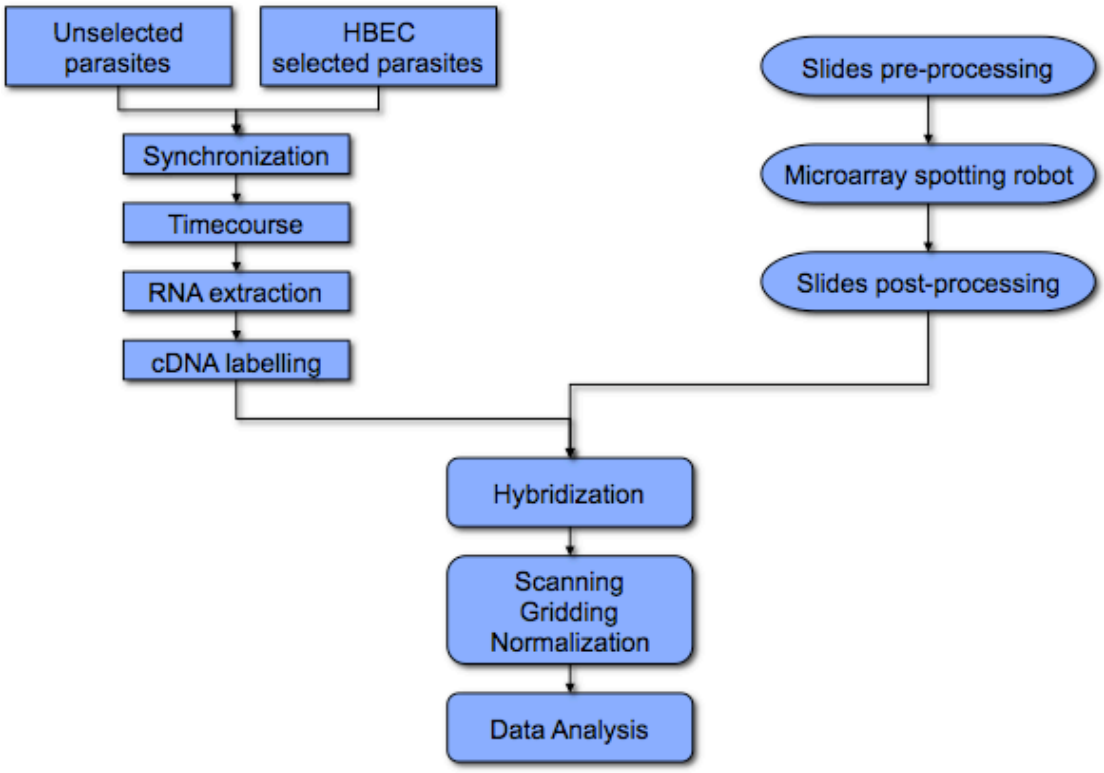


Figure 5-1. Overview of the transcriptome analysis described in this chapter.

5.4.1 Tight synchronization of parasites

For microarray experiments, tightly synchronous parasite populations are required and the selected and unselected parasite populations being compared need to be at the same stage of development (otherwise differences in the timing of transcription can give artifactual results, see section 1.4.3)

In order to synchronise parasites, a smear was taken every 2-3 hours to record the stage of development. When a schizont-rich parasite population was observed, a two-stage synchronisation procedure was carried out. Different protocols were tested and optimized: for the pilot experiment, i.e. the selection of HB3-HBEC1 and the HB3-Uns1 control, cultures were Percoll-treated while for all other selections schizont stage parasites were purified by MACS columns. Both methods are described here under.

5.4.1.1 Percoll-sorbitol procedure (pilot experiment)

Overview: The Percoll procedure separates the population into two layers: the pellet where ring stages and rosetting parasites can be found, and an upper layer with mostly pigmented trophozoite and schizont stage parasites. This upper layer is kept and fresh uninfected RBC (uRBC) are added for merozoites to reinvade. About 5 hours later the culture should contain mainly very young rings and a sorbitol treatment removes all remaining pigmented trophozoite and schizont stages parasites.

Percoll method: Parasite cultures were resuspended in 5ml complete RPMI (see chapter 2 for composition) and carefully layered over 5ml 60% Percoll (27ml Percoll (Sigma), 3ml 10x RPMI (Sigma), 15ml incomplete RPMI) then centrifuged at 1500g for 10 min. The upper layer was collected and wash twice in incomplete RPMI. uRBC were added in order to reach a parasitaemia of about 1 to 2% schizonts. Fresh complete RPMI was added to obtain a haematocrit of 2% and the flask was incubated at 37^0C.

Sorbitol method: see materials & methods chapter.

However, the Percoll protocol was judged not sensitive enough because too many rings were found in the upper layer (see results section). Thus, after this pilot experiment, schizonts were purified using MACS columns.

5.4.1.2 MACS-sorbitol procedure

Overview: Late stages parasites have accumulated hemozoin that has magnetic properties. This can be used to separate pigmented trophozoites and schizonts from ring stages using a strong magnet (QuadroMACS Separator, Milteny Biotec) (Ribaut, et al., 2008). Pigmented trophozoites and schizonts are harvested and fresh uRBC are added for merozoites to reinvade. About 5 hours later the culture should contain mainly very young rings and a sorbitol treatment removes all remaining pigmented trophozoite and schizont stage parasites. This results in a 5-hour window of synchronization.

MACS Method: Up to 200µl packed cell volume (pcv) of culture at 10-15% parasitaemia was used per LD column (MACS, Milteny Biotec). The culture was spun down and resuspended in 4mL of buffer (2% BSA in sterile Phosphate Buffered Saline (PBS, Sigma)). The suspension was poured into a LD column in the separator stand (magnet). Once all the liquid had gone through, another 1mL of buffer was added. This step was repeated a second time. The LD column was then removed from the magnet and placed on a new 15mL Falcon tube. 3mL of buffer was added and the cells were eluted using a plunger. The eluted cells were spun down and resuspended with complete medium. A smear was taken to verify there were no or very few rings in the purified preparation. A purification of over 98% schizonts was typically achieved. uRBC were added to the flask of parasites to reach a parasitaemia of about 3 to 4% schizonts.
Sorbitol method: see materials & methods chapter.

If the amount of parasites necessary for microarray experiments was not reached after this procedure, parasites were allowed to reinvade for another cycle and then sorbitol treated 6 to 7 hours after the first ring was seen.

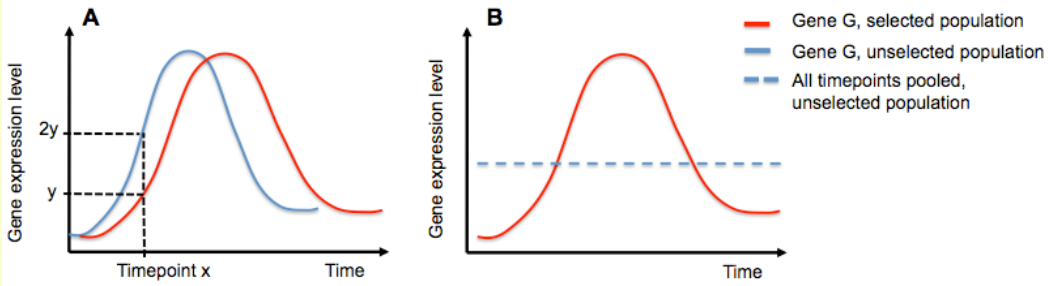
5.4.2 Time-course

Once cultures reached the appropriate quantity of material (about 1.5ml pcv at 7% parasitaemia for selected parasites, triple this amount for unselected), a time-course study was performed by taking a sample of the culture every 8 hours, starting 3 hours after the sorbitol treatment (see section 5.5.2 for amount of parasites sampled). The sample was spun down at 400 g for 5 minutes and the supernatant removed. TRIzol Reagent (mono-phasic solution of phenol and guanidine isothiocyanate, Invitrogen 15596-026) was added to the pelleted sample at a 10:1 ratio and mixed vigorously. After incubating for 5 min at room temperature (RT), the mixture was stored at -80°C.

RNA extraction (see chapter 2 section 2.5.1.) was only performed once samples from all time points were collected.

5.4.3 Pooling and reverse transcription to cDNA

Overview: In order to compare the expression of a gene before and after selection, both parasite populations need to be at the same stage of development. Synchronisation of *P. falciparum* cultures is difficult and a scenario where all schizonts would rupture at the same time is never obtained. A way to overcome this problem, after a time-course experiment, is to pool the RNA of all time points of one of the two populations to be compared (see Box 5-1). All RNA samples (time points and pools) are then reverse transcribed with the incorporation of amino-allyl dUTP to allow fixation of the dye at a later stage.



Box 5-1. Pooling all time points of one population minimizes the significance of synchronization.

Graph A indicates the expression level of the same gene in two different populations. In this example the overall amount of mRNA is the same but the synchronisation is not perfect and the selected population is slightly "ahead" of the unselected parasites. As shown on the graph, even that slight shift between the 2 populations would lead, at time point x, to a difference in gene expression of magnitude 2. Thus if we were to compare two populations that are not perfectly synchronised we run the risk of misinterpreting a shift of expression timing as a differentially regulated gene.

To overcome this issue, one can pool all time points from a population and compare this average level of gene expression against the second population (graph B). The advantage is that we are able to find out if a gene is up or downregulated after selection even if the two populations are not perfectly synchronised. Note that each time point sample from the unselected population is also hybridised against the pool.

Method: For each strain (HB3, 3D7 and IT) 12µg of RNA from the unselected parasites at each of the 6 time points was pooled together. Pools and time point samples were used for first-strand cDNA synthesis as follows: DEPC-H_2O was added to the RNA to reach a volume of 28.5 µl. 2µl of random 9-mer primers (2 µg/µl) and 2µl of oligo-dT-25 (2 µg/µl) were added to the mixture. This was heated at 70°C for 10 min and incubated on ice for 10 min. Reverse transcription was initiated by adding 9 µl of RT buffer (Fermentas EP0451: 250 mM Tris-HCl [pH 8.3 at 25°C], 250 mM KCl, 20 mM MgCl, 50 mM DTT), 1.5 ml of

aa-dUTP dNTPs 30X stock (30X stock is 30 mM dATP, 15mM dTTP, 15mM dCTP, 15mM dGTP, 15mM 5-(3-aminoallyl)-2'-deoxyuridine-5'-triophosphate, (aa-dUTP, Sigma)), 2.5 µl H_2O and 1.5 µl of reverse transcriptase (RevertAid H Minus M-MulV Reverse Transcriptase, Fermentas EP0451). The reaction was carried out at 42°C for 2 h and then the remaining RNA was hydrolysed with 0.1 mM EDTA and 0.2 M NaOH at 65°C for 15 min.

The resulting aa-dUTP-containing cDNA samples were cleaned using MinElute PCR Purification Kit (Qiagen 28006) as described in chapter 2, section 1.5.3. "PCR product purification". The cDNA was resuspended in 10mM Tris-HCl (pH 8.5) and quantified using a spectrophotometer (NanoDrop). Samples were stored at -20°C.

5.4.4 Making of microarray chips

Overview: The microarray chips, which contain oligos specific to HB3/Dd2/IT VSA as well as all 3D7 oligos, were printed on glass slides treated with polylysine. Slides that were dusty or misprinted were discarded. They were later post-processed to reduce background noise of cDNA binding to free polylysine.

5.4.4.1 Preparing polylysine slides

Glass slides were covered with polylysine at least 10 days prior to printing DNA oligos.

Up to 300 Gold Seal Microslides were placed in plastic racks (25 slides/rack). Racks were placed in large beakers with wash solution (200g pure NaOH pellets in 800ml H_2O with 1200ml of 95% ethanol). The beakers were gently shaken for 1 to 3 hours. This wash removes any residual oil and debris from the slides. Each rack was then individually rinsed by swirling for 30s in 3 different beakers containing ultrapure water (MilliQ H_2O). The water was replaced every 4 racks. After rinsing the racks were left overnight in MilliQ H_2O. Racks were then submerged in polylysine solution (300ml poly-l-lysine [0.1% (w/v) in H_2O; Sigma], 350ml PBS and 2850ml MilliQ H_2O). After being gently shaken for up to one hour in this solution, racks were again rinsed for 30s in 3 different beakers

containing MilliQ H_2O. They were spun in tabletop centrifuge (GS-6KR) at 600rpm for 4min to dry. Racks were then placed in a vacuum oven for 30min at 50°C. Slides were finally stored in a clean plastic box.

5.4.4.2 Printing microarray chips

The microarray for the *P. falciparum* genome was designed by Hu *et al.*, consisting of 10166 70-mer long oligonucleotide elements (oligos) for 5363 genes with one unique oligo every 2 kb per gene (Hu, et al., 2007). To these were added oligos specific to VSA from HB3, Dd2 and IT strains (Chapter 4). 3× SSC (20X stock = 3.0 M Sodium Chloride, 0.3 M Sodium Citrate, pH 7.0) was added to the customised oligos (Invitrogen) to yield 20 μM. The oligos were lyophilised and stored at -20°C in 384-well microtitre plates. Prior to printing, all oligos were hydrolysed at room temperature in H_2O up to a concentration of 20 μM using a Gilson 940 workstation (this was performed by Sachel Mok and Dr Arshna Gupta in Dr Zbynek Bozdech laboratory, NTU, Singapore).

The program for the microarray robot (VersArray Chipwriter pro system, Biorad) was developped by Dr Zbynek Bozdech and Sachel Mok.

Before usage, the 24 printing pins (ChipMaker™ Micro Spotting Pins) were washed in an ultrasonic bath filled with 5% Micro Cleaning Solution (ArrayIT™, unspecified composition) in distilled water. They were sonicated for 20min then rinsed exhaustively with distilled H_2O. Pins were sonicated again in distilled H_2O for 5 min. After leaving them to dry, they were placed in the robot.

Oligos were spun for 4min at 600rpm then each plate was placed in the appropriate slot in the robot. 120 polylysine-covered slides were aligned and the robot was run for printing (2 to 3 days).

Slides with dust or obvious misprint were discarded and the rest were kept in a clean plastic box.

5.4.4.3 Post-processing of polylysine slides

The oligonucleotide spots are not necessarily evenly formed, therefore for a more uniform distribution, the spots were rehydrated and snap-dried. The

slides were hydrated one by one in slide warmer (Cole Parmer) containing a hydration tray with 0.5× SSC at 42°C for 90s with the printed side facing down. The slides were immediately snap-dried on a flat metal surface in a heat block at 100°C. Oligos were cross-linked to the slide to enhance binding to the hydrophobic surface by UV irradiation. The slides were placed array side up in a Stratagene UV 1800 Stratalinker and exposed to 800 mJ energy-start-modus.

To reduce background noise the remaining free lysine groups are modified to minimise their ability to bind labelled probe DNA. The slides were placed into a metal rack and soaked in 65°C pre-warmed 3× SSC with 0.2% SDS (Sodium dodecyl sulfate) for 5 min. The slides were instantly plunged for 30s in ddH_2O and then in 95% ethanol. For the blocking solution, 5.5 g succinic anhydride (Sigma, S7626) was dissolved in 500ml ddH_2O and 335ml of pure 1,2-methyl pyrrolidinone (Sigma, M6762) was added. Immediately after the succinic anhydride dissolved, 15 ml of 1 M sodium borate, pH 8.0 was added, and mixed until the solution was clear. The slides were immediately immersed in the blocking solution and plunged up and down for 30s and then rotated gently for 5 min on a rotating platform. The slides were washed in ddH_2O by plunging up and down for 1 min and placed back into the blocking solution, plunged for 30s and then rotating for 5 min. The slides were washed again in ddH_2O for 1 min then transferred to another ddH_2O-containing dish and moved up and down for 30s. Lastly, the slides were transferred to a chamber containing 95% ethanol and moved up and down for 30s and then centrifuged to dry at 600 rpm for 5 min. The slides were then ready for hybridization.

5.4.5 cDNA labelling, microarray hybridization, washing and scanning

Overview: Time points samples (selected or unselected) were labelled with Cy5 (red dye) and pool aliquots with Cy3 (green dye). Each time point sample was hybridized on a microarray chip with the same amount of labelled cDNA from the pool. After overnight hybridization, slides were washed and scanned.

Method: 1.5µg of each cDNA sample was thawed and $NaHCO_3$ pH 9.0 added to give a final concentration of 0.1M. Cy3 and Cy5 dyes (RPN5661, Amersham,

unspecified concentration) were resuspended with 14µl DMSO (Sigma). From now on all steps were carried out in the dark until the microarray chips were scanned. 1 µl of Cy5 was added to each time point sample while 6 µl of Cy3 was added to the pool (for 6 reactions). Cy3 and Cy5 reactive dyes are coupled to aminoallyl-cDNA by incubation for a minimum of 2 h at room temperature. The labelled product was purified using QIAquick PCR purification system (Qiagen 28006) as described in chapter 2 in section 1.5.3. "PCR product purification". Cy5-labelled time point samples were mixed with the same amount of Cy3-labelled pool sample. 10mM Tris-HCl pH 8.5 was added to reach a volume of 37.1 µl. To each sample was added: 6.75µl 20x SSC, 1.125µl 1M Hepes, 1 µl 10% SDS and mixed by pipetting. Samples were then boiled for 5 min and cooled down at RT for 5 min. Samples were loaded in a Maui chamber (BioMicro Systems) using a micropipette. Great care was taken to avoid any air bubbles inside the chamber. Microarray hybridizations were incubated for 14–16 h using a Maui hybridization system (Bio Micro Systems) at 65°C.

The next day arrays were washed in 2x SSC with 0.2% SDS and then 0.1x SSC at room temperature for 5 min per wash. Arrays were centrifuged for 5min at 500 rpm in a table top centrifuge. The microarrays were scanned with a GenePix 4000B scanner (Axon Instruments). The GMT gain for the green channel was fixed to 420 while the GMT gain for the red channel was modified from one scan to the other in order to equilibrate the red and green signal from each array. This ensures an overall similar intensity for the both signals.

5.4.6 Gridding and normalization

All arrays were visually inspected using GenePix and any bad quality spots (signal below background or dust on the chip) were flagged out (see also section 5.5.3 for an example).

After gridding, the data were loaded onto the Acuity 4.0 software. Within this database, each spot was expressed as:

$$\frac{F635Median - B635}{F532Median - B532}$$

'F' is the foreground signal intenity, 'B' is the background signal intensity, '635' is the wavelength of the red channel, '532' is the wavelength of the green channel. Thus, the data for each spot is the ratio between red and green signal.
Each array was then normalized with Lowess (locally weighted least squares regression). Lowess takes continuous sections of the data and fit a linear regression line to that area of data. A dataset with all time points was created using the following parameters:

Cutoff : Discard flagged spots AND (% > B532+2SD >= 95 OR %>B635 >= 95)

In other words, only unflagged spots and spots with median intensities (green or red) greater than the local background plus 2 times the standard deviation of the background were used.

5.4.7 Microarray data analysis

Values from oligos specific to the same genes were averaged using OligoAverage.pl (Hu, et al., 2007). For the analysis of non-VSA genes (section 5.5.6) all data specific to *var*, *rif*, *stevor* and rRNA were deleted. Most rRNA spots are unreliable because they reach signal saturation, due to very high content of rRNA (80% of total RNA) (Dr Zbynek Bozdech, personal communication).
The gene annotation was based on PlasmoDB v5. The latest information on predicted exported proteins and VSA was found in the following studies:

Reference	**Information**
(Sargeant, et al., 2006)	Prediction score ("ExportPred").
(Kraemer, et al., 2007)	Classification of *var* genes for 3D7, HB3 and IT strains.
(Maier, et al., 2008)	iRBC phenotype after gene knock-out.
(Joannin, et al., 2008)	Rifin family subdivision (type A and type B).
(Schreiber, et al., 2008)	Stevor family subdivision (subtype A and subtype B)
(van Ooij, et al., 2008)	Secretome prediction based on the signal peptide and the Pexel motif.
(Wang, et al., 2009a)	Rifin typeA family subdivision (type A1, A2 and A3).

The gene annotation was updated using PERL scripts (see appendix).

Basic data analysis was carried out using Microsoft Excel, Cluster (http://bonsai.ims.utokyo.ac.jp/~mdehoon/software/cluster/software.htm#ctv) and Jalview (http://jtreeview.sourceforge.net/) for data visualization. Numerous Macros in Excel were used in order to replicate the same handling to each parasite selection.

The MADIBA website (http://www.bi.up.ac.za/MADIBA/) was used for enzymatic pathways and chromosomal visualization (Law, et al., 2008).

The statistical data analysis was performed using StatPlus (an add-on for Microsoft Excel) and Multiexperiments Viewer (MeV) (Saeed, et al., 2006, Saeed, et al., 2003).

Paired T-tests (Significance level: $\alpha<0.05$) were run with various parameters described in section 5.5.6.2. Each unselected time point [Unselected/POOL] was paired to its equivalent [Selected/POOL].

BETR (Bayesian Estimate of Temporal Regulation) and Limma were run as "Time Course" with significance level: $\alpha<0.05$ (Aryee, et al., 2009).

Significance Analysis of Microarray (SAM) is a statistical technique for finding significant genes in a set of microarray experiments (Tusher, et al., 2001). SAM computes a statistic d_i for each gene i, measuring the strength of the relationship between gene expression and the response variable (in this case, the response variable is the grouping Selected-Unselected). Missing values in the input data matrix are imputed by K-nearest neighbors, i.e. the most similar genes to the gene with a missing value are used to impute the missing value. Two-class Paired Significance Analysis for Microarrays was run with default parameters (K-nearest neighbour imputer) unless otherwise stated.

The statistic d, or relative difference in gene expression, is defined as:

$$d(i) = \frac{\bar{x}_{Sel}(i) - \bar{x}_{Uns}(i)}{s(i) + s_0} \qquad \text{(eq. 1)}$$

"$\bar{x}_{Sel}(i) - \bar{x}_{Uns}(i)$" is the difference between the average levels of expression for gene (i) in Selected and Unselected conditions. The gene-specific scatter s(i) is the standard deviation of repeated expression measurements:

$$s(i) = \sqrt{\left(\frac{\frac{1}{n_{Sel}} + \frac{1}{n_{Uns}}}{n_{Sel} + n_{Uns} - 2}\right)\left\{\sum_m [x_m(i) - \bar{x}_{Sel}(i)]^2 + \sum_n [x_n(i) - \bar{x}_{Uns}(i)]^2\right\}} \qquad \text{(eq. 2)}$$

where "n" is the number of measurements (arrays) in Selected and Unselected populations. "Σ_m" and "Σ_n" are the summation of the expression measurements in Selected and Unselected populations, respectively. In other words, $s(i)$ is an estimate of the standard deviation of the numerator in eq. 1. To compare *d(i)* across all genes, the distribution of *d(i)* should be independent of the level of gene expression and of *s(i)* thus "s_0" (a small positive constant) is added. SAM uses repeated permutations of the data to determine if the expression of any genes is significantly related to the response: First, genes are ranked by their *d(i)* values so that $d(1) \geq d(2) \geq d(3)\ldots$. The data matrix is then permuted N times (5000 times in this case). For each permutation, the relative difference d_P(i) is calculated and ranked so that $d_P(1)) \geq d_P(2) \geq d_P(3)\ldots$. The expected relative difference is calculated as:

$$d_E(i) = \sum_p \frac{d_p(i)}{N} \qquad \text{(eq. 3)}$$

d(i) is plotted versus d_E(i) (see Figure 5-22 as an example). The user determines the cutoff for significance based on the false positive rate (FDR). The FDR is the expected proportion of false positives used to correct for multiple comparisons (Verducci, et al., 2006):

$$FDR \approx \frac{\frac{1}{N}\sum_{p=1}^{N}\{i \mid d_p(i) \geq t_1 \vee d_p(i) \leq t_2\}}{\{i \mid d(i) \geq t_1 \vee d(i) \leq t_2\}}$$

Where N is the number of permutations, t_1 and t_2 are the smallest positive and largest negative *d(i)*, respectively (Figure 5-22). The numerator is an estimate of the number of falsely significant genes while the denominator is the number of genes called significant. The FDR basically calculates the average number of

genes that exceed the values of t_1 and t_2 in the permutations. This is presented as a *q value* for each gene in the final list of significant genes.

5.5 Results

5.5.1 *P. falciparum* synchronisation and time-course

The selection of *Plasmodium falciparum* on HBEC-5i has been described in chapter 3. As a high amount of RNA material is needed for the microarray experiments, the last round of selection was performed with 8 HBEC-5i-covered Petri dishes instead of a single one. This was to minimize the number of life cycles between the last round of selection and the time-course experiment.

Selected and unselected *P. falciparum* parasite cultures had to be tightly synchronized for the time-course experiment. For the pilot experiment (HB3-HBEC1 and HB3-Uns1), the Percoll procedure was tested. The purity of schizonts in the upper layer was only 68%, thus MACS columns were used for all other selections (purity > 98% schizonts). The synchronization window, i.e. the time elapsed between the MACS/Percoll treatment and the sorbitol treatment, is indicated in Table 5-1.

For the time-course, the first sample for RNA was collected 3 hours after the sorbitol treatment, and subsequent samples were taken from the parasite culture every 8 hours over a 48-hour period so as to cover the entire intra-erythrocytic life cycle (Figure 5-2). The quantity of packed cell volume (pcv) sampled for each time point is indicated in Table 5-2, along with the amount of RNA and cDNA generated.

	HB3-HBEC1	HB3-Uns1	HB3-HBEC2	HB3-HBEC-TNF[6]	HB3-Uns2	3D7-HBEC	3D7-Uns	IT-HBEC	IT-Uns	Dd2
Rounds of selection[1]	5	/	5	6	/	7	/	6	/	*5* but no phenotype
Synchronization method[2]	Percoll + Sorbitol	Percoll + Sorbitol	MACS + Sorbitol	MACS + Sorbitol	MACS + Sorbitol	MACS + Sorbitol	MACS + Sorbitol	MACS + Sorbitol	MACS + Sorbitol	/
Synchronization window[3]	5 hours	5 hours	7 hours	7 hours	6 hours	7 hours	7 hours	7 hours	5 hours	/
Time between last selection and time-course[4]	13 days	/	12 days	12 days	/	14 days	/	13 days	/	/
Parasitaemia[5]	4.5%	7.5%	4.6%	3.4%	5.0%	4%	5.6%	9.5%	8.2%	/

Table 5-1. Summary of synchronisations for time-course purposes. Selected and unselected parasites were synchronised before the time-course experiment.

[1]: Number of rounds of selection on HBEC-5i before the time-course.

[2]: See text and materials & methods chapter for details.

[3]: Time between the first ring appeared (or end of MACS treatment) and the Sorbitol treatment. The shorter the time, the more synchronised the parasites are.

[4]: Number of days elapsed between the last round of selection and the start of the time-course.

[5]: Percentage of iRBC during the time-course.

[6]: HB3 parasites selected on HBEC-5i activated with TNF.

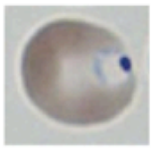
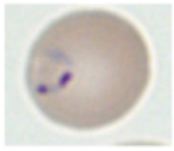
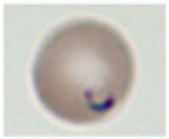
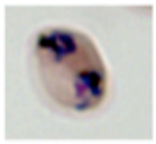
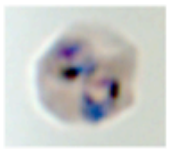
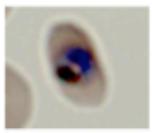
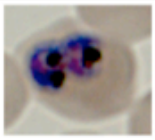
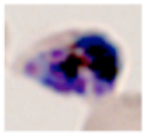
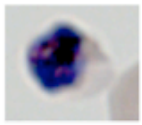
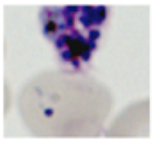
Time-point	Time post invasion	HB3 Unselected	HB3-HBEC Selected
T1 Early ring	8h (range: 3-8h)		
T2 Ring	16h (range: 11-16h)		
T3 Late ring/early troph	24h (range: 19-24h)		
T4 Troph	32h (range: 27-32h)		
T5 Schizont	40h (range: 35-40h)		
T6 Mature schizont	48h (range: 43-48h)		

Figure 5-2. Example of a time-course experiment (here HB3-Uns and HB3-HBEC1). Every 8 hours after the first ring invasion a sample was taken from the culture, mixed with TRIzol reagent and frozen. A smear was performed to record the development stage of parasites. "Troph" = pigmented trophozoite stage.

	T.	pcv (µl)	RNA harvested (µg)	[cDNA] (µg/µl)
HB3-HBEC1 4.5% parasitaemia	T1	200	4.5	0.08
	T2	200	3.3	0.07
	T3	200	11.1	0.28
	T4	200	37.3	0.09
	T5	200	43.3	0.25
	T6	200	33.0	0.09

	T.	pcv (µl)	RNA harvested (µg)	[cDNA] (µg/µl)
HB3-Uns1 7.5% parasitaemia	T1	130	7.4	0.14
	T2	130	5.4	0.53
	T3	130	17.4	0.26
	T4	130	25.9	0.21
	T5	130	48.5	0.34
	T6	130	30.0	0.31
HB3-HBEC2 4.6% parasitaemia	T1	800	11.8	0.14
	T2	800	6.7	0.20
	T3	400	23.8	0.14
	T4	300	46.8	0.20
	T5	350	40.0	0.22
	T6	200	1.2	0.04
HB3-HBEC-TNF 3.4% parasitaemia	T1	800	11.6	0.21
	T2	800	14.1	0.27
	T3	400	7.5	0.21
	T4	300	21.2	0.19
	T5	300	24.0	0.18
	T6	300	28.0	0.22
HB3-Uns2 5% parasitaemia	T1	3000	4.1	0.46
	T2	3000	5.1	0.50
	T3	600	17.3	0.49
	T4	450	27.7	0.28
	T5	450	42.3	0.38
	T6	450	24.9	0.34
3D7-HBEC 4% parasitaemia	T1	900	28.8	0.18
	T2	1000	15.3	0.37
	T3	900	36.0	0.32
	T4	350	43.6	0.35
	T5	350	84.0	0.32
	T6	150	19.5	0.38
3D7-Uns 5.6% parasitaemia	T1	1350	26.8	0.24
	T2	1400	26.0	0.34
	T3	1300	11.0	0.22
	T4	400	36.0	0.51
	T5	400	40.0	0.54
	T6	250	35.7	0.49
IT-HBEC 9.5% parasitaemia	T1	1350	42.8	0.20
	T2	1300	59.2	0.66
	T3	1100	40.0	0.83
	T4	500	68.4	0.54
	T5	400	103.6	0.54
	T6	400	67.6	0.48

	T.	pcv (µl)	RNA harvested (µg)	[cDNA] (µg/µl)
IT-Uns 8.2% parasitaemia	T1	850	30.8	0.49
	T2	750	34.2	0.50
	T3	550	50.1	0.50
	T4	250	84.4	0.39
	T5	250	64.8	0.40
	T6	250	14.4	0.16

Table 5-2. Time-course results: amount of RNA and cDNA harvested for each time point. T. = time point. Pcv = Packed cell volume sampled; RNA harvested = Total quantity of RNA obtained after extraction. [cDNA] = Concentration of cDNA after reverse transcription of 12 µg of RNA (or less if that amount was not available).

5.5.2 RNA extraction, pooling, and cDNA labelling

In order to compare the expression of a gene before and after selection, both parasite populations need to be at the same stage of development. A way to overcome this problem, after a time-course experiment, is to pool the RNA of all time points of one of the two populations to be compared (Box 5-1). Here it was arbitrarily chosen to pool some of the RNA from unselected parasites. Each time point of each population is then hybridized against the same amount of pool cDNA.

Practically, for each unselected population, about two third of the RNA of each time point was pooled. Thus ending up with 3 pools: HB3-Uns-Pool, 3D7-Uns-Pool and IT-Uns-Pool ("Uns" stands for "Unselected") (Figure 5-3). All RNA samples (time points and pools) were reverse transcribed with the incorporation of amino-allyl dUTP (Figure 5-4) to allow fixation of the dye (Cy3 or Cy5).

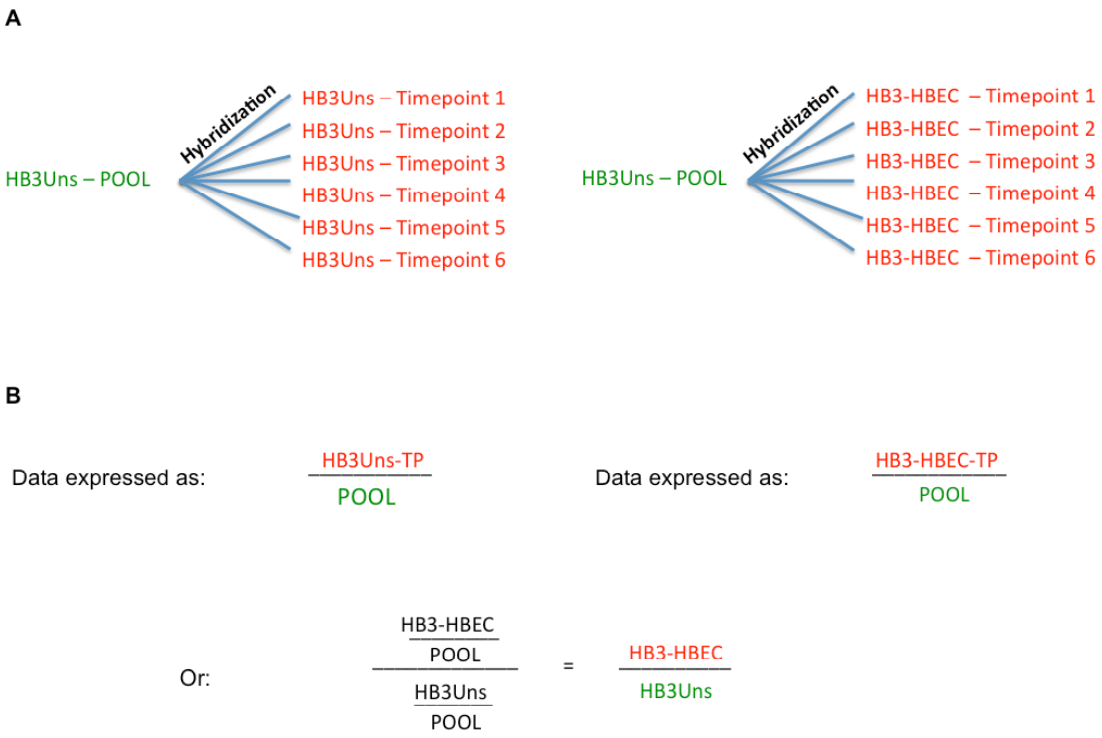


Figure 5-3. Schematic representation of the pooling and hybridizations. Here an example is shown with HB3 selected parasites. The pool is made of an equal amount of RNA from the 6 time points of an unselected parasite population. (A) Each time point, whether from a selected or unselected population, is hybridized against the pool. (B) The resulting ratios correspond to the signal from a time point divided by the signal from the pool. The data can also be expressed as the ratio between selected and unselected populations for each time point because the pool is identical in both cases.

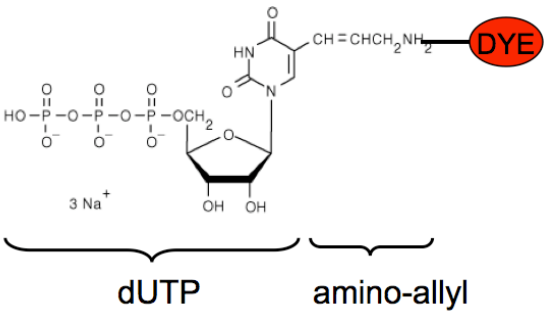


Figure 5-4. amino-allyl dUTP is used to allow dye (Cy3 or Cy5) fixation.

5.5.3 Hybridization

Each red dye (Cy5)-labelled time point sample was hybridized with the same amount of pool cDNA (green dye Cy3-labelled) on a microarray chip (Figure 5-3). Note that for the pilot experiment (HB3-HBEC1), due to the low yield of RNA (Table 5-2), it was not possible to make a pool. Thus each time point of both populations (selected and unselected) were hybridized together, i.e. cDNA from HB3-HBEC1-time point1 is hybridized with the same amount of cDNA from HB3-Uns1-time point1 and so on.

After scanning the microarray slides, all spots were automatically and manually gridded (Figure 5-5). A few hybridizations had to be discarded because of dust on the array, very high background or Cy5 dye being too weak. These hybridizations were repeated when there was enough material to do so (Table 5-2) and only data for HB3-HBEC2 time point 6 (T6) is missing while data for T2 of the same strain and T6 for IT-Uns are partial (Table 5-3).

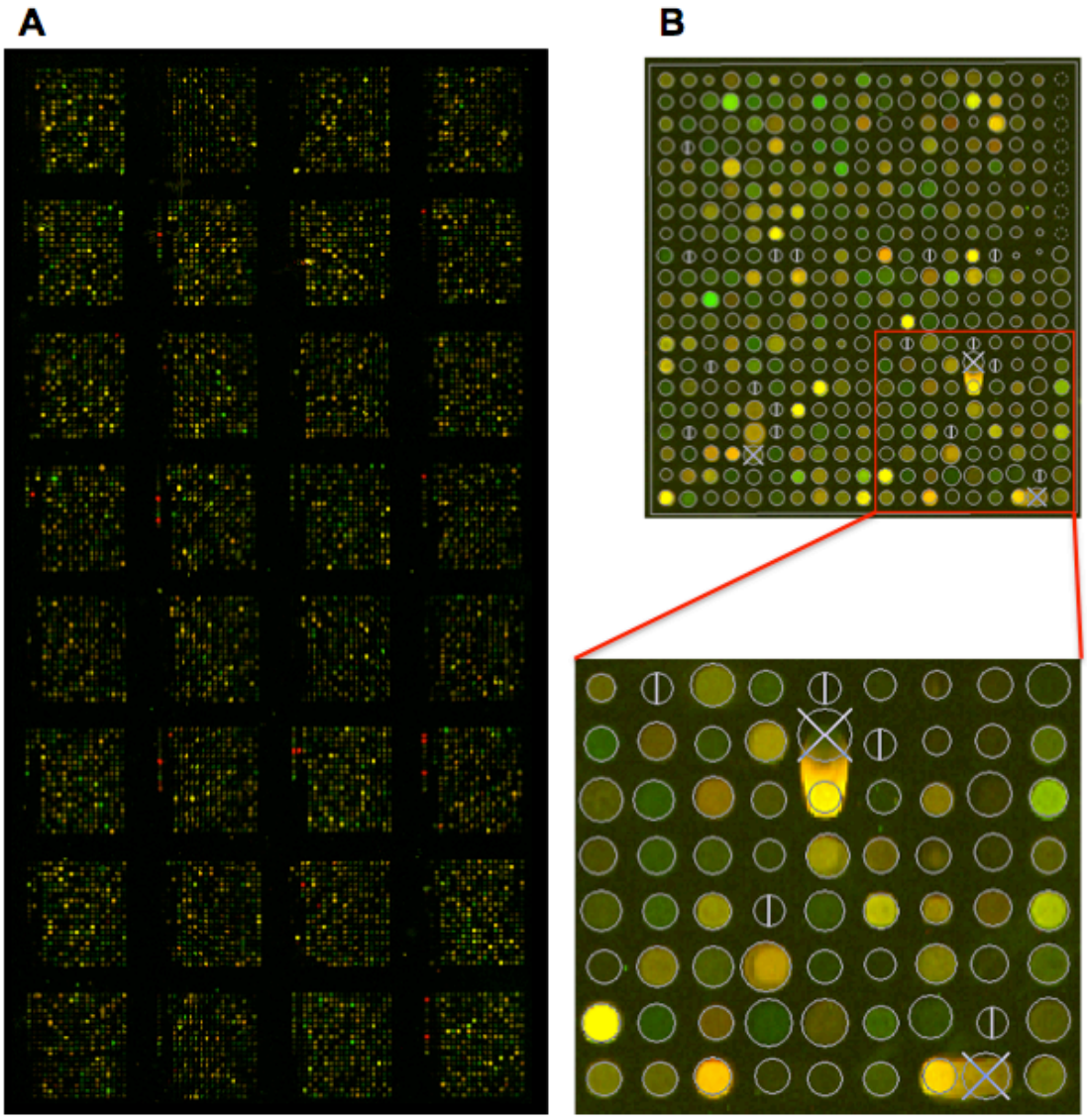


Figure 5-5. Example of a typical microarray scan and grid. (A) The entire microarray chip. Over 10 000 spots, each representing the signal from unique oligos, can be seen. The red signal is due to the time point sample (selected or unselected) labelled with Cy5 while the green signal comes from the pool labelled with Cy3. The same amount of both signals (red and green) appears yellow. (B) A grid labelling each spot is automatically generated and flags out (vertical line within a circle) spots with a signal below background level. Each grid is then visually inspected and extra spots are manually flagged out (crossed circles) if necessary. For example, in the zoomed out square, 4 automatically flagged out spots and 2 manually flagged out spots can be seen. The later 2 spots were considered "bad" because a neighbouring spot "leaked". Thus the signal could come from the other spot.

	T1	T2	T3	T4	T5	T6
HB3-HBEC1	54%	50%	76%	78%	78%	71%
HB3-Uns2	80%	64%	65%	89%	83%	81%
HB3-HBEC-TNF	86%	83%	82%	90%	85%	85%
HB3-HBEC2	77%	27%	79%	88%	84%	N/A
3D7-Uns	89%	75%	80%	75%	84%	85%
3D7-HBEC	77%	78%	88%	75%	87%	84%
IT-Uns	72%	67%	74%	73%	73%	50%
IT-HBEC	75%	72%	75%	72%	65%	76%

Table 5-3. Percentage of oligos where the expression is above the background cutoff. All time points were hybridized against a pool except for "HB3-HBEC1" were selected and unselected cDNA were hybridized with each other.

All data was loaded onto Acuity software 4.0 for normalization. Apart from a few exceptions, about 70 to 85% of oligonucleotide probes (abbreviated as "oligos") show expression above the background cutoff defined in section 5.4.7 (Table 5-3). Output files from Acuity were converted into an Excel spreadsheet (Figure 5-6). Ratios were converted to $\log_2$ to get a normal distribution.

Unique Oligo ID | Gene ID and annotation | Log ratios for selected parasites | Log ratios for unselected parasites

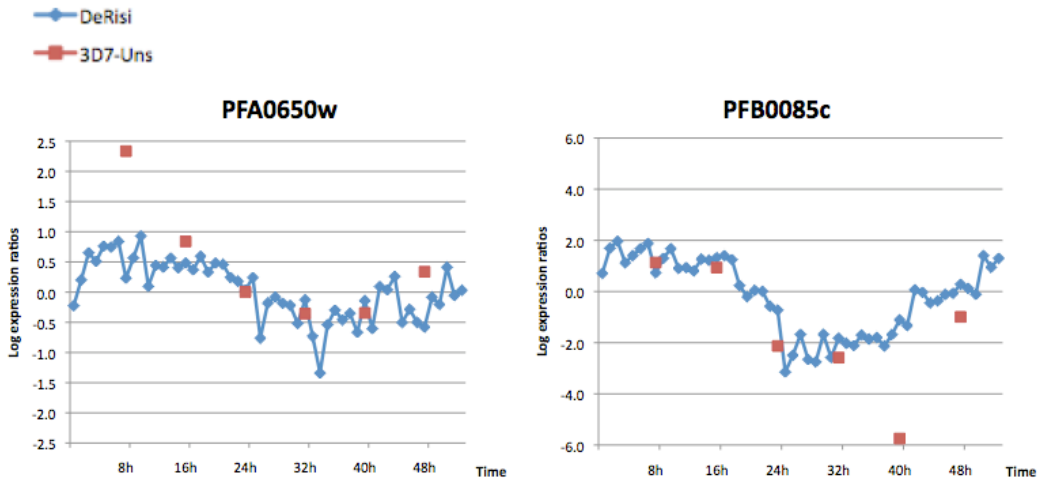
	A	B	C	D	E	F	G	H	I	J	K	L	M	N
1	id	NAME	HBEC-T1	HBEC-T2	HBEC-T3	HBEC-T4	HBEC-T5	HBEC-T6	Uns-T1	Uns-T2	Uns-T3	Uns-T4	Uns-T5	Uns-T6
2	aMAL13P1.100_1	MAL13P1.100::hypothetical protein,	-0.60	<no data>	-0.84	0.54	0.96	0.51	-0.59	-0.76	-1.11	0.12	0.90	0.42
3	aMAL13P1.102_0	MAL13P1.102::hypothetical protein,	-1.15	-2.09	-2.33	-6.19	-1.50	3.01	-0.17	-2.72	-3.11	-4.19	-1.45	2.42
4	aMAL13P1.102_1	MAL13P1.102::hypothetical protein,	<no data>	-1.75	-2.39	-4.39	-1.72	2.45	-0.21	-2.44	-3.21	-4.59	-1.54	2.28
5	aMAL13P1.103_0	MAL13P1.103::hypothetical protein,	-0.07	-2.00	-2.78	-0.21	1.35	0.07	-0.59	-5.21	-2.35	-0.18	0.98	0.02
6	aMAL13P1.105_0	MAL13P1.105::hypothetical protein,	-1.05	-0.80	-1.24	0.48	0.62	0.28	<no data>	-0.03	0.17	0.55	0.88	0.16
7	aMAL13P1.105_1	MAL13P1.105::hypothetical protein,	-1.14	-1.35	-1.24	0.59	0.88	<no data>	-0.55	<no data>	-0.71	0.53	<no data:	0.08
8	aMAL13P1.106_0	MAL13P1.106::hypothetical protein	0.48	1.32	0.94	<no data>	-0.63	0.04	0.83	1.79	1.04	0.09	-0.13	0.53

Figure 5-6. Screenshot of a typical Excel table with microarray data. Note that for example the gene MAL1P1.100 is represented by a single oligo (aMAL1P1.100_1) while the gene MAL1P1.102 is represented by two different oligos (aMAL1P1.102_0 and aMAL1P1.102_1). The data for the latter two oligos will be averaged later in the analysis. "<no data>" indicates a spot that did not pass the cutoff defined in section 5.4.6 because the intensity was below background level or because it was manually flagged out. Log ratios shown here correspond to the [timepoint / POOL] data.

5.5.4 Synchronicity of parasite preparations

The first published transcriptome analysis of *P. falciparum* revealed an unprecedented way of regulating genome transcription (Bozdech, et al., 2003). Most genes follow a "just in time" transcription pattern, being turned on and off at a very specific time and only once during the intra-erythrocytic life cycle. Thus in order to analyze the transcriptome of a population it is crucial for all parasites to be at the same stage of development. The pooling of time points from one population (unselected parasites) was a way to overcome this difficulty (Box 5-1 in section 5.4.3).

As a first way to verify the synchronicity of the parasites, Giemsa smears for each time point were carefully inspected (Figure 5-2 in section 5.5.1). Also, the expression timing of 10 randomly selected genes was compared with PlasmoDB data (Data for 3D7-Uns only is shown in Figure 5-7). Almost all genes in this study followed the same expression pattern as in the original microarray study (Llinas, et al., 2006), indicating that there was no obvious issue with the synchronisation of parasites.



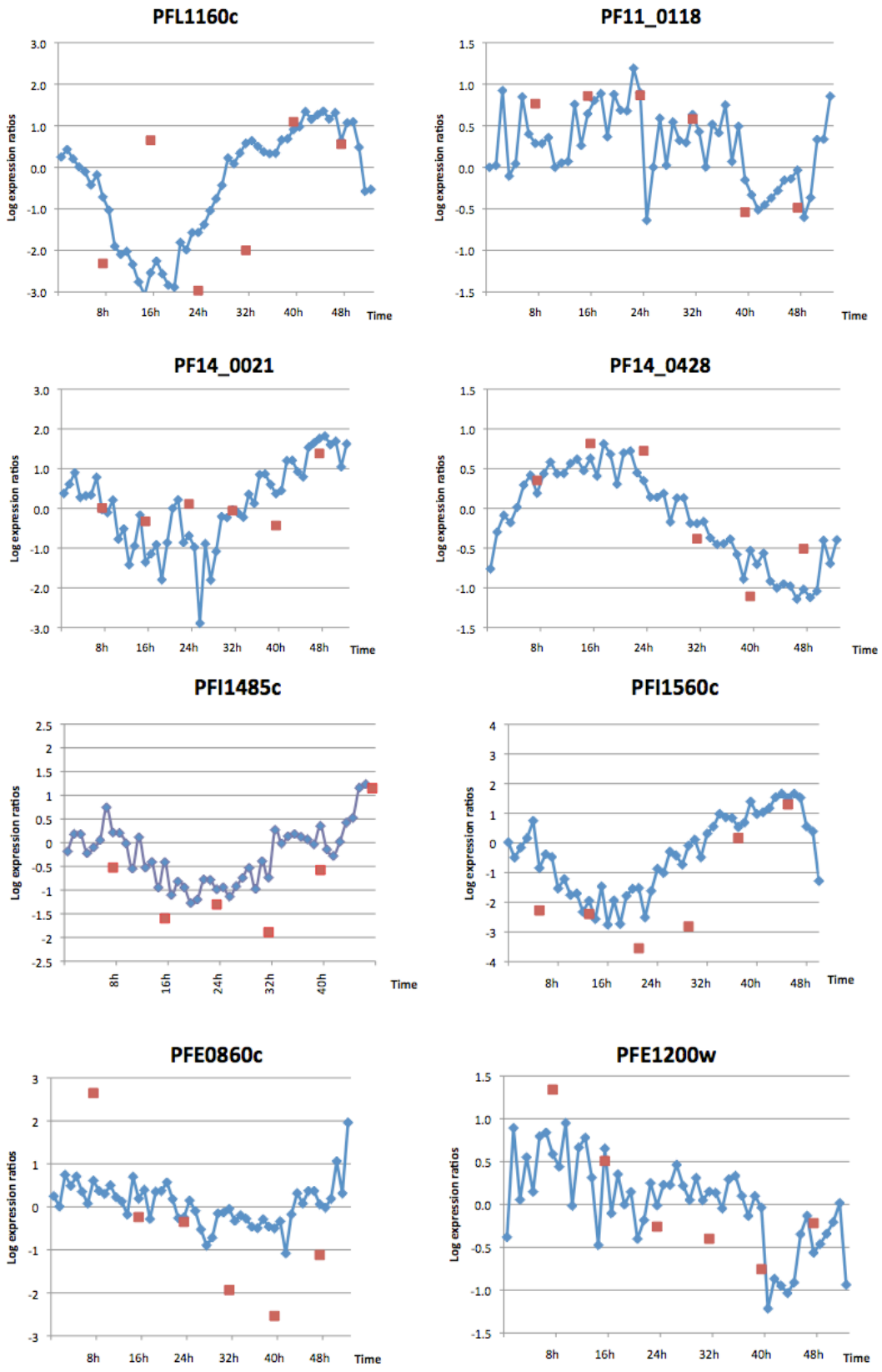


Figure 5-7. Time-course expression profile of 3D7 parasites from DeRisi lab (PlasmoDB) and this work (3D7-Uns). 10 genes were randomly selected from

the 3D7-Uns data (orange squares). The vast majority of them follow the same pattern of expression as in the original microarray analysis (blue squares and lines) from the DeRisi lab (Llinas, et al., 2006)).

A last and more thorough approach was the statistical evaluation by Pearson correlation of oligos showing data at all time points (Table 5-4). All oligos of one time point in an unselected strain were set in correlation with all oligos of one time point of the selected strain. A Pearson correlation close to 1 shows a strong positive correlation and a correlation close to -1 shows a strong negative correlation. Here, in almost all cases, the same time point in an unselected strain showed a strong positive correlation with the same time point in the selected strain (Table 5-4, fields with gray background). The largest disparity was found in time point 3 between HB3-HBEC-TNF and HB3-Uns2 (Pearson correlation coefficient 0.34). Gene expression for that particular time point should therefore be interpreted cautiously. Time point 6 in the IT strain also showed a relatively weak positive correlation (Pearson correlation coefficient 0.51). All other time points and strains showed a strong positive correlation with correlation coefficients of 0.72 or greater, with many being greater than 0.9 (Table 1.4).

		HB3-Uns2					
		T1	**T2**	**T3**	**T4**	**T5**	**T6**
HB3-HBEC2	**T1**	0.84	0.66	0.12	-0.20	-0.36	N/A
	T2	0.74	0.86	0.29	-0.18	-0.50	N/A
	T3	0.24	0.65	0.78	0.23	-0.35	N/A
	T4	-0.12	0.11	0.71	0.79	0	N/A
	T5	-0.38	-0.54	-0.10	0.56	0.78	N/A
	T6	N/A	N/A	N/A	N/A	N/A	N/A

		HB3-Uns2					
		T1	**T2**	**T3**	**T4**	**T5**	**T6**
HB3-HBEC-TNF	**T1**	0.88	0.63	0.12	-0.21	-0.32	0.38
	T2	0.26	0.72	0.83	0.28	-0.50	-0.45
	T3	0.73	0.89	0.34	-0.17	-0.51	0.05
	T4	-0.21	0.11	0.71	0.83	-0.09	-0.55
	T5	-0.46	-0.54	-0.07	0.59	0.76	0.1
	T6	-0.01	-0.46	-0.49	-0.11	0.7	0.72

		3D7-Uns					
		T1	**T2**	**T3**	**T4**	**T5**	**T6**
3D7-HBEC	**T1**	0.75	0.77	0.68	0.39	-0.2	-0.3
	T2	0.71	0.88	0.81	0.39	-0.35	-0.48
	T3	0.52	0.73	0.93	0.68	-0.13	-0.51
	T4	0.19	0.38	0.64	0.94	0.40	-0.37
	T5	-0.39	-0.31	-0.17	0.39	0.96	0.33
	T6	-0.24	-0.45	-0.49	-0.26	0.45	0.92

		IT-Uns					
		T1	**T2**	**T3**	**T4**	**T5**	**T6**
IT-HBEC	**T1**	0.91	0.63	0.17	-0.18	-0.37	0.17
	T2	0.84	0.93	0.43	-0.16	-0.58	-0.1
	T3	0.36	0.7	0.92	0.29	-0.46	-0.39
	T4	-0.19	0.03	0.73	0.89	0.18	-0.34
	T5	-0.5	-0.58	-0.12	0.68	0.89	0.11
	T6	-0.33	-0.58	-0.5	0.1	0.86	0.51

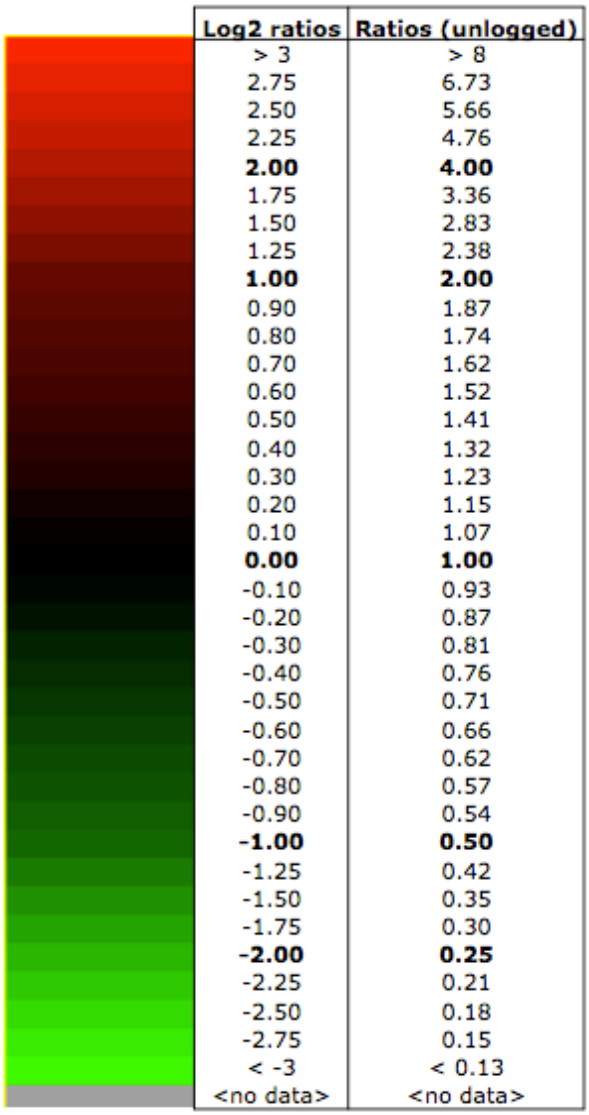
Table 5-4. Pearson correlation of time points between selected and unselected strains. Time points [Unselected/POOL] were correlated with time points [Selected/POOL]. Pearson correlation numbers close to 1 indicate a high correlation between both time points.

5.5.5 Analysis of variant surface antigen gene expression in selected and unselected parasites

In the first instance, the microarray data analysis focused on VSA genes because they are the major candidate ligands for cytoadherence. For ease of understanding, the data will be presented as log ratios of Selected versus Unselected expression:

$$\frac{\frac{Selected}{POOL}}{\frac{Unselected}{POOL}} = \frac{Selected}{Unselected}$$

Thus if there is a higher amount of cDNA in the Selected compared to the Unselected population this will result in a positive log ratio, while lower expression in the Selected will result in a negative log ratio. A colour scheme is used to facilitate the data visualization (Figure 5-8).



Log2 ratios	Ratios (unlogged)
> 3	> 8
2.75	6.73
2.50	5.66
2.25	4.76
2.00	**4.00**
1.75	3.36
1.50	2.83
1.25	2.38
1.00	**2.00**
0.90	1.87
0.80	1.74
0.70	1.62
0.60	1.52
0.50	1.41
0.40	1.32
0.30	1.23
0.20	1.15
0.10	1.07
0.00	**1.00**
-0.10	0.93
-0.20	0.87
-0.30	0.81
-0.40	0.76
-0.50	0.71
-0.60	0.66
-0.70	0.62
-0.80	0.57
-0.90	0.54
-1.00	**0.50**
-1.25	0.42
-1.50	0.35
-1.75	0.30
-2.00	**0.25**
-2.25	0.21
-2.50	0.18
-2.75	0.15
< -3	< 0.13
<no data>	<no data>

Figure 5-8. Colour legend used for all microarray data shown in this work. See the appendix (CD attached) for the actual expression ratios of all genes.

5.5.5.1 *Var* gene expression in selected and unselected HB3

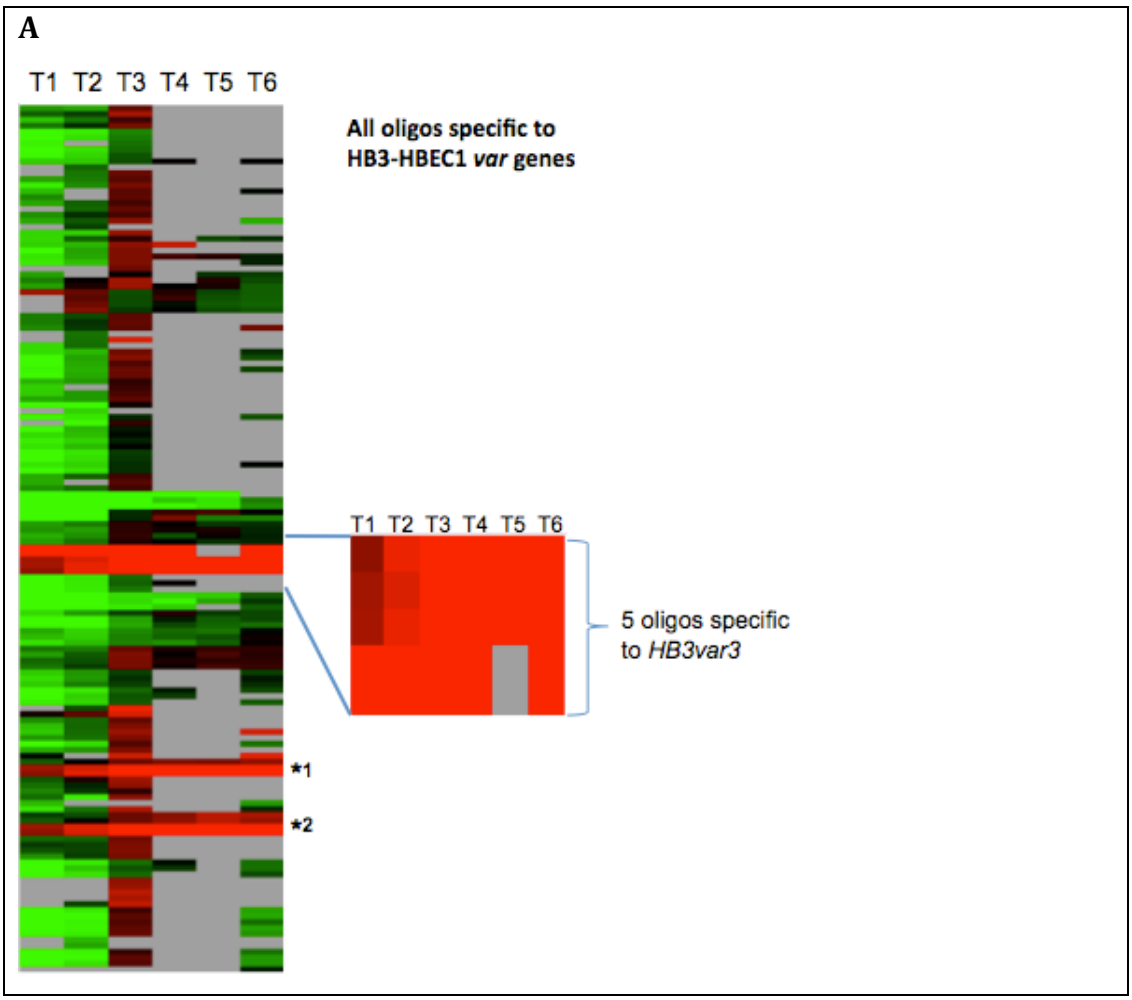
The first selection of HB3 on HBEC-5i resulted in a parasite population showing a marked upregulation of a single *var* gene, *HB3var3* (Figure 5-9), member of the group A subfamily (Kraemer, et al., 2007). There were five oligos on the microarray chip for this gene, and all five showed strongly upregulated hybridisation signals (8 to 30 fold) in HB3-HBEC1 compared to unselected HB3 (Figure 5-9A). In addition, marked upregulation of *HB3var3* was seen at all six time points. Four other oligos also showed marked upregulation (asterisked in

Figure 5-9A), however, they were found to be probes for *HB3var5* and *HB3var46p* that share the same 3' end as *HB3var3.* The specific probes for the 5' end of *HB3var5* and *HB3var46p* did not show increased hybridisation signals, suggesting that it is only *HB3var3*, and not *HB3var5* or *HB3var46p* that is upregulated on selection for binding to HBEC5i. A few other *var* genes were slightly upregulated at a single time point (time point 3). However, it is clear that *HB3var3* stands out as being the only *var* gene to be highly upregulated at all time points and with all available probes for the gene. Virtually all other genes with expression data were downregulated in HB3-HBEC1.

The second independently selected parasite line HB3-HBEC2 gave very similar results, with *HB3var3* being the only *var* gene that was highly upregulated with all probes and multiple time points (time points 1, 3 and 4, Figure 5-9B). Data were not available for time points 2 and 6 because of technical problems as described in section 5.5.3. In this case, upregulation of *HB3var3* was most marked at time points 1 and 3 (6 and 11 fold increase, respectively). Transcription of full length *var* genes occurs mostly between 3-18 hours (Kyes, et al., 2000), therefore time points 1-3 are the most critical and meaningful for examination of *var* gene transcription patterns.

Selection of HB3 parasites on TNF-activated HBEC5i also resulted in a parasite population with upregulated transcription of *HB3var3* (Figure 5-9C). Many other *var* genes were upregulated at a single time point (time point 3), particularly in HB3-HBEC-TNF (Figure 5-9C). However, as stated in section 5.5.4, technical artefacts cannot be excluded for that time point (Table 5-4). Once again, *HB3var3* was the only *var* gene to be consistently highly upregulated (5 to 37 fold) with multiple probes and multiple time points. Therefore, according to the data presented here, the activation of HBEC-5i with TNF for each round of selection has not modified the upregulated *var* gene in selected HB3 parasites.

Taken together, these three independent selections show very strikingly that transcription of *HB3var3* is upregulated after parasite selection for binding to HBEC5i, making it a leading candidate for the cytoadherence ligand.


A
T1 T2 T3 T4 T5 T6
All oligos specific to
HB3-HBEC1 var genes
T1 T2 T3 T4 T5 T6
5 oligos specific
to HB3var3
*1
*2

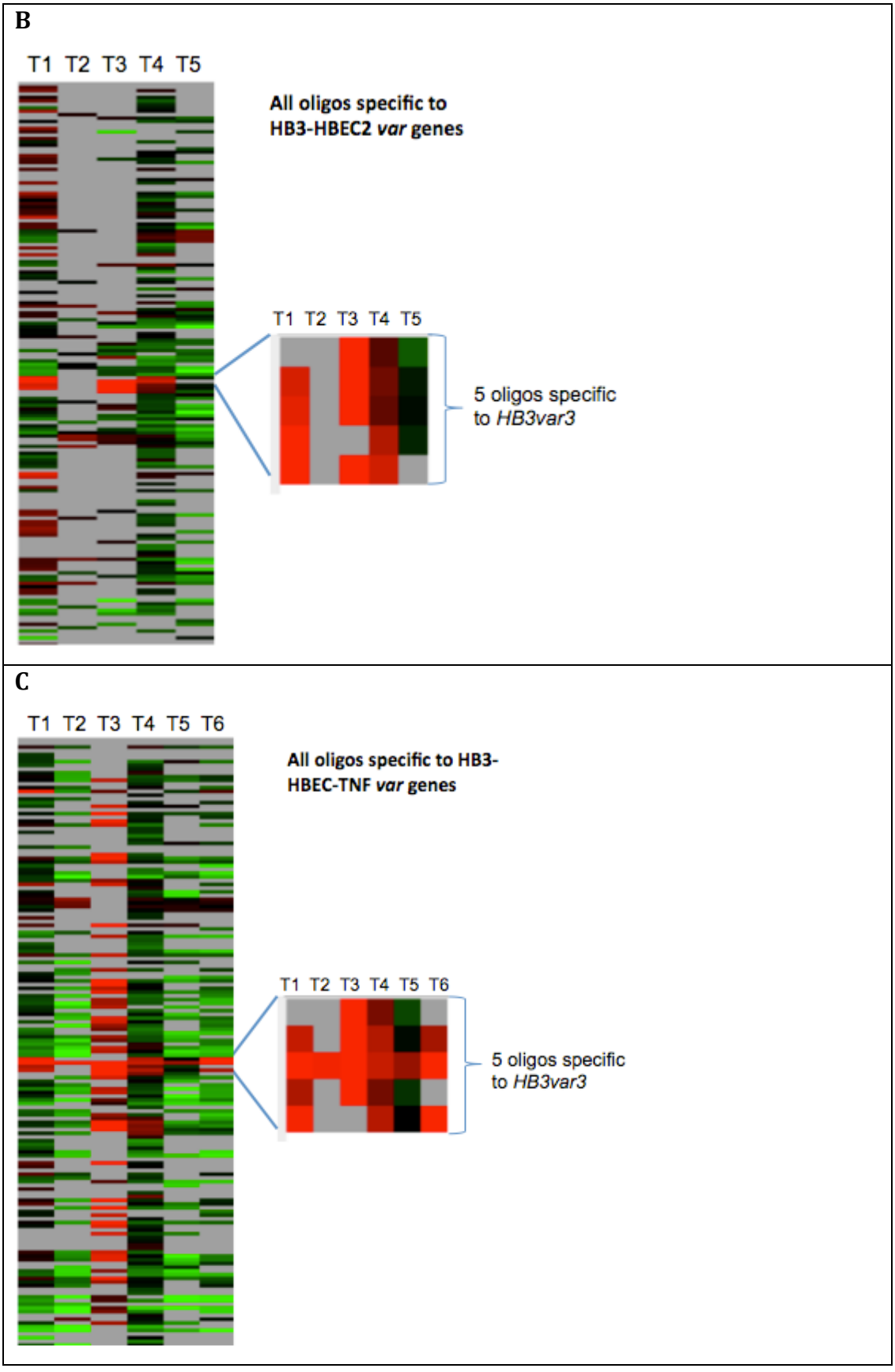

B
T1 T2 T3 T4 T5
All oligos specific to HB3-HBEC2 var genes
T1 T2 T3 T4 T5
5 oligos specific to HB3var3
C
T1 T2 T3 T4 T5 T6
All oligos specific to HB3-HBEC-TNF var genes
T1 T2 T3 T4 T5 T6
5 oligos specific to HB3var3

Figure 5-9. *var* genes expression ratios in HB3 derived selections. Each row is a different oligo, each column is a time point. All oligos are shown except for those without any expression data at all. Data represented here are the ratio [Selected/POOL] divided by the ratio [Unselected/POOL], which is mathematically equivalent to a [Selected/Unselected] ratio. Red rectangles indicate higher amount of cDNA in the selected compared to the unselected population. Green rectangles indicate higher expression in the unselected population. A gray rectangle indicates the lack of data. It is a spot that did not pass the cutoff defined in section 5.4.6 because the signal intensity was below background level or, less likely, because the spot was manually flagged out. Note that HBEC1 was hybridised "HB3-HBEC1" with "HB3-Uns1" because there was no pooling. For each selection, the most highly upregulated *var* gene(s) has been zoomed out. As Kraemer *et al* discovered, a few *var* genes have part of their sequence identical to other *var* genes, either within or in between strains. For example, the second half of *HB3var3* shows similarities with *HB3var5* and *HB3var46p*. Therefore some oligos are not unique to a single sequence. *1: Oligos HB3var46p_2 and HB3var46p_3 also match the *HB3var3* gene. Oligos HB3var46p_0 and HB3var46p_1 are however unique to *HB3var46p* and are not upregulated. *2: Oligos HB3var5_2 and HB3var5_3 also match *HB3var3*. Oligos HB3var5_0 and HB3var5_1 are however unique to *HB3var5* and are not upregulated.

5.5.5.2 *Var* gene expression in selected and unselected 3D7

In a similar way to the *var* family expression pattern in HB3 selections, 3D7-HBEC shows downregulation of a wide range of *var* genes while a single variant is highly upregulated (Figure 5-10). The six oligos specific to *PFD0020c* show upregulation by 4 to 22 fold from time point 2 to 6. Time point 1 of the [3D7-HBEC/POOL] hybridization is surprisingly downregulated. A technical artefact is plausible as the Pearson correlation for that time point was lower than for others (Table 5-4).

A few other oligos also show upregulation at different time points (Figure 5-10). However, no other *var* variant than *PFD0020c* is consistently and highly upregulated after selection on HBEC-5i. PFD0020c is part of the group A subfamily (Lavstsen, et al., 2003b).

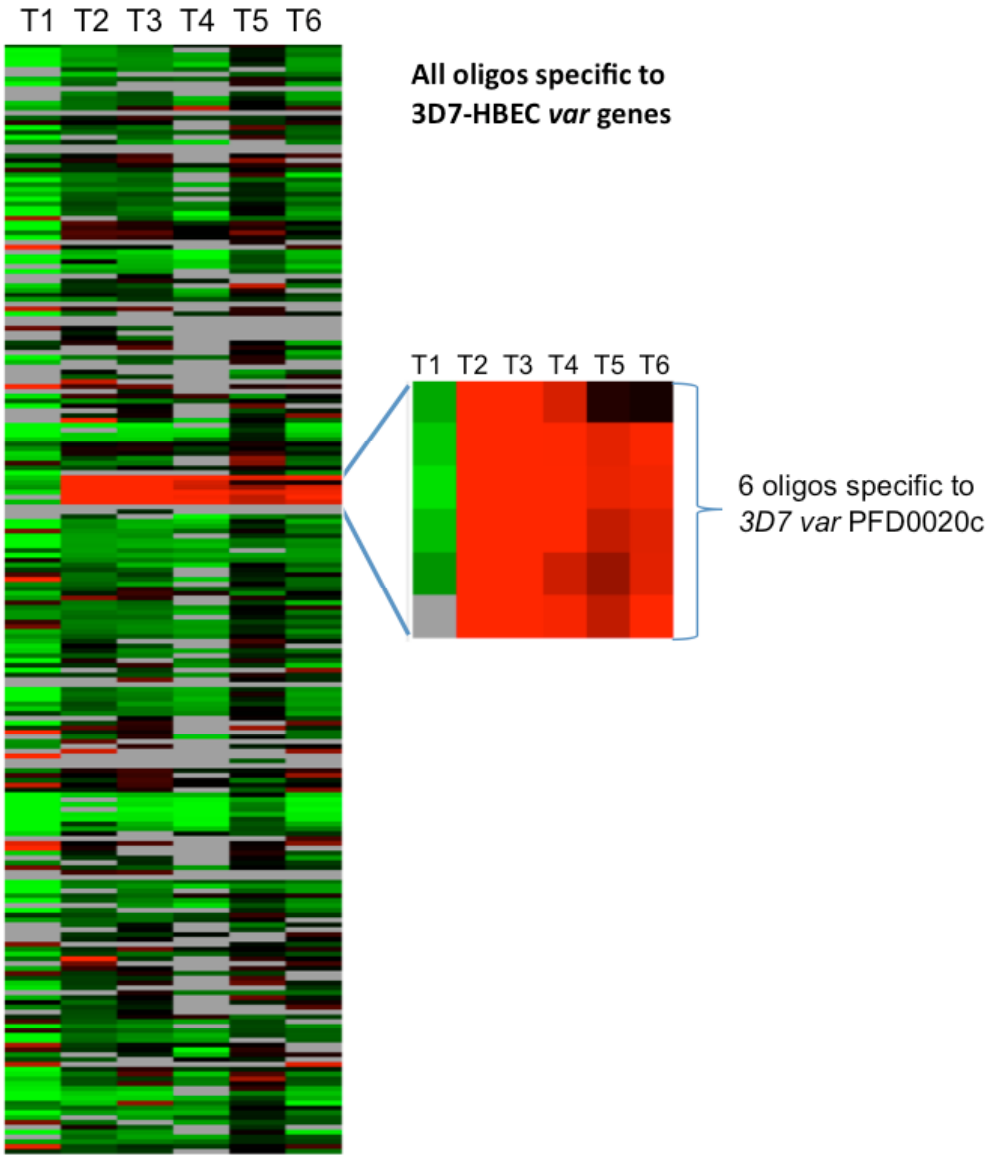


Figure 5-10. *var* genes expression ratios in 3D7 parasites. All *var* oligos are shown except for those without any expression data at all. Data represented here is the ratio [Selected/Unselected]. PFD0020c is the most highly upregulated 3D7 *var* gene after selection on HBEC-5i.

5.5.5.3 *Var* gene expression in selected and unselected IT

As observed with all other selections, the selection of IT on HBEC-5i resulted in most *var* genes being greatly downregulated (Figure 5-11). With this strain however two *var* genes were found highly upregulated: *ITvar7* (group A subfamily) and *ITvar19* (group B subfamily) (Kraemer, et al., 2007). The five

oligos specific to each of these two genes show a 10 to over 100 fold upregulation on average. The expression is particularly strong in time points 2 and 3, when *var* genes have been shown to be at their highest peak of transcription (Kyes, et al., 2000).

Three other oligos also showed marked upregulation (asterisked in Figure 5-11). However, these oligos (ITvar32_2, ITvar32_3 and ITvar6_0) also perfectly match *ITvar19*. This results from the fact that *ITvar19* is partly identical to *ITvar6* and *ITvar32* (Kraemer, et al., 2007). Oligos specific to *ITvar6* and *ITvar32* do not show upregulation thus it can be safely concluded that only *ITvar7* and *ITvar19* show high and consistent upregulation after selection of the IT strain on HBEC-5i.

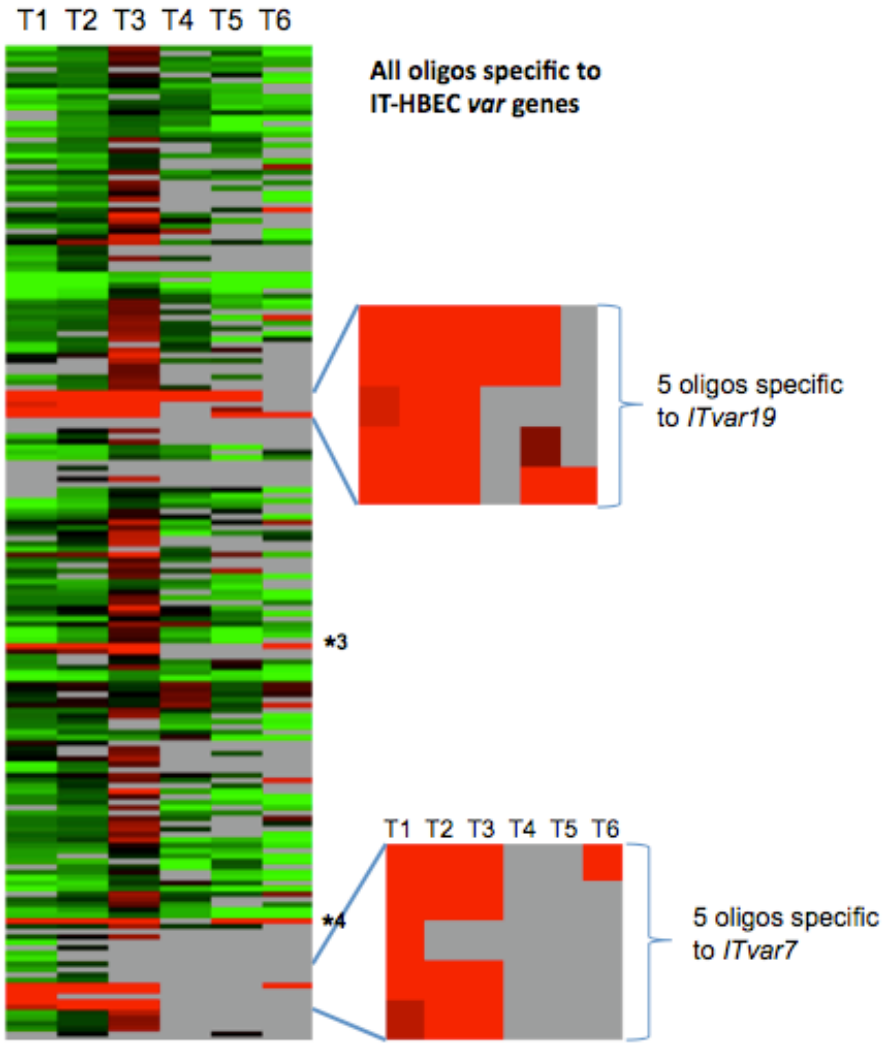


Figure 5-11. *var* genes expression ratios in IT parasites. All *var* oligos are shown except for those without any expression data at all. Data represented here is the ratio [Selected/Unselected]. *ITvar7* and *19* are the most highly upregulated IT *var* gene after selection on HBEC-5i. Because a few *var* genes share part of their sequence with other *var* genes (Kraemer, et al., 2007), some oligos are not specific to a single gene. For example, *ITvar32* and *ITvar6* are partly identical to *ITvar19*. *3 and *4: Oligos ITvar32_2, ITvar32_3 and ITvar6_0 (*4) also match *ITvar19*. However, other oligos specific to *ITvar32* (ITvar32_0 and 1) and *ITvar6* (ITvar32_1, 2 and 3) are not upregulated.

Considering the five selections together, the microarray data for the *var* gene family is striking. In all 5 selections, one (or two in IT-HBEC) *var* variant is very highly upregulated in the selected parasites while plenty of variants are

downregulated. At time point 3 (16 to 24 hours post invasion), there is an 11 to 320 fold increase of these *var* genes in the selected population (Table 5-5). No other *var* gene was upregulated by at least 2 fold across more than one time point. In fact, the upregulation of these particular *var* genes (*HB3var3* in HB3-HBEC1, 2 and TNF; *PFD0020c* in 3D7-HBEC; *ITvar7* and *ITvar19* in IT-HBEC) was so high that it was immediately visible on the scanned slides (see Figure 5-12 as an example).

	T1	T2	T3	T4	T5	T6
HB3-HBEC1: *var3*	8.5	13.4	34.1	61.0	9.8	25.1
HB3-HBEC2: *var3*	6.4	NA	11.2	3.0	0.8	NA
HB3-HBEC-TNF: *var3*	5.1	2.3	37.5	3.5	1.3	5.6
3D7-HBEC: *PFD0020c*	0.4	22.0	19.6	7.0	4.2	6.3
IT-HBEC: *var7*	13.1	14.2	177.2	NA	NA	10.3
IT-HBEC: *var19*	9.2	32.8	319.2	14.7	12.7	13.8

Table 5-5. Expression fold ratios (unlogged) of the most upregulated *var* genes in each selection. Numbers represent the average of all oligos specific to that gene. Note that if data is missing for one oligo, the unlogged ratio is assumed to be 1 for calculating the average ratio. NA = no data available in any oligo.

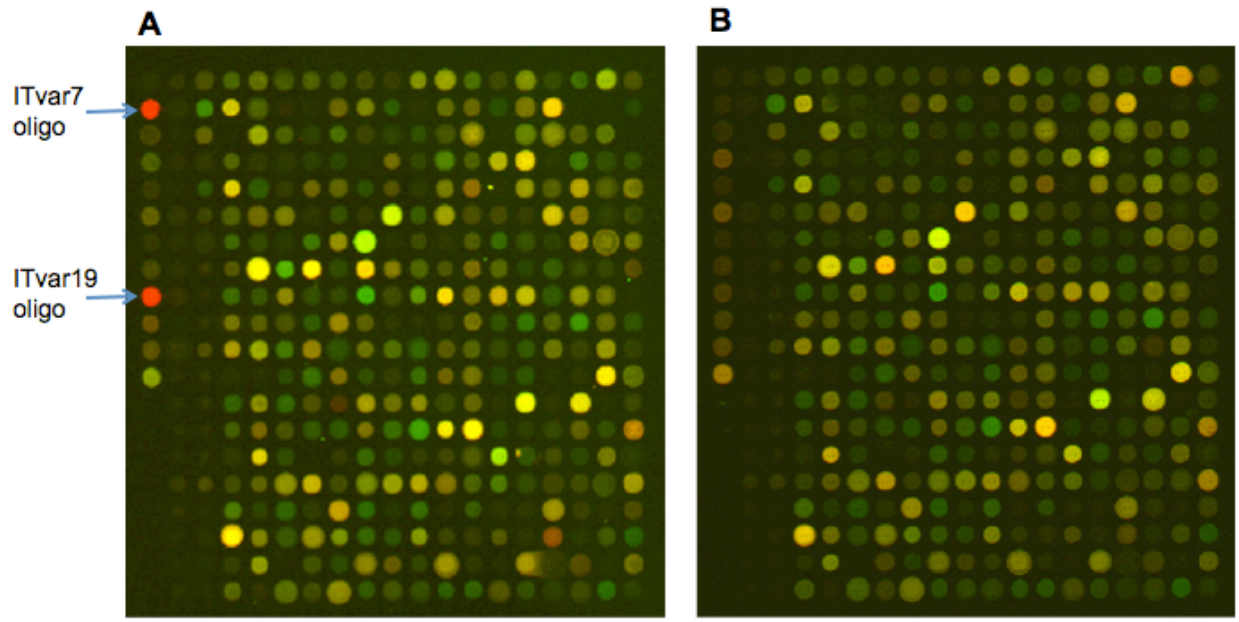


Figure 5-12. Comparison between IT-HBEC (A) and IT-Uns (B) microarray scans at time point 2. The same 380 spots of both chips are shown, before any gridding. Note how, apart from 2 spots in (A), the colour pattern is very similar from one chip to the other.

5.5.5.4 *Rif* and *stevor* gene expression in selected and unselected parasites

5.5.5.4.1 Differentially regulated rif *genes in HB3 parasites*

HB3-HBEC1, HB3-HBEC2 and HB3-HBEC-TNF show upregulation of many *rif* variants at time point 3 and 4 (Figure 5-13).

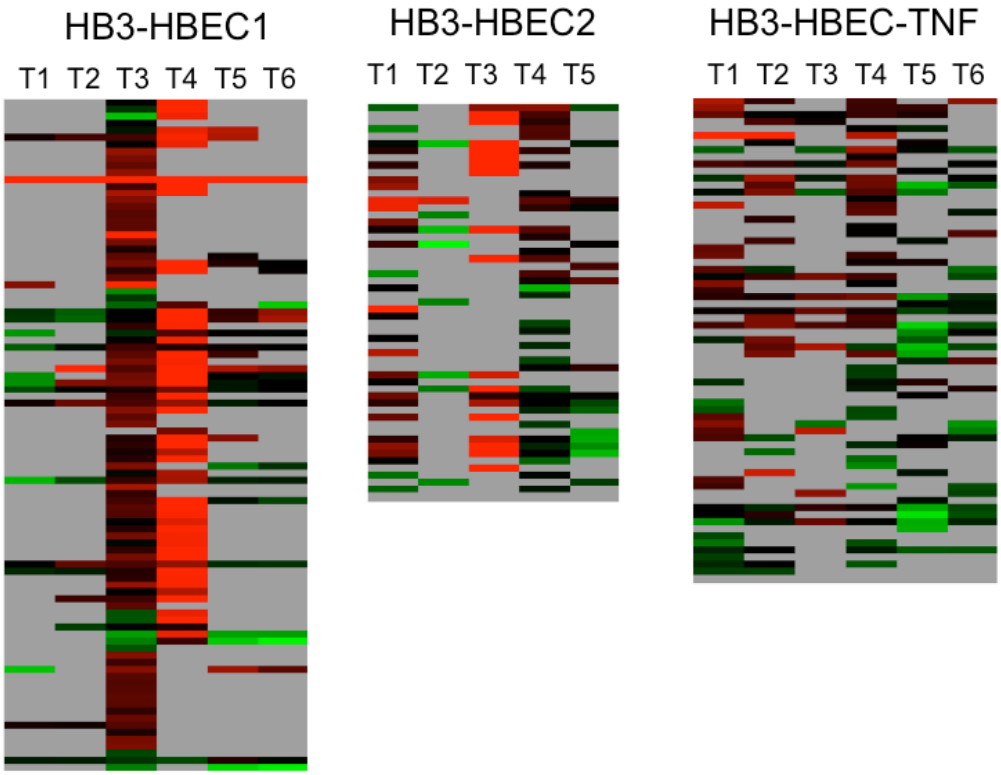


Figure 5-13. *Rif* expression in all 3 HB3 selections. Only oligos that show expression data in at least one time point are shown. Each row is a different oligo, each column is a time point. Most *rif* genes are represented by a single oligo on the chip. The most highly upregulated variants are also shown in Figure 5-14.

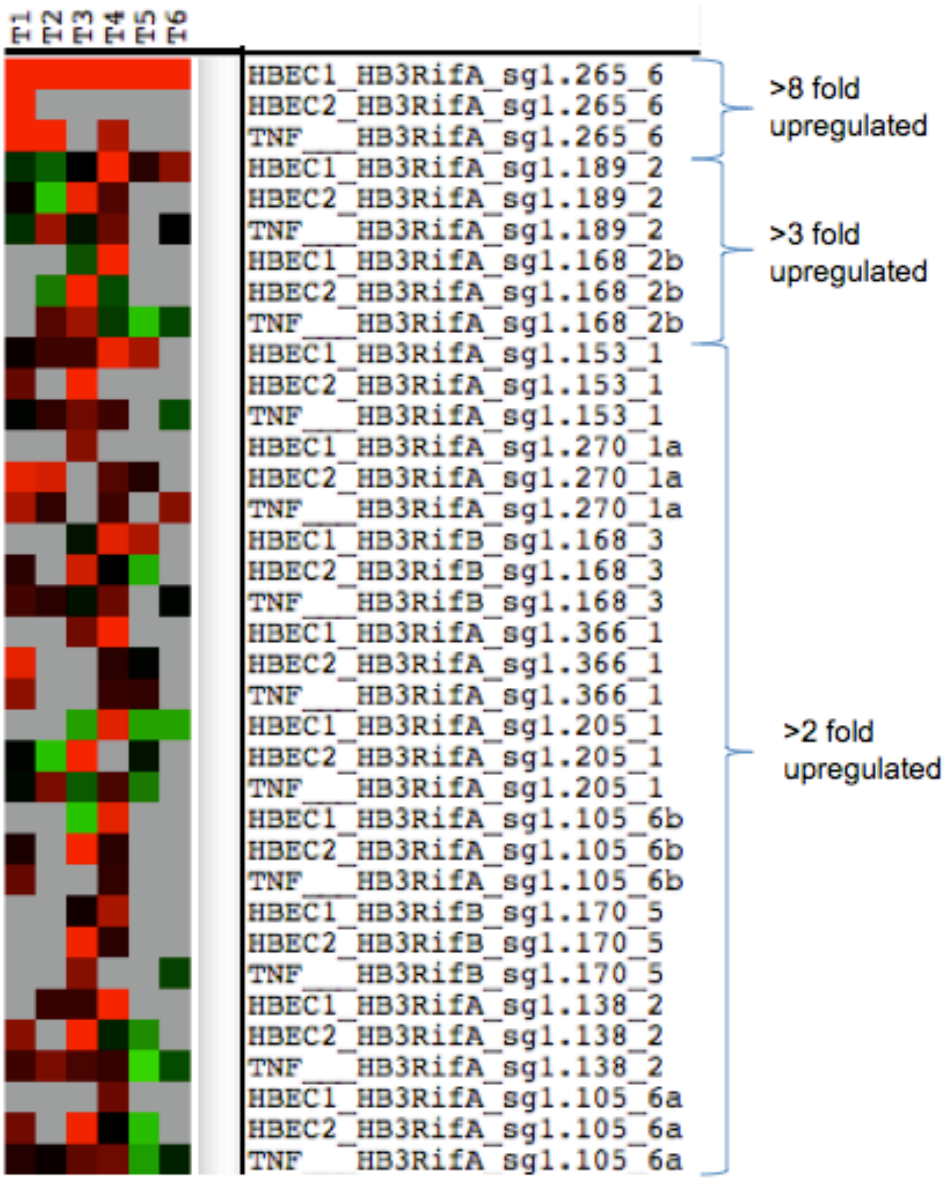


Figure 5-14. 12 Oligos specific to *rif* genes at least 2 fold upregulated in the 3 HB3-derived strains. The name of each *rif* gene is given by the supercontig number where it is found as well as which strand (e.g., "HB3RifA_sg1.265_6" is a HB3 *rif* gene, subgroup A, found in supercontig 265 on the reverse complement frame 6). An "a" or "b" letter is added where many genes on the same supercontig are encountered. "TNF" = the HB3-HBEC-TNF strain.

As the same *var* gene (*HB3var3*) was to found to be upregulated with or without the activation of HBEC-5i with TNF, we investigated whether we could identify *rif* genes upregulated in all 3 HB3 derived selections. In other words, we

examined the possibility that one or more HB3 *rif* genes may act as a ligand to HBEC-5i, regardless of the endothelial cells activation with TNF. In the *rif* family, 12 genes are upregulated by 2 fold or more in at least one time point, 3 of them are 3 fold or more upregulated (Figure 5-14). Only one is highly upregulated: *HB3_RifA_265_6*, by 8 to 100 fold (Table 5-6). It is represented on the microarray chip by a single oligo. Very interestingly, this *rif* gene is located on the same supercontig as *HB3var3*, the most highly upregulated *var* gene (Figure 5-15, second panel). These two genes lay next to each other but on different strands and are transcribed in opposite directions. This is a common feature of group A *var* genes: a *rif* gene (subfamily *Rif_A2*) is found "head to head" with the *var* gene (Lavstsen, et al., 2003a). Thus the selection of HB3 parasites on HBEC-5i, with or without prior activation with TNF, led to the upregulation of *HB3var3* and its "head to head" *HB3_RifA_265_6* gene, as well as other *rif* variants but to a lower level. The selection on TNF-activated HBEC-5i has not greatly modified the *rif* expression pattern of HB3 parasites.

	T1	T2	T3	T4	T5	T6
HBEC1: *HB3_RifA_265_6*	15.4	18.9	17.9	99.9	16.0	32.9
HBEC2: *HB3_RifA_265_6*	10.1	NA	NA	NA	NA	NA
HB3-HBEC-TNF: *HB3_RifA_265_6*	7.8	16.0	NA	3.8	NA	NA
3D7-HBEC: *rif_PFD0025w*	0.8	NA	15.6	NA	0.9	1.3
IT-HBEC: IT_RifA_2006_6b	NA	NA	NA	NA	NA	NA

Table 5-6. Expression fold ratios (unlogged) of the *rif* genes located "head to head" to the most upregulated *var* genes in each selection. Data comes from a single oligo, except for *PFD0025w* that is represented by two oligos (numbers given are the average of both oligos). NA = No data available.

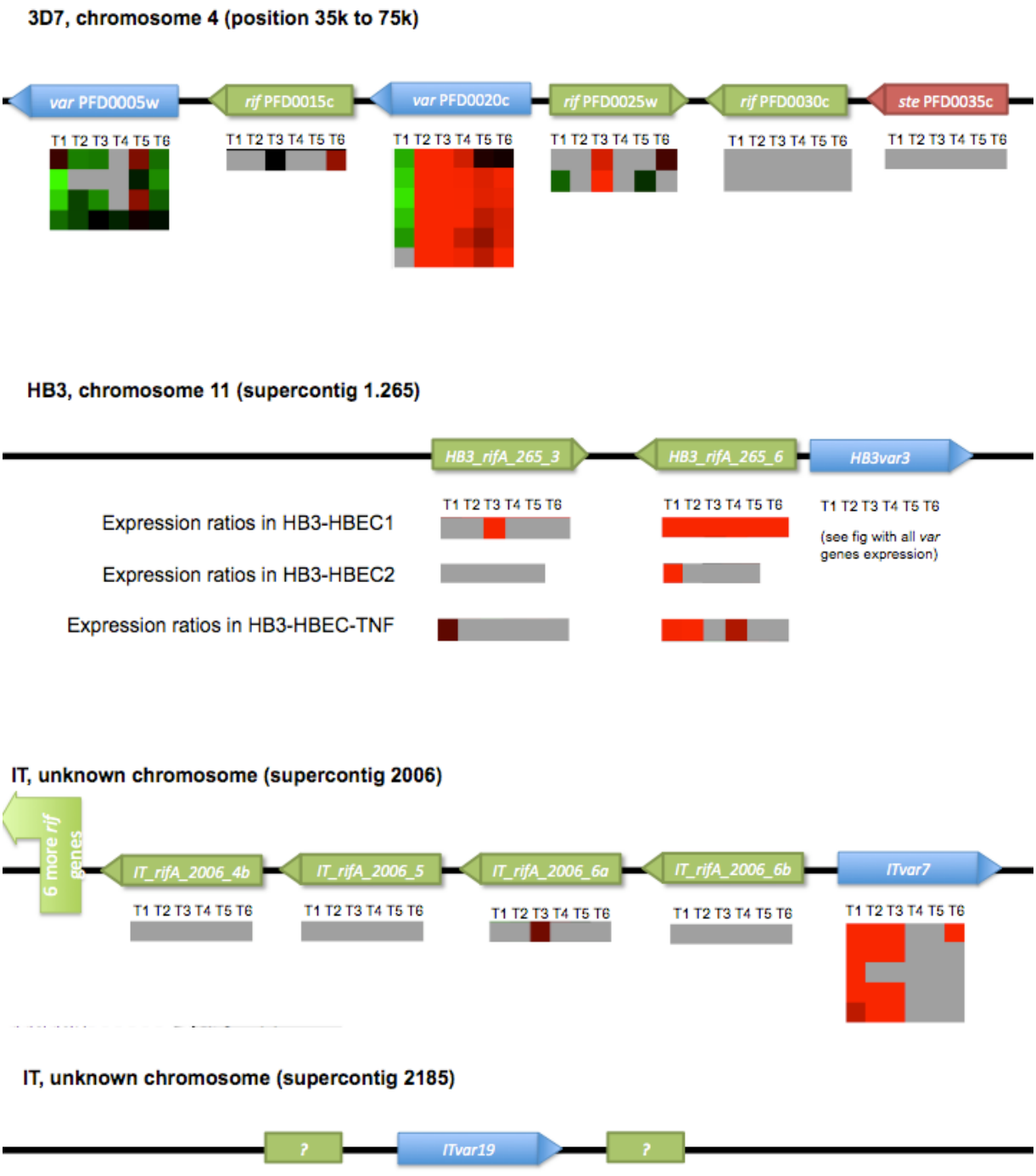


Figure 5-15. Chromosomal representation of all upregulated *var* and *rif genes*. Only the 3D7 map is 'complete' as the genome assembly for HB3 and IT is not finished. For example, it is not known if there are VSA genes surrounding *ITvar19*. Expression data of all oligos is shown below each gene when available. Drawings are not to scale.

5.5.5.4.2 Differentially regulated rif *genes in 3D7 parasites*

In 3D7-HBEC, the most highly upregulated *rif* gene is *PFD0025w* (represented by two oligos, Figure 5-16 below and Table 5-6 above) that is physically found next to the *PFD0020c var* gene (Figure 5-15, top panel). Thus the group A *var* and its "head to head" *rif* gene seem to have been upregulated together, similar to what was observed with the HB3 selections. Importantly, the expression of other VSAs in the close vicinity of the upregulated *var* and *rif* genes seems unaffected. This rules out the possibility that the entire chromosomal region is in a transcriptionally active state resulting from the selection on HBEC-5i.

No *rif* gene was upregulated in more than one time point and none to the same extent as *PFD0025w*. Thus with 3D7 parasites, the selection on HBEC-5i has enriched for parasites expressing *var PFD0020c* and *rif PFD0025w*, two VSA genes located "head to head" with each other.

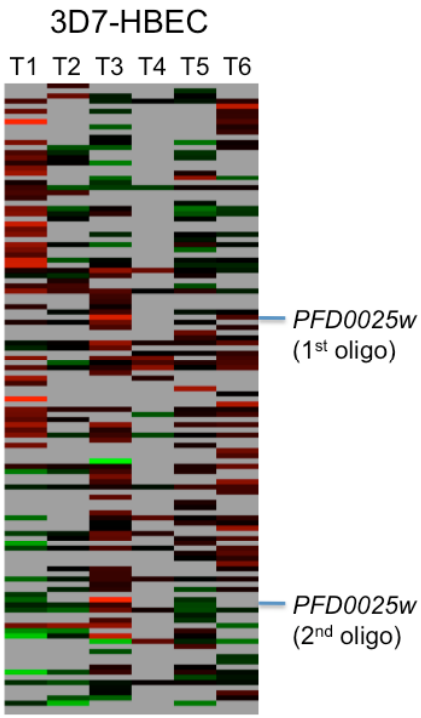


Figure 5-16. *Rif* expression in 3D7. Only oligos that show expression data in at least one time point are shown. *PFD0025w*, represented by two oligos, is the most highly upregulated *rif* gene in 3D7-HBEC.

5.5.5.4.3 Differentially regulated rif *genes in IT parasites*

In IT-HBEC, many *rif* genes are upregulated in time point 3 (Figure 5-17). Just five *rif* variants show a ratio greater than 3 fold in a single time point: *IT_RifA_647_3*, *IT_RifA_2004_6*, *IT_RifA_2157_3a*, *IT_RifA_p_246_1* and *IT_RifA_1466.* The latter is the most upregulated with a 6 fold ratio (average of two oligos). *IT_RifA_2006_6b*, the *rif* gene located next to the *ITvar7* gene that is upregulated in selected parasites, shows "no data" at all time points (Figure 5-15, third panel). Therefore this gene was probably not expressed in IT-HBEC, although it is possible that a technical issue impeded the signal (for example, misprinting of the relevant oligo).

The contig where the group B *ITvar19* lays is too short to be able to tell if there is any *rif* sequence in its surrounding. This is unexpected anyway as "head to head" *rif* genes are only found next to group A *var* genes (Lavstsen, et al., 2003b).

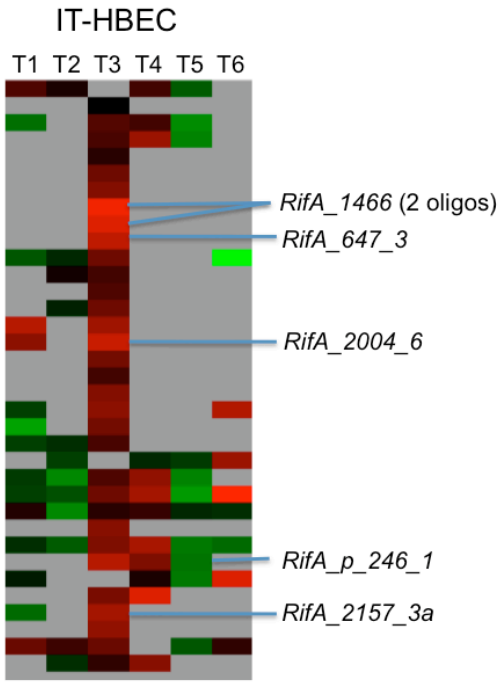


Figure 5-17. *Rif* expression in IT. Only oligos that show expression data in at least one time point are shown. Five *rif* variants that show a ratio greater than 3 fold in a single time point are indicated.

All in all, the five selections on HBEC-5i (one of which with TNF activated HBEC-5i) all show many upregulated *rif* genes and few downregulated ones. Interestingly, in HB3 and 3D7 selections, the most highly upregulated *rif* is located "head to head" with the upregulated *var* genes previously identified (section 5.5.5.1). In 3D7-HBEC, other VSAs located in the vicinity of the upregulated *var*/*rif* do not show upregulation, suggesting a very specific control of gene transcription. In IT-HBEC the "head-to head" *rif* gene next to the upregulated var gene was not upregulated, therefore it does not appear to be generally true that *var* genes and their head-to-head *rif* genes are always co-regulated.

5.5.5.4.4 Differentially regulated stevor *genes*

In HB3-HBEC1, a wide range of *stevor* variants was found to be upregulated in time point 4 of this pilot experiment (Figure 5-18). This expression window (24 to 32 hours post invasion) exactly corresponds to *stevor* transcription timing (Kaviratne, et al., 2002). However, none of these upregulated *stevor* genes were expressed in the repeat of this experiment (HB3-HBEC2). As HB3-HBEC-TNF shares a very similar *var* and *rif* genes expression pattern with HB3-HBEC1 and 2, it was postulated that some *stevor* genes would also be found upregulated in common to all 3 selections. However, only one *stevor* (*HB3_Ste_195_6*, subfamily A) is upregulated in HB3-HBEC1 and HB3-HBEC-TNF. No *stevor* gene was upregulated in all 3 HB3 derived selections. Altogether, because of the lack of overlap between HB3-HBEC1 and HB3-HBEC2, no Stevor protein is likely to be involved in the cytoadhesion to HBEC-5i, at least for the HB3 clone.

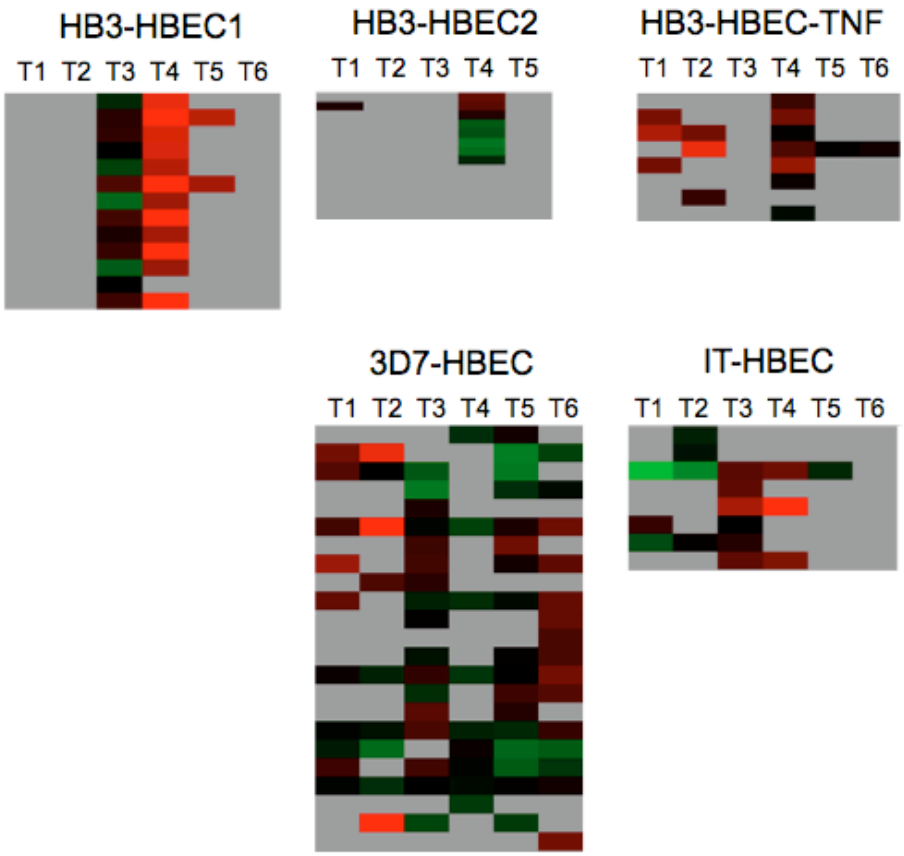


Figure 5-18. *Stevor* expression in all 5 selections. Only oligos that show that expression data in at least one time point are shown. Each row is a different oligo, each column is a time point. The vast majority of *stevor* genes are represented by a single oligo.

In IT-HBEC, a pseudogene is the most highly upregulated *stevor*: *IT_ste_p_2164_32* (6 fold at time point 4). No other variant is upregulated by at least 2 fold.

In 3D7-HBEC, 4 *stevor* genes are upregulated more than 3 fold at time point 2: *PFA0750w* (3 fold), *MAL7P1.218* (6 fold), *PF10_0395* (9 fold) and *PFC1105w* (11 fold). The other time points however are only slightly up or even down regulated. These 4 upregulated 3D7 *stevor*, out of 37 family members, have to be put into the perspective that ~10% of all oligos on the chip show at least one time point differentially expressed by 3 fold or more (Table 5-7). Thus an experimental repeat with IT-HBEC and 3D7-HBEC would be needed before drawing any conclusion on *rif* and *stevor* in these 2 strains.

	Total non-VSA genes	1 TP > 2 fold	1 TP > 3 fold	1 TP > 4 fold	2 TPs > 2 fold
HB3-HBEC1	4837	1191	405	233	324
HB3-HBEC2	5083	2025	932	529	769
HB3-HBEC-TNF	5140	2326	1057	651	1030
3D7-HBEC	5096	1461	580	331	384
IT-HBEC	4959	2472	1196	638	818

Table 5-7. Number of non-VSA genes (averaged oligo values) differentially regulated in at least one time point. The column "Total non-VSA genes" identifies genes with expression in at least one time point. "1 TP > 2 fold" indicates the number of genes that are up or down regulated by at least 2 fold in at least one time point. "2 TPs" means in at least 2 time points.

An interesting feature about *rif* and *stevor* expression data is that, only about a quarter of all oligos show expression above background level. In each strain, 11 to 34% of *rif* and *stevor* oligos were expressed (see full set of microarray data in appendix). Within the genome as a whole, with the same background cutoff, percentage of oligos with data is around 70 to 85% (Table 5-3 in section 5.5.3). This indicates that most of these VSA are not expressed in *in vitro* cultures, which has been reported previously (Blythe, et al., 2009, Mackinnon, et al., 2009).

It is also interesting to note that very few *rif* oligos show downregulation after selection on HBEC-5i (i.e. few "green spots", Figure 5-13, Figure 5-16 and Figure 5-17). This contrasts with the *var* genes expression pattern where the majority of oligos showed downregulation.

Overall, the analysis of the microarray data for VSA expression has revealed, in HB3 and 3D7-HBEC selections, a single group A *var* and its "head to head" *rif* genes to be the most consistent and highly upregulated VSA genes after selection on HBEC-5i. In IT-HBEC, two *var* genes (a group A and a group B family members) were found to be upregulated. This data fits very well with the hypothesis that the selected populations of parasites express a restricted

repertoire of VSA that are the main ligand candidates for cytoadherence to HBEC-5i.

5.5.6 Analysis of non-VSA genes expression in selected and unselected parasites

The 4 *var* genes identified in section 5.5.5 are unequivocal: they are by far the most highly upregulated genes after selection. However, even if these PfEMP1 variants (and their associated Rifins for 3D7-HBEC and HB3 selections) are now strong ligand candidates, this does not exclude the possibility that other non-VSA genes could be involved in the cytoadherence to HBEC-5i. Here again, the hypothesis is that any gene that would explain the change of phenotype from unselected (non-binding) parasites to selected (binding) parasites would be upregulated after selection. The vast majority of non-VSA genes have a virtually identical sequence from one strain to the other therefore the 3 clones (HB3, 3D7 and IT) can be considered as replicates of each other (Llinas, et al., 2006). Moreover, HB3-HBEC-TNF showed very similar VSA expression pattern with HB3-HBECs. Thus, in the first instance, we analyzed the non-VSA data of all 5 selections together. The aim of this section is to discover whether other non-VSA genes may be involved, directly or indirectly, in cytoadherence to HBEC-5i.

For the analysis of non-VSA genes, oligos specific to the same genes were averaged together (Table 5-7 above). In cases where one oligo had no data for a particular time point and another oligo specific to the same gene does have a value, the "no data" was averaged with a value of 1 (i.e. no change of expression). This is a conservative approach in order to weigh down outliers. Three different approaches to the analysis of non-VSA genes were tested and are described in detail below:

- Approach 1: Genes differentially regulated in all 5 selections.
- Approach 2: Statistical approach.
- Approach 3: "Area under the curve" (and statistical tests).

5.5.6.1 Approach 1: Differentially regulated genes in common to all 5 selections

This is the most intuitive type of analysis: a gene involved in general cytoadherence to HBEC-5i (with or without prior activation with TNF) should be upregulated in all selections. Using an arbitrary cutoff of 2 fold in at least one time point (Table 5-7), 15 genes were found to be upregulated (Figure 5-19) and 58 genes were downregulated in all 5 selections. Out of a total of about 5000 genes (the full *P. falciparum* genome minus the VSA genes), only one gene is upregulated by at least 3 fold in all 5 selections: *PF14_0472*, member of the PHISTa family. The Plasmodium helical interspersed subtelomeric (PHIST) family, with 72 members in *P. falciparum*, encodes proteins of unknown functions but predicted to be exported (Sargeant, et al., 2006). 6 other upregulated genes encode proteins predicted or proven to be exported: *P. falciparum* Erythrocyte Membrane Protein 3 (PfEMP3, exported (Pasloske, et al., 1993)), Ring-infected Erythrocyte Surface Antigen (RESA-1, exported (Brown, et al., 1985)), Membrane Associated Histine Rich Protein (MAHRP-1, exported (Spycher, et al., 2003)) and 3 predicted to be exported proteins with a Pexel motif: PF14_0740, PF11_0035 and PFF0055w (Sargeant, et al., 2006). These 6 genes and *PF14_0472* are upregulated at time point 3 (16 to 24 hours post invasion) in almost all selections, indicating that they could be translated on time for cytoadherence at the pigmented trophozoite stage. The functions of these proteins and the possibility that they could play a role in cytoadherence are discussed further in section 5.6.6.

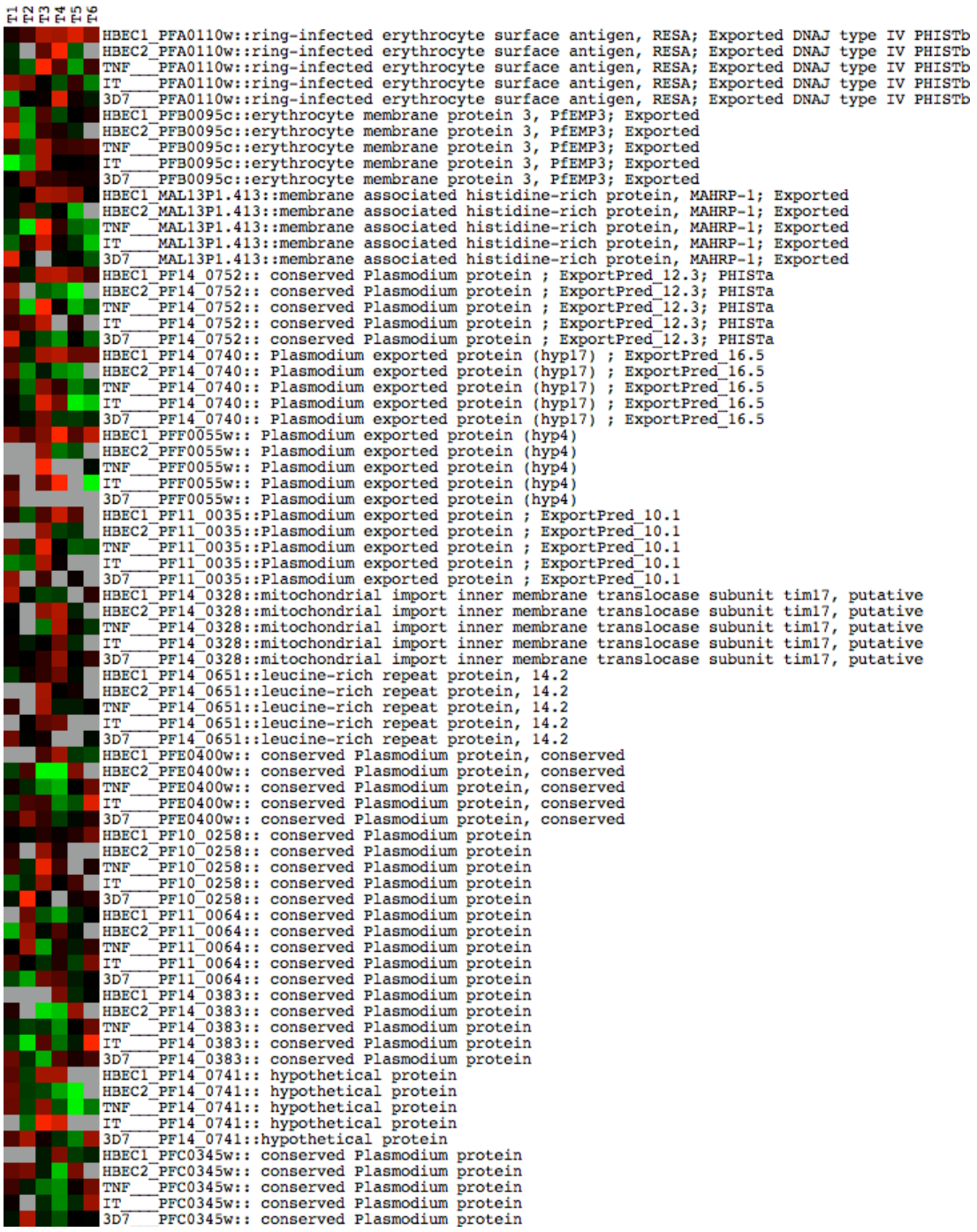


Figure 5-19. 15 genes upregulated in at least one time point by 2 fold or more in all 5 selections. Data for each gene represents the average of many oligos where available. The top 7 genes are proven or predicted to be exported. The gene annotation was updated with PlasmoDB 6.4 (released on 13 May 2010). "ExportPred" = Export prediction score (Sargeant, et al., 2006). A score of 4.3 or above corresponds to a 95% chance of the protein to be exported. *PF14_0752* (PHISTa) is the only gene to be upregulated by 3 fold in all selections.

The 8 other upregulated genes (Figure 5-19) do not show a Pexel motif, however there are examples of proteins being exported despite lacking such a motif (Skeleton binding protein 1, MAHRP-1, ring-exported proteins 1 and 2 are all trafficked to the Maurer's Cleft (Saridaki, et al., 2009, Spielmann, et al., 2006, Spycher, et al., 2003)). Alternatively, even within the parasite, they could be indirectly involved in cytoadherence, for example by facilitating PfEMP1 trafficking. Finally, note that many of these "up" regulated genes are also downregulated in other time points (Figure 5-19). For these genes the selection may have change the timing of expression rather than the actual overall amount of mRNA.

Within the 58 downregulated genes, 11 are downregulated by at least 3 fold in at least one time point (Figure 5-20). Intriguingly, 4 invasion-related proteins are found within these 11 highly downregulated genes: Reticulocyte binding protein Homolog 4 (RH4), merozoite surface protein-6 (MSP6), subtilisin-like protease 1 (PfSUB-1) and Apical Membrane Antigen (AMA-1). The rest of the "downregulated dataset" also contains invasion-related members: RH3, MSP3, MSP-7, Erythrocyte Binding Antigen-140 (EBA 140), EBA-175, EBA-181, CLAG 3.2, SPATR protein (Curtidor, et al., 2008), merozoite-TRAP-like protein ((Baum, et al., 2006)), protein Kinase 2 (Kato, et al., 2008), PF10_0352 (a merozoite surface protein (Hu, et al., 2009)), PF10_0351 (a.k.a. MSP3-related protein H103 (Pearce, et al., 2005)) (all reviewed in (Gaur, et al., 2004) unless otherwise specified). Thus 16 out of the 58 most consistently downregulated genes encode proteins known to be associated with merozoite invasion. Moreover, a very recent study predicted the functions of hypothetical proteins based on their association with known proteins (Hu, et al., 2009). Using their function prediction, 25 other genes in the "downregulated dataset" were classified as invasion-related (Figure 5-20). Thus, after selection on HBEC-5i, all five selected lines show a marked downregulation of 58 genes in common, 69% of which encode proteins proven or predicted to be involved with merozoite invasion. They were mostly downregulated in time points 1, 3 and 5 (Table 5-8). Note that at the time where invasion genes are expected to be transcribed, i.e.

time point 6, there was no downregulation on average (Table 5-8). Thus the actual amount of invasion proteins necessary for merozoites to invade in RBC may still be the same in HBEC-5i selected parasites. In fact, although it was not specifically tested, the invasion rate did not seem to differ before or after selection.

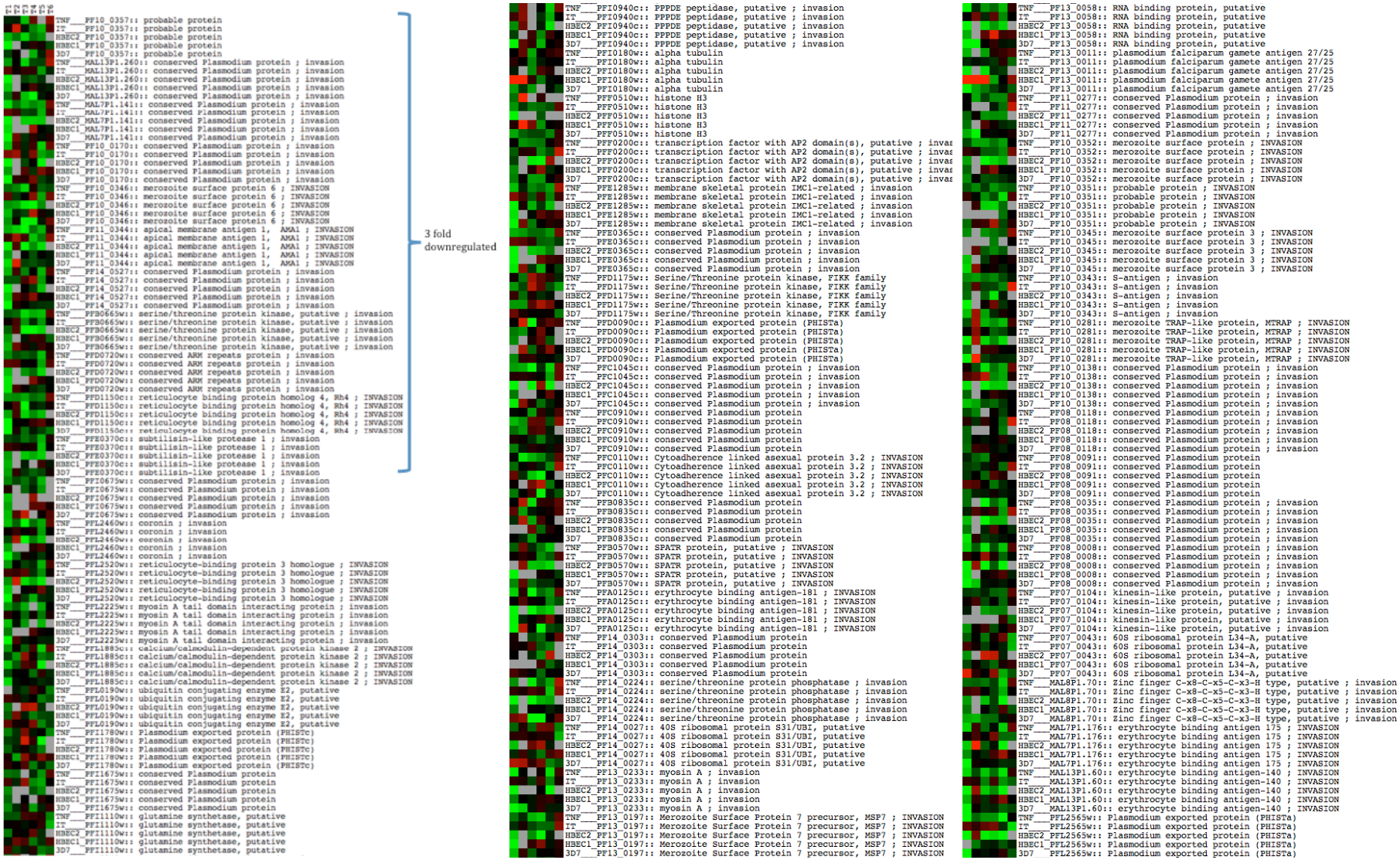

T12
T24
T36
T48
T60
TNF___PF10_0357:: probable protein
IT___PF10_0357:: probable protein
HBEC2_PF10_0357:: probable protein
HBEC1_PF10_0357:: probable protein
3D7___PF10_0357:: probable protein
TNF___MAL13P1.260:: conserved Plasmodium protein ; invasion
IT___MAL13P1.260:: conserved Plasmodium protein ; invasion
HBEC2_MAL13P1.260:: conserved Plasmodium protein ; invasion
HBEC1_MAL13P1.260:: conserved Plasmodium protein ; invasion
3D7___MAL13P1.260:: conserved Plasmodium protein ; invasion
TNF___MAL7P1.141:: conserved Plasmodium protein ; invasion
IT___MAL7P1.141:: conserved Plasmodium protein ; invasion
HBEC2_MAL7P1.141:: conserved Plasmodium protein ; invasion
HBEC1_MAL7P1.141:: conserved Plasmodium protein ; invasion
3D7___MAL7P1.141:: conserved Plasmodium protein ; invasion
TNF___PF10_0170:: conserved Plasmodium protein ; invasion
IT___PF10_0170:: conserved Plasmodium protein ; invasion
HBEC2_PF10_0170:: conserved Plasmodium protein ; invasion
HBEC1_PF10_0170:: conserved Plasmodium protein ; invasion
3D7___PF10_0170:: conserved Plasmodium protein ; invasion
TNF___PF10_0346:: merozoite surface protein 6 ; INVASION
IT___PF10_0346:: merozoite surface protein 6 ; INVASION
HBEC2_PF10_0346:: merozoite surface protein 6 ; INVASION
HBEC1_PF10_0346:: merozoite surface protein 6 ; INVASION
3D7___PF10_0346:: merozoite surface protein 6 ; INVASION
TNF___PF11_0344:: apical membrane antigen 1, AMA1 ; INVASION
IT___PF11_0344:: apical membrane antigen 1, AMA1 ; INVASION
HBEC2_PF11_0344:: apical membrane antigen 1, AMA1 ; INVASION
HBEC1_PF11_0344:: apical membrane antigen 1, AMA1 ; INVASION
3D7___PF11_0344:: apical membrane antigen 1, AMA1 ; INVASION
TNF___PF14_0527:: conserved Plasmodium protein ; invasion
IT___PF14_0527:: conserved Plasmodium protein ; invasion
HBEC2_PF14_0527:: conserved Plasmodium protein ; invasion
HBEC1_PF14_0527:: conserved Plasmodium protein ; invasion
3D7___PF14_0527:: conserved Plasmodium protein ; invasion
TNF___PFB0665w:: serine/threonine protein kinase, putative ; invasion
IT___PFB0665w:: serine/threonine protein kinase, putative ; invasion
HBEC2_PFB0665w:: serine/threonine protein kinase, putative ; invasion
HBEC1_PFB0665w:: serine/threonine protein kinase, putative ; invasion
3D7___PFB0665w:: serine/threonine protein kinase, putative ; invasion
TNF___PFD0720w:: conserved ARM repeats protein ; invasion
IT___PFD0720w:: conserved ARM repeats protein ; invasion
HBEC2_PFD0720w:: conserved ARM repeats protein ; invasion
HBEC1_PFD0720w:: conserved ARM repeats protein ; invasion
3D7___PFD0720w:: conserved ARM repeats protein ; invasion
TNF___PFD1150c:: reticulocyte binding protein homolog 4, Rh4 ; INVASION
IT___PFD1150c:: reticulocyte binding protein homolog 4, Rh4 ; INVASION
HBEC2_PFD1150c:: reticulocyte binding protein homolog 4, Rh4 ; INVASION
HBEC1_PFD1150c:: reticulocyte binding protein homolog 4, Rh4 ; INVASION
3D7___PFD1150c:: reticulocyte binding protein homolog 4, Rh4 ; INVASION
TNF___PFE0370c:: subtilisin-like protease 1 ; invasion
IT___PFE0370c:: subtilisin-like protease 1 ; invasion
HBEC2_PFE0370c:: subtilisin-like protease 1 ; invasion
HBEC1_PFE0370c:: subtilisin-like protease 1 ; invasion
3D7___PFE0370c:: subtilisin-like protease 1 ; invasion
TNF___PFI0675w:: conserved Plasmodium protein ; invasion
IT___PFI0675w:: conserved Plasmodium protein ; invasion
HBEC2_PFI0675w:: conserved Plasmodium protein ; invasion
HBEC1_PFI0675w:: conserved Plasmodium protein ; invasion
3D7___PFI0675w:: conserved Plasmodium protein ; invasion
TNF___PFL2460w:: coronin ; invasion
IT___PFL2460w:: coronin ; invasion
HBEC2_PFL2460w:: coronin ; invasion
HBEC1_PFL2460w:: coronin ; invasion
3D7___PFL2460w:: coronin ; invasion
TNF___PFL2520w:: reticulocyte-binding protein 3 homologue ; INVASION
IT___PFL2520w:: reticulocyte-binding protein 3 homologue ; INVASION
HBEC2_PFL2520w:: reticulocyte-binding protein 3 homologue ; INVASION
HBEC1_PFL2520w:: reticulocyte-binding protein 3 homologue ; INVASION
3D7___PFL2520w:: reticulocyte-binding protein 3 homologue ; INVASION
TNF___PFL2225w:: myosin A tail domain interacting protein ; invasion
IT___PFL2225w:: myosin A tail domain interacting protein ; invasion
HBEC2_PFL2225w:: myosin A tail domain interacting protein ; invasion
HBEC1_PFL2225w:: myosin A tail domain interacting protein ; invasion
3D7___PFL2225w:: myosin A tail domain interacting protein ; invasion
TNF___PFL1885c:: calcium/calmodulin-dependent protein kinase 2 ; INVASION
IT___PFL1885c:: calcium/calmodulin-dependent protein kinase 2 ; INVASION
HBEC2_PFL1885c:: calcium/calmodulin-dependent protein kinase 2 ; INVASION
HBEC1_PFL1885c:: calcium/calmodulin-dependent protein kinase 2 ; INVASION
3D7___PFL1885c:: calcium/calmodulin-dependent protein kinase 2 ; INVASION
TNF___PFL0190w:: ubiquitin conjugating enzyme E2, putative
IT___PFL0190w:: ubiquitin conjugating enzyme E2, putative
HBEC2_PFL0190w:: ubiquitin conjugating enzyme E2, putative
HBEC1_PFL0190w:: ubiquitin conjugating enzyme E2, putative
3D7___PFL0190w:: ubiquitin conjugating enzyme E2, putative
TNF___PFI1780w:: Plasmodium exported protein (PHISTc)
IT___PFI1780w:: Plasmodium exported protein (PHISTc)
HBEC2_PFI1780w:: Plasmodium exported protein (PHISTc)
HBEC1_PFI1780w:: Plasmodium exported protein (PHISTc)
3D7___PFI1780w:: Plasmodium exported protein (PHISTc)
TNF___PFI1675w:: conserved Plasmodium protein
IT___PFI1675w:: conserved Plasmodium protein
HBEC2_PFI1675w:: conserved Plasmodium protein
HBEC1_PFI1675w:: conserved Plasmodium protein
3D7___PFI1675w:: conserved Plasmodium protein
TNF___PFI1110w:: glutamine synthetase, putative
IT___PFI1110w:: glutamine synthetase, putative
HBEC2_PFI1110w:: glutamine synthetase, putative
HBEC1_PFI1110w:: glutamine synthetase, putative
3D7___PFI1110w:: glutamine synthetase, putative
3 fold downregulated
TNF___PFI0940c:: PPPDE peptidase, putative ; invasion
IT___PFI0940c:: PPPDE peptidase, putative ; invasion
HBEC2_PFI0940c:: PPPDE peptidase, putative ; invasion
HBEC1_PFI0940c:: PPPDE peptidase, putative ; invasion
3D7___PFI0940c:: PPPDE peptidase, putative ; invasion
TNF___PFI0180w:: alpha tubulin
IT___PFI0180w:: alpha tubulin
HBEC2_PFI0180w:: alpha tubulin
HBEC1_PFI0180w:: alpha tubulin
3D7___PFI0180w:: alpha tubulin
TNF___PFF0510w:: histone H3
IT___PFF0510w:: histone H3
HBEC2_PFF0510w:: histone H3
HBEC1_PFF0510w:: histone H3
3D7___PFF0510w:: histone H3
TNF___PFF0200c:: transcription factor with AP2 domain(s), putative ; invas
IT___PFF0200c:: transcription factor with AP2 domain(s), putative ; invas
HBEC2_PFF0200c:: transcription factor with AP2 domain(s), putative ; invas
HBEC1_PFF0200c:: transcription factor with AP2 domain(s), putative ; invas
3D7___PFF0200c:: transcription factor with AP2 domain(s), putative ; invas
TNF___PFE1285w:: membrane skeletal protein IMC1-related ; invasion
IT___PFE1285w:: membrane skeletal protein IMC1-related ; invasion
HBEC2_PFE1285w:: membrane skeletal protein IMC1-related ; invasion
HBEC1_PFE1285w:: membrane skeletal protein IMC1-related ; invasion
3D7___PFE1285w:: membrane skeletal protein IMC1-related ; invasion
TNF___PFE0365c:: conserved Plasmodium protein ; invasion
IT___PFE0365c:: conserved Plasmodium protein ; invasion
HBEC2_PFE0365c:: conserved Plasmodium protein ; invasion
HBEC1_PFE0365c:: conserved Plasmodium protein ; invasion
3D7___PFE0365c:: conserved Plasmodium protein ; invasion
TNF___PFD1175w:: Serine/Threonine protein kinase, FIKK family
IT___PFD1175w:: Serine/Threonine protein kinase, FIKK family
HBEC2_PFD1175w:: Serine/Threonine protein kinase, FIKK family
HBEC1_PFD1175w:: Serine/Threonine protein kinase, FIKK family
3D7___PFD1175w:: Serine/Threonine protein kinase, FIKK family
TNF___PFD0090c:: Plasmodium exported protein (PHISTa)
IT___PFD0090c:: Plasmodium exported protein (PHISTa)
HBEC2_PFD0090c:: Plasmodium exported protein (PHISTa)
HBEC1_PFD0090c:: Plasmodium exported protein (PHISTa)
3D7___PFD0090c:: Plasmodium exported protein (PHISTa)
TNF___PFC1045c:: conserved Plasmodium protein ; invasion
IT___PFC1045c:: conserved Plasmodium protein ; invasion
HBEC2_PFC1045c:: conserved Plasmodium protein ; invasion
HBEC1_PFC1045c:: conserved Plasmodium protein ; invasion
3D7___PFC1045c:: conserved Plasmodium protein ; invasion
TNF___PFC0910w:: conserved Plasmodium protein
IT___PFC0910w:: conserved Plasmodium protein
HBEC2_PFC0910w:: conserved Plasmodium protein
HBEC1_PFC0910w:: conserved Plasmodium protein
3D7___PFC0910w:: conserved Plasmodium protein
TNF___PFC0110w:: Cytoadherence linked asexual protein 3.2 ; INVASION
IT___PFC0110w:: Cytoadherence linked asexual protein 3.2 ; INVASION
HBEC2_PFC0110w:: Cytoadherence linked asexual protein 3.2 ; INVASION
HBEC1_PFC0110w:: Cytoadherence linked asexual protein 3.2 ; INVASION
3D7___PFC0110w:: Cytoadherence linked asexual protein 3.2 ; INVASION
TNF___PFB0835c:: conserved Plasmodium protein
IT___PFB0835c:: conserved Plasmodium protein
HBEC2_PFB0835c:: conserved Plasmodium protein
HBEC1_PFB0835c:: conserved Plasmodium protein
3D7___PFB0835c:: conserved Plasmodium protein
TNF___PFB0570w:: SPATR protein, putative ; INVASION
IT___PFB0570w:: SPATR protein, putative ; INVASION
HBEC2_PFB0570w:: SPATR protein, putative ; INVASION
HBEC1_PFB0570w:: SPATR protein, putative ; INVASION
3D7___PFB0570w:: SPATR protein, putative ; INVASION
TNF___PFA0125c:: erythrocyte binding antigen-181 ; INVASION
IT___PFA0125c:: erythrocyte binding antigen-181 ; INVASION
HBEC2_PFA0125c:: erythrocyte binding antigen-181 ; INVASION
HBEC1_PFA0125c:: erythrocyte binding antigen-181 ; INVASION
3D7___PFA0125c:: erythrocyte binding antigen-181 ; INVASION
TNF___PFF14_0303:: conserved Plasmodium protein
IT___PFF14_0303:: conserved Plasmodium protein
HBEC2_PFF14_0303:: conserved Plasmodium protein
HBEC1_PFF14_0303:: conserved Plasmodium protein
3D7___PFF14_0303:: conserved Plasmodium protein
TNF___PFF14_0224:: serine/threonine protein phosphatase ; invasion
IT___PFF14_0224:: serine/threonine protein phosphatase ; invasion
HBEC2_PFF14_0224:: serine/threonine protein phosphatase ; invasion
HBEC1_PFF14_0224:: serine/threonine protein phosphatase ; invasion
3D7___PFF14_0224:: serine/threonine protein phosphatase ; invasion
TNF___PFF14_0027:: 40S ribosomal protein S31/UBI, putative
IT___PFF14_0027:: 40S ribosomal protein S31/UBI, putative
HBEC2_PFF14_0027:: 40S ribosomal protein S31/UBI, putative
HBEC1_PFF14_0027:: 40S ribosomal protein S31/UBI, putative
3D7___PFF14_0027:: 40S ribosomal protein S31/UBI, putative
TNF___PFF13_0233:: myosin A ; invasion
IT___PFF13_0233:: myosin A ; invasion
HBEC2_PFF13_0233:: myosin A ; invasion
HBEC1_PFF13_0233:: myosin A ; invasion
3D7___PFF13_0233:: myosin A ; invasion
TNF___PFF13_0197:: Merozoite Surface Protein 7 precursor, MSP7 ; INVASION
IT___PFF13_0197:: Merozoite Surface Protein 7 precursor, MSP7 ; INVASION
HBEC2_PFF13_0197:: Merozoite Surface Protein 7 precursor, MSP7 ; INVASION
HBEC1_PFF13_0197:: Merozoite Surface Protein 7 precursor, MSP7 ; INVASION
3D7___PFF13_0197:: Merozoite Surface Protein 7 precursor, MSP7 ; INVASION
TNF___PFF13_0058:: RNA binding protein, putative
IT___PFF13_0058:: RNA binding protein, putative
HBEC2_PFF13_0058:: RNA binding protein, putative
HBEC1_PFF13_0058:: RNA binding protein, putative
3D7___PFF13_0058:: RNA binding protein, putative
TNF___PFF13_0011:: plasmodium falciparum gamete antigen 27/25
IT___PFF13_0011:: plasmodium falciparum gamete antigen 27/25
HBEC2_PFF13_0011:: plasmodium falciparum gamete antigen 27/25
HBEC1_PFF13_0011:: plasmodium falciparum gamete antigen 27/25
3D7___PFF13_0011:: plasmodium falciparum gamete antigen 27/25
TNF___PFF11_0277:: conserved Plasmodium protein ; invasion
IT___PFF11_0277:: conserved Plasmodium protein ; invasion
HBEC2_PFF11_0277:: conserved Plasmodium protein ; invasion
HBEC1_PFF11_0277:: conserved Plasmodium protein ; invasion
3D7___PFF11_0277:: conserved Plasmodium protein ; invasion
TNF___PFF10_0352:: merozoite surface protein ; INVASION
IT___PFF10_0352:: merozoite surface protein ; INVASION
HBEC2_PFF10_0352:: merozoite surface protein ; INVASION
HBEC1_PFF10_0352:: merozoite surface protein ; INVASION
3D7___PFF10_0352:: merozoite surface protein ; INVASION
TNF___PFF10_0351:: probable protein ; INVASION
IT___PFF10_0351:: probable protein ; INVASION
HBEC2_PFF10_0351:: probable protein ; INVASION
HBEC1_PFF10_0351:: probable protein ; INVASION
3D7___PFF10_0351:: probable protein ; INVASION
TNF___PFF10_0345:: merozoite surface protein 3 ; INVASION
IT___PFF10_0345:: merozoite surface protein 3 ; INVASION
HBEC2_PFF10_0345:: merozoite surface protein 3 ; INVASION
HBEC1_PFF10_0345:: merozoite surface protein 3 ; INVASION
3D7___PFF10_0345:: merozoite surface protein 3 ; INVASION
TNF___PFF10_0343:: S-antigen ; invasion
IT___PFF10_0343:: S-antigen ; invasion
HBEC2_PFF10_0343:: S-antigen ; invasion
HBEC1_PFF10_0343:: S-antigen ; invasion
3D7___PFF10_0343:: S-antigen ; invasion
TNF___PFF10_0281:: merozoite TRAP-like protein, MTRAP ; INVASION
IT___PFF10_0281:: merozoite TRAP-like protein, MTRAP ; INVASION
HBEC2_PFF10_0281:: merozoite TRAP-like protein, MTRAP ; INVASION
HBEC1_PFF10_0281:: merozoite TRAP-like protein, MTRAP ; INVASION
3D7___PFF10_0281:: merozoite TRAP-like protein, MTRAP ; INVASION
TNF___PFF10_0138:: conserved Plasmodium protein ; invasion
IT___PFF10_0138:: conserved Plasmodium protein ; invasion
HBEC2_PFF10_0138:: conserved Plasmodium protein ; invasion
HBEC1_PFF10_0138:: conserved Plasmodium protein ; invasion
3D7___PFF10_0138:: conserved Plasmodium protein ; invasion
TNF___PFF08_0118:: conserved Plasmodium protein ; invasion
IT___PFF08_0118:: conserved Plasmodium protein ; invasion
HBEC2_PFF08_0118:: conserved Plasmodium protein ; invasion
HBEC1_PFF08_0118:: conserved Plasmodium protein ; invasion
3D7___PFF08_0118:: conserved Plasmodium protein ; invasion
TNF___PFF08_0091:: conserved Plasmodium protein
IT___PFF08_0091:: conserved Plasmodium protein
HBEC2_PFF08_0091:: conserved Plasmodium protein
HBEC1_PFF08_0091:: conserved Plasmodium protein
3D7___PFF08_0091:: conserved Plasmodium protein
TNF___PFF08_0035:: conserved Plasmodium protein ; invasion
IT___PFF08_0035:: conserved Plasmodium protein ; invasion
HBEC2_PFF08_0035:: conserved Plasmodium protein ; invasion
HBEC1_PFF08_0035:: conserved Plasmodium protein ; invasion
3D7___PFF08_0035:: conserved Plasmodium protein ; invasion
TNF___PFF08_0008:: conserved Plasmodium protein ; invasion
IT___PFF08_0008:: conserved Plasmodium protein ; invasion
HBEC2_PFF08_0008:: conserved Plasmodium protein ; invasion
HBEC1_PFF08_0008:: conserved Plasmodium protein ; invasion
3D7___PFF08_0008:: conserved Plasmodium protein ; invasion
TNF___PFF07_0104:: kinesin-like protein, putative ; invasion
IT___PFF07_0104:: kinesin-like protein, putative ; invasion
HBEC2_PFF07_0104:: kinesin-like protein, putative ; invasion
HBEC1_PFF07_0104:: kinesin-like protein, putative ; invasion
3D7___PFF07_0104:: kinesin-like protein, putative ; invasion
TNF___PFF07_0043:: 60S ribosomal protein L34-A, putative
IT___PFF07_0043:: 60S ribosomal protein L34-A, putative
HBEC2_PFF07_0043:: 60S ribosomal protein L34-A, putative
HBEC1_PFF07_0043:: 60S ribosomal protein L34-A, putative
3D7___PFF07_0043:: 60S ribosomal protein L34-A, putative
TNF___MAL8P1.70:: Zinc finger C-x8-C-x5-C-x3-H type, putative ; invasion
IT___MAL8P1.70:: Zinc finger C-x8-C-x5-C-x3-H type, putative ; invasion
HBEC2_MAL8P1.70:: Zinc finger C-x8-C-x5-C-x3-H type, putative ; invasion
HBEC1_MAL8P1.70:: Zinc finger C-x8-C-x5-C-x3-H type, putative ; invasion
3D7___MAL8P1.70:: Zinc finger C-x8-C-x5-C-x3-H type, putative ; invasion
TNF___MAL7P1.176:: erythrocyte binding antigen 175 ; INVASION
IT___MAL7P1.176:: erythrocyte binding antigen 175 ; INVASION
HBEC2_MAL7P1.176:: erythrocyte binding antigen 175 ; INVASION
HBEC1_MAL7P1.176:: erythrocyte binding antigen 175 ; INVASION
3D7___MAL7P1.176:: erythrocyte binding antigen 175 ; INVASION
TNF___MAL13P1.60:: erythrocyte binding antigen-140 ; INVASION
IT___MAL13P1.60:: erythrocyte binding antigen-140 ; INVASION
HBEC2_MAL13P1.60:: erythrocyte binding antigen-140 ; INVASION
HBEC1_MAL13P1.60:: erythrocyte binding antigen-140 ; INVASION
3D7___MAL13P1.60:: erythrocyte binding antigen-140 ; INVASION
TNF___PFL2565w:: Plasmodium exported protein (PHISTa)
IT___PFL2565w:: Plasmodium exported protein (PHISTa)
HBEC2_PFL2565w:: Plasmodium exported protein (PHISTa)
HBEC1_PFL2565w:: Plasmodium exported protein (PHISTa)
3D7___PFL2565w:: Plasmodium exported protein (PHISTa)

Figure 5-20. 58 genes downregulated in at least one time point by 2 fold or more in all 5 selections. Data for each gene represents the average of many oligos where available. The gene annotation is according to PlasmoDB 6.4. The annotation "INVASION" or "invasion" was added in order to distinguish proteins proven or predicted to be involved in invasion, respectively (Haase, et al., 2008, Hu, et al., 2009). The top 11 genes are downregulated by at least 3 fold in one or more time point.

	T1	T2	T3	T4	T5	T6	Average of 6 time points
Downregulated dataset	0.39	1.10	0.61	0.75	0.56	1.10	0.68

Table 5-8. Average unlogged fold ratios of the 58 genes downregulated in 5 selections. As ratios are expressed as [Selected/Unselected], a ratio of "0.5" is a 2 fold downregulation. "T" = time point.

The MADIBA website allows visualization of metabolic pathways and chromosomal localizations. The "downregulated dataset" (58 genes) was tested to find out if any metabolic pathway was overall differentially regulated (Table 5-9). No pathway was significantly downregulated (Fisher's exact test). There is no known enzyme in the "up" regulated dataset (Figure 5-19). Thus no metabolic pathway is significantly differentially regulated after selection on HBEC-5i.

Gene ID	Annotation	Found in pathway	P-value*
PFI1110w	Glutamine synthetase	Nitrogen metabolism	0.57
PFI1110w	Glutamine synthetase	Glutamate metabolism	0.40
PFI1110w	Glutamine synthetase	Peptidoglycan biosynthesis	0.20
PFC0910w	Conserved Plasmodium protein	Nicotinate and nicotinamide metabolism	0.38

Table 5-9. Downregulated enzymes found in metabolic pathways. In each metabolic pathway there was at most one downregulated and no upregulated enzyme. Thus no pathway is significantly differentially regulated. *Fisher's exact test.

All 73 differentially regulated genes (58 "down" + 15 "up") were plotted on the 14 *P. falciparum* chromosomes to show their localization (Figure 5-21). Differentially regulated genes are evenly spread along the 14 chromosomes.

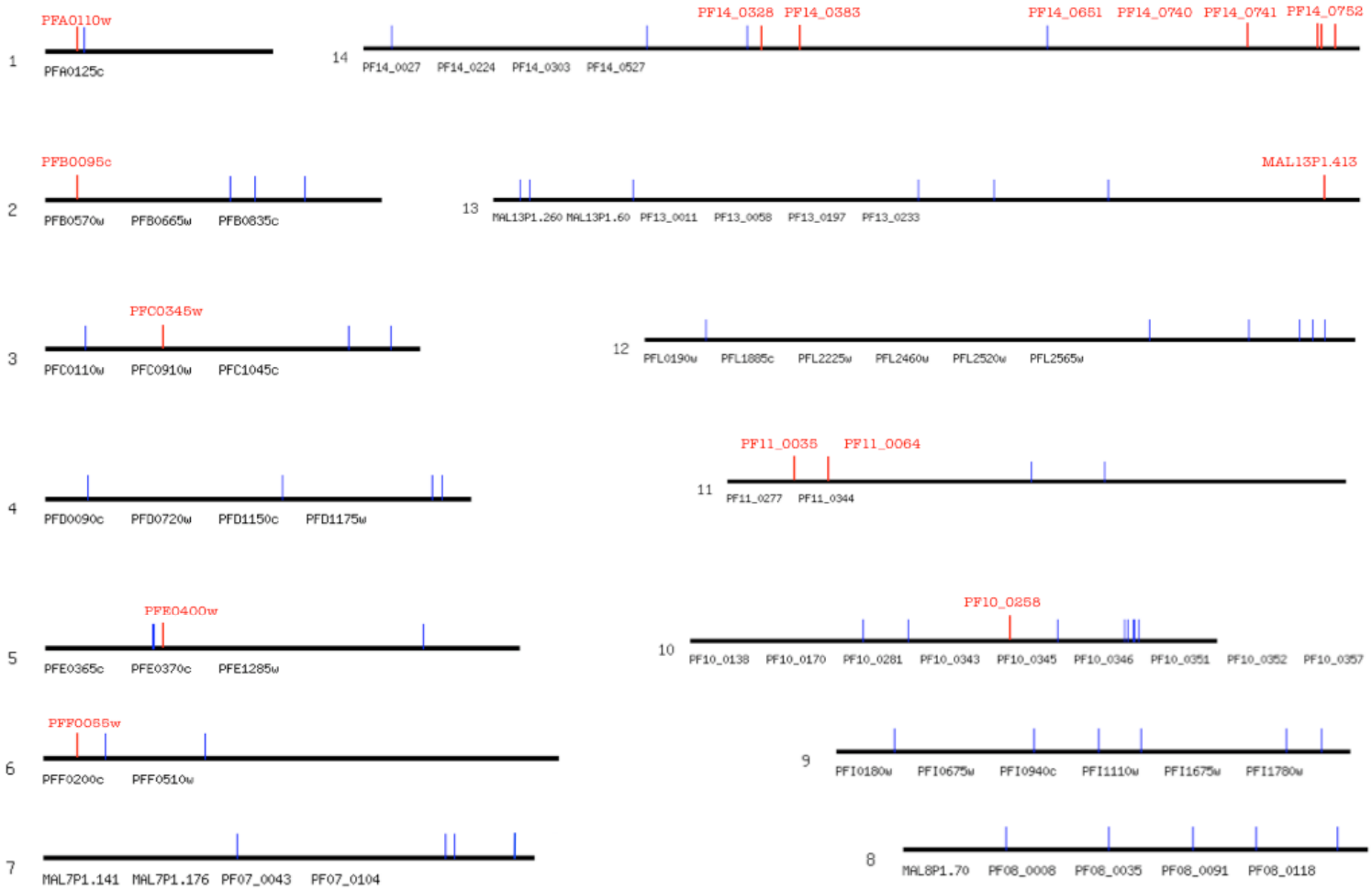


Figure 5-21. Chromosomal localization of differentially regulated genes. The 14 *P. falciparum* chromosomes are represented to scale. The 15 upregulated genes are indicated in red, the 58 downregulated genes are indicated in blue (vertical bars) and black (gene ID).

Tuikue Ndam and colleagues compared gene expression of *P. falciparum* placental isolates to that of the 3D7 laboratory strain (Tuikue Ndam, et al., 2008). They noticed that the proportion of over-expressed genes predicted to be exported was higher than expected compared to the whole genome. This finding has recently been confirmed by another group (Mackinnon, et al., 2009). Here, we tested whether proteins predicted to be exported were overall differentially regulated. Expression data of 96 non-VSA genes with an ExportPred score above 4.3 (Sargeant, et al., 2006)) were averaged (Table 5-10). Altogether, they were not differentially regulated as the average expression ratio of all exported proteins is very close to 1 in all time points and all selections. Therefore, unlike what has been found in field isolates, there is no overall upregulation of the "exported proteins family" (Mackinnon, et al., 2009, Tuikue Ndam, et al., 2008).

	T1	T2	T3	T4	T5	T6	Average of 6 time points
HB3-HBEC1	0.69	0.56	1.16	1.55	0.98	0.92	**0.97**
HB3-HBEC2	1.06	0.69	0.80	0.96	0.55	NA	**0.81**
HB3-HBEC-TNF	1.11	0.78	1.10	1.21	0.75	0.97	**0.98**
3D7-HBEC	0.97	1.16	1.09	0.95	1.00	0.84	**0.99**
IT-HBEC	0.82	0.88	1.49	1.32	0.79	NA	**1.03**
Average of 5 selections	**0.92**	**0.79**	**1.11**	**1.18**	**0.80**	**0.90**	**0.96**

Table 5-10. Overall fold ratios of all non-VSA exported proteins. Numbers indicate the average fold ratios of all proteins (without VSA) with an ExportPred score above 4.3. This is the threshold above which 95% of proteins are predicted to be exported. Average ratios are very close to 1, i.e. no change in expression between selected and unselected population.

This first approach has identified genes that are differentially regulated by at least two fold in all selections. In other words, five independent selections with three different clones (HB3, 3D7 and IT), two different protocols ("pooling" of all time points or not) and two activation states of HBEC-5i (TNF activated or

not) altogether show 15 upregulated and 58 downregulated genes in common. The downregulated dataset indicates a massive bias towards invasion related genes. Among these 15 upregulated genes are 7 proteins predicted or proven to be exported and could therefore be involved in cytoadherence to HBEC-5i.

5.5.6.2 Approach 2: Statistical approach

Some non-VSA genes were identified as upregulated after selection with the previous approach. However, many of these interesting genes show a high variability in expression across time points and across selections. Although from a biological point of view an upregulation seen in a single time point might be enough to influence parasite cytoadherence, a gene upregulated across multiple time points would be considered as more reliable, as it is the case with the upregulated *var* genes. Therefore this statistical approach tests whether there are genes consistently upregulated across selections, without using a fold-based arbitrary cutoff.

Because HB3-HBEC1 was processed in a different way (there was no pool, time points were hybridized with each other directly) it is not compared with other selections in the first instance.

For all statistical tests described in this section, the data was loaded on Multi-experiment Viewer (MeV, (Saeed, et al., 2006)) and each [Unselected / POOL] time point was paired with its [Selected / POOL] equivalent. Therefore there were four replicates (HB3, HB3-TNF, 3D7 and IT) for each of the six time points (except for T6 where data for HB3-HBEC2 is missing).

BETR (Aryee, et al., 2009) and Limma have been developed specifically for statistical analysis of time-course experiments. However they cannot be applied directly to our datasets because they compare each time point against a "time point 0" which would represent the baseline level of gene expression before the start of the time-course experiment. These tests are thus not appropriate for our data.

Paired t-tests allow to estimate the error variance for each gene from the log ratios (reviewed in (Cui and Churchill, 2003)). A standard *t* test can be conducted for each gene and the resulting *t* statistic can be used to determine

which genes are significantly expressed. However, due to the large amount of t-tests, their *p*-values have to be adjusted by applying a correction method.

Paired t-tests based on permutations or on t-distribution with an adjusted Bonferroni correction found no gene to be significant (Table 5-11). This is probably due to the high variability among the data (between strains and between time points) and because the Bonferroni correction is usually regarded as too stringent for microarray data (Leung and Cavalieri, 2003). The t-test analysis could be repeated with the Benjamini-Hochberg correction as it is less conservative (Benjamini and Hochberg, 1995). However this option is not available on MeV.

	Significant differentially regulated genes	
	Positive (upregulated)	**Negative (downregulated)**
T-test (two-class paired) Adjusted Bonferroni correction	0	0
T-test (two-class paired) 100 permutations. False significant genes proportion should not exceed 5%.	0	0
SAM (two-class paired) 5000 permutations FDR median <5%	30 genes (1% of total)	55 genes (2% of total)

Table 5-11. Significant differentially regulated genes with T-test and SAM. The total number of non-VSA gene in this dataset is 4573.

The same statistical test cannot directly be applied to VSA genes as their oligo sequences are specific to each strain. Therefore they cannot be used as replicates of each other, as it is the case with non-VSA genes. However, the VSA analysis (section 5.5.5) clearly showed a similar pattern in all strains (HB3, 3D7 or IT) and in all selection methods (with or without TNF activation): a single *var* gene is highly upregulated (or two in the case of IT-HBEC). Therefore, we argue that the expression data of the upregulated *var* can be used as a positive control for the paired t-tests (Table 5-11). For the purpose of these t-tests only, the upregulated *var* expression data (Table 5-5) was added to the non-VSA data as if it was the same *var* gene in all strains (for IT-Uns and IT-HBEC, the data from

ITvar7 and *ITvar19* were averaged together). This made-up *var* gene was renamed "*ligand_average*". Running the same t-tests (Table 5-11) with the added *ligand_average* gene data found a single significant differentially expressed gene: the *ligand_average* gene (adjusted p-value = 0.00374). This highly and consistently upregulated *var* gene was the only gene to reach statistical significance. Although this "trick" should be used carefully as the upregulated *var* oligo sequences are different from one strain to the other, it indicates that there is probably no other gene differentially regulated to the same extent and with the same consistency as these upregulated *var* genes. In other words, the PfEMP1 family is clearly the strongest candidate as a ligand mediating the cytoadherence to HBEC-5i.

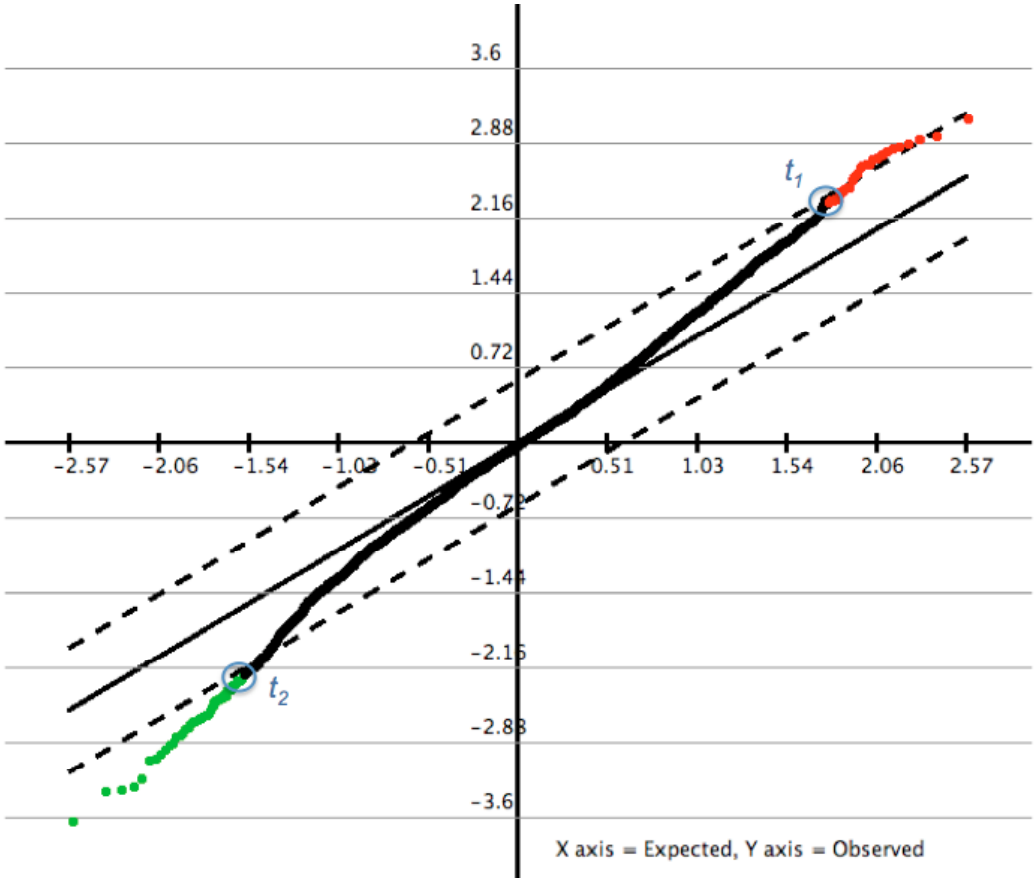


Figure 5-22. SAM graph showing the threshold (FDR < 5%) used in this analysis. Red dots are significant positively differentially regulated genes, green dots are significant negatively differentially regulated genes. t_1 and t_2 are the smallest positive and largest negative *d(i)*, respectively.

SAM (Significance Analysis of Microarray) is probably the most used statistical test for microarray data analysis. It is a statistical technique for finding significant genes in a set of microarray experiments (Tusher, et al., 2001). The data for each gene are permuted, and a test statistic *d* is computed for both the original and the permuted data for each gene. *d* captures the difference among mean expression levels of experimental conditions, scaled by a measure of variance in the data. Full details of the SAM approach are given in the methods section 5.4.7. The default number of permutations of MeV is set at 100. There was variability in the output from one run to the other so we used 5000 permutations. With a false discovery rate (FDR) median chosen to be less than 5%, 86 genes were significant: 30 positively and 55 negatively (Figure 5-22 above and Table 5-11). This is a fairly non-stringent cutoff implying that, on average, 5% of the 85 genes are false positives. Only one of the 30 upregulated genes (PF14_0612) is predicted to be exported (Sargeant, et al., 2006). It reaches 8 fold expression in HB3-HBEC3 and HB3-HBEC-TNF; however in HB3-HBEC1, IT-HBEC and 3D7-HBEC it is at most 1.4 fold expressed. Thus the evidence for this gene to be involved with cytoadhesion is weak. None of the significantly upregulated genes was upregulated by at least 2 fold on average (Table 5-12). Thus there is no overlap with genes identified in Figure 5-19. On the other hand, the expression pattern of these significant genes (Figure 5-23) is clearly more homogenous than the expression from Figure 5-19. Thus, as expected, the SAM analysis identified genes that are consistently upregulated. The level of upregulation is however minor compared to the upregulated *var* genes (Table 5-5) and cannot fully explain the substantial change of phenotype before and after selection. Therefore none of the genes identified in this approach are strong ligand candidates for cytoadhesion to HBEC-5i.

GeneID	Annotation (PlasmoDB 6.4)	d_E	d	Num.	Den.	Fold	q
PF14_0067	LCCL domain-containing protein CCP3	-0.14	2.38	0.49	0.21	1.69	4.97
PFF0415c	conserved Plasmodium protein	0.61	2.87	1.31	0.46	1.58	2.36
PF10_0288	conserved Plasmodium protein	-0.54	2.57	0.53	0.21	1.52	2.87
PF11_0119	SNARE protein, putative	-0.46	2.78	0.49	0.18	1.51	2.36
PF10_0113	conserved Plasmodium protein	-0.63	2.47	0.65	0.26	1.48	4.43
PF10_0270	conserved Plasmodium protein	-0.55	2.96	0.42	0.14	1.45	2.36
(MAL8P1.158)	*Not a predicted gene in PlasmoDB6.4*	*-0.90*	*2.49*	*0.42*	*0.17*	*1.42*	*4.66*
PF14_0645	conserved Plasmodium protein	0.08	2.45	0.44	0.18	1.39	4.43
PF11_0190	haloacid dehalogenase-like hydrolase, putative	-0.43	2.36	0.42	0.18	1.37	4.97
PFL0400w	apicoplast ribosomal protein L29 precursor, putative	1.02	3.15	0.42	0.13	1.36	2.36
PFB0160w	ERCC1 nucleotide excision repair protein, putative	0.18	2.37	0.42	0.18	1.35	4.97
PFE0790c	BolA-like protein, putative	0.50	2.63	0.37	0.14	1.33	3.24
PFC0126c	PFMNL-1 CISD1-like iron-sulfur protein, putative	0.25	2.38	0.48	0.2	1.32	4.97
PFE0275w	conserved Plasmodium protein	0.45	2.6	0.4	0.15	1.32	3.18
PF14_0692	conserved Plasmodium membrane protein	0.10	2.46	0.33	0.13	1.31	4.43
PFB0855c	apicoplast RNA methyltransferase precursor, putative	0.24	2.69	0.41	0.15	1.31	2.13
PFD0890	conserved Plasmodium protein	0.41	2.87	0.34	0.12	1.3	2.36
PF14_0612	conserved Plasmodium protein ; ExportPred_7.1	0.07	2.8	0.73	0.26	1.29	2.36
MAL13P1.142	conserved Plasmodium protein	-1.70	2.39	0.36	0.15	1.28	4.97
PF07_0070	drug metabolite transporter, putative	-0.79	2.71	0.44	0.16	1.28	2.13
PFF1075w	conserved Plasmodium protein	0.68	2.92	0.29	0.1	1.27	2.36
PFF0175c	conserved Plasmodium protein	0.59	2.99	0.35	0.12	1.26	2.36
MAL13P1.290	high mobility group protein 4, putative	-1.27	2.77	0.42	0.15	1.25	2.36
PFD1080w	conserved Plasmodium protein	0.42	2.49	0.32	0.13	1.24	4.66
MAL13P1.271	V-type ATPase, putative	-1.31	2.72	0.32	0.12	1.23	2.13
PF13_0068	mitochondrial ribosomal protein S35 precursor, putative	-0.28	2.37	0.53	0.22	1.22	4.97
PF14_0178	Ubiquitin fusion degradation protein UFD1, putative	-0.10	2.38	0.28	0.12	1.22	4.97
PF11_0263	conserved Plasmodium protein	-0.40	2.84	0.3	0.11	1.22	2.36
PFE0740c	kinase, putative	0.49	2.44	0.26	0.11	1.21	4.43
PF13_0357	conserved Plasmodium protein	-0.17	2.7	0.3	0.11	1.21	2.13

Table 5-12. 30 significant positively differentially regulated genes from the SAM analysis (FDR < 5%). Gene annotation was updated with PlasmoDB 6.4. Note that MAL13P1.291 (PlasmoDB 5.0) is now referred as MAL13P1.290. MAL8P1.158 does not exist anymore on PlasmoDB 6.4 (i.e. it is not a predicted gene). d_E = Expected score. d = Observed score. Num = Numerator = $\bar{x}_{Sel}(i) - \bar{x}_{Uns}(i)$. Den = Denominator = $s(i) + s_0$. Fold = unlogged fold change. q = *q-value* (in %).

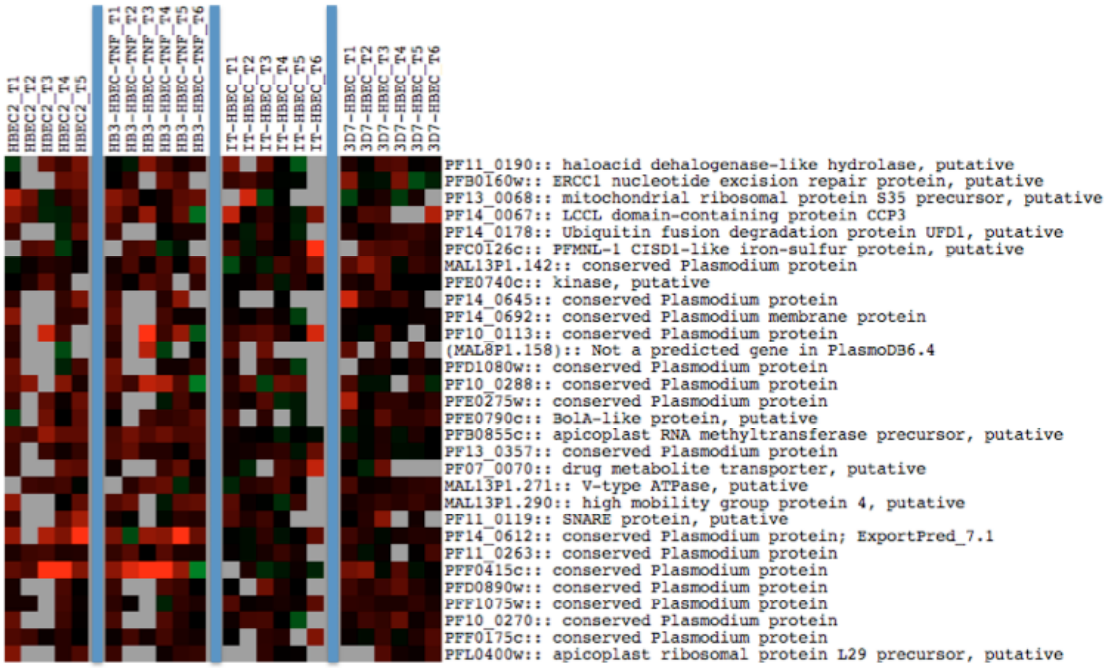


Figure 5-23. 30 significant positively differentially regulated genes from the SAM analysis (FDR < 5%). Note how the expression pattern is much more homogenous than with the first approach (Figure 5-19).

The same SAM analysis also identified 55 significant negatively differentially regulated genes (Figure 5-22 and Table 5-11). Just over half of them (23 genes asterisked in Table 5-13) had already been found in the first approach, as they are downregulated by at least 2 fold in all selections (Figure 5-20). Unlike with upregulated genes, where there was no overlap between the first and this second approach, most downregulated genes are identified by both methods. Note that the first approach was based on the 5 selections while here only the data from HB3, HB3-TNF, 3D7 and IT is used. In the pilot experiment (HB3-HBEC1) time point samples were hybridized with each other directly, thus it is not possible to pair Selected with Unselected time points data for this SAM statistical test. Interestingly, out of the 55 genes identified here, 15 have been shown to encode invasion related proteins (Haase, et al., 2008) and another 26 are predicted to be involved with the same process (Hu, et al., 2009) (Table 5-13 and Figure 5-24). Thus 75% of SAM-identified downregulated genes are predicted or proven to be involved with invasion. This is a very similar result to that which was obtained with the first approach. The

[timepoint/POOL] data allows visualization of the timing of expression of these significant genes (Figure 5-25A). Virtually all 55 genes are expressed at time point 5 and even more at time point 6, corresponding to the schizont stage, where invasion-related genes are transcribed (Bozdech, et al., 2003). This strikingly contrasts with the expression timing of genes found to be significantly upregulated (Figure 5-25B). Thus, just like it was observed in the first approach, the selection on HBEC-5i may have selected for parasites transcribing lower levels of schizont stage genes, rather than invasion genes *per se*. In any case, it is important to heed that these schizont stage genes are downregulated over most time points, not just at T5 and T6 (Table 5-8 and Figure 5-24).

GeneID	Annotation (PlasmoDB 6.4)	d_E	d	Num.	Den.	Fold	q
PF10_0352	merozoite surface protein ; INVASION*	-0.51	-3.60	-0.95	0.26	0.79	0.00
PFD1150c	reticulocyte binding protein homolog 4, Rh4 ; INVASION*	0.43	-3.32	-1.00	0.30	0.75	0.00
MAL13P1.60	erythrocyte binding antigen-140 ; INVASION*	-1.13	-3.31	-1.16	0.35	0.48	0.00
PFL1565c	CG2-related protein, putative ; invasion	1.28	-3.27	-0.75	0.23	0.78	0.00
PFL2225w	myosin A tail domain interacting protein ; invasion*	1.58	-3.20	-0.85	0.26	0.68	0.00
PF14_0425	fructose-bisphosphate aldolase	0.00	-3.02	-0.57	0.19	0.76	0.00
PF14_0761	acyl-CoA synthetase	0.12	-3.00	-0.92	0.31	0.57	0.00
MAL7P1.119	conserved Plasmodium protein ; INVASION	-1.07	-2.96	-1.29	0.44	0.93	0.00
PF10_0346	merozoite surface protein 6 ; INVASION*	-0.51	-2.92	-0.98	0.34	0.83	0.00
MAL8P1.70	Zinc finger C-x8-C-x5-C-x3-H type, putative ; invasion*	-0.85	-2.87	-0.83	0.29	0.78	0.00
PFD0715c	conserved Plasmodium protein; invasion	0.39	-2.86	-0.88	0.31	0.87	0.00
PF11_0442	transcription factor with AP2 domain(s), putative ; invasion	-0.32	-2.80	-0.97	0.35	1.09	0.00
PFL2565w	Plasmodium exported protein (PHISTa) ; ExportPred_14.9 *	2.28	-2.78	-1.48	0.53	0.45	0.00
PFI0265c	RhopH3 ; INVASION	0.75	-2.76	-1.17	0.42	1.28	0.00
PFB0315w	41 kDa antigen ; invasion	0.19	-2.72	-0.59	0.22	0.96	0.00
PFL0245w	probable protein ; invasion	0.99	-2.71	-0.59	0.22	0.72	0.00
PFL0870w	Thrombospondin-related apical membrane protein ; INVASION	1.10	-2.68	-0.58	0.22	0.89	0.00
PFB0665w	serine/threonine protein kinase, putative ; invasion*	0.22	-2.65	-0.90	0.34	0.82	0.00
PF08_0008	conserved Plasmodium protein ; invasion*	-0.75	-2.64	-1.05	0.40	0.71	0.00
PFE0365c	conserved Plasmodium protein ; invasion*	0.46	-2.63	-0.91	0.35	0.68	0.00
PF14_0108	conserved Plasmodium protein ; invasion	-0.13	-2.61	-0.67	0.26	0.92	0.00
MAL8P1.6	early transcribed membrane protein 8, ETRAMP 8	-0.86	-2.60	-0.60	0.23	0.76	0.00
PFE0865c	splicing factor, putative	0.50	-2.60	-0.39	0.15	0.73	0.00
PFA0125c	erythrocyte binding antigen-181 ; INVASION*	0.13	-2.58	-1.10	0.43	0.61	0.00
PFL2460w	coronin ; invasion*	1.86	-2.58	-0.91	0.35	0.74	0.00
MAL13P1.480	histidine-rich protein III ; ExportPred_5.5	-1.14	-2.56	-1.15	0.45	0.44	0.00
PF13_0011	plasmodium falciparum gamete antigen 27/25 *	-0.30	-2.54	-0.95	0.37	0.74	0.00
PFL2100w	ubiquitin conjugating enzyme E2, putative ; invasion	1.49	-2.49	-0.61	0.24	1.01	2.03
PF11_0277	conserved Plasmodium protein ; invasion*	-0.39	-2.45	-0.71	0.29	1.25	3.24
PFB0275w	metabolite/drug transporter, putative ; invasion	0.19	-2.45	-0.66	0.27	0.65	3.24
PFI1475w	merozoite surface protein 1 precursor ; INVASION	0.91	-2.45	-0.83	0.34	0.84	3.24
PFE0370c	subtilisin-like protease 1 ; INVASION*	0.46	-2.43	-0.68	0.28	0.69	3.24
PF14_0578	conserved Plasmodium protein ; invasion	0.06	-2.43	-0.54	0.22	0.89	3.24

PFI0540w	conserved Plasmodium protein ; invasion	0.78	-2.42	-0.88	0.36	0.78	3.24
PF11_0344	apical membrane antigen 1, AMA1 ; INVASION*	-0.36	-2.41	-0.99	0.41	0.80	3.24
MAL13P1.176	reticulocyte binding protein 2, homolog b ; INVASION	-1.54	-2.41	-0.78	0.32	0.95	3.24
PFA0445w	conserved Plasmodium protein ; invasion	0.15	-2.41	-0.58	0.24	0.67	3.24
PF08_0035	conserved Plasmodium protein ; invasion*	-0.73	-2.40	-0.87	0.36	0.94	3.24
MAL13P1.268	conserved Plasmodium protein	-1.32	-2.38	-0.77	0.32	0.63	3.12
PF13_0211	calcium-dependent protein kinase, putative ; invasion	-0.22	-2.35	-0.76	0.32	0.81	2.91
PF10_0351	probable protein ; INVASION*	-0.51	-2.35	-0.67	0.29	0.67	2.91
PFB0670c	conserved Plasmodium protein ; invasion	0.22	-2.34	-0.82	0.35	0.95	2.91
PF13_0233	myosin A ; invasion*	-0.21	-2.34	-0.96	0.41	0.69	2.91
PFD0310w	sexual stage-specific protein precursor	0.36	-2.30	-0.47	0.21	0.79	3.97
PFC0120w	Cytoadherence linked asexual protein 3.1 ; INVASION	0.25	-2.30	-0.66	0.29	0.86	3.97
PFC0060c	Serine/Threonine protein kinase, FIKK family	0.25	-2.29	-0.68	0.30	0.78	3.97
PFC0110w	Cytoadherence linked asexual protein 3.2 ; INVASION*	0.25	-2.29	-0.73	0.32	0.89	3.97
MAL7P1.22	conserved Plasmodium protein	-1.00	-2.29	-0.54	0.24	0.68	3.97
PF08_0119	conserved Plasmodium protein ; invasion	-0.69	-2.26	-0.61	0.27	0.51	3.75
PF13_0058	RNA binding protein, putative *	-0.28	-2.26	-1.08	0.48	0.63	3.75
PFD0395c	conserved Plasmodium protein ; invasion	0.37	-2.26	-0.56	0.25	0.69	3.75
PFL1170w	polyadenylate-binding protein, putative	1.17	-2.25	-0.31	0.14	0.83	3.75
PFI1675w	conserved Plasmodium protein *	0.94	-2.25	-0.55	0.25	0.91	4.79
PFL1090w	glideosome-associated protein 45 ; invasion	1.14	-2.24	-0.77	0.34	0.79	4.79
MAL7P1.141	conserved Plasmodium protein ; invasion*	-1.05	-2.24	-0.87	0.39	0.80	4.79

Table 5-13. 55 significant negatively differentially regulated genes from the SAM analysis (FDR < 5%). Gene annotation was updated with PlasmoDB 6.4. The annotation "INVASION" or "invasion" was added in order to distinguish proteins proven or predicted to be exported, respectively (Haase, et al., 2008, Hu, et al., 2009). Genes already identified in the first approach (Figure 5-20) are asterisked. d_E = Expected score. d = Observed score. Num = Numerator = $\bar{x}_{Sel}(i) - \bar{x}_{Uns}(i)$. Den = Denominator = $s(i) + s_0$. Fold = unlogged fold change. q = *q-value* (in %).

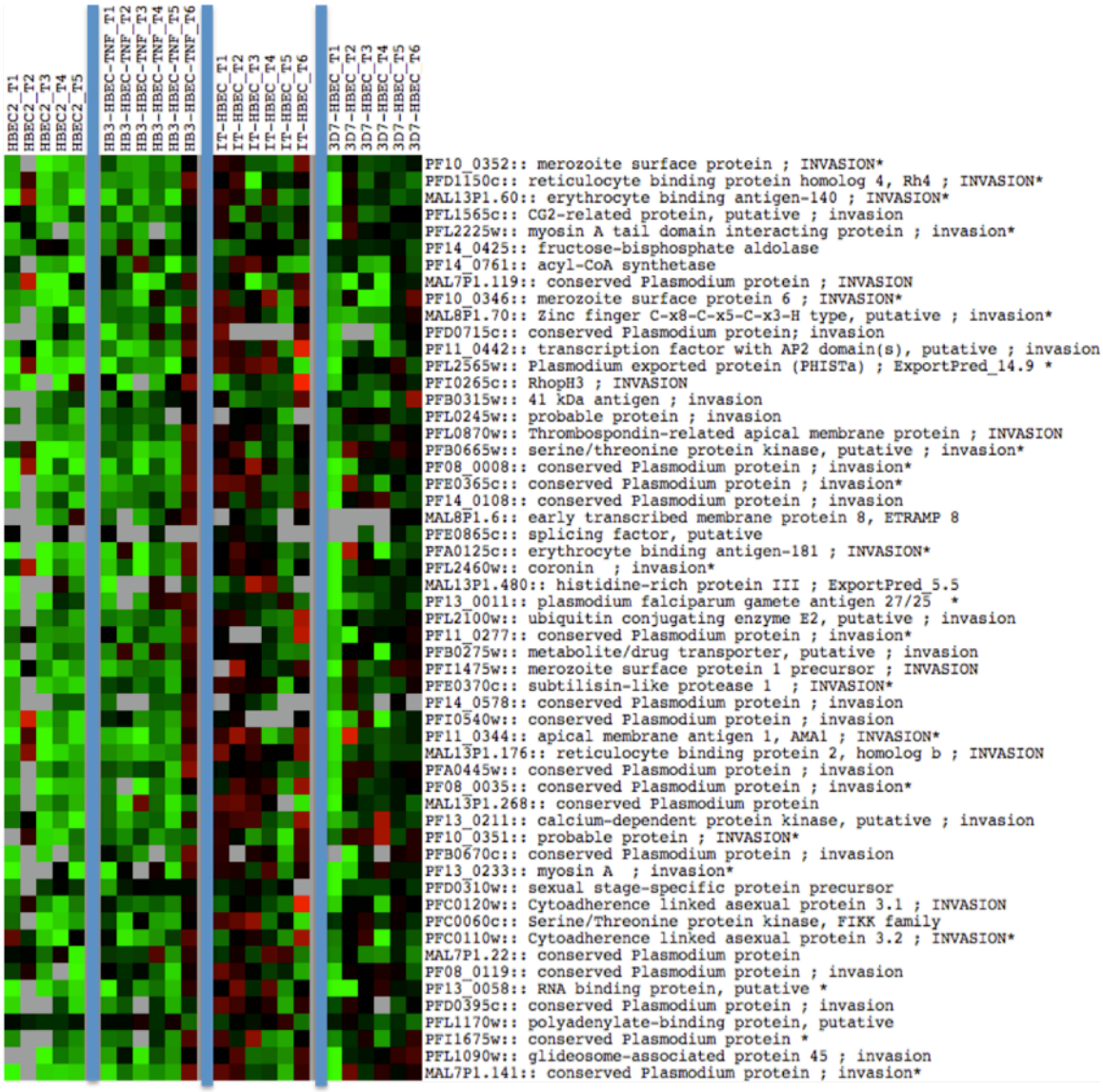


Figure 5-24. 55 significant negatively differentially regulated genes from the SAM analysis (FDR < 5%). Gene annotation was updated with PlasmoDB 6.4. The annotation "INVASION" or "invasion" was added in order to distinguish proteins proven or predicted to be involved in erythrocyte invasion, respectively (Haase, et al., 2008, Hu, et al., 2009). Genes already identified in the first approach (Figure 5-20) are asterisked.

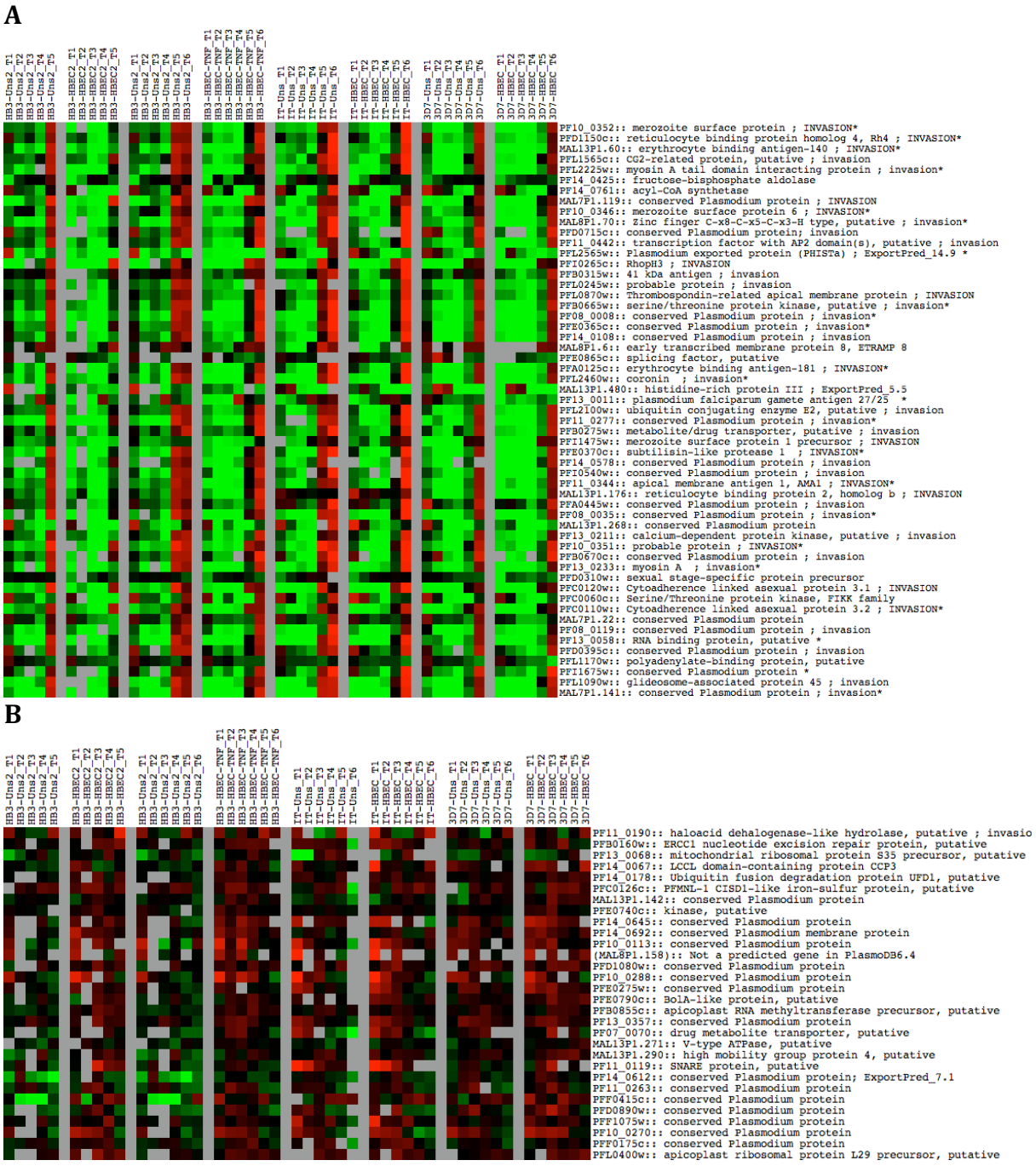


Figure 5-25. 88 significant differentially regulated genes from the SAM analysis (FDR < 5%). Data is shown as it was used for the SAM test: data for each time point is paired as [Unselected/POOL] with [Selected/POOL]. A gray column was added in between time points from different selections for clarity. Note that the HB3-Uns2 time points 1 to 5 are represented twice as they are used for HB3-HBEC2 as well as HB3-HBEC-TNF. (A) 55 negatively differentially regulated gene. Figure 5-24 legend also applies here. This representation also allows to visualize the timing of expression in both conditions (Selected or Unselected): genes are somewhat

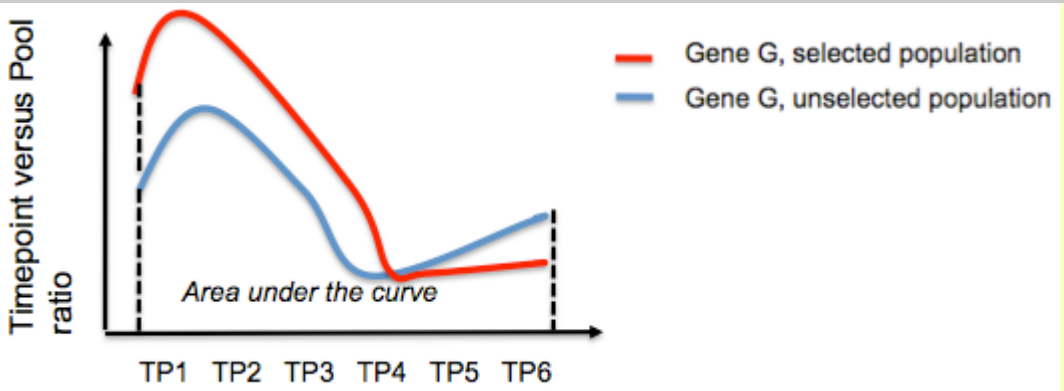
expressed at time point 5 and mostly at time point 6 (late schizont stage). (B) 30 positively differentially regulated gene.

Overall, this second approach found no significant non-VSA genes differentially regulated using t-test statistics with the parameters described above. When data for the upregulated *var* gene in each strain was added, using the different strains as replicates, this upregulated *var* gene was the only significant gene. This implies that the PfEMP1 family is the best candidate as the HBEC-5i ligand. The SAM test was run with less stringent parameters than the t-tests and identified 85 significant genes. As previously noticed, almost all downregulated genes are schizont stage transcribed and most of them are invasion related. The upregulated non-VSA genes show a consistent but low level of transcription in the HBEC-selected lines. None of them was previously identified as 2 fold upregulated in all selections. Therefore this statistical approach found no new candidate that could play a direct role in HBEC-5i cytoadhesion. The overall low number of significant genes highlights the high variability found among the different replicates but also that *var* genes were the only major differentially regulated genes.

5.5.6.3 Approach 3: "Area under the curve"

The first approach focused on the most highly differentially regulated non-VSA genes, the second one searched for consistent gene expression. They revealed lots of variation across time points for many genes. A way to overcome this is to sum all time points in the [Selected/POOL] as well as in the [Unselected/POOL] arrays, then divide the first sum by the second (Box 5-2). In effect this calculates the area under the expression curve of each gene. Genes with the highest Area Ratio [Selected Area / Unselected Area] are considered to be the most upregulated genes across the entire life cycle. The question that can be answered here is "which genes are most upregulated across all time points?" or in other words "which gene has most increased its quantity of mRNA after selection?" As only upregulated genes are HBEC-5i ligand candidates, I will not focus on downregulated genes here.

This approach cannot be used with HB3-HBEC1 data because time points were directly hybridised with each other for this strain.



	T1	T2	T3	T4	T5	T6	Sum (Area)	Area Ratio [Sel./Uns.]
Gene G [Selected/POOL]	2	2.5	2	1.5	0.5	0.5	9	1.5
Gene G [Unselected/POOL]	1	1.5	1.5	0.5	0.5	1	6	

Box 5-2. "Area under the curve approach". Unlogged ratios [time points/POOL] are summed to calculate an area representative of the gene expression. The area from the Selected data is divided from the unselected one. This final ratio corresponds to the overall amount of gene expression before and after selection.

For statistical analysis, the Selected area was paired with the Unselected area.

Non-VSA genes data from 4 strains (HB3-HBEC2, HB3-HBEC-TNF, 3D7-HBEC, IT-HBEC) and their unselected equivalent was unlogged. The "Area" was calculated by summing the data of all 6 time points. The "Area Ratio" is then defined as the Selected Area divided by the Unselected Area. The "Overall Area Ratio" for each gene is the mean of the 4 Area Ratios from the 4 strains. As expected, the distribution of all Overall Area Ratios is centred on 1, i.e. no change in gene expression after selection (Figure 5-26).

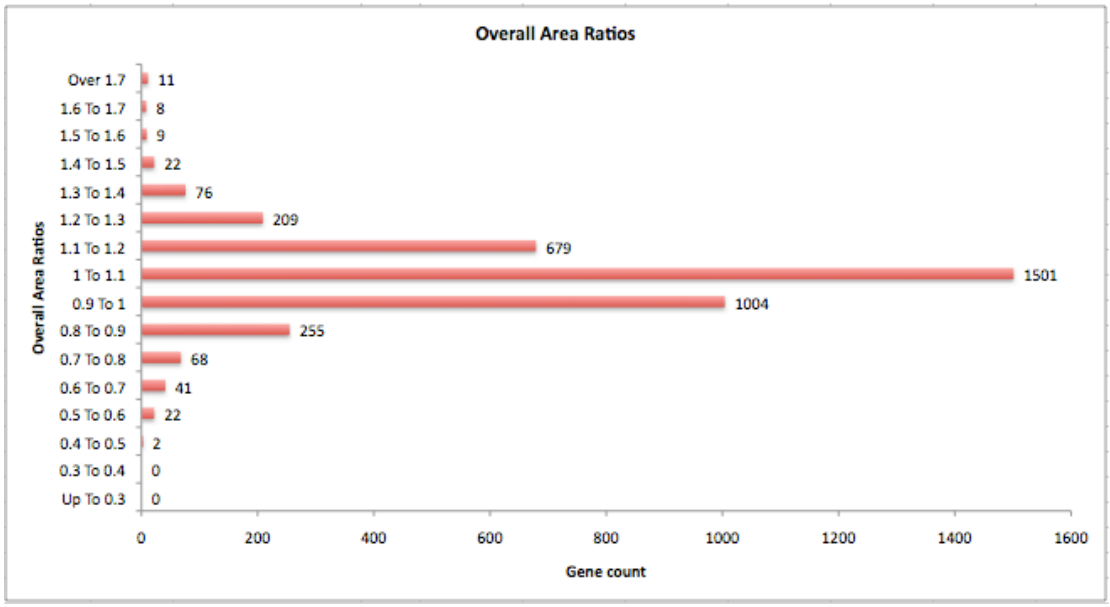


Figure 5-26. Histogram of the Overall Area Ratios. The unlogged value for each gene is the average of the Area Ratios from each of the 4 selections.

Genes that had no Area Ratio below 1 in any selection (i.e. never "downregulated") were ranked by their Overall Area Ratio (Table 5-14).

Gene ID and annotation	HBEC 2 Area	TNF Area	3D7 Area	IT Area	Overall Area
PF14_0752 :: Plasmodium exported protein (PHISTa) ; ExportPred_12.3	2.80	1.22	3.13	1.64	**2.20**
PFD0075w :: conserved Plasmodium falciparum protein family	2.11	1.79	1.62	2.99	**2.13**
PF11_0512 :: RESA-2 protein with PHIST and DnaJ domains ; ExportPred_10.5	1.06	1.34	4.03	1.64	**2.02**
PF14_0612 :: conserved Plasmodium protein ; ExportPred_7.1	3.39	1.57	1.16	1.03	**1.79**
PF14_0067 :: LCCL domain-containing protein CCP3	1.44	1.50	1.80	2.09	**1.71**
PF11_0319 :: mitochondrial rpoD precursor, putative	2.91	1.45	1.27	1.18	**1.71**
PF10_0288 :: conserved Plasmodium protein	1.98	2.06	1.18	1.31	**1.63**
PF10_0391 :: Plasmodium exported protein (hyp4) ; ExportPred_12.5	1.75	1.79	1.31	1.63	**1.62**
PFA0060w :: Plasmodium exported protein (hyp4) ; ExportPred_12.5	1.77	1.99	1.58	1.13	**1.62**
PFC0735w :: 40S ribosomal protein S15A, putative	2.40	1.43	1.36	1.27	**1.62**
MAL13P1.61 :: Plasmodium exported protein (hyp8) ; ExportPred_16.2	1.73	2.35	1.18	1.09	**1.59**
PF11_0024 :: Plasmodium exported protein (hyp4) ; ExportPred_12.5	1.41	1.78	1.38	1.63	**1.55**

Table 5-14. Top 12 of the highest Area Ratios. Genes that are significantly upregulated are in bold (SAM, FDR median < 5%).

Interestingly, according to these criteria, out of all non-VSA genes, the highest ranked gene is *PF14_0752*, the PHISTa gene already identified as the only non-VSA to be upregulated by at least 3 fold in all selections. Although the first approach and this one are based on different criteria, they both identify *PF14_0752* as the top candidate for HBEC-5i binding. Within the 12 genes with the highest Overall Area Ratios, half of them (including *PF14_0752*) encode proteins predicted to be exported (Sargeant, et al., 2006). Therefore the selection on HBEC-5i resulted in an enrichment of parasites that tend to express some exported proteins (indicated by their ExportPred score in Table 5-14). No function has ever been ascribed to any of these 6 genes. The expression at each time point of the "top 12" genes is indicated in Figure 5-27. Only 3 genes reach an Overall Area Ratio greater than 2 fold: *PF14_0752* (PHISTa), *PFD0075w* and *PF11_0512* (RESA-2) (Table 5-14). For comparison, the "*ligand_average*" (the made-up upregulated *var* gene described in section 5.5.6.2) shows an Overall Area Ratio of 12.5. Although the predicted to be exported proteins identified in this "Area under the curve" approach could be considered as cytoadhesion ligand candidates, their relatively weak upregulation has to be put in perspective with the very high increase of *var* gene expression.

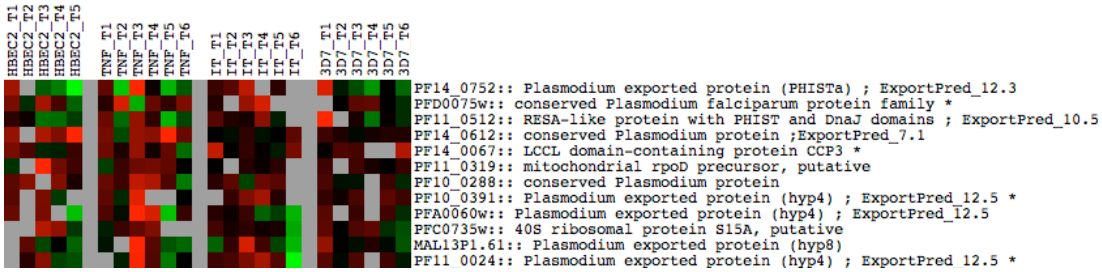


Figure 5-27. Time point expression of the top 12 of the highest Area Ratios.
Genes with a significant Area ratio are asterisked.

A SAM analysis was also performed on the Area data. The Selected Area was paired with its Unselected Area for each strain. The parameters used were the same as in section 5.5.6.2. Out of all non-VSA genes, the SAM test found 31

genes with significant upregulated Area ratio (Table 5-15 and Table 5-16). Four of them had already been identified by SAM in approach 2 in section 5.5.6.2. Four other genes happened to be in the "top 12" of the highest Overall Area Ratios (in bold in Table 5-14). Two significant genes encode exported proteins (PF10_0391 and PF11_0024). PF14_0752 (PHISTa), the best candidate identified in this approach, was not retained as significant by the SAM test. This can be explained by the relatively high differences in Area ratios in between the different strains. The Area ratios for PF14_0752 are high in HB3-HBEC2 and 3D7-HBEC but lower in HB3-HBEC-TNF and IT-HBEC (Table 5-14). The 4 significant genes show more consistent Area ratios.

	Significant differentially regulated genes	
	Upregulated	**Downregulated**
SAM (two-class paired) 5000 permutations FDR median <5%	31 genes (1%)	0 genes (0%)
T-test (two-class paired) Adjusted Bonferroni correction	0	0
T-test (two-class paired) 100 permutations. False significant genes proportion should not exceed 5%.	0	0

Table 5-15. Statistical tests performed for the "Area under curve" approach. The 31 genes identified here by "SAM" are listed in Table 5-16.

GeneID::Annotation (PlasmoDB 6.4)	d_E	d	Num.	Den.	Fold	q
PF14_0513:: RNA binding protein, putative	0.28	3.07	0.33	0.11	1.25	2.42
PFB0660w:: conserved Plasmodium protein	0.28	3.08	0.46	0.15	1.41	2.42
(MAL8P1.44):: Not a predicted gene in PlasmoDB6.4	*-0.05*	*3.11*	*0.45*	*0.15*	*1.41*	*2.59*
PFC0420w:: calcium-dependent protein kinase-3	0.96	3.12	0.31	0.10	1.23	2.59
PF14_0519:: mitochondrial ribosomal protein S11 precursor, putative	0.54	3.13	0.31	0.10	1.24	2.59
PFL1350w:: RNA pseudouridylate synthase, putative	-0.12	3.22	0.27	0.08	1.20	2.88
PFD0565c:: DEAD box ATP-dependent RNA helicase,	-0.81	3.22	0.30	0.09	1.23	2.88
PF11_0023:: Plasmodium exported protein (hyp5) ;	0.08	3.25	0.41	0.13	1.33	2.88
PFF0435w:: ornithine aminotransferase	-0.67	3.25	0.28	0.09	1.22	2.88
PF11_0048:: casein kinase II beta chain	-0.45	3.30	0.36	0.11	1.28	3.41
PF07_0044:: conserved Plasmodium protein	-0.09	3.31	0.39	0.12	1.32	3.41
PF08_0067:: conserved Plasmodium protein	-0.99	3.36	0.22	0.07	1.17	3.75
PF10_0270:: conserved Plasmodium protein*	0.26	3.39	0.50	0.15	1.38	3.95
PF14_0240:: 60S ribosomal protein L21e, putative	-0.75	3.44	0.41	0.12	1.33	4.17
PF11_0284:: methyltransferase, putative	-0.53	3.45	0.39	0.11	1.33	4.17
PF14_0130:: conserved Plasmodium protein	-0.22	3.47	0.40	0.11	1.28	4.17

MAL13P1.271:: V-type ATPase, putative*	0.60	3.47	0.32	0.09	1.24	4.17
PFF1530c:: Plasmodium exported protein (hyp4)	0.15	3.52	0.45	0.13	1.45	4.17
PF14_0651:: leucine-rich repeat protein, 14.2	0.58	3.58	0.43	0.12	1.34	4.17
PF10_0341:: tRNA pseudouridine synthase D, putative	0.26	3.58	0.48	0.13	1.37	4.17
PF14_0490:: conserved Plasmodium protein	-0.53	3.63	0.40	0.11	1.31	4.17
PF11_0047:: actin-like protein, putative	0.27	3.65	0.38	0.10	1.31	4.17
PFB0995w:: hypothetical protein	0.11	3.69	0.35	0.09	1.27	4.17
PF14_0251:: Sel4 protein	1.19	3.93	0.37	0.09	1.29	0.00
PF10_0269:: DNA-directed RNA polymerase II, put.	-0.13	3.97	0.28	0.07	1.22	0.00
PF14_0067:: LCCL domain-containing protein CCP3*	0.27	4.11	0.76	0.18	1.74	0.00
PFD0075w:: conserved Plasmodium f. protein family	-0.71	4.12	1.05	0.25	2.05	0.00
PF10_0391:: Plasmodium exported protein (hyp4) ;	0.31	4.22	0.69	0.16	1.57	0.00
PF11_0024:: Plasmodium exported protein (hyp4) ;	0.33	4.23	0.63	0.15	1.52	0.00
PFE0790c:: BolA-like protein, putative*	-0.89	4.34	0.42	0.10	1.34	0.00
PFD0890w:: conserved Plasmodium protein*	-0.79	4.87	0.44	0.09	1.38	0.00

Table 5-16. 31 Significant positively differentially regulated genes analyzed by their area ratios. Genes already identified by SAM in approach 2 (Table 5-12) are asterisked.

All in all, the strongest non-VSA candidate from this "Area under the curve" approach is *PF14_0752* (PHISTa), the same gene identified in the first approach. Among the "top 12" list of highest Overall Area ratios, 5 other genes encode proteins predicted to be exported. 2 of them show statistical significance (SAM analysis) making them cytoadherence-related candidates. However, all genes detected here are relatively weak candidates when compared to the upregulated *var* genes expression pattern of each strain.

5.5.6.4 Summary of non-VSA candidates for HBEC-5i cytoadhesion.

The analysis of VSA genes expression showed a clear-cut result: All parasite lines selected on HBEC-5i highly express one (or two) *var* variants, as well as the "head to head" *rif* gene for the HB3 and 3D7 strains. Results from the 3 approaches on the non-VSA genes also identify many genes that could be involved in cyotadhesion, albeit none as highly and consistently upregulated in all strains as the upregulated *var* genes. The relatively few genes significantly differentially regulated illustrate this lack of consistency in between time points and strains. Thus no other ligand candidate pointed out in this microarray data analysis is as likely as PfEMP1 to be involved in binding to HBEC-5i. However, from a biological point of view, a gene upregulated in a single time point, especially at ring stage, may be enough to influence cytoadherence.

The microarray data alone cannot give definite answer on to which gene is or is not involved in cytoadherence. Nevertheless, the 3 approaches have met their goal of identifying putative HBEC-5i ligand candidates that should be further investigated. Upregulated genes encoding a Pexel motif are given priority as their resulting proteins are predicted to be exported. Figure 5-28 summarizes the Pexel proteins with the highest probability of being involved in cytoadherence. The most promising candidates are discussed in section 5.6.6 based on this microarray data but also previous published experiments when available.

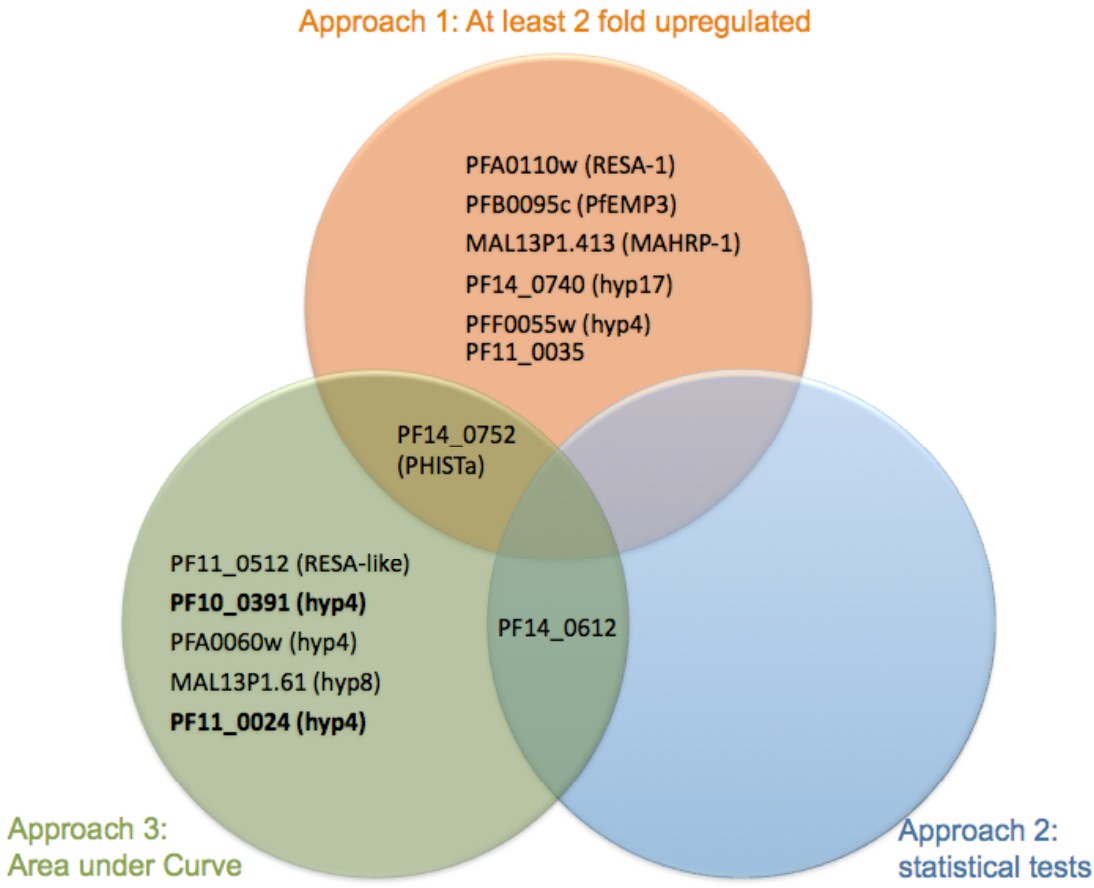


Figure 5-28. Summary of upregulated exported proteins identified in each approach. Genes that were found to be significant by SAM test are shown in bold. For approach 3, it was arbitrarily chosen to focus on the top 12 genes with highest Overall Area ratio. *PF14_0612* is upregulated at low level but identified in Approach

2 and 3. The best non-VSA ligand candidate is *PF14_0752*, encoding a PHISTa protein, as it is the most upregulated gene in Approach 1 and Approach 3. "hyp4", "hyp8" and "hyp17" are a temporary family identifier based on multiple alignments (Sargeant, et al., 2006). No function has been assigned to any of these gene families yet.

5.6 Discussion

Despite decades of research on cerebral malaria, the *P. falciparum* ligands mediating binding to human brain endothelial cells have never been directly investigated. Moreover, very few studies have considered the possibility that other genes than the *var* family may be involved in cytoadherence (Mok, et al., 2007). This chapter attempted to fill both gaps in our knowledge of cerebral malaria: by selecting *P. falciparum* iRBCs for binding to HBEC-5i, it was postulated that genes necessary for cytoadherence would be upregulated in the selected population of parasites. Furthermore, by applying a method that measures the expression of the entire transcriptome, we investigated the ligand(s) question in an unbiased way.

The major finding presented in this chapter was that, of all strains selectable for binding to HBEC-5i, a single group A *var* gene (or 2 *var* genes in the case of IT-HBEC) is always the most highly and consistently upregulated gene. These *var* genes will be discussed in more detail below (and in chapter 6), followed by discussion of the other candidate genes found to be upregulated after selection. Finally, the limitations of the microarray method will be discussed.

5.6.1 Parasites were well synchronised.

The first method tested for tight synchronization of parasite cultures was with Percoll (HB3-HBEC1 parasites). The Percoll procedure separates the population into two layers: the pellet where ring stages and rosetting parasites can be found, and an upper layer with mostly pigmented trophozoite stages parasites. Thus this process involuntarily selects against rosetting parasites. In this particular case it is of no consequence because both unselected and selected

parasites hardly form any rosettes (chapter 3). In any case, the Percoll procedure was abandoned because, in our hands, the purity obtained with the MACS column was much higher.

The MACS-Sorbitol method is validated by the good parasite cultures synchronization obtained. This was verified by checking blood smears at each time point, comparing the expression timing with the published *P. falciparum* transcriptome (Bozdech, et al., 2003, Llinas, et al., 2006) and calculating the Pearson correlation between Selected and Unselected time points. The latter approach detected issues in HB3-HBEC-TNF time point 3. Gene expression for that particular time point should therefore be interpreted cautiously.

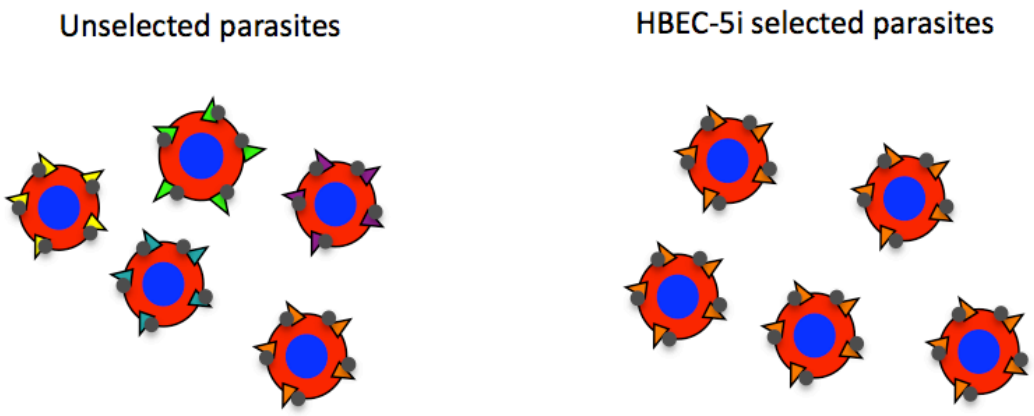
5.6.2 Limitations of the microarray approach

The fact that this research analyzed the entire transcriptome does not imply that we would definitely identify the ligand(s).

The putative "ligands" we try to identify fall into two categories: they can either be the molecule directly binding to HBEC-5i, in which case they have to be located on the iRBC surface, or they can be indirectly involved in cytoadherence, for example by helping PfEMP1 trafficking. They can also be specific ligands, i.e. necessary for binding to HBEC-5i only, or unspecific, i.e. involved in any cytoadherence phenotype. We would expect a specific ligand to be upregulated after selection, but not necessarily the unspecific ligand as it could already be expressed in the unselected population.

Using the example of a protein being involved in PfEMP1 expression or trafficking, and there could be hundreds of them, if one such protein were found in the selected parasites only then one would expect the corresponding gene to be upregulated after selection to the same extent as the upregulated *var* genes (roughly 20 fold). In other words, in the example of the HB3 strain, if there were a gene that is necessary for trafficking of the HB3Var3 variant, and for that VSA only, then this gene would be expressed at very low level in the unselected population and highly upregulated after selection just like *HB3var3*. However there was no non-VSA gene upregulated to the same extend as *HB3var3*. Thus, based on these microarray data, it is unlikely that a non-VSA gene is *specifically* involved in HBEC-5i cytoadhesion.

On the other hand, assuming the total amount of PfEMP1 is more or less the same in unselected and HBEC-selected parasites, a non-VSA gene involved in trafficking of all *var* genes would be expressed at similar levels in both populations, no matter how crucial the gene is for cytoadherence (Box 5-3). Thus, the microarray approach cannot detect unspecific ligands that would be expressed at similar levels before and after selection.



Box 5-3. Hypothesis of a cytoadherence-related protein found in both unselected and selected parasites. As shown in this chapter, the unselected population of parasites expresses a wide repertoire of VSAs (coloured triangles) while the selected population is limited to parasites expressing a group A *var* gene (orange triangles). In the above cartoon, the grey circles represent a protein crucial for mediating any type of cytoadherence but already expressed in most parasites of the unselected population. This grey protein could be involved indirectly in cytoadherence (e.g. PfEMP1 trafficking to the RBC membrane) or even directly mediating the binding if it is found at the surface. It would not be associated with any particular PfEMP1 but would nevertheless be necessary for binding to a receptor. This correlates with the fact that unselected parasites are already able to bind to CD36 for example (chapter 3). However, the selection on HBEC-5i for a particular VSA does not need to influence the transcription of this constitutively expressed grey protein. As a result if another protein is necessary for cytoadherence but is expressed at similar level in both populations then the microarray approach would not detect it.

5.6.3 HB3var3 is consistently upregulated in HB3-HBEC1, 2 and TNF.

Very few unselected parasites bind to HBEC-5i. The most likely explanation is that the appropriate *var* gene, i.e. the one encoding the putative PfEMP1 ligand, is only expressed at low level in this parasite population. An issue that can arise when parasites are selected from a small subset of the population is a "cloning out" effect, i.e. some genes can randomly be enriched in the selected population. The repeat selection from scratch with HB3-HBEC2 resulted in the same *var* gene being upregulated, hence confirming that the HB3var3 PfEMP1 variant is a major candidate ligand for binding to HBEC-5i. However, these data do not rule out the possibility that other PfEMP1 molecules could have the ability to bind HBEC-5i but were not detected in these experiments. Indeed, if other potential binding variants were not expressed at all in the unselected population, then they could not be enriched after selection.

This "cloning out" effect can explain why there are more non-VSA genes down than up regulated (Figure 5-20 and Figure 5-19). This is typically seen in subcloned parasites lines, where the parental population express a wider variety of genes altogether (Sachel Mok, Zbynek Bozdech, unpublished data).

As detailed in chapter 1, TNF is thought to play an important role in cerebral malaria and high levels of this cytokine are associated with the disease (reviewed in (Gimenez, et al., 2003)). It can induce the expression of many surface receptors on HBEC-5i including known receptors for *P. falciparum* adhesion such as ICAM-1 ((Wassmer, et al., 2005) and chapter 3). Thus, it was hypothesized that different parasite ligands could potentially be upregulated after selection on TNF activated HBEC-5i compared to unactivated cells. HB3-HBEC-TNF however showed the same *var* gene upregulated after the selection on TNF activated HBEC-5i. The number of parasites binding to cells was similar with or without TNF (chapter 3). It is still unknown from our data whether PfEMP1 is binding to a TNF-induced receptor, but in all likelihood HB3-HBEC and HBE-HBEC-TNF are binding to the same (unknown) receptor.

5.6.4 *Var* PFD0020c in 3D7-HBEC, ITvar7 and ITvar19 in IT-HBEC.

Repeating the *P. falciparum* selections with different strains, 3D7 and IT, led to a similar *var* gene expression pattern: most of them are downregulated after selection and only one or two variants are highly upregulated. The expression of these *var* genes at almost all time points may seem surprising as they are normally express during mid-late ring stage (Kyes, et al., 2000). However, the signal observed does not necessarily imply active transcription. The expression seen around time points 4 and 5 could be due to mRNA transcribed at time point 2 or 3 that would not have decayed yet (Shock, et al., 2007). The signal seen at time point 6 could be due to very early ring parasites (next cycle).

A validation of the *var* gene results using a different method (RT-PCR), and thorough analysis of all upregulated *var* genes can be found in chapter 6.

5.6.5 Adjacent *rif* genes tend to be upregulated with *var* genes

In all HB3 derived strains and in 3D7-HBEC, the most highly upregulated *rif* gene is located "head to head" to the upregulated group A *var* gene. This association in expression has already been shown in 3D7 parasites using the *PfSir*2 knockout line (Tham, et al., 2007) as well as in 3D7 and IT/FCR3 parasites selected for group A *var* gene expression with children's serum from a malaria endemic area (Wang, et al., 2009a). Unselected 3D7 parasites however do not seem to co-regulate group A *var* and their associated *rif* genes (Tham, et al., 2007). Our microarray data strongly suggests that the neighbouring *var* and *rif* genes are under the control of a common promoter. In fact, it has recently been shown that a titratable factor activates the transcription of all VSA families (Howitt, et al., 2009). DNA fluorescent *in situ* hybridization demonsrate that a transcriptionally active episomal *rif* promoter colocalizes with an active *var* promoter, indicating that these genes families utilize the same subnuclear expression site (Howitt, et al., 2009). The lack of expression of IT_RifA_2006_6b in IT-HBEC seems to contradict this hypothesis, however a technical issue with the microarray cannot be ruled out (for example, the oligo specific to that *rif* gene could have been badly printed). In the IT/FCR3 serum selected parasites

from Wang *et al*, it is a different *var* (*ITvar2*) and its neighbouring *rif* gene that are upregulated (Wang, et al., 2009b). Further experiments, for example RT-PCR with *rif* specific primers, are needed before drawing conclusions on the expression of IT_RifA_2006_6b.

The major discrepancy between the *var* and *rif* expression patterns is in the amount of downregulated genes after selection: most of them for the *var* gene family and hardly any for the *rif* family. This low level of *rif* (and *stevor*) gene expression in unselected parasites has been previously described as many studies show that non-var VSAs are poorly expressed in unselected *in vitro* cultures (Blythe, et al., 2009, Daily, et al., 2005, Niang, et al., 2009). This can be explained by the lack of both the immune pressure and the need for cytoadherence capacity in a culturing flask. In that sense the physiology of a selected line of parasites probably resembles more *in vivo* parasites because of the intense selective pressure that parasites must face in a human body.

The possibility that other VSAs than *var* genes may be involved in cytoadherence had almost never been investigated, let alone the interaction with human brain endothelial cells. Our data show an expression increase of many *rif* variants. This increase is however not as high or consistent as the upregulated *var* genes, therefore the PfEMP1 family is still the main ligand candidates. But these "head to head" *rif* genes, which happened to be somewhat conserved (Wang, et al., 2009b), deserve further investigation. They could also be necessary for HBEC-5i binding. Raising specific antibodies to test their surface expression would be the first step. Secondly, one could knockout the "head to head" *rif* gene. If that mutant parasite line is not selectable on HBEC-5i anymore, this would imply that the *rif* gene expression is a requirement for cytoadherence. A quicker experiment would be to trypsinize iRBC at very low trypsin concentration. PfEMP1, unlike Rifin, has been shown to be highly trypsin sensitive (Fernandez, et al., 1998, Kyes, et al., 1999). Thus removing PfEMP1 from the iRBC surface might indicate its necessity for HBEC-5i binding. However, the sensitivity of other parasite proteins is not known thus this experiment would be of limited value.

5.6.6 Non-VSA genes indirectly involved in cytoadherence to HBEC-5i

The main advantage of using microarray technology was to have an unbiased approach about which genes may act as cytoadherence ligands. The *var* gene expression is a clear-cut result, however hundreds of other genes were found to be differentially regulated to a lesser extent after selection on HBEC-5i (Table 5-7). The 3 different approaches used here pointed out many non-VSA candidates that could be involved with cytoadherence (Figure 5-28). The aim was not to obtain an exhaustive list of putative ligands but identifying the best candidates that are worth following-up by other methods (e.g. Northen blot, Western blot).

The selection on HBEC-5i induced a change of phenotype from a few to a lot of adhering parasites (see chapter 3). Therefore one would expect a specific and direct ligand to be highly upregulated in the selected (binding) parasites. A similar result should be seen with all 3 clones (HB3, 3D7 and IT). Also, this ligand candidate should be located at the surface of iRBCs. This involves featuring a Pexel motif, although exceptions exist (e.g. SBP-1 or MAHRP-1, reviewed in (Maier, et al., 2009)). Only the upregulated *var* genes, or possibly the "head to head" *rif* genes, fit all criterias. A 2 or 3 fold upregulation, as observed with some non-VSA genes, is not sufficient to explain the strong change of phenotype before and after selection. Consequently, according to our data, there is no non-VSA gene that is likely to be a direct and specific ligand.

Nevertheless, non-VSA genes could indirectly be involved with cytoadherence, for example via PfEMP1 trafficking. In fact, there are at least 11 proteins known to be essential for PfEMP1 to be functional (Table 5-17). Using our microarray data, a gene encoding a protein predicted to be exported and showing upregulation in all strains would be a candidate for indirect cytoadherence to HBEC-5i. That gene would not necessarily have to be involved with PfEMP1 trafficking.

Gene	Function	Reference
PFB0106c	Involved in the transport of PfEMP1 to Maurer's Cleft.	(Maier, et al., 2008)
MAL7P1.171	Involved in the transport of PfEMP1 to Maurer's Cleft.	(Maier, et al., 2008)
PF10_0025	Involved in the transport of PfEMP1 to Maurer's Cleft.	(Maier, et al., 2008)
MAHRP-1	Involved in the transport of PfEMP1 to Maurer's Cleft.	(Spycher, et al., 2008)
SBP1	Involved in the transport of PfEMP1 to Maurer's Cleft and iRBC surface.	(Cooke, et al., 2006)
MAL7P1.172 (PHISTc)	Involved in the transport of PfEMP1 from Maurer's Cleft to iRBC surface.	(Maier, et al., 2008)
PF14_0758	Involved in the transport of PfEMP1 from Maurer's Cleft to iRBC surface.	(Maier, et al., 2008)
PF13_0076	Involved in the transport of PfEMP1 from Maurer's Cleft to iRBC surface.	(Maier, et al., 2008)
PFD1170c (PHISTb)	Essential knobs on iRBC surface and involved in cytoadherence.	(Maier, et al., 2008)
PF10_0381 (DNAJ)	Essential for knobs on iRBC surface and for cytoadherence.	(Maier, et al., 2008)
KAHRP	Essential for knobs formation.	(Rug, et al., 2006)

Table 5-17. List of proteins known to be essential for PfEMP1 function. Adapted from (Sam-Yellowe, 2009).

In this final section, we classify putative ligands (Figure 5-28) into 3 categories: (1) " true positive", i.e. an upregulated gene that has previously been shown to be essential for cytoadherence; (2) "probably false negative", i.e. an upregulated gene that has previously been shown not to be essential for cytoadherence; (3) "New ligand candidates", i.e. an upregulated gene encoding an exported protein of unknown function that would be worthy of further investigation. Note that for the "probably false negative" category, genes included in that category were shown not to be essential for cytoadherence to CD36 or CSA. Thus they could still be important for HBEC-5i binding. However they would not be the first genes to be tested for further analysis, hence their inclusion in that category.

Finally, this last section shows the expression of each oligo specific to the ligand candidate in all selections as well as the timing of expression according to the original transcriptome analysis as it is a much more precise timing resolution (Bozdech, et al., 2003, Llinas, et al., 2006). For each candidate, the

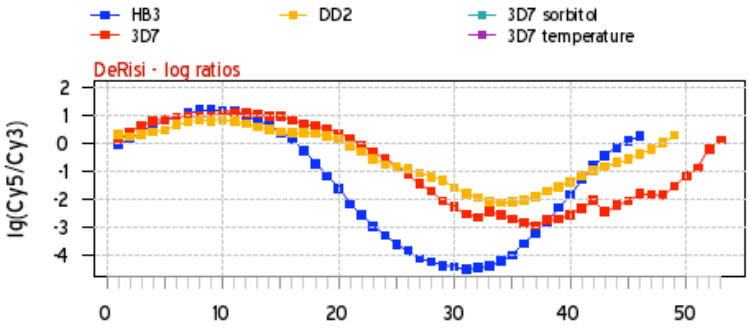
details of gene expression are shown first, followed by discussion of the known characteristics of the protein and the likelihood of its involvement in cytoadherence.

5.6.6.1 MAHRP-1 is essential for cytoadherence (true positive).

MAL13P1.413: Membrane Associated Histidine-Rich Protein (MAHRP-1)

Function: Necessary for translocation of PfEMP1 to the iRBC surface.

PlasmoDB transcription pattern:



HB3-HBEC1	HB3-HBEC2	HB3-HBEC-TNF	3D7-HBEC	IT-HBEC
T1 T2 T3 T4 T5 T6	T1 T2 T3 T4 T5 T6	T1 T2 T3 T4 T5 T6	T1 T2 T3 T4 T5 T6	T1 T2 T3 T4 T5 T6

Figure 5-29. Expression details of MAHRP-1. The first graph, from PlasmoDB, precisely indicates the timing of expression in the HB3, Dd2 and 3D7 strain (Bozdech, et al., 2003, Llinas, et al., 2006). The peak of transcription of *MAHRP-1* occurs about 10 hours post invasion. The bottom panels show the expression ratios (one oligo) in each selected HBEC-5i selected strain.

The membrane associated histidine-rich protein (MAHRP-1) is transcribed in ring-stage iRBC and the resulting protein is located in the Maurer's Cleft despite the fact that it is lacking a Pexel motif (Spycher, et al., 2003, Spycher, et al., 2006). This suggests MAHRP-1 uses a Pexel-independent pathway to reach the RBC cytosol. Interestingly, deletion of the *MAHRP1* gene leads to an accumulation of PfEMP1 in the PV membrane and a depletion of surface-exposed PfEMP1 (Spycher, et al., 2008). This in turn results in a decrease in cytoadherence to CD36. The complementation of the mutant

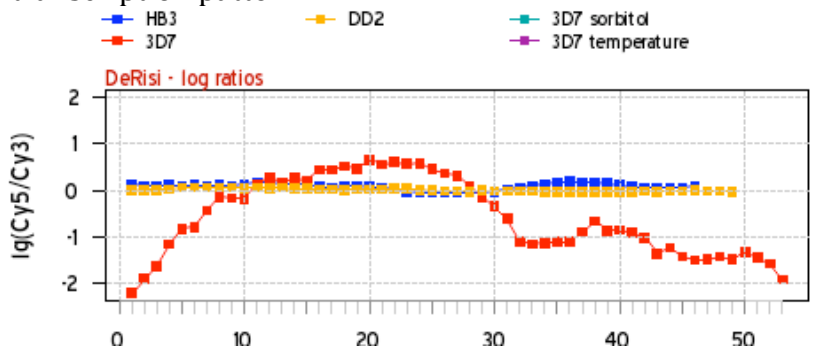
parasites can restore PfEMP1 localization and cytoadherence properties. Altogether this strongly suggests that MAHRP1 is involved in PfEMP1 trafficking (Maier, et al., 2009). As MAHRP-1 is upregulated by at least two fold in all selections, we can hypothesize that it indirectly mediates adhesion of selected parasites to HBEC-5i via the trafficking of PfEMP1 ligands. If this were true, it would not be possible to select the knockout line for HBEC-5i binding.

5.6.6.2 PfEMP3 is upregulated but probably not essential for HBEC-5i binding (false positive).

PFB0095c: Erythrocyte Membrane Protein 3 (PfEMP3)

Function: Located near the RBC membrane. Binds to Spectrin. Not essential for PfEMP1 expression.

PlasmoDB transcription pattern:



HB3-HBEC1	HB3-HBEC2	HB3-HBEC-TNF	3D7-HBEC	IT-HBEC
T1 T2 T3 T4 T5 T6	T1 T2 T3 T4 T5 T6	T1 T2 T3 T4 T5 T6	T1 T2 T3 T4 T5 T6	T1 T2 T3 T4 T5 T6

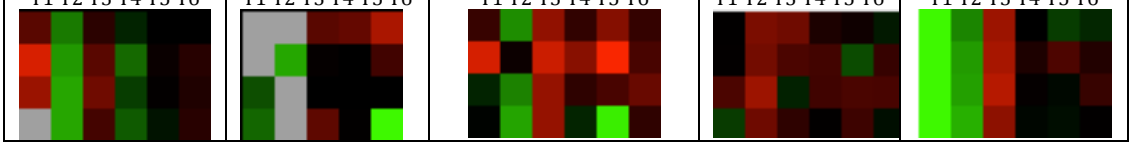


Figure 5-30. PfEMP3 expression. The 4 oligos specific to this gene are shown.

The upregulation of PfEMP3 expression is interesting as it is also upregulated in parasites selected for platelet-mediated clumping of iRBC (Monica Arman, unpublished data) or rosetting (Ashfaq Ghumra and Antoine Claessens, unpublished data). PfEMP3 is a bulky protein interacting with the iRBC membrane skeleton (Waller, et al., 2007) and spectrin (Pei, et al., 2007). *P. falciparum* mutants with truncated *PfEMP3* gene show an accumulation of truncated PfEMP3 under the iRBC membrane which disrupts PfEMP1 surface

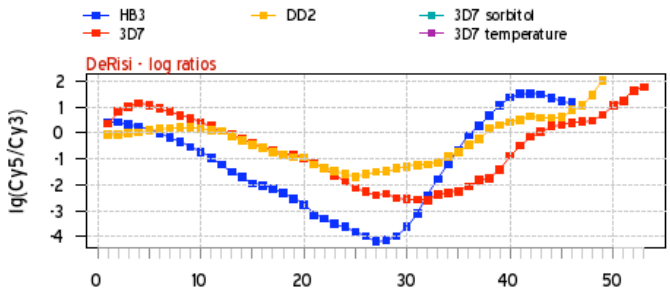
expression and binding to CD36 (Waterkeyn, et al., 2000). However the full-length knockout line of *PfEMP3* is fully functional in terms of CD36 adhesion under flow conditions (Waterkeyn, et al., 2000). Thus, unless another protein complemented the function of PfEMP3 in the full-length knockout line, a role for this protein as PfEMP1 trafficking or in cytoadherence is unlikely. It is then difficult to find an explanation about why *PfEMP3* is consistently upregulated. One possibility is that the selection on HBEC-5i enriched for iRBC with the appropriate shape or rigidity where PfEMP3 could have a role. This does not fit with the fact that parasites cytoadhere even in the absence of PfEMP3 (Waterkeyn, et al., 2000), except again if other proteins can complement its function. To test this hypothesis one could analyze the transcriptome of the PfEMP3-Knockedout line and find out whether other rigidity-related genes are upregulated to complement the lack of PfEMP3. Also, PfEMP3-knockout parasites could be tested for selection on HBEC-5i.

5.6.6.3 RESA-1 is upregulated but probably not essential for HBEC-5i binding (false positive).

PFA0110w: RESA, DNAJ, PHISTb

Function: Binds to Spectrin and protects cytoskeleton rigidity during febrile episode.

PlasmoDB transcription pattern:



HB3-HBEC1	HB3-HBEC2	HB3-HBEC-TNF	3D7-HBEC	IT-HBEC
T1 T2 T3 T4 T5 T6	T1 T2 T3 T4 T5 T6	T1 T2 T3 T4 T5 T6	T1 T2 T3 T4 T5 T6	T1 T2 T3 T4 T5 T6

Figure 5-31. RESA-1 expression. The 2 oligos specific to this gene are shown.

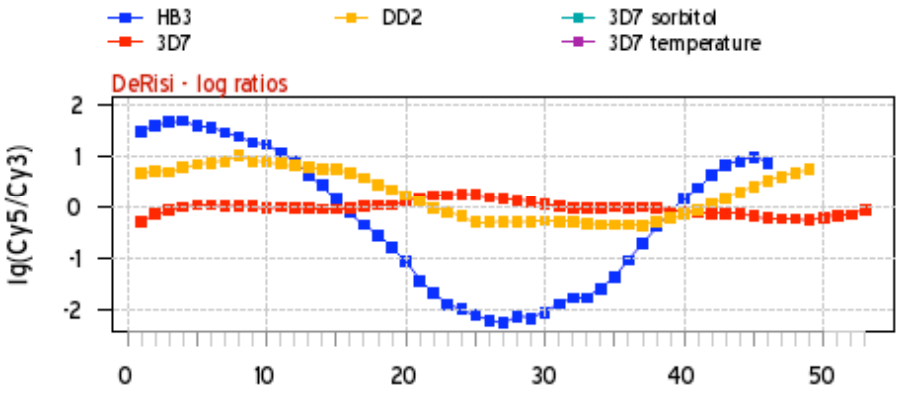
The first protein to be exported after the invasion of the merozoite in the RBC is RESA-1 (Ring-Infected Surface Antigen), a PHISTb family member (Rug, et al., 2004). It binds to spectrin via a motif located next to the DNA-J domain. RESA is thought to stabilize the RBC membrane during febrile episodes (Silva, et al., 2005). Antibodies reacting with RESA inhibit merozoite invasion (Berzins, et al., 1986). The lack of RESA does not decrease cytoadherence nor does it affect parasite virulence in monkeys (Fandeur, et al., 1993, Mills, et al., 2007, Silva, et al., 2005). Knocking-out the gene neither disrupts the formation of knobs nor the expression of PfEMP1 (Maier, et al., 2008). Despite this absence of evidence for a role in cytoadhesion, RESA-1 is upregulated in parasites in pregnant women (compared to the 3D7 strain) (Tuikue Ndam, et al., 2008). The reason for the change of expression level is unknown. Further investigation is needed to ascertain why the gene is upregulated in HBEC-5i selected parasites.

5.6.6.4 RESA-2 is upregulated in some HBEC-5i selections and in other studies.

PF11_0512 : RESA-2, DNAJ, PHIST

Function: unknown (similar to RESA-1?).

PlasmoDB transcription pattern:



HB3-HBEC1	HB3-HBEC2	HB3-HBEC-TNF	3D7-HBEC	IT-HBEC
T1 T2 T3 T4 T5 T6	T1 T2 T3 T4 T5 T6	T1 T2 T3 T4 T5 T6	T1 T2 T3 T4 T5 T6	T1 T2 T3 T4 T5 T6



Figure 5-32. RESA-2 expression. The 2 oligos specific to this gene are shown.

Interestingly, RESA-2, a homologue to RESA-1, has also been pointed out in this microarray data analysis due to its Overall Area ratio. The function of this protein has never been studied, although it could be similar to RESA-1. Importantly, RESA-2 is upregulated in field isolates (Daily, et al., 2005) and in rosetting parasites (Mok, et al., 2007) indicating a possible role in cytoadherence. However, a Δ*resa-2* knockout line found no change in rigidity of the RBC membrane and no change in cytoadherence to CSA (Maier, et al., 2008). Nevertheless, the same line, which normally expresses the var2csa PfEMP1 variant, showed a ”partially reduced” reactivity with serum antibodies from malaria-exposed multigravid women, pointing towards a reduced amount of PfEMP1 surface expression. Whether the Var2csa protein was actually expressed at a lower level in this Δ*resa-2* knockout line was not tested by the authors (Maier, et al., 2008). In our microarray analysis, the 2 oligos specific to PF11_0512 (*resa-2*) only show consistent upregulation in HB3-HBEC1, HB3-HBEC-TNF and IT-HBEC. Therefore our data and the Maier *et al* study are inconclusive in the role of RESA-2 in cyotadherence. Further research is needed to investigate its function.

5.6.6.5 PF11_0035 is upregulated but is not necessary for PfEMP1 expression (probably false negative).

PlasmoDB transcription pattern:

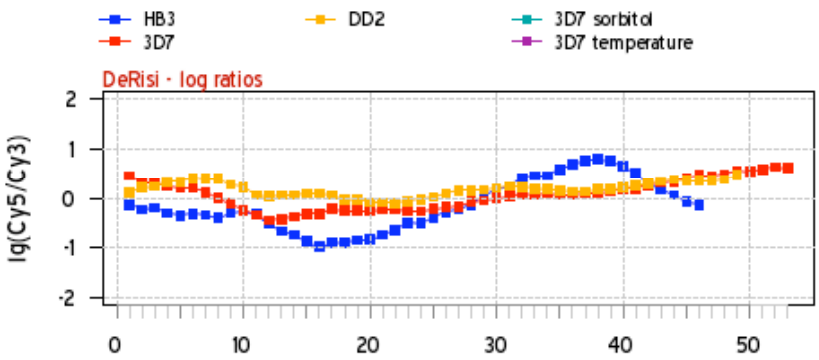


Figure 5-33. A single oligo is specific to *PF11_0035*; its expression can be seen in **Figure 5-19**.

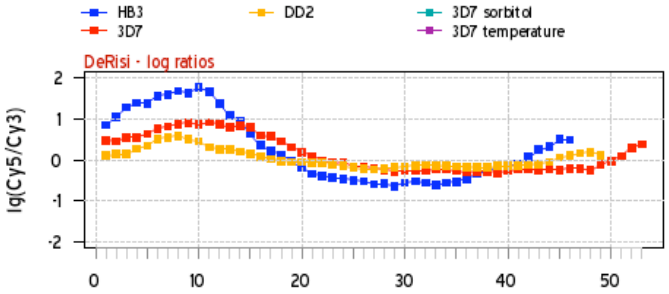
PF11_0035 shows a Pexel motif and was one of the 83 genes that were individually knocked out (Maier, et al., 2008). The mutant line did not show any change in RBC rigidity, cytoadhesion to CSA or PfEMP1 expression. Therefore PF11_0035 is unlikely to be essential for cytoadherence.

5.6.6.6 Two PHIST members are HBEC-5i ligand candidates.

PF14_0752: PHISTa family

Function: unknown.

PlasmoDB transcription pattern:



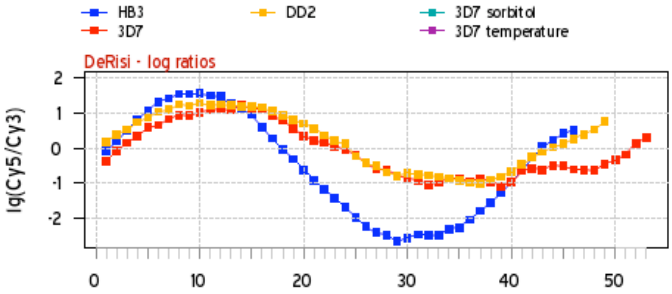
HB3-HBEC1	HB3-HBEC2	HB3-HBEC-TNF	3D7-HBEC	IT-HBEC
T1 T2 T3 T4 T5 T6	T1 T2 T3 T4 T5 T6	T1 T2 T3 T4 T5 T6	T1 T2 T3 T4 T5 T6	T1 T2 T3 T4 T5 T6

Figure 5-34. PF14_0752 (PHISTa) expression. The gene is encoded by a single oligo.

PF11_0503: PHISTc family

Function: unknown.

PlasmoDB transcription pattern:



HB3-HBEC1	HB3-HBEC2	HB3-HBEC-TNF	3D7-HBEC	IT-HBEC
(no data available)	T1 T2 T3 T4 T5 T6	T1 T2 T3 T4 T5 T6	T1 T2 T3 T4 T5 T6	T1 T2 T3 T4 T5 T6

Figure 5-35. PF11_0503 (PHISTc) expression. The gene is encoded by a single oligo.

The microarray analysis revealed a PHISTa gene, *PF14_0752*, as one of the best candidate for involvement in cytoadherence. The PHIST family was recently discovered by bioinformatics analysis (Sargeant, et al., 2006). PHISTa is a sub-family of 25 relatively short genes with a signal sequence and a Pexel motif. They are all entirely specific to *P. falciparum*, which indicates a function unique to that parasite species. Interestingly, I noticed that *PF14_0752* is one of the most highly upregulated gene in CD36–selected parasites (Mok, et al., 2007), in field isolates (Daily, et al., 2005) and in 3D7 gametocytes (Eksi, et al., 2005). All results come from microarray data and were confirmed by RT-PCR. Furthermore, *PF14_0752* is under strong evolutionary pressure as it is one of the 234 non-VSA genes to evolve twice as fast as normal rate (Kidgell, et al., 2006). All in all, based on our data and on other publications, *PF14_0752* is the first non-VSA candidate that should be further scrutinized.

Equally interesting is PF11_0503, a PHISTc protein (Figure 5-35). It shows an extremely similar expression pattern as *PF14_0752* (Figure 5-34) in all strains even though the gene sequence and its oligo are unrelated to *PF14_0752*. There was no oligo for this gene in the pilot experiment hence the lack of data for HB3-HBEC1. Thus PF11_0503 is equally as likely as PF14_0752 to be involved in cytoadherence to HBEC-5i. However, PF11_0503 has not been mentioned in any publication yet.

Thus we postulate that PF14_0752 (PHISTa) and PF11_0503 (PHISTc) are involved in cytoadhesion to HBEC-5i.

5.6.6.7 Other upregulated and exported proteins.

All other predicted to be exported proteins identified in this microarray data analysis have never been directly studied. To our knowledge, a knock-out attempt has never been performed on any of these genes (Maier, et al., 2009). More experiments are needed to investigate their putative role in binding to HBEC-5i. The best candidates are summarized in Table 5-18.

TRUE POSITIVES Genes identified in any approach and already known to be involved in cytoadherence	**"FALSE POSITIVE"** Genes identified in any approach and already known to be not necessary for cytoadherence	**NEW CYTOADHESION CANDIDATES** Genes identified in any approach and could potentially be involved in cytoadherence
MAHRP-1	PfEMP3	PF14_0752 (PHISTa)
	RESA-1	*PF11_0503 (PHISTc)*
	PF11_0035	PF14_0740 (hyp17)
	RESA-2?	PFF0055w (hyp4)
		PF11_0035
		PF10_0391 (hyp4)
		PFA0060w (hyp4)
		MAL13P1.61 (hyp8)
		PF11_0024 (hyp4)

Table 5-18. Summary of the exported non-VSA ligand candidates. A "true positive" is a gene identified in the microarray data analysis with previously published studies indicating a role in cytoadherence, A "false positive" is a gene identified in the microarray data analysis with previously published studies indicating the gene is not necessary for cytoadherence. Important note: no study had ever focused on HBEC-5i cytoadhesion before. Therefore the gene necessity for cytoadhesion refers to other of types cytoadhesion (for example, binding to CSA). A gene not essential for cytoadherence to CSA might be important for HBEC-5i binding. By "false positive", we mean genes that are less likely to be involved with HBEC-5i cytoadhesion. PF11_0503 was not identified in any of the 3 approaches because there was no oligo specific to that gene in the HB3-HBEC1 experiment. Its expression with all other strains is however very similar to PF14_0752.

All in all, this chapter fulfilled its aim of identifying parasite ligand candidates, with PfEMP1 being the major one. This comprehensive approach also detected new putative candidates, including "head to head" Rifins and PHIST family members. The putative PfEMP1 ligands are further characterized in chapter 6.

6 Chapter VI: Further analysis of the putative *var* gene ligands

6.1 Abstract

The microarray data indubitably indicated *P. falciparum* erythrocyte membrane protein 1 (PfEMP1) as strong ligand candidates for binding to human brain microvascular endothelial cells (HBEC-5i). In this chapter, the *var* genes expression was also profiled by Reverse Transcriptase-PCR (RT-PCR) using degenerate primers specific to conserved motifs within the DBLα domains of *var* genes. The RT-PCR results perfectly correlate with the microarray data as *HB3var3*, *PFD0020c*, *ITvar7* and *ITvar19* are the most upregulated *var* genes in HB3, 3D7 and IT selections, respectively. We also investigated whether these putative ligands are specifically binding to HBEC-5i only. HB3 parasites were selected on human pulmonary and dermal microvascular endothelial cells (HPMEC and HDMEC, respectively) as sequestration in these tissues has been reported in cerebral malaria cases. Both selections led to the same *var* gene (*HB3var3)* being highly upregulated. Thus HB3var3 may be the ligand binding to HBEC-5i, HPMEC and HDMEC, possibly using the same receptor.

Interestingly, upregulated *var* genes from HB3, 3D7 and IT are all part of the group A or group-A like family and all harbour a CIDR1α1 domain. More experiments, including developing an antibody against the CIDR1α1 domain, will be needed to determine whether these PfEMP1 variants are the parasite ligands for binding to HBEC-5i. All in all, these findings are consistent with previous work showing an association between Group A *var* genes and cerebral malaria.

6.2 Introduction

The selection of *Plasmodium falciparum* parasites on HBEC-5i resulted in a considerable upregulation of one or two *var* genes (out of 50 to 60 variants) in each strain (chapter 5). This chapter focuses on: (i) the confirmation of the microarray data, (ii) analyzing the specificity of the *var* "ligands" for binding to brain endothelial cells, and (iii) performing bioinformatics analyses on the candidate *var* sequences to identify common features among them.

Despite their high divergence in sequence, *var* genes show some conserved features. For example the DBLα domains are found in all PfEMP1s sequenced to date (except for Var2CSA) (Kraemer, et al., 2007). This characteristic has allowed the development of a pair of 'universal primers' that are specific to two conserved regions within the DBLα domain (Bull, et al., 2005, Taylor, et al., 2000a). A stretch of about 300 hypervariable nucleotides is found in between these conserved regions (see section 6.4, Figure 6-1, central panel). Thus the universal primers are used to amplify the conserved regions plus the hypervariable region included in between. Then this unique hypervariable stretch within the 'DBLα tag' will allow for the identification of the corresponding *var* gene. In theory, these primers can amplify any *var* gene (except for Var2CSA and type 3 *var* that do not show this conserved feature). This method has also been used to sequence DNA or cDNA of DBLα tags of unknown genomes (Afonso Nogueira, et al., 2002, Bull, et al., 2005, Bull, et al., 2008, Ikenoue, et al., 2002, Kaestli, et al., 2006, Kaestli, et al., 2004, Kyriacou, et al., 2006, Normark, et al., 2007, Warimwe, et al., 2009).

Sequestration of *P. falciparum* iRBC in brain microvasculature is the hallmark of cerebral malaria. However, cerebral malaria cases also show parasites sequestered in many other organs, including lungs, dermis, liver, kidney, spleen, intestine and heart (see also chapter 1). In fact, in all postmortem cerebral malaria studies where autopsies of the rest of the body were carried out, sequestration was found in other organs (Genrich, et al., 2007, MacPherson, et al., 1985, Montgomery, et al., 2006, Nakazawa, et al., 1995, Pongponratn, et al., 1991, Pongponratn, et al., 2003, Seydel, et al., 2006,

Wilairatana, et al., 2000). Importantly, identical parasite clones have been shown to cytoadhere in different organs (Montgomery, et al., 2006), indicating that the adhesion capacity of a clonal parasite population is not restricted to a single type of endothelial cell. The parasite might achieve this by either binding to common receptors found in different body parts (as suggested by (Seydel, et al., 2006)) or by expressing different VSA that allow it to sequester in various locations over the body. A pilot experiment has attempted to solve the issue by profiling the *var* transcriptome in brain, lung, heart and spleen (Montgomery, et al., 2007). Although the number of patients was too small to draw any conclusion, expression of many specific var DBLα tags was detected in different organs simultaneously.

Although parasites can be found in different organs, the relative amount of sequestration is difficult to estimate. Indeed, there is extensive heterogeneity in the intensity of parasitisation, even within very small areas (Silamut, et al., 1999). Moreover, the level of peripheral parasitaemia does not correlate with the number of sequestered parasites in tissues (Montgomery, et al., 2006). An alternative approach is to estimate the parasite burden by measuring the concentration of parasite-derived lactate dehydrogenase (pLDH) in tissue samples obtained at autopsy (Piper, et al., 1999). Using this technique, the highest parasite load was found in brain, dermis and intestine of comatose Malawian children (Seydel, et al., 2006). The same study also demonstrated that patients with high concentrations of pLDH in one tissue were likely to have high concentrations elsewhere.

Most studies have reported iRBC sequestration in the dermis and lungs (chapter 1). Microvascular endothelial cell primary lines derived from these human tissues have recently been made commercially available (ScienCell). Although HBEC-5i selected *P. falciparum* parasites were shown to bind to HDMEC and HPMEC (Human Dermal and Pulmonary Microvascular Endothelial Cells, respectively) in chapter 3, it remained to be tested whether selection on these cells from unselected parasites would enrich for the same *var* genes. An interesting feature about HPMEC and HDMEC is that, unlike HBEC-5i, they are positive for CD36 expression ((Shen, et al., 1995, Swerlick, et al., 1992b) and

chapter3). Binding to CD36 has been shown to be a property of most groups B and C but not group A PfEMP1 proteins (Robinson, et al., 2003). This leads to a hypothesis where parasites would tend to express group A PfEMP1s for sequestration in the brain microvasculature, where CD36 receptor is scarce or inexistent (Silamut, et al., 1999), but group B and C for sequestration in other organs. By selecting HB3 parasites on HDMEC and HPMEC and characterising the resulting *var* transcription profile, we are testing whether *HB3var3* expression is preferentially selected for binding to brain endothelial cells (HBEC-5i).

6.3 Aims of this chapter

The first aim of this chapter is to test the validity of the microarray data. As *var* genes were the most differentially regulated genes, an RT-PCR experiment is performed to profile the *var* gene trancriptome in selected and unselected parasites.

Secondly, in order to test whether *HB3var3* upregulation is specific to HBEC-5i selection, HB3 parasites were selected on HDMEC and HPMEC. HB3-HDMEC and HB3-HPMEC *var* gene expression is analysed using the same RT-PCR method.

Finally, various bioinformatics approaches are used to identify common features among the PfEMP1 sequences from HB3, 3D7 and IT that are putative ligands for binding to brain endothelial cells.

6.4 Methods

The method for profiling the *var* transcriptome by DBLα RT-PCR is laid out in Figure 6-1.

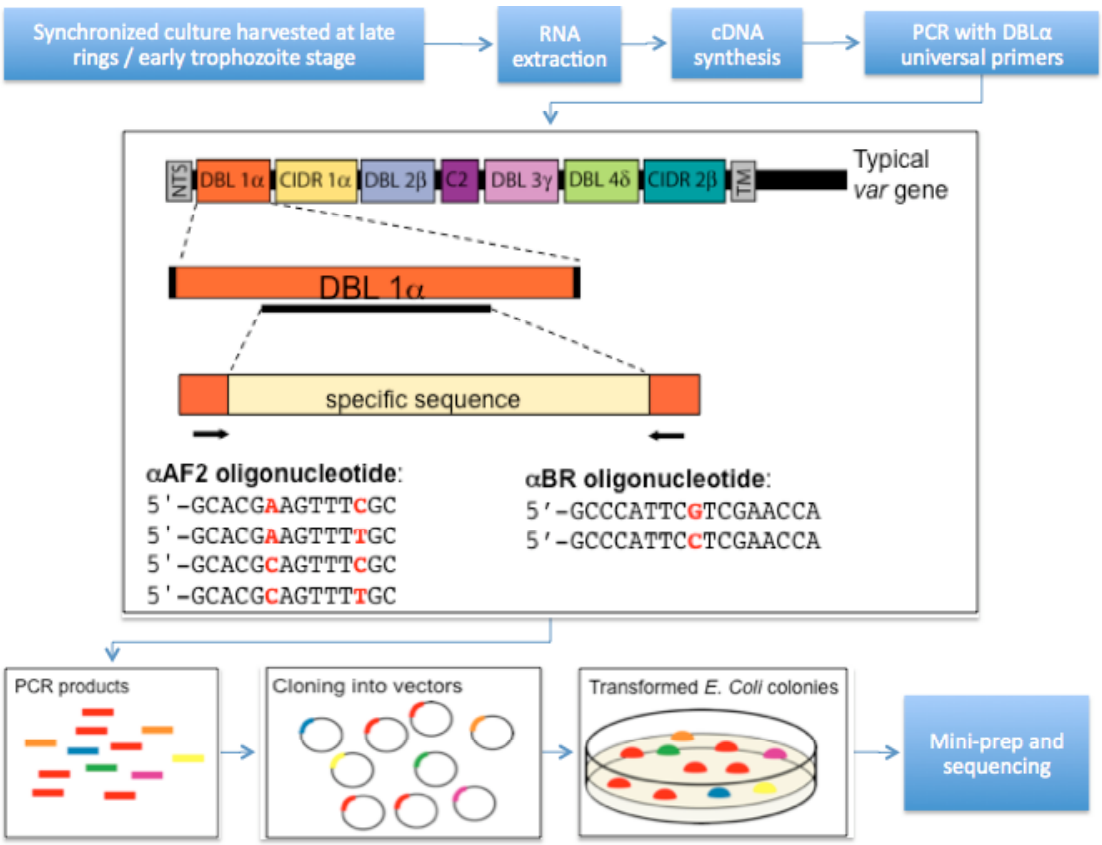


Figure 6-1. Overview of the *var* transcription profile by DBLα RT-PCR. The basic principle is that the mRNA from late rings/ early trophozoite cultures is harvested and reverse-transcribed into cDNA. The DBL1α domains are amplified by PCR using the universal primers (sequences are in the central rectangle). The resulting products are cloned into vectors. *Escherichia coli* is then transformed with these vectors and colonies that have integrated them are picked the day after for sequencing. The number of times that a given sequence ("DBLα tag") is found is proportional to the expression of each *var* gene. Figure modified from Monica Arman (unpublished).

6.4.1 RNA extraction

P. falciparum iRBC cultures were grown to late rings/ early trophozoite stages. At least 300µl packed cell volume at 5% parasitaemia or higher was harvested as described in chapter 2.

6.4.2 DNase treatment

For RT-PCR purposes, but not for microarray applications, RNA samples were DNase treated to remove any contaminating genomic DNA (gDNA).

1 µg of RNA from each parasite culture was treated with DNAse 1 (Invitrogen) for 20 min at RT. In a microcentrifuge tube was added: 5 µl RNA, 7 µl DEPC H_20, 1.5 µl 10x DNAse buffer (400mM Tris-HCl, pH 7.5, 100mM Sodium Chloride, 60mM Magnesium Chloride), 1.5 µl DNAse 1. The reaction was stopped with 1.5 µl 25mM EDTA, incubated for 10 min at 65˚C and kept on ice.

6.4.3 cDNA synthesis

For RT-PCR purposes, cDNA was synthesized using Superscript III First Strand Synthesis (Invitrogen 18080-051).

To the RNA sample was added: 50 ng random hexamers, 1 nmol dNTP and 2 µl DEPC-H_20. This was gently mixed and heated to 65˚C for 5 min. The tube was left on ice for 2 min to cool. It was split into two tubes: "Plus RT" (RT: reverse transcriptase) and "RT Control" (to detect gDNA contamination in the RT-PCR reaction). 4 µl of 5x first strand synthesis buffer (200 mM Tris-HCl, pH 8.4, 500 mM KCl), 0.4 µmol DTT, 100 nmol $MgCl_2$ and 1 µl DEPC-H_20 was added to each, mixed gently and incubated (25˚C, 2 min). 0.5 µl Superscript III reverse transcriptase (RT) was added to the plus RT tube while 0.5µl DEPC-H_20 was added to the control tube. These were incubated at 25˚C for 10 min, 50˚C for 50 min and 85˚C for 15 min. The cDNA was then stored at –20˚C.

6.4.4 PCR

To amplify DBLα domains of *var* genes, the modified version (Bull, et al., 2005) of universal primers was used (Taylor, et al., 2000b).

To autoclaved 0.5 ml centrifuge tubes were added: 20.75µl H_2O, 4µl 25mM $MgCl_2$, 8µl 10mM dNTPs, 25pmol αAF2 primer (GCACG(A/C)AGTTT(C/T)GC), 25 pmol αBR primer (GCCCATTC(G/C)TCGAACCA), 0.25µl AmpliTaq Gold (10 000 units/ml, Applied Biosystems N8080246). The PCR machine used was a PCT- 100 Peltier thermal cycler PCR machine (MJ Research) with the following

program: 5 min at 95˚C, (20s at 95˚C, 20 s at 42˚C, 1 min at 60˚C) repeated 35 times, 10 min at 60˚C, 4˚C forever.

6.4.5 Agarose gel electrophoresis

All PCR products were run on an agarose gel as described in chapter 2.

6.4.6 PCR product purification

If no genomic DNA contamination was detected in the agarose gel, PCR products were purified as described in chapter 2.

6.4.7 Ligation and cloning

In order to clone the PCR product into a vector, 7 µl purified PCR product was ligated into 1µl PCR II TA cloning vector (TA cloning kit, Invitrogen) using 4 units T4 DNA ligase and 1 µl ligation buffer (500 mM Tris-HCl, 100 mM $MgCl_2$, 10 mM ATP, 100 mM Dithiothreitol, pH 7.5) overnight at 14°C.

Competent cells (E. coli, TOP10F' from Invitrogen) were thawed on ice and 2 µl of the resulting ligated plasmid was gently mixed into the vial. After incubation on ice for 30 min, cells were heat shocked (30 s, 42°C) and put on ice again. 250µl SOC media (Invitrogen) was added to these transformed cells and incubated at 37°C for 1 hr with shaking.

Plates (100mm) were prepared with Luria Bertani (LB) agar (Sigma), 50 µg/ml ampicillin, 40 µl of 20 µg/ml X-gal and 20 µg/ml IPTG for blue/white screening. Cells were plated on these LB plates and incubated overnight at 37°C. Individual white colonies were selected for overnight culture in LB medium (5ml vial or 96-well plate) with 50 µg/ml ampicillin at 37°C.

6.4.8 Mini-prep

DNA was extracted from overnight culture with a mini-prep kit (Qiagen).

Bacterial cultures (from individual colonies) were pelleted by centrifugation at 13000rpm for 3min and resuspended in 250 µl buffer P1 (6.06 g/l Tris base, 3.72 g/l EDTA, pH 8.0). Cells were lysed with 250 µl P2 buffer (8 g/l NaOH, 1% (w/v) SDS in water) and neutralised in 350 µl N3 buffer (confidential

composition). Cell debris was removed by centrifugation (13000 rpm, 10 min). The supernatant was applied to a spin column and centrifugated. From here all centrifugations were at 13000rpm for 1min in a bench-top centrifuge. The columns with bound plasmids were washed with 750 µl wash buffer PE and spun down. The flow-through was discarded and the column spun again to remove any residual ethanol. Plasmids were then collected in a fresh tube after addition of 50 µl elution buffer (10 mM Tris-HCl, pH 8.5) to the column and a final spin.

6.4.9 *Eco*RI restriction enzyme digestion

5 µl of the DNA extraction in elution buffer was digested with 0.5 µl EcoRI (12u/µl Promega R6011) and 1 µl buffer H (90mM Tris-HCl, pH 7.5, 10mM $MgCl_2$, 50mM NaCl; Promega) which was incubated at 37°C for about 90 min. 5 µl of the digested plasmid preparation was visualised by running an agarose gel (section 6.4.5). Plasmids containing an insert were sequenced.

6.4.10 Sequencing

Plasmids were sequenced using the DNA Sequencing Kit (Applied Biosystems). Per sample: 4 µl BigDye, 1.6 pmol VR1 primer (AGATGCATGCTCGAG CGG), 5 µl DNA. The mix was incubated for 25 cycles of 96°C for 30 s, 50°C for 15 s and 60°C for 4 min. Sequencing was carried out by the GenePool sequencing facility (University of Edinburgh).
Sequences were analysed using TranSeq and ClustalW.

6.4.11 Large scale sequencing by GenePool

For larger numbers of samples, when white colonies on LB plates were picked (section 6.4.7), bacteria were inoculated in 150 µl LB medium with ampicillin in a 96-well plate. The plate was incubated overnight at 37°C. Half the amount of culture was then transferred to a new plate and given to the GenePool for PCR and sequencing reactions.
Sequences were analysed using TranSeq and ClustalW.

6.4.12 Bioinformatics tools and Statistical analysis

Website details of all bioinformatics software are given in chapter 2. Statistical tests were performed using GraphPad Prism 5.0. P-values were calculated with a Two-tailed Fisher's exact test (confidence interval: 95%).

6.5 Results

6.5.1 DBLα RT-PCR confirms the microarray data for the *var* gene family

The purpose of the DBLα RT-PCR experiment is to analyze the *var* genes transcription before and after selection on HBEC-5i. The number of different DBLα tags found among the *E. coli* colonies is representative of the variety of *var* genes expressed in the parasite population; and the percentage of *E. coli* colonies that contain each specific DBLα tag group indicates the relative expression of that *var* gene within the population.

For RT-PCR purposes, RNA was extracted from populations that were at late ring to early pigmented trophozoite stages. This corresponds to time point 3 in the microarray time-course analysis. Each sample was reverse transcribed; a control to check for genomic DNA contamination was included in all cases (i.e. mock reverse transcription reaction done without adding the reverse transcriptase enzyme). DBLα transcripts were amplified by PCR using degenerate primers to DBLα domains (Figure 6-1 in section 6.4). Samples were run on an agarose gel (Figure 6-2). Multiple bands around 400bp can be seen, representing multiple DBLα domain transcripts of slightly different lengths. Control samples (without reverse transcriptase) lanes remained blank, indicating that there is no genomic DNA contamination. These DBLα RT-PCR products were purified before ligation into plasmids. The recombinant plasmids were transformed into *Escherichia coli* and plated on agar/ampicillin plates. The antibiotic selects for bacteria having integrated the plasmid, which contains a gene conferring drug resistance. Bacterial colonies were picked and expanded in LB broth.

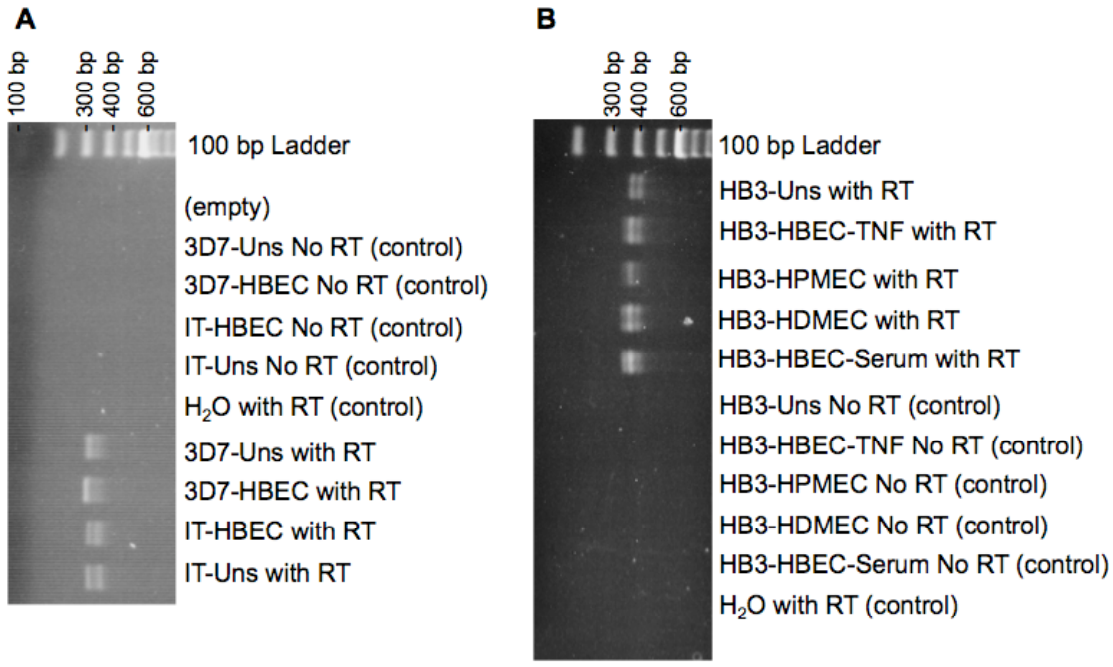


Figure 6-2. Representative gels of DBLα domain RT-PCR products. RT-PCR products from amplification of DBLα domains from selected and unselected cDNA with primers DBLαAF2 and DBLαBR, were visualised by electrophoretic separation on a 1.5% agarose gel. As a control, a PCR was also performed with samples where water was added instead of the reverse transcriptase ("No RT"). Empty lanes indicate no genomic DNA contamination.

For HB3-Uns and HB3-HBEC1, recombinant plasmids were extracted by miniprep. The presence of an insert of the expected length was verified by digestion with *Eco*RI enzyme. Samples that did show an insert on an agarose gel (27 for HB3-Uns, 29 for HB3-HBEC1) were given to the GenePool facility (Edinburgh) for sequencing. For all other selections, picked bacterial colonies were grown in LB broth in a 96-well plate and immediately given to the GenePool facility.

The resulting nucleotide sequences (DBLα tags) were translated into peptides using TranSeq. These amino acid sequences were aligned by ClustalW with all PfEMP1 sequences from the same clone in order to identify each tag. An

example is shown in Figure 6-3. The proportion of each DBLα tag defines the *var* gene expression profile.

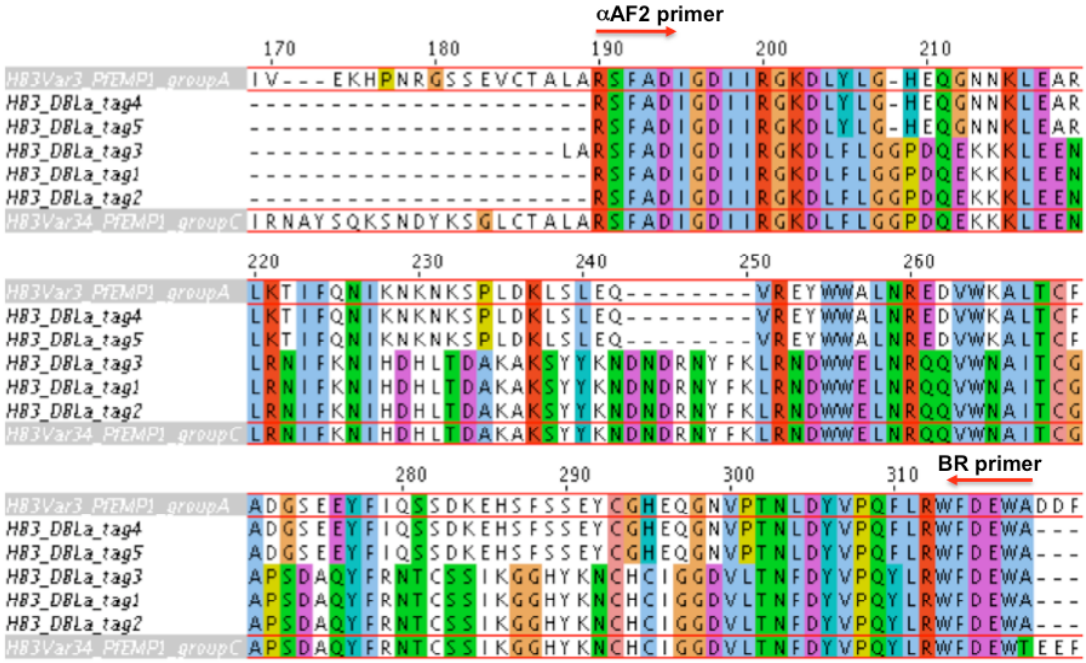


Figure 6-3. Partial protein alignment of 2 PfEMP1 sequences and 5 typical translated DBLα tags. PfEMP1 sequences "HB3var3" and "HB3var34" are outlined in red. Tags 1, 2 and 3 perfectly match HB3var34 while tags 4 and 5 match HB3var3.

6.5.1.1 *Var* gene expression profile in HB3 selections

The main change in the *var* gene expression profile after selection of HB3 parasites on HBEC-5i is the marked upregulation of *HB3var3* (Figure 6-4A). A single tag, out of 27, matched *HB3var3* in the HB3-Uns populations while there were 13 out of 25 tags in HB3-HBEC1. Thus the selection resulted in a significant 14 fold upregulation of the group A *var* gene *HB3var3* (p-value = 0.0001, Fisher's exact test).

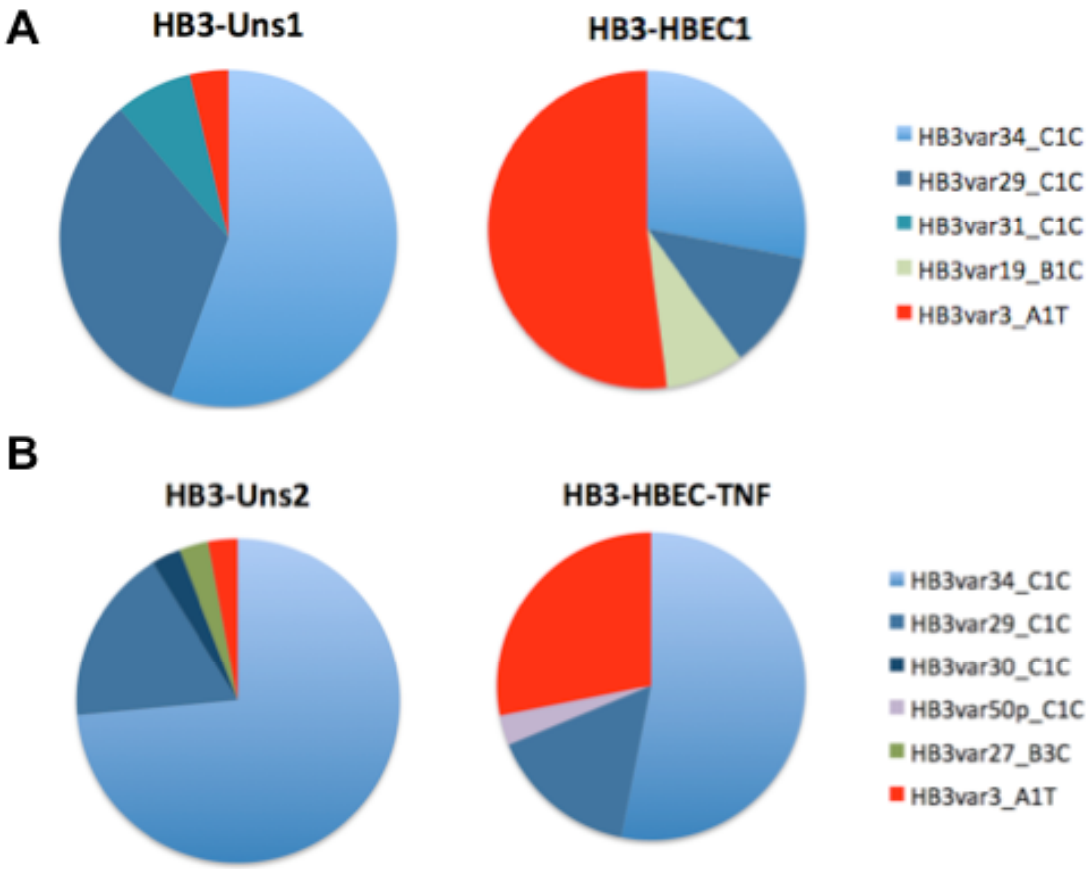


Figure 6-4. Frequencies of DBLα tags in HB3 unselected (Uns) and selected (HBEC) parasites. The pie charts represent the percentage of different DBLα *var* gene sequences detected in each parasite population by RT-PCR with universal primers. 25 to 34 transformed colonies were sequenced for each strain. Colour scheme for *var* subgroups: group A genes are in red, group B in green, group C in blue.

A similar result was obtained after the HB3 selection on HBEC-5i activated with TNF (Figure 6-4B). 9 out of 32 tags in the HB3-HBEC-TNF parasites matched *HB3var3*. This is a 10 fold increase compared to the HB3-Uns parasites (p-value = 0.0054, Fisher's exact test).

HB3-HBEC2, the parasite line derived from the second selection of HB3 for binding to HBEC-5i, was not tested, as it is already a replicate of HB3-HBEC1. Altogether, the DBLα RT-PCR *var* genes profile of HB3-HBEC1 and HB3-HBEC-TNF selections correlates well with the results from the microarray data analysis. The unselected HB3 parasites express mostly group C *var* genes while

a single group A is upregulated after selection on HBEC-5i. The activation of these cells with TNF, which induces the expression of many surface receptors (chapter 3), did not influence the *var* gene expression profile of the selected HB3 parasites, i.e. the changes in the *var* gene profile are similar to the ones found after selection on untreated HBEC-5i. Finally, these results validate the microarray data.

6.5.1.2 Var gene expression profile in 3D7 and IT selections

The microarray data also indicated a single group A *var* gene to be highly upregulated in the 3D7 selected strain: *PFD0020c*. This result is faithfully reproduced in this DBLα RT-PCR approach (Figure 6-5A). Out of 41 tags in 3D7-Uns, only one matches *PFD0020c* while 14 out of 36 tags are specific to that gene in 3D7-HBEC. Thus the selection of 3D7 on HBEC-5i resulted in a 16 fold upregulation of *PFD0020c* (p-value < 0.0001, Fisher's exact test). This upregulation is mostly at the expense of *PFF0010w*, a telomeric group B *var* gene (Figure 6-5B). *PFF0010w* was downregulated by up to 90 fold in the microarray analysis (see appendix for fold changes of all genes in the microarray data).

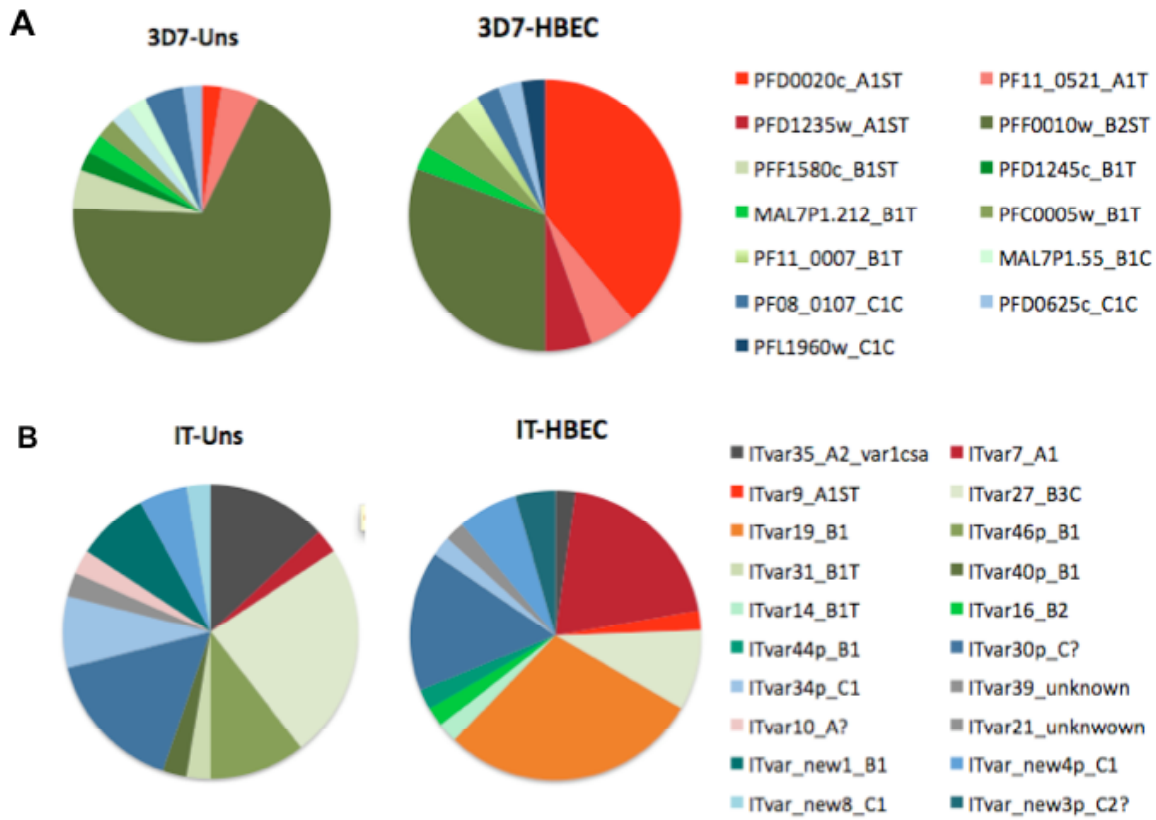


Figure 6-5. Frequencies of DBLα tags in unselected (Uns) and selected (HBEC) parasites. The pie charts represent the percentage of different DBLα *var* gene sequences detected in each parasite population by RT-PCR with universal primers. 36 to 45 transformed colonies were sequenced for each strain. Colour scheme for *var* subgroups: group A genes are in red, group B in green, group C in blue and unknown group in grey. Note that *ITvar19_B1*, a group B *var* gene but with group A-like features, is in orange.

Selection of the IT strain on HBEC-5i resulted in 2 *var* genes being upregulated (Figure 6-5B). *ITvar7* was represented by a single tag in IT-Uns (total: 38 tags) but 9 in IT-HBEC (total: 45 tags). There was no *ITvar19* tag in IT-Uns and 13 tags in IT-HBEC. Thus both *ITvar7* and *19*, part of the group A and group B subfamily, respectively, are significantly upregulated after selection on HBEC-5i (p-value = 0.0184 and 0.0001, respectively, Fisher's exact test). Note how the IT strain expresses a much wider range of *var* genes compared to HB3 (Figure 6-4).

In summary, all four pairs of DBLα RT-PCR experiments presented here confirmed the *var* gene expression profile observed with the microarray method. This adds confidence to the rest of the microarray data. It also validates the four upregulated *var* genes (*HB3var3*, *PFD0020c*, *ITvar7* and *ITvar19*) as encoding the primary ligand candidates for binding to HBEC-5i.

6.5.2 Quantitative PCR

RNA samples used for DBLα RT-PCR were also analyzed by Quantitative PCR (Q-PCR). This work was performed by our collaborators Sanne Schou and Thomas Lavstsen in Copenhagen. Q-PCR results again perfectly correlate with microarray and RT-PCR data (Table 6-1).

	Method		
	Microarray	DBLα RT-PCR	Q-PCR
HB3-HBEC	*HB3var3*	*HB3var3*	*HB3var3*
HB3-HBEC-TNF	*HB3var3*	*HB3var3*	*HB3var3*
3D7-HBEC	*PFD0020c*	*PFD0020c*	*PFD0020c*
IT-HBEC	*ITvar7* *ITvar19*	*ITvar7* *ITvar19*	*ITvar7* *ITvar19*

Table 6-1. Summary of the main *var* genes upregulated after selection on HBEC-5i.

6.5.3 HB3-HBEC-Serum parasites also transcribe *HB3var3*

All *P. falciparum* parasites selections on HBEC-5i were performed with binding medium, i.e. without serum. To show that this selection method was physiologically relevant, HB3 parasites were also selected using the exact same protocol but with the addition of 10% human pooled serum (see chapter 3 section 3.5.3.1).

The main concern was whether these selected parasites (HB3-HBEC-Serum) would express the same *var* genes as HB3-HBEC. Thus HB3-HBEC-Serum was harvested for DBLα RT-PCR to profile the *var* genes transcription. As it was observed with HB3-HBEC (Figure 6-4A), the only major change in

transcription pattern in HB3-HBEC-Serum (Figure 6-6) is the upregulation of *HB3var3*, albeit to a lesser extent (6 fold instead of 14 fold). Thus it can be safely concluded that the presence of serum or not does not have a major influence on the HBEC-5i-parasite interaction.

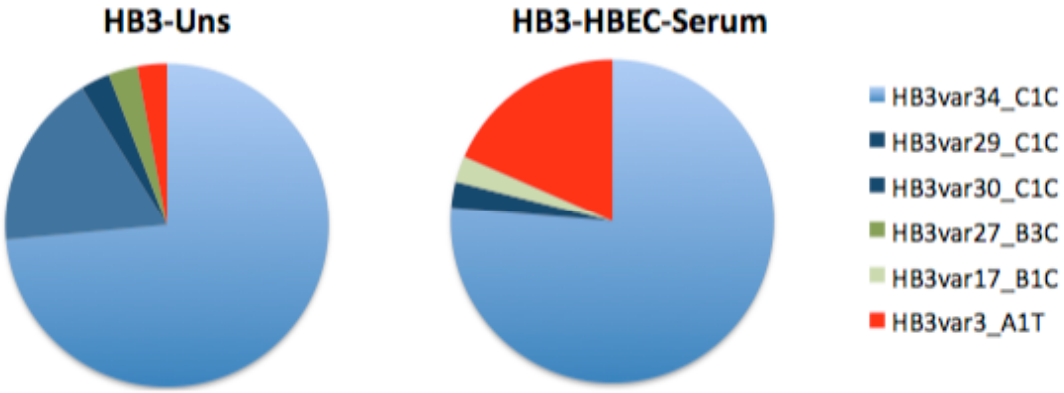


Figure 6-6. Frequencies of DBLα tags in unselected (Uns) and selected (HBEC) HB3 parasites with the addition of human serum. Pie charts represent 34 and DBLα tags from the HB3-Uns and HB3-HBEC-Serum parasites, respectively.

6.5.4 HB3 selection on Dermal and Pulmonary cells

Together, the microarray and RT-PCR experiments pointed towards the PfEMP1 variants that are the most likely to be HBEC-5i ligands. However, assuming these candidates are indeed ligands, the question of whether these PfEMP1s are *specific* to HBEC-5i has not been addressed yet. Just like placental iRBC bind to Chondroitin Sulfate A (CSA) and not other glycoaminoglycans (GAG) (Dahlback, et al.); would HB3var3, PFD0020c, ITvar7 and 19 bind to HBEC-5i only and not other type of endothelial cells? The binding assay experiments with HB3-HBEC1 on Human Pulmonary Microvascular Endothelial Cell (HPMEC) and Human Dermal Microvascular Endothelial Cell (HDMEC) already indicated that HBEC-5i

selected parasites bind to other endothelial cell types (chapter 3). However, it remained to be tested whether selecting *P. falciparum* parasites from an unselected population would result in the same *var* genes being upregulated.

HB3 parasites were selected on HPMEC and HDMEC in parallel using the exact same procedure as for the selection on HBEC-5i described in chapter 2. An unselected population (HB3-Uns3) was also grown alongside the selections. RNA was extracted from all cultures at late ring/early pigmented trophozoite stage after 4 rounds of selection. The RT-PCR was performed with the degenerate primers to DBLα domains. No genomic DNA contamination was seen (Figure 6-2B). Products were cloned and sequenced as previously described (section 6.5.1).

In HB3-HDMEC, 11 out of 34 tags match *HB3var3*, compared to a single tag (out of 34) matching the same gene in HB3-Uns (Figure 6-7). This is an 11 fold increase after selection (p-value = 0.0015, Fisher's exact test). The same trend was seen in HB3-HPMEC as 9 out of 35 tags match *HB3var3*, resulting in a 9 fold upregulation (p-value = 0.0062, Fisher's exact test). Note that in both selections as well as in HB3-Uns, the most common tag refers to *HB3var34*, a group C *var* gene that is expressed at high levels in all HB3 lines (Figure 6-4). In summary, the selection of HB3 parasites on HDMEC and HPMEC resulted in the upregulation of a single *var* variant: *HB3var3*. This is the same gene that was found upregulated after selection on HBEC-5i. It indicates that HB3var3 could be the PfEMP1 ligand binding to HBEC-5i, HDMEC and HPMEC.

Due to time constraints, 3D7 and IT were not selected on HPMEC or HDMEC.

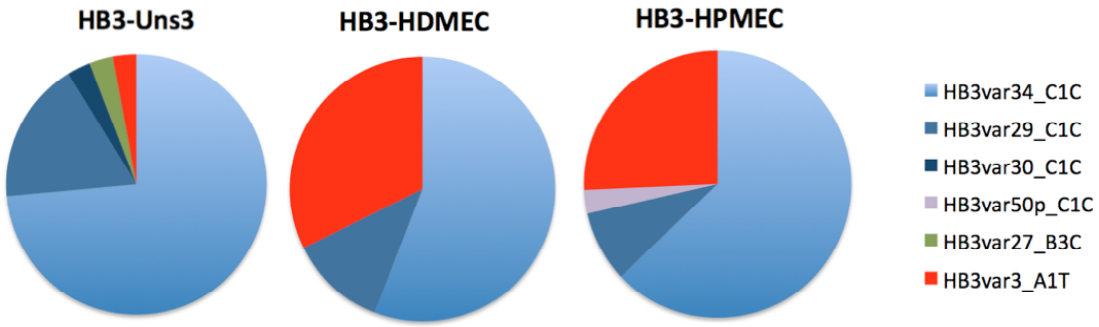


Figure 6-7. Frequencies of DBLα tags in unselected (Uns), dermal (HDMEC4) and pulmonary (HPMEC4) selected HB3 parasites. Pie charts represent 34, 34 and 35 DBLα tags from the HB3-Uns, HB3-HDMEC and HB3-HPMEC parasites, respectively.

6.5.5 Further analysis of the upregulated *var* genes

The following sections focus on various biophysical characteristics of PfEMP1, especially the four upregulated variants.

6.5.5.1 Glyosaminoglycans predicted binding motifs are found in most PfEMP1s

Endothelial cells are covered with glycosaminoglycans (GAG) that can interact with various ligands (Klein, et al., 1992, Taylor and Gallo, 2006).

Some motifs containing basic amino acid clusters (histidine, arginine and lysine) occur in proteins known to bind to heparin, a highly negatively charged GAG. One of these motifs ("XBBXBX", where B is a basic residue and X is a hydropathic residue) is found in all 4 putative "ligand" PfEMP1s (Table 6-2). However, that motif also occurs in about half of PfEMP1 variants encoded in each clone, including PfEMP1 variants that were not upregulated after binding to endothelial cells. In fact, the total number of predicted putative motifs in the PfEMP1 family is similar to what would be expected by chance (bottom part of Table 6-2). Thus, based on this sequence analysis only, there is no reason to think that the selection on HBEC-5i would have selected for PfEMP1 variants binding to GAG.

	Motif A: XBBBXXBX	Motif B: XBBXBX	Motif C: TXXBXXTBXXXTBB
HB3 (50 PfEMP1s)	1 (1 seq)	39 (22 seq)	1 (1 seq)
3D7 (62 PfEMP1s)	2 (2 seq)	45 (30 seq)	None
IT (56 PfEMP1s)	1 (1 seq)	38 (27 seq)	None
With shuffled sequences:			
HB3 (50 shuffled PfEMP1s)	*1 (1 seq)*	*30 (24 seq)*	*None*
3D7 (62 shuffled PfEMP1s)	*3 (3 seq)*	*25 (19 seq)*	*None*
IT (56 shuffled PfEMP1s)	*1 (1 seq)*	*19 (15 seq)*	*None*

Table 6-2. Numbers of predicted putative heparin binding motifs in the PfEMP1 family. Shown is the total number of motifs followed by the number of sequences with at least one motif in parenthesis. Motif B occurs twice in HB3var3 and ITvar19, once in PFD0020c and ITvar7. X = hydrophobic residue, B = basic residue, T = turn. In order to test the likelihood that these motifs may occur by chance in these large protein sequences, each PfEMP1 sequence was shuffled using ScanProSite from ExPASy (bottom part of the table, in italics). Thus numbers shown would slightly differ every time the sequences are shuffled.

6.5.5.2 CIDR1α1 domain is found in all upregulated *var* genes

With the exception of *ITvar19* (group B *var* gene, unknown chromosomal location), the other upregulated *var* genes in all selections are group A *var* genes (subtelomeric location) (Kraemer, et al., 2007). This classification was verified by alignment of the upstream regions of these genes. As expected for group A PfEMP1 variants, HB3var3, PFD0020c and ITvar7 show a DBL1α_1 domain while ITvar19 has a DBL1α_0 domain (see chapter 1 for *var* gene nomenclature). Despite its upstream region and its DBL1α_0 domain*, ITvar19* has got a couple of "group A-like features": it is large (7 domains, compared to about 4 for a typical group B gene) and has got a CIDR1α1 domain (usually only seen in group A variants). Remarkably, 5 consecutive domains of *ITvar19* are the same domain types as in *HB3var3* (Table 6-3). All four upregulated *var* genes contain CIDR1α1, DBL2β-C2, DBLγ, DBLδ, and CIDR2β type domains.

Var gene name	Upstream	Extracellular domain structure
HB3var3	A1	DBL1α1 CIDR1α1 DBL2β-C2 DBL3γ DBL4δ CIDR2β DBL5β-C2
3D7 PFD0020c	A1	DBL1α1 CIDR1α1 DBL2β-C2 DBL3γ DBL4γ DBL5δ CIDR2β
ITvar7	A1	DBL1α1 CIDR1α1 DBL2β-C2 DBL2β-C2 DBL4γ DBL5δ CIDR2β
ITvar19	B1	DBL1α CIDR1α1 DBL2β-C2 DBL3γ DBL4δ CIDR2β DBL5γ

Table 6-3. Schematic representation of the 4 upregulated *var* genes. The domains structure was defined by Kraemer *et al (Kraemer, et al., 2007)*. The only domains found in all 4 strains are: CIDR1α1, DBL2β-C2, DBLγ, DBLδ, CIDR2β.

Var gene name	Upstream	Extracellular domain structure
HB3var34	C1	DBL1α CIDR1α DBL2β-C2 DBL3γ DBL4δ CIDR2β
HB3var29	C1	DBL1α CIDR1α DBL2β CIDR2β
HB3var31	C1	DBL1α CIDR1α DBL2β CIDR2β
ITvar27	B3	DBL1α CIDR1α DBL2β-C2 DBL3γ DBL4δ CIDR2β
ITvar34	C1	DBL1α CIDR1α DBL2δ + other domains to determine
ITvar46	B1	DBL1α CIDR1α DBL2δ + other domains to determine
3D7 PFF1580c	C1	DBL1α CIDR1α DBL2β-C2 DBL3γ DBL4δ CIDR2β DBL5ε DBL6ε DBL7ε
3D7 PFF0010w	B2	DBL1α CIDR1γ DBL2β-C2 DBL3γ DBL4β DBL5ε

Table 6-4. Schematic representation of 8 "non-ligand" PfEMP1s. These *var* were downregulated after selection on HBEC-5i. It is unlikely that they are able to bind to HBEC-5i.

The upregulated *var* genes thus share many characteristics. The next question is whether there are any features that distinguish the upregulated genes (potential "ligands") from other *var* genes that were not upregulated after selection and therefore are unlikely to encode PfEMP1 ligands for HBEC-binding. For example, is there any stretch of amino acids that would be found in these "ligand" sequences only and could mediate the interaction with HBEC-5i? The first difficulty in answering that question lies in the lack of good negative controls. It is not known whether the other group A PfEMP1 variants are unable to bind to HBEC5i or whether they simply were not expressed in the unselected parasites and thus could not be upregulated. However at least 8 *var* genes, from group B and C, were downregulated after selection (Table 6-4). Thus they can confidently be called "non-ligands" for HBEC5i-binding. An interesting feature found in many ligands and non-ligands is the chain of DBL2β-C2-DBL3γ-DBL4δ-CIDR2beta domains, making it unlikely for these 4 domains to be of crucial importance for the specificity of binding onto HBEC-5i. Thus the only domain that is uniquely found in the "ligands" group is CIDR1α1. Unlike CIDR1α, CIDR1α1 is unable to bind to CD36 (Robinson, et al., 2003). It is particularly interesting because it is uncommonly found in *var* genes. Out of 160 var genes (3D7 + IT + HB3), only 16 show a CIDR1α1 domain. All 4 upregulated *var* genes harbour a CIDR1α1 domain, thus the occurrence of CIDR1α1 domains in the upregulated var gene occurs more frequently than would be expected by chance given their frequency in the genome (χ^2 test, *p-value < 0.001*). Note also that non-ligand PFF0010w shows a CIDR1γ domain (Table 6-4), thus it seems that a CIDR1α1 domain is a prerequisite for *var* gene to be upregulated after selection, as opposed to just a lack of CIDR1α domain.

6.5.5.3 Upregulated CIDR1α1 domains are basic

Although there is no obvious difference between "ligand" and "non-ligand" PfEMP1 sequences, the analysis with each domain taken individually reveals a much lower isoelectric point (pI) for the CIDR1α (pI = 5.0) compared to CIDR1α1 domains (pI = 7.7) (Table 6-5). Thus at physiological pH, CIDR1α1 will be positively charged and CIDR1α highly negatively charged. Electrostatic

interactions are known to play a role in many adhesion processes (for example (Chou, et al., 2010)). Therefore this may indicate that group A or group A-like PfEMP1s are binding to a negatively charged receptor.

The 4 CIDR1α1 domains also appear to be more conserved with each other (average identity score: 48%) than CIDR1α domains (average identity score: 34%). This difference in conservation does not appear with the DBL1α domains for example (52% for DBL1α ligands compared to 51% for non-ligands).

	Full length PfEMP1		**CIDR1 only**	
	Average of the 4 ligands	Average of 8 non-ligands	**CIDR1α1** Average of the 4 ligands	**CIDR1α** Average of 7 non-ligands
Isoelectric point	6.27	5.80	7.72	4.98
Amino acids (a.a.)	3105	2361	425	481
Negative a.a. (D + E)	518 (17%)	394 (17%)	65 (15%)	99 (21%)
Positive a.a. (K + R)	494 (16%)	354 (15%)	70 (16%)	72 (15%)
Cysteines	122 (4%)	83 (4%)	19.5 (5%)	17 (4%)

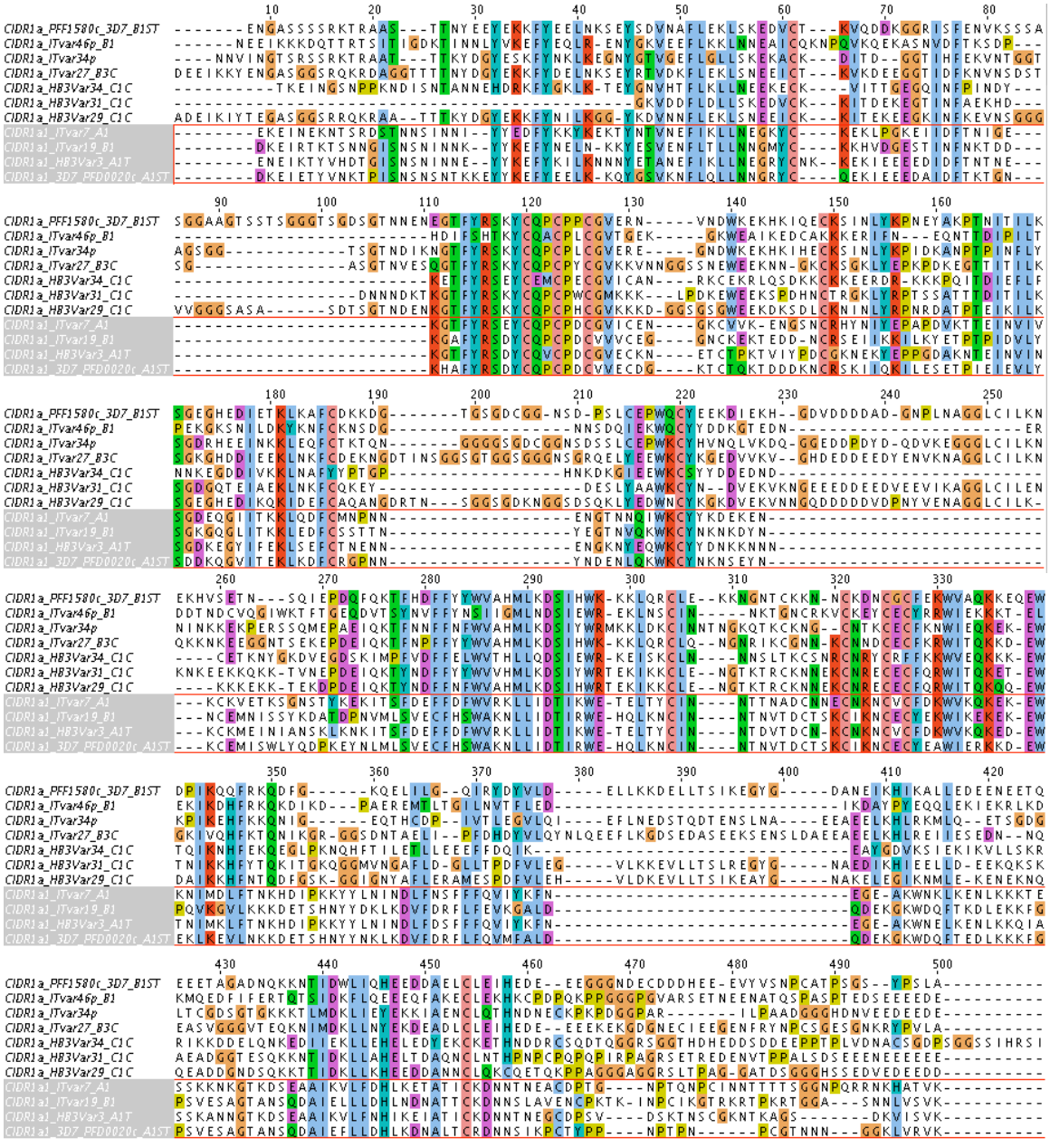
Table 6-5. Biophysical characteristics of ligand and non-ligand PfEMP1s. The isoelectric point is shown, as well as the numbers of negatively and positively charged amino acids and cysteine residues, with the relative percentage in parenthesis. The analysis for the CIDR1 domains includes the 7 CIDR1α non-ligand domains shown in **Table 6-4** and not the CIDR1γ domain.

6.5.5.4 No obvious motif distinguishes CIDR "ligand" to "non-ligand" domains

If the CIDR1α1 domain does confer upon PfEMP1 variants the ability to bind to HBEC-5i, the next obvious question is whether these sequences harbour any conserved motif. Both CIDR1α and CIDR1α1 are characterized by high variability between sequences and only a few amino acids differentiate a CIDR1α from a CIDR1α1 domain (Robinson, et al., 2003). The hypothesis, albeit somewhat unlikely, is that some "ligand" CIDR1α1 domains could show a unique stretch of amino acids, not found in CIDR1α domains.

An alignment of 7 "non-ligand" CIDR1α and the 4 "ligand" CIDR1α1 domains is shown in Figure 6-8. There is no motif longer than 2 amino acids

uniquely found in CIDR1α1 “ligands”. Motifs that differentiate a CIDR1α1 from a CIDR1α domain include a “KW” and a “LK” motif uniquely found in CIDR1α1 (Robinson, et al., 2003). The lack of these motifs and the surrounding region are thought to be important for binding to CD36 (Gamain, et al., 2001, Robinson, et al., 2003).



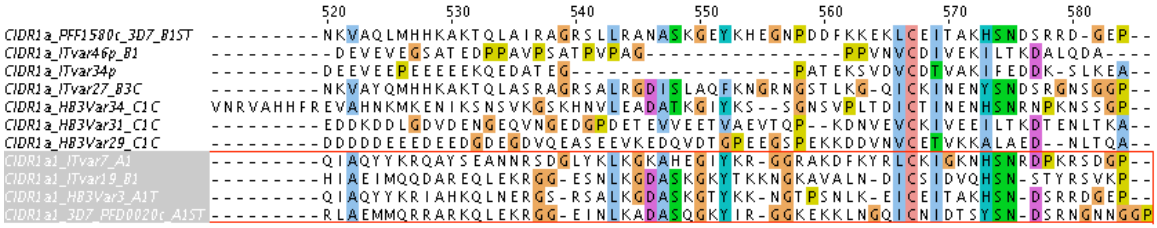


Figure 6-8. Alignment of 7 CIDR1α "non-ligand" and 4 CIDR1α1 "ligand". Domain boundaries were defined in (Smith, et al., 2000b). CIDR1α1 domains from the 4 ligand candidate PfEMP1s are outlined in red. There is no stretch of more than 2 amino acids unique to CIDRα1 domains .

The motif discovery tool MEME is used to identify statistically over-represented motifs in a given set of sequences (Bailey and Elkan, 1994). Our dataset of "ligand" and "non-ligand" is however relatively small and cannot be directly analysed with MEME as the data consists of two different domains types (CIDR1α and CIDR1α1). In other words, MEME would detect motifs that are specific to the CIDR1α and to the CIDR1α1 domain, rather than motif that would be unique to binding domains. It is possible that the few differences ("KW" and "LK") in sequences between the two domain types confer the binding ability of PfEMP1 to HBEC-5i. If this hypothesis were true, all PfEMP1s harbouring a CIDR1α1 domain would be capable of cytoadherence. Assuming PfEMP1 is indeed the ligand binding to HBEC-5i, more experiments should be done to pinpoint the exact amino acid region mediating the binding to HBEC-5i.

Taking all of the above analysis together, we hypothesise that the CIDR1α_1 domain of the upregulated PfEMP1 variants may have a functional role in adhesion to brain endothelial cells. Further experiments to test this hypothesis are discussed in section 6.6.3.2.

6.6 Discussion

The RT-PCR data presented in this chapter validated the microarray results as the same *var* genes (*HB3var3*, *PFD0020c*, *ITvar7* and *ITvar19*) were found highly upregulated. The only domain in common to all 4 PfEMP1 "ligands" is CIDR1α1.

Finally, the HB3 parasite selection on HDMEC and HPMEC indicates that these putative ligands are not specific to HBEC-5i but may also possibly mediate binding to other endothelial cell types.

The following sections discuss each finding in detail in the context of other relevant studies, and outline the further experiments required to test whether the PfEMP1 variants identified here are the parasite ligands for HBEC5i binding.

6.6.1 Limitations of the DBLα RT-PCR approach

The DBLα RT-PCR method has some limitations. The original study using the universal primers on genomic 3D7 DNA sequenced 140 tags and only found 45 different DBLα tags (out of 61 possibilities) (Taylor, et al., 2000a). However the primers were a slightly different version to those currently in use (Bull, et al., 2005). Normark *et al* sequenced 272 DBLα tags from 3D7 genomic DNA (gDNA) and could only amplify 39 *var* genes (Normark, et al., 2007). Nevertheless, a direct comparison between this technique and real-time RT-PCR found that the results were generally in good agreement (Gatton, et al., 2006). Thus, although the method will easily detect the change of *var* gene expression in two parasite populations, it might miss out one or more *var* genes that would not be amplified by the universal primers. In this thesis, both the microarray and the qRT-PCR experiments showed virtually identical results to the RT-PCR method. This adds confidence to the RT-PCR results obtained with the selected parasite lines used in this work.

Note that one recent study analysed the *var* transcriptome of 3D7 by real-time PCR and RT-PCR with universal primers. They found a high discrepancy between the results of the two methods (Golnitz, et al., 2008). They conclude on the unreliability of the universal primers, however without further analysis it is not possible to differentiate which method is accurate.

6.6.2 HB3var3 is the main ligand candidate binding to HBEC-5i, HDMEC and HPMEC

The DBLα RT-PCR using universal primers is a fundamentally different approach from the microarray analysis. For example, the RT-PCR amplifies the

cDNA while the microarray does not. Importantly, both methods point to the same results in terms of *var* gene expression. Therefore it can safely be concluded that the selection on HBEC-5i has enriched for a population of parasites transcribing group A (or group-A like in IT-HBEC) *var* genes. This is in concordance with the current hypothesis that group A *var* genes are associated with severe malaria and more specifically cerebral malaria (Kyriacou, et al., 2006, Normark, et al., 2007, Tembo and Montgomery, 2010, Warimwe, et al., 2009).

HB3 parasites were also selected on human primary cell lines extracted from the microvasculature of the dermis and the lungs (HDMEC and HPMEC). A microarray analysis was not performed on the two selected lines (HB3-HDMEC and HB3-HPMEC), but the RT-PCR method showed *HB3var3* to be the only upregulated *var* gene after selection. This and the fact that HB3-HBEC1, but not HB3-Uns, binds to HPMEC and HDMEC (chapter 3), indicate that the PfEMP1 variant encoded by *HB3var3* is the main ligand candidate for all three cell lines (HBEC-5i, HDMEC and HPMEC). It implies that HB3var3 variant would not specifically bind to HBEC-5i.

This result does not render our cerebral malaria *in vitro* model any less valid. All cerebral malaria postmortem studies have found sequestration in other organs, often at high level (Genrich, et al., 2007, MacPherson, et al., 1985, Montgomery, et al., 2006, Nakazawa, et al., 1995, Pongponratn, et al., 1991, Pongponratn, et al., 2003, Seydel, et al., 2006, Wilairatana, et al., 2000). Thus the same parasite ligand may bind to various locations in the human body, possibly even to the same receptor. Whether *P. falciparum* parasites use the same ligand molecules to attach to endothelial cells *in vivo* and *in vitro* of course remains to be tested.

6.6.3 The role of group A PfEMP1 and CIDR1α1 in severe malaria

6.6.3.1 Group A *var* gene expression is associated with cerebral malaria

The use of the DBLα RT-PCR universal primers has allowed researchers to analyse the *var* gene transcriptional profiles of field isolates. As the upstream

sequence of these expressed *var* genes cannot be known from the DBLα tags, the DBL1α/DBL1α_1 distinction is used instead, because the vast majority of group B and C *var* genes show a DBL1α (also called DBL1α_0) domain, while group A genes have a DBL1α_1 domain. Interestingly, the expression of DBL1α_1 domain has been repeatedly associated with severe malaria (Kirchgatter and Portillo Hdel, 2002, Kyriacou, et al., 2006, Normark, et al., 2007, Warimwe, et al., 2009). Other studies however did not find this association (Bull, et al., 2005, Kaestli, et al., 2006, Kalmbach, et al., 2010, Rottmann, et al., 2006). Discrepancy in these results may be attributed to the differences in disease classification and/or geographical differences (see also chapter 7 for a detailed discussion on group A *var* genes). In all our selections, a group A *var* gene (and a group A-like in IT-HBEC) is found highly expressed. Our *in vitro* model tallies with the current hypothesis that group A *var* gene expression is linked to cerebral malaria (Kyriacou, et al., 2006).

Recently, publications based on the DBLα RT-PCR universal primers have subdivided the DBLα domains according to the presence or absence of two mutually-exclusive motifs: REY and MFK (Bull, et al., 2005, Bull, et al., 2007, Warimwe, et al., 2009). The MFK motif is only found in the DBL1α domain of group A PfEMP1s but not all of them, while the REY motif can be found in any type of PfEMP1. However they have never been found together in the same gene. Interestingly, REY has been associated with severe anaemia and MFK with impaired consciousness (Warimwe, et al., 2009). HB3var3 has got a REY motif, PFD0020c a MFK motif and the upregulated IT PfEMP1s neither. Our dataset of PfEMP1 sequences is obviously too small to investigate whether there is any correlation between the MFK/REY genotype and the binding to HBEC-5i phenotype.

6.6.3.2 CIDR1α1 domains are commonly recognized by human semi-immune serum

CIDR1α1 is the only domain found in common to all 4 upregulated *var* genes, belonging to the group A or group A-like subgroup. Unfortunately it is not possible to tell whether other, non-upregulated, group A *var* genes could act as

cytoadherence ligands or not. Indeed, if the gene encoding a potential HBEC-5i ligand was not expressed at all in the unselected population, the selection would not increase its expression. Note for example that *PFD0020c* in 3D7-Uns and *HB3var3* in HB3-Uns were the only group A *var* genes detected by RT-PCR. Therefore genes that are not upregulated after selection cannot be confidently classified as "non-ligands". This renders the identification of a putative motif in common to all upregulated *var* genes (like CIDR1α1) difficult due to the lack of good "negative control".

If the CIDR1α1 domain is indeed directly involved in binding to HBEC-5i, which remains to be proven, it is possible that patients immune to cerebral malaria would develop antibodies against these domains. The interaction of 3D7 PfEMP1 variants with human sera has been reported in at least three studies. (1) Selection of 3D7 parasites with semi-immune serum from malaria endemic area leads to the enrichment of PfEMP1 PFD1235w (Jensen, et al., 2004a). Although this is a different group A PfEMP1 from the one found in 3D7-HBEC, PFD1235w also has got a CIDR1α1 domain. (2) A study tested the recognition of 20 recombinant 3D7 PfEMP1 domains with serum from endemic areas (Joergensen, et al., 2007). The antibody response of each serum sample was analysed by ELISA on the recombinant PfEMP1 domains (DBL and CIDR of various subtypes). PfEMP1 grouping (A, B or C) could not predict the recognition (i.e. the binding of an antibody to the recombinant domain) by the immune sera. However, I noticed that the CIDR1α1 domain (from PFD1235w) is significantly better recognized than the CIDR1α or CIDR1γ domains in high transmissions areas (Joergensen, et al., 2007). (3) Furthermore, a larger study analyzed 42 3D7 PfEMP1 recombinant domains with over one thousand serum samples from areas of various malaria endemicity (Cham, et al., 2009). Again, the amount of antibodies from the serum samples binding to each recombinant domain was measured. The serum recognition data indicated that natural antibodies to CIDR are acquired faster than to DBL domains (Cham, et al., 2009). Interestingly, out of 16 CIDR domains tested, the most recognized one is a CIDR1α1 (63% of individuals had antibodies binding to the CIDR1α1 domain of PF11_0521). In summary, all studies published to date are consistent with the

hypothesis that children rapidly acquire anti-CIDR1α1 antibodies. Whether these antibodies would protect against cerebral malaria remains to be tested.
To our knowledge, the interaction between PfEMP1s domains from the HB3 or IT clone and human serum has never been studied.

Ideally, assuming the upregulated *var* genes are indeed the ligands binding to HBEC-5i, one would try to identify common motifs in all ligand sequences. If these amino acids turn out to be essential for mediating this interaction, they could in theory be used as a target for a PfEMP1-based vaccine to prevent cerebral malaria. According to our hypothesis, antibodies would block the sequestration of parasites expressing CIDR1α1 domains in the brain microvasculature. A similar approach is currently being developed on Var2csa as this PfEMP1 variant is well-conserved in all *P. falciparum* isolates and it is necessary for binding to CSA in the placenta (reviewed in (Tuikue Ndam and Deloron, 2008)). It is however too early to know whether a similar approach could be used with cerebral malaria. Currently the main drawback is the lack of known conserved region. Our dataset of PfEMP1 "ligands" is too small to hypothesize on which amino acid motifs would be crucial for the binding to HBEC-5i. This issue resembles more the CD36-PfEMP1 interaction, where thousands of PfEMP1 variants are thought to be able to cytoadhere to the receptor and yet no clear sequence consensus can be identified among all ligands (Ge and Elghetany, 2005, Robinson, et al., 2003).

6.6.3.3 Future work

Data presented here has only focused on the transcription levels of putative ligands. Although there is a general correlation between abundance of mRNA and protein in *P. falciparum* (Le Roch, et al., 2004, Wang, et al., 2010), it will be necessary to prove that HB3var3, PFD0020c, ITvar7 and 19 proteins are indeed expressed in HBEC-selected parasites but also located at the iRBC surface. This can be tested for HB3-HBEC with antibodies specific to the DBLα1 and CIDR1α1 domains of HB3var3 currently being developed by Ash Ghumra (Rowe group). Antibodies to PFD0020c (DBL and CIDR domains) are also available (Sanne Schou, Copenhagen). They will be used to test HB3var3 and PFD0020c proteins

expression in HB3-HBEC and 3D7-HBEC parasites by Western Blot. A band should be seen in the protein lysate from these parasites but no band, or a weak band, should be obtained with unselected parasites. Antibodies should also react with these PfEMP1 ligand candidates in an immunofluoresence assay on live selected iRBC, indicating their surface expression.

These antibodies could also be attached to beads and used to select new parasites (similar experiment as (Jensen, et al., 2004a)). These parasites should in turn show a greater binding to HBEC-5i than the unselected population, further indicating that the upregulatd *var* genes were indeed the ligands.

In summary, both the microarray and RT-PCR methods identified 4 *var* genes that are the main ligand candidates for cytoadherence to HBEC-5i, but also HDMEC and HPMEC. The main common feature to these 4 sequences is the CIDR1α1 domain. Although more experiments are obviously needed, we hypothesize that this domain is crucial for binding to an unknown receptor on microvascular endothelial cells.

7 Chapter VII: Conclusion

The general aim of this thesis was to identify the protagonists involved in the interaction between the *P. falciparum* parasites and the human brain microvascular endothelial cell line (HBEC-5i) (Figure 7-1). To answer these questions, three *P. falciparum* strains (HB3, 3D7 and IT/FCR3) were successfully selected for cytoadherence to HBEC-5i. This change of phenotype also led to a significant reduction in platelet-mediated clumping as well as a large increase in binding to primary cell lines (HBMEC, HDMEC and HPMEC). The rosetting frequency however remained the same.

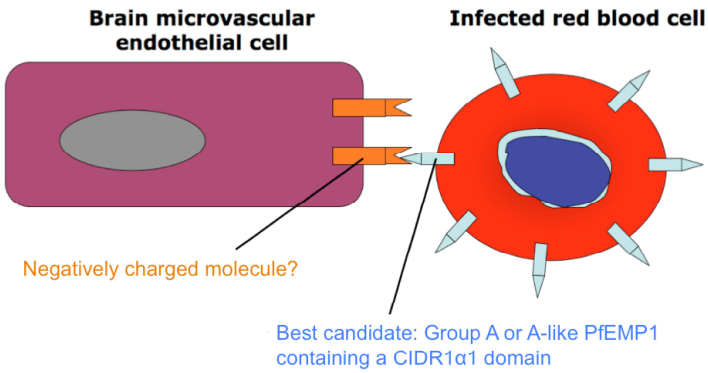


Figure 7-1. Model of the *P. falciparum* iRBC and HBEC-5i interaction.

The question as to the identity of the host receptor was investigated by using a combination of static binding assays on soluble molecules as well as binding inhibition assays on HBEC-5i with various antibodies and receptors. Although a definite receptor has not been identified, preliminary data indicate that selected HB3 and IT parasites (HB3-HBEC and IT-HBEC, respectively) bind significantly better than unselected parasites to the immobilised soluble receptors Integrin αV and gC1qR. This interaction may however be unspecific. Interestingly, heparin blocks binding while NCAM and Integrin antibodies somewhat reduce it. Curdlan Sulphate and heparin-like compounds, all known to inhibit rosetting, also show anti-cytoadhesion activity even at low concentrations. As Integrin αV and gC1qR are predicted to carry a net negative

charge and heparin is highly negatively charged, these data may indicate that *P. falciparum* parasites are binding to a negatively charged receptor on HBEC-5i.

The question of the *P. falciparum* ligand was investigated by comparing the transcriptome of selected and unselected parasites by microarray analysis. A clear-cut result, later validated by RT-PCR, was observed in all strains: *HB3var3*, *3D7_PFD0020c*, *ITvar7* and *ITvar19* were highly upregulated (11 to over 100 fold) in HB3-HBEC, 3D7-HBEC and IT-HBEC selected parasites, respectively. As no other gene was so consistently and highly transcribed, PfEMP1 antigens encoded by these genes are the main ligand candidates for cytoadhesion to HBEC-5i (Figure 7-1). *HB3var3*, *3D7_PFD0020c and ITvar7* belong to the group A subfamily while *ITvar19* is a group B *var* gene but with group A-like features (chapter 6). The activation of HBEC-5i with TNF prior to each round of selection with HB3 parasites also resulted in *HB3var3* being the main ligand candidate. The *rif* genes *HB3_RifA_256_6* and *3D7rif_PFD0025w* located "head to head" with the upregulated *var* genes were also expressed at a higher level (16 to 18 fold) in HB3-HBEC, HB3-HBEC-TNF and 3D7-HBEC than in unselected parasites. This coregulation of group A *var* genes and their adjacent *rif* genes had been previously reported (Tham, et al., 2007, Wang, et al., 2009b) and may indicate a common way of transcription activation (Howitt, et al., 2009). The microarray approach also revealed many other genes upregulated in all selections, including genes encoding proteins predicted to be exported (e.g. MAHRP-1 and PF14_0752 (PHISTa)). These proteins could also be involved in cytoadherence, directly or indirectly, for example in the trafficking of PfEMP1 to the iRBC surface. Finally, HB3 parasites selected for cytoadherence to HDMEC and HPMEC also showed upregulation of *HB3var3*. Assuming PfEMP1 is indeed the ligand, these results indicate that HB3var3 would not bind specifically to HBEC-5i only. The implications of these findings within the current knowledge about cerebral malaria are discussed below.

7.1 The elusive HBEC-5i receptor

How do *P. falciparum* iRBC bind to the microvascular endothelium? Decades of research on sequestration have identified over a dozen host receptor

candidates, yet none show significant binding to parasites isolated from cerebral malaria patients or show polymorphisms associated with protection from the disease (chapter 1 and (Rowe, et al., 2009a)). The *in vitro* model developed in this thesis should, in theory, shed light on the characterization of the receptor.

ICAM1 is often cited as the main receptor candidate involved in cerebral malaria. In this work, although ICAM1 is strongly expressed on the surface of HBEC-5i, several pieces of evidence indicate that it is not the receptor for HBEC-selected parasites: (1) HB3-HBEC, unlike the ICAM-selected line A4, does not bind to recombinant ICAM1 in a static assay; (2) two anti-ICAM1 antibodies do not block adhesion of HB3-HBEC to HBEC-5i; (3) A4 parasites only poorly adhere to HBEC-5i or HBMEC; (4) IT-HBEC express *ITvar7* and *19* which have been shown to be ICAM1 non-binders (Howell, et al., 2008).

A4 and HB3-Uns parasites bind to ICAM1 and CD36, respectively (chapter 3). The fact that these parasites show very little binding to any endothelial cell line may seem surprising as ICAM1 and CD36 are found at the surface of these cells (except for CD36 on HBEC-5i). However, the adhesion of A4 and HB3-Uns was tested on a static binding assay on isolated receptors. The total amount of ICAM1 or CD36 proteins on the surface of endothelial cells might be much lower than what was used in those assays (25 µg/ml). Also, it has to be remembered that the surface of endothelial cells is covered with the glycocalyx, consisting of proteoglycans, glycoproteins and glycosaminoglycan (GAG) (Bartlett and Park, 2010, Reitsma, et al., 2007). Numerous GAG - ligand proteins interactions have been described (Delehedde, et al., 2001). Thus it is possible that, although ICAM1 and CD36 are surface exposed on the cultured cell lines, they are "not available" for binding to iRBC. The glycocalyx would "mask" them and prevent the interaction with the appropriate PfEMP1. This hypothesis will be tested using various enzymes (heparinase, hyaluronidase, chondroitinase ABC, neuraminidase) in order to cleave parts of the glycocalyx.

Anti-NCAM and anti-Integrin antibodies, and to a larger extent soluble heparin, did reduce the binding of HB3-HBEC to HBEC-5i. Due to time constraints, the binding inhibition assays were not repeated enough times to

conclusively determine the extent of the inhibitory effect. However, taking the three receptor identification approaches together (static binding assays, binding inhibition assays with soluble molecules and antibodies), it seems that none of the "usual suspects" was directly involved in the adhesion of selected parasites. This indicates that a novel host surface molecule that has never been linked with malaria may act as a parasite receptor. As HB3-HBEC bind slightly better to the negatively charged proteins gC1qR and Integrin αV, and because the highly negatively charged molecule heparin blocks the adhesion to HBEC-5i, these data point towards an electrostatic based interaction with selected parasites. This correlates with the fact that the selection on endothelial cells results in parasites expressing *var* genes with positively charged CIDR domains.

It is important to emphasize that neither this study nor any other publication has investigated the full repertoire of endothelial cell receptors for their propensity to adhere to iRBC. In other words, only about 15 receptors out of hundreds of endothelial cells surface molecules have been studied in the context of malaria (Rowe, et al., 2009a). It is thus plausible that the receptor mediating the cytoadherence of iRBC in cerebral malaria cases has yet to be discovered. In fact, a non-exhaustive PubMed search reveals that various pathogens attach to at least 10 HBMEC surface receptors, which, to our knowledge, have never been tested for cytoadherence to *P. falciparum* (Table 7-1).

Pathogen	**Ligand protein**	**HBMEC receptor**	**Reference**
E. coli K1	OmpA	**Ec-gp96**	(Shin, et al., 2005)
	IbeA(Ibe10)	Unknown	(Huang, et al., 2001)
	IbeA	**Vimentin**	(Zou, et al., 2006)
	IbeB	Unknown	(Huang, et al., 1999)
	IbeT	Unknown	(Zou, et al., 2008)
	CNF1	**67LR**	(Kim, et al., 2005)
	FimH	**CD48**	(Khan, et al., 2007)
Streptococcus agalactiae	Lmb	**Laminin**	(Tenenbaum, et al., 2007)
	ScpB	**Fibronectin**	(Beckmann, et al., 2002)
	FbsA	**Fibrinogen**	(Tenenbaum, et al., 2005)

Neisseria meningitidis	MspA	Unknown	(Turner, et al., 2006)
	Opc	**Integrin α5β1**	(Unkmeir, et al., 2002)
Balamuthia mandrillaris	Galactose Binding Protein	**Galactose**	(Matin, et al., 2007)
Cronobacter sakazakii	OmpA	**Fibronectin**	(Nair, et al., 2009)
Babesia bovis	VESA1 (>300 members)	Unknown	(Al-Khedery and Allred, 2006)
Cryptococcus neoformansi	HA	**CD44**	(Jong, et al., 2008)
Measles virus	Unknown?	**CD46**	(Andres, et al., 2003)
Polio Virus	Unknown?	**PVR** (CD155)	(Coyne, et al., 2007)
	gp140, SDF-1	**CXCR4**	(Mendu, et al., 2007)

Table 7-1. List of known interactions between pathogen ligands and human brain microvascular endothelial cell (HBMEC) receptors.

This illustrates the need to apply a more comprehensive approach to endothelial cells receptor identification. One possibility is to use the parasite ligand as a probe that would bind to biotinylated HBEC-5i surface receptors ((Zou, et al., 2006) detailed in chapter 3, section 1.6.9). The molecule bound to the ligand (i.e. the receptor candidate) is identified by mass spectrometry. Assuming PfEMP1 is the ligand, a recombinant domain of that protein, like CIDR1α1, would be used. Alternatively, the full-length PfEMP1 molecules could be attached to beads coated with an anti-ATS antibody (ATS being the C-terminal intracellular part of the protein, relatively well conserved in all PfEMP1 variants). This technique demonstrated the interaction with P-selectin (Senczuk, et al., 2001).

7.2 Group A or group A-like PfEMP1 are the main ligand candidates

The strong upregulation of group A or group A-like *var* genes found in all selected parasites is consistent with many observations from chapter 3:

(1) **HBEC-selected parasites do not form rosettes**. Although rosetting is thought to be a phenotype mediated by group A *var* genes, the upregulated *var* variants (*HB3var3* and *ITvar7* and *19*) are different from the genes expressed in rosetting parasites (*HB3var6* and *ITvar60* and *ITvar9*) ((Rowe, et al., 1997) and Rowe group, unpublished data).

(2) **HBEC-selected parasites and CD36 adhesion**. Microarray, DBLα and quantitative RT-PCR methods all show some expression of group B and C *var* genes, even in the HBEC-5i selected populations. This explains why HB3-HBEC selected parasites bind to CD36 on a static binding assay (chapter 3). Some parasites within the HB3-HBEC population (almost half of them according to the DBLα RT-PCR data) express *var* variants that are predicted to bind to CD36 via their CIDR1α domain. Even if the percentage of parasites expressing group B and C is lower in HB3-HBEC, it is likely that the high amount of binding to CD36 is due to these unselected parasites among the HB3-HBEC population. A "re-binding assay" of HBEC-5i bound parasites detached and added to CD36 would settle the issue.

(3) **HBEC-selected parasites reduce their platelet-mediated clumping frequency**. This is a related explanation as above because clumping is thought to be mainly CD36 mediated ((Pain, et al., 2001) and Arman, unpublished data). Unlike binding assay experiments, the platelet-mediated clumping assay results in a ratio of clumping and non-clumping parasites. This ratio is reduced (i.e. less clumps) in HBEC-selected parasites which is consistent with the upregulation of group A *var* genes (CD36 non-binders). In other words, all strains of HBEC-selected parasites upregulate *var* genes containing a CIDR1α1 domain, which does not confer the ability to bind to CD36, hence correlating with the reduction of platelet-mediated clumping.

(4) **HBEC-selected parasites lose their phenotype over time**. Assuming PfEMP1 is indeed the ligand, this could be explained by the switching of group A *var* genes back to a group B or C *var* as in the unselected population. To test this hypothesis, a HBEC-selected line could be cultured for a few weeks without any further selection while recording the change of binding ability to HBEC-5i and *var* gene transcription over time. One would then expect to observe a correlation between the ratio of group A *var* genes transcribed and the cytoadherence to endothelial cells.

Although group A or group A-like *var* genes are the primary ligand candidates, the microarray analysis revealed that many other genes might also be implicated. The "head to head" *rif* genes found upregulated in HB3-HBEC and 3D7-HBEC do not necessarily mean they are ligand candidates as they could have been transcribed by the same activation factor (assuming there is one) that activated *HB3var3* and *PFD0020c* (Howitt, et al., 2009). *PF14_0752* (PHISTa), the most highly upregulated non-VSA gene in common to all strains, is the best target for a follow-up study. In the first instance, the gene could be disrupted by using a knockout strategy as it was performed on many other Pexel proteins (Maier, et al., 2008). Note that an antibody to PF14_0752 would not necessarily block the cytoadhesion to HBEC-5i if the function of this protein is carried out within the iRBC (e.g. trafficking of PfEMP1 within the RBC cytosol). Other genes potentially involved in cytoadherence and plans for future experiments can be found in chapter 5.

7.3 HBEC-5i and group A var genes, a model for cerebral malaria?

Although there is still much controversy about the variant surface antigens (VSA) involved in cerebral malaria (see chapter 1 section 1.5 and chapter 6 section 6.6.3), the majority of studies addressing the question have found an association between group A *var* gene expression in field isolates and severe or cerebral malaria (Jensen, et al., 2004a, Kirchgatter and Portillo Hdel, 2002, Kyriacou, et al., 2006, Normark, et al., 2007, Warimwe, et al., 2009). The disparity in results probably illustrates the complexity of the disease and the multitude of components implicated. It is therefore quite clear that, if group A PfEMP1 were indeed necessary for causing cerebral malaria, they would certainly not be the only factor. It is also possible that the current *var* gene classification into group A, B and C does not represent the actual pathogenesis effect of these antigens. Note that studies linking group A *var* gene expression with severe/cerebral malaria have done so using the DBLα RT-PCR universal primers. Thus only about a thirtieth of the *var* mRNA is sequenced and analysed via this method. It is possible that the crucial amino acids associated with

cerebral malaria lay in another domain, for example the CIDR1α1, which would be missed using the DBLα primers. The future of *var* genes transcriptional studies in field isolates may reside in second generation sequencing techniques which could sequence the entire mRNA product (Otto, et al., 2010).

Importantly, the upregulation of group A (or A-like) *var* genes seen in our *in vitro* model resembles what is thought to happen in cerebral malaria cases. This is also, with the selection of parasites using semi-immune serum from children (Jensen, et al., 2004a) and the selection for rosetting (Rowe group, unpublished data), a novel way of selecting parasites for their group A *var* gene expression. However, the selection of HB3 on HDMEC and HPMEC also upregulated the expression of *HB3var3* (chapter 6). This does not render our cerebral malaria model any less valid. Indeed, postmortem studies of cerebral malaria cases consistently find sequestered parasites in other organs (Genrich, et al., 2007, MacPherson, et al., 1985, Montgomery, et al., 2006, Nakazawa, et al., 1995, Pongponratn, et al., 1991, Pongponratn, et al., 2003, Seydel, et al., 2006, Wilairatana, et al., 2000) (see also Table 1-3 in chapter 1). Therefore the same parasite ligand(s) may be used for sequestration in various tissues. The ultimate question remains whether *P. falciparum* iRBC are binding to the same receptor *in vivo* as they do *in vitro* on HBEC-5i. In order to investigate that question it is of course necessary to identify the HBEC-5i receptor first.

7.4 Future work

To determine whether PfEMP1 is indeed the ligand binding to HBEC-5i, specific antibodies will be used to detect surface expression and test their blocking abilities (see discussion of chapter 6). In addition, the selection could be repeated with the PfEMP1 mutant line DC-J. This transgenic line expresses a *var* gene in which the PfEMP1 coding region has been replaced by a drug selectable marker leading to the silencing of all other *var* genes in the *P. falciparum* genome (Dzikowski, et al., 2006b). Thus parasites cultured without drug (PfEMP1 expressed) should be selectable on HBEC-5i while parasites cultured in the presence of the drug would not cytoadhere (PfEMP1 not expressed).

In order to validate this sequestration model, it is essential to test the cytoadherence of field isolates on HBEC-5i. Two hypotheses will be tested: do field isolates sampled from cerebral malaria patients bind better to HBEC-5i (and other endothelial cell lines) than isolates from uncomplicated malaria? And are parasites expressing *var* genes with a CIDR1α1 domain more likely to bind than isolates expressing other types of CIDR domains? These experiments could be coupled with rosetting and platelet-mediated clumping assays.

Equally important would be to test the anti-cytoadherence activity of semi-immune and immune sera. Ideally, one would want to perform a binding inhibition assays with serum from acute and convalescent cerebral malaria patients. This could assess whether the disease led to the production of anti-cytoadherence antibodies. Similar experiments in Thailand and Malawi with field isolates binding to melanoma cells showed that sera had some anti-cytoadherence property but that was very strain-specific (Goldring, et al., 1992, Singh, et al., 1988).

All binding assays performed here should also be repeated under flow conditions as it is more physiologically relevant (see for example (Ho, et al., 1998, Serirom, et al., 2003)).

The significance of CIDR1α1 domains could be experimented by testing the recognition of the recombinant domains (Ash Ghumra, unpublished data) with sera from cerebral and non-cerebral malaria cases (very similar experiment as (Cham, et al., 2009)).

Skin biopsies are potentially a new approach to study sequestration (Nakano, et al., 1996, Nakazawa, et al., 1995). Although they would not be a model for cerebral malaria directly, they offer the possibility to investigate binding of *P. falciparum* iRBC to human endothelial cells *ex vivo* by, for example, characterisation of the *var* gene expression pattern of sequestered parasites.

7.5 Could the immense sequence diversity of group A PfEMP1 be a vaccine target?

The very basic principle that antibodies to DBL and CIDR domains of PfEMP1 can confer some immunity to malaria has been shown in monkeys (Baruch, et al., 2002, Chen, et al., 2004, Moll, et al., 2007). By far the most likely PfEMP1-based vaccine candidate today is Var2csa as it is fairly conserved among all *P. falciparum* strains (reviewed in (Tuikue Ndam and Deloron, 2008)) (see also section 1.5.1 in chapter 1). To develop a Var2csa-based vaccine, researchers are trying to define epitopes that are both conserved among clones and that would inhibit iRBC adhesion to CSA (Hviid, 2010). This vaccine would protect specifically against pregnancy-associated malaria by mimicking the immunity acquired by multigravid women. Here one wants to identify an antigen, conserved in most *P. falciparum* strains, which would elicit antibodies preventing cerebral malaria.

As detailed in section 1.5 in chapter 1, children living in malaria endemic areas tend to quickly develop protection against VSA associated with severe malaria (VSA_{SM}). One current hypothesis is that group A PfEMP1 represent these VSA_{SM} (Tembo and Montgomery, 2010). Their expression would dominate in young patients with little pre-existing immunity and cause severe disease (Hviid, 2010). Even if antibodies to group A PfEMP1 can be proven to confer immunity to severe malaria (and cerebral malaria in particular), this subset of *var* genes still represent an enormous diversity of sequence, rendering the development of a vaccine based on these antigens challenging. On the other hand, despite the sequence diversity, many variants bind to the same receptor, for example group B and C PfEMP1s binding to CD36. This may indicate that the conformation of each PfEMP1 is conserved, allowing the attachment to the receptor. Thus, if the precise molecular mechanism mediating the iRBC adhesion to endothelial cells can be decoded, then one would have, in principle, found a vaccine target. This idea is being applied to the development of a vaccine against antigens conserved in most Streptococci (reviewed in (Steer, et al., 2009)).

Finally, one piece of evidence is important to keep in mind: children in endemic areas almost never develop cerebral malaria more than once (Snow, et al., 1993); i.e. a single episode is enough to generate immunity to the disease. Again, if one can pinpoint how the immune system develops this protection, then a vaccine against cerebral malaria is feasible.

Abracadabra.

8 Appendix

8.1 Perl scripts

Summary of the principal custom made Perl scripts:

Program name	**Description**
Program3b.pl	Parse the output file from HMMer to get the coordinates of sequences
Program6b.pl	With the output file from "Program3b.pl", it returns the actual protein sequences.
Program7a.pl	Search for the exon 1 in a list of full length *var* genes. If the exon boundary is different from the typical *var* gene, the output will be blank.
Program7b.pl	Similar to Program7a.pl but for exon 2 of *var* genes.
Program7c.pl	Search for exon 1 and 2 in *rif* genes.
Program8c.pl	From a file with fasta format sequences, it returns the headers only (i.e. the gene/protein sequences are erased).
Program10.pl	Search for the start (i.e. the first Methionine) of each protein sequence. Note: there is a bug if the start of the sequence is missing due to a supercontig too short.
Program11a.pl	With a list of fasta format headers with coordinates (output from Program8c.pl), it returns the appropriate DNA sequence.
Program11_ups.pl	Similar to Program11a.pl but it returns the 500bp upstream of the start codon.
Program15.pl	Similar to Program3b.pl. With an output file from OligoRankPick, it returns a fasta format list of oligos.

The scripts can be found in the file "Perl scripts.doc" on the attached CD (see last page of this thesis).

8.2 Extracted VSA sequences

Here are indicated coordinates of all VSA sequences extracted with HMMer.

The GeneID indicates on which supercontig and on which frame the translated sequence is found. For example "HB3var_1.8_6" is a *var*/PfEMP1 sequence found in the HB3 genome on supercontig 1.8 on frame 6. The start and end coordinates are indicated in order to retrieve the protein sequence from that supercontig. Also shown is the length of the protein as well as the E-value score from the HMMer analysis. If more than one VSA sequence is found on the same supercontig, a letter ("a", "b"…) is added to differentiate between VSA sequences.

8.2.1 PfEMP1 sequences

8.2.1.1 HB3 PfEMP1 sequences

Gene ID - Start - End - Length - E-value					Gene ID - Start – End – Length - E-value				
HB3var_1.8_6	4709	7084	2376	0	HB3var_1.183_6	4170	5870	1701	0
HB3var_1.47_1	25695	27419	1725	0	HB3var_1.193_2	3783	5803	2021	0
HB3var_1.47_1	15994	17683	1690	0	HB3var_1.200_6	6017	7737	1721	0
HB3var_1.47_2	11483	14002	2520	0	HB3var_1.203_6	1104	2878	1775	0
HB3var_1.47_3	30566	32308	1743	0	HB3var_1.220_5	7744	9962	2218	0
HB3var_1.47_5	18752	21780	3029	0	HB3var_1.226_6	3936	5715	1780	0
HB3var_1.54_1	8064	10493	2430	0	HB3var_1.243_5	2758	5518	2761	0
HB3var_1.54_2a	25123	26879	1757	0	HB3var_1.245_4	1	2420	2420	0
HB3var_1.54_2b	17842	20474	2633	0	HB3var_1.105_3	8471	10263	1793	0
HB3var_1.54_3	14191	16707	2517	0	HB3var_1.138_2	6091	8466	2376	0
HB3var_1.88_2	9845	11526	1682	0	HB3var_1.142_5	15395	17220	1826	0
HB3var_1.88_4	8994	11991	2998	0	HB3var_1.226_5	7014	9786	2773	0
HB3var_1.96_2	9404	11154	1751	0	HB3var_1.253_6	1006	4378	3372	0
HB3var_1.100_1	8985	10765	1781	0	HB3var_1.265_2	4341	7268	2928	0
HB3var_1.100_1	14092	15883	1792	0	HB3var_1.54_1	2316	4734	2418	0
HB3var_1.100_3	19217	21026	1810	0	HB3var_1.114_4	10620	12428	1809	0
HB3var_1.118_1	8687	11038	2352	0	HB3var_1.243_6	1	1616	1616	0
HB3var_1.125_4	9417	12002	2586	0	HB3var_1.189_4	8275	10206	1931	0
HB3var_1.130_1	12026	14524	2499	0	HB3var_1.368_1	2735	4848	2110	1e-60
HB3var_1.142_6	7194	8970	1777	0	HB3var_1.463_6	2	999	998	4e-124
HB3var_1.142_6b	10131	12721	2591	0	HB3var_1.508_3	1	745	745	2e-13
HB3var_1.144_5	11864	13670	1807	0	HB3var_1.528_5	1	663	663	7e-22
HB3var_1.153_4	10187	13051	2865	0	HB3var_1.529_4	1	675	675	4e-20
HB3var_1.168_5	5030	7553	2524	0					

8.2.1.2 Dd2 PfEMP1 sequences

Gene ID - Start - End - Length - E-value					Gene ID - Start – End – Length - E-value				
Dd2var_1.2_3	23290	25630	2341	0	Dd2var_1.35_1	1692	4376	2683	0
Dd2var_1.2_4	17029	19643	2616	0	Dd2var_1.35_4	7642	9380	1739	0
Dd2var_1.2_5a	7689	10285	2598	0	Dd2var_1.37_6	8571	11837	3267	0
Dd2var_1.2_5b	1151	2914	1763	0	Dd2var_1.48_3	9696	12645	2953	0
Dd2var_1.2_5c	21269	24064	2797	0	Dd2var_1.54_6	7629	10382	2754	0
Dd2var_1.2_6	11462	13658	2197	0	Dd2var_1.58_6	7585	9296	1707	0
Dd2var_1.5_3	3701	6922	3225	0	Dd2var_1.64_4	7353	9951	2595	0
Dd2var_1.6_2	10097	13285	3189	0	Dd2var_1.80_2	7613	10773	3159	0
Dd2var_1.9_1	16783	18846	2063	0	Dd2var_1.93_2	4098	5798	1687	0
Dd2var_1.10_1	17710	20682	2972	0	Dd2var_1.93_4	1645	4374	2728	0
Dd2var_1.13_4	9974	12748	2776	0	Dd2var_1.187_3	5648	7877	2228	0
Dd2var_1.14_3	1704	4218	2515	0	Dd2var_1.193_2	1271	3045	1770	0
Dd2var_1.14_6	12323	14766	2436	0	Dd2var_1.208_2	1193	3029	1823	0
Dd2var_1.17_5	10661	12372	1712	0	Dd2var_1.208_3	5814	7552	1729	0
Dd2var_1.19_2	9876	11935	2060	0	Dd2var_1.218_1	3403	5602	2200	0
Dd2var_1.21_3	14301	16568	2268	0	Dd2var_1.274_4	3424	5829	2400	0
Dd2var_1.25_4	12032	14418	2373	0	Dd2var_1.308_1	2044	3814	1771	0
Dd2var_1.26_4	6333	8113	1782	0	Dd2var_1.339_4	2891	4605	1711	0
Dd2var_1.26_5	10311	12002	1682	0	Dd2var_1.344_4	2124	4521	2398	0
Dd2var_1.26_6	2575	4353	1779	0	Dd2var_1.394_3	1329	3509	2181	0

8.2.1.3 IT PfEMP1 sequences

As mentioned in the main text, IT *var* genes were published by Kraemer *et al* 2007. When the Sanger Institute released a new version of the IT genome, the HMMer approach was used to extract 8 "new" *var* sequences. Also, I was able to complete 7 truncated *var* sequences from the Kraemer *et al* study.(Afonso Nogueira, et al., 2002)

"new" *var* sequences (i.e. not mentioned in the Kraemer *et al* 2007 publication)

New PfEMP1 sequences	Status (gene/pseudogene)	Gene ID - Start – End – Length - E-value			
ITvar_NEW1	Gene	0000000_4c_NEW10	5598	7590	1993
ITvar_NEW2	Gene	0002160_5a_NEW20	8913	10731	1819
ITvar_NEW3p	Truncated	0002160_5c6_NEW3 6798	8131	1333	2.6e-227
ITvar_NEW4p	Pseudogene	0002047_456_NEW4p	477	3000	2523
ITvar_NEW5p	Pseudogene	0000093_5_SHORT	2045	2596	551
ITvar_NEW6p	Truncated	0002173_23_NEW6p	2261	4858	2598
ITvar_NEW7	Gene	0002013_1_NEW7 4208	5875	1668	0
ITvar_NEW8	Gene	0000093_4_NEW8 5518	7233	1716	0

"Elongated" *var* sequences from the Kraemer *et al* 2007 publication

Kraemer *et al* name	New status (gene/pseudogene)	Gene ID - Start – End – Length - E-value
ITvar10	Gene	0000033_3 2339 5254 2916 0
ITvar23p	Gene	0002012_2 5554 7370 1878 0
ITvar58p	Pseudogene	0002012_31 798 2676 1879 1.4e-130
ITvar30p	Start truncated	0002011_1 4060 5751 1692 0
ITvar46p	Gene	0002157_6 3895 6654 2760 0
ITvar51p	Gene	0000000_6 10423 12281 1923 0
ITvar34p	Gene	0002011_3 9162 10952 1791 0

Here under is the subgrouping of *var* genes (A, B or C) not indicated in the Kraemer *et al* study. This is based on upstream sequences alignment as described in Lavstsen *et al* 2003.

Var name	**Probable var group**
NEW1	B1
NEW2	B1
NEW3p	C2?
NEW4p	C1
NEW5p	C1
NEW6p	C1
NEW7	B1
NEW8	C1
10_Elong	A(?)
58p_Elong	B3
30p_Elong	C???
51p_Elong	C1
34p_Elong	C1
Var6	B1
Var21	B (2?)

8.2.2 Rifin sequences

8.2.2.1 3D7 Re-annotated Rifin sequences 3D7

I re-annotated the Rifin family as part of the PlasmoDB reannotation effort, using the same HMMer approach described in this manuscript.

For the *rif* family, 8 genes had their annotation modified, 23 had their sequence modified and 2 'new' *rif* sequences were found (both pseudogenes). When the sequence was modified, the new coordinates are indicated in the last 2 columns.

Gene ID	Genomic location from PlasmoDB	Product Description from PlasmoDB	Pseudo/gene	Sequence modified?	Type (A or B)	Start Coordinate	End Coordinate
PFA0010c	MAL1: 39,205 - 40,430 (-)	RIFIN	gene	no	A		
PFA0020w	MAL1: 50,586 - 51,859 (+)	RIFIN	gene	no	A		
PFA0030c	MAL1: 54,001 - 55,229 (-)	RIFIN	gene	no	B		
PFA0040w	MAL1: 60,005 - 61,236 (+)	RIFIN	gene	no	A		
PFA0045c	MAL1: 62,420 - 63,633 (-)	RIFIN	gene	no	A		
PFA0050c	MAL1: 66,050 - 67,222 (-)	RIFIN	gene	no	A		
PFA0080c	MAL1: 81,998 - 83,339 (-)	RIFIN	gene	no	A		
PFA0095c	MAL1: 90,475 - 91,653 (-)	RIFIN	gene	no	B		
PFA0710c	MAL1: 565,425 - 566,564 (-)	RIFIN	pseudo	**yes**	B	565,425	566,599
PFA0740w	MAL1: 593,569 - 594,907 (+)	RIFIN	gene	no	A		
PFA0745w	MAL1: 596,822 - 597,993 (+)	RIFIN	gene	no	B		
PFA0760w	MAL1: 605,882 - 607,251 (+)	RIFIN	gene	no	A		
PF10_0002	MAL10: 38,051 - 39,004 (-)	RIFIN	gene	**yes**	A	38,444	39,397
PF10_0003	MAL10: 41,774 - 42,964 (-)	RIFIN	gene	no	B		
PF10_0004	MAL10: 44,817 - 46,134 (-)	RIFIN	gene	no	A		
PF10_0005	MAL10: 48,053 - 50,279 (-)	RIFIN	gene	no	A		

PF10_0006	MAL10: 51,350 - 52,600 (-)	RIFIN	gene	no	B		
PF10_0393	MAL10: 1,606,689 - 1,607,866 (+)	RIFIN	gene	no	A		
PF10_0394	MAL10: 1,609,724 - 1,610,778 (+)	RIFIN	gene	no	B		
PF10_0396	MAL10: 1,615,852 - 1,617,211 (+)	RIFIN	gene	no	A		
PF10_0397	MAL10: 1,619,319 - 1,620,524 (+)	RIFIN	gene	no	B		
PF10_0398	MAL10: 1,622,593 - 1,623,859 (+)	RIFIN	gene	no	A		
PF10_0399	MAL10: 1,625,875 - 1,627,033 (+)	RIFIN	gene	no	B		
PF10_0400	MAL10: 1,629,157 - 1,630,473 (+)	RIFIN	gene	no	A		
PF10_0401	MAL10: 1,632,561 - 1,633,613 (+)	RIFIN	**pseudo**	**yes**	B	1,632,561	1,633,652
PF10_0402	MAL10: 1,635,703 - 1,636,812 (+)	RIFIN	gene	no	B		
PF10_0403	MAL10: 1,639,187 - 1,640,454 (+)	RIFIN	gene	no	A		
PF10_0404	MAL10: 1,642,385 - 1,643,568 (+)	RIFIN	gene	no	B		
PF10_0405	MAL10: 1,645,960 - 1,647,307 (+)	RIFIN	gene	no	A		
PF11_0009	MAL11: 45,056 - 46,233 (+)	RIFIN	gene	no	A		
PF11_0010	MAL11: 48,112 - 49,307 (+)	RIFIN	gene	no	A		
PF11_0011	MAL11: 51,623 - 52,751 (-)	RIFIN	gene	no	A		
PF11_0529	MAL11: 66,686 - 67,965 (-)	RIFIN	gene	no	A		
PF11_0020	MAL11: 70,081 - 71,289 (-)	RIFIN	gene	no	B		
PF11_0021	MAL11: 73,244 - 74,442 (-)	RIFIN	gene	no	A		
PF11_0022	MAL11: 76,820 - 78,000 (-)	RIFIN pseudogene	pseudo	no	A		
PF11_0515	MAL11: 2,003,616 - 2,004,739 (+)	RIFIN	gene	no	B		
PF11_0517	MAL11: 2,010,297 - 2,011,226 (+)	RIFIN	gene	**yes**	A	2,009,898	2,011,226
PF11_0518	MAL11: 2,012,562 - 2,013,419 (-)	RIFIN pseudogene	pseudo	no	B		
PF11_0519	MAL11: 2,015,624 - 2,016,877 (-)	RIFIN	gene	no	A		
PF11_0520	MAL11: 2,018,764 - 2,019,944 (-)	RIFIN	gene	no	A		
PFL0010c	MAL12: 26,321 - 27,687 (-)	RIFIN	gene	no	A		
PFL0015c	MAL12: 30,078 - 31,261 (-)	RIFIN	gene	no	B		
PFL0025c	MAL12: 43,800 - 45,106 (-)	RIFIN	gene	no	A		
PFL1965w	MAL12: 1,728,762 - 1,729,754 (+)	RIFIN pseudogene	pseudo	**yes**	A	1,728,762	1,729,994
PFL2580w	MAL12: 2,188,743 - 2,189,593 (+)	RIFIN, pseudogene	pseudo	no	?		
PFL2585c	MAL12: 2,190,466 - 2,191,753 (-)	RIFIN	**pseudo**	**yes**	A	2,190,498	2,191,753

PFL2605w	MAL12: 2,201,478 - 2,202,669 (+)	RIFIN	gene	no	B		
PFL2615w	MAL12: 2,207,813 - 2,209,098 (+)	RIFIN	gene	no	A		
PFL2625w	MAL12: 2,214,654 - 2,216,002 (+)	RIFIN	gene	no	A		
PFL2630w	MAL12: 2,218,435 - 2,219,516 (+)	RIFIN	**pseudo**	yes	B?	2,218,435	2,219,531
PFL2640c	MAL12: 2,224,980 - 2,226,184 (-)	RIFIN	gene	no	A		
PFL2645c	MAL12: 2,228,615 - 2,229,723 (-)	RIFIN	gene	no	A		
PFL2655w	MAL12: 2,234,583 - 2,235,775 (+)	RIFIN	gene	no	B		
PFL2660w	MAL12: 2,238,193 - 2,239,400 (+)	RIFIN	gene	no	A		
MAL13P1.2	MAL13: 30,708 - 31,984 (-)	RIFIN	gene	no	A		
PF13_0004	MAL13: 47,686 - 48,872 (+)	RIFIN	gene	no	A		
PF13_0005	MAL13: 50,765 - 51,960 (+)	RIFIN	gene	no	A		
PF13_0006	MAL13: 54,170 - 55,362 (-)	RIFIN	gene	no	B		
MAL13P1.4	MAL13: 57,212 - 58,525 (-)	RIFIN	gene	no	A		
MAL13P1.8	MAL13: 65,651 - 66,919 (-)	RIF pseudogene	pseudo	**yes**	A		
MAL13P1.495	MAL13: 2,828,796 - 2,830,233 (+)	RIFIN	**pseudo**	**yes**	B	2,828,373	2,830,272
MAL13P1.500	MAL13: 2,832,373 - 2,833,648 (+)	RIFIN	gene	no	A		
MAL13P1.515	MAL13: 2,841,133 - 2,842,372 (+)	RIFIN	gene	no	A		
MAL13P1.520	MAL13: 2,844,073 - 2,845,298 (-)	RIFIN	gene	no	A		
MAL13P1.530	MAL13: 2,850,118 - 2,851,348 (+)	RIFIN	gene	no	B		
MAL13P1.535	MAL13: 2,853,801 - 2,855,163 (+)	RIFIN	gene	no	A		
PF14_0002	MAL14: 7,209 - 8,539 (-)	RIFIN	gene	no	A		
PF14_0003	MAL14: 10,975 - 12,118 (-)	RIFIN	gene	no	B		
PF14_0004	MAL14: 14,127 - 15,364 (-)	RIFIN	gene	no	A		
PF14_0005	MAL14: 17,470 - 18,809 (-)	RIFIN	gene	no	B		
PF14_0006	MAL14: 20,898 - 22,233 (-)	RIFIN	gene	no	A		
PF14_0008	MAL14: 27,322 - 28,429 (-)	RIFIN	gene	no	B		
PF14_0766	MAL14: 3,265,206 - 3,266,447 (+)	RIFIN	gene	no	B		
PF14_0768	MAL14: 3,271,971 - 3,272,918 (+)	RIFIN	gene	**yes**	B	3,271,648	3,272,918
PF14_0769	MAL14: 3,275,300 - 3,276,571 (+)	RIFIN	gene	no	A		
PF14_0770	MAL14: 3,278,570 - 3,279,732 (+)	RIFIN	gene	no	B		
PF14_0772	MAL14: 3,284,970 - 3,286,073 (+)	RIFIN	gene	no	A		

PFB0015c	MAL2: 33,030 - 34,259 (-)	rifin	gene	no	A		
PFB0030c	MAL2: 41,515 - 42,858 (-)	rifin	gene	no	A		
PFB0035c	MAL2: 45,286 - 46,800 (-)	rifin	gene	no	A		
PFB0040c	MAL2: 48,923 - 50,147 (-)	rifin	gene	no	A		
PFB0055c	MAL2: 57,344 - 58,421 (-)	rifin	gene	no	B		
PFB0060w	MAL2: 63,157 - 64,376 (+)	rifin	gene	no	A		
PFB1000w	MAL2: 886,915 - 887,802 (+)	rifin	gene	no	A		
PFB1005w	MAL2: 889,660 - 890,745 (+)	rifin	gene	no	B		
PFB1010w	MAL2: 892,856 - 894,206 (+)	rifin	gene	no	A		
PFB1015w	MAL2: 896,226 - 897,420 (+)	rifin	gene	no	B		
PFB1035w	MAL2: 904,346 - 905,775 (+)	rifin	gene	no	A		
PFB1040w	MAL2: 907,678 - 908,861 (+)	rifin	gene	no	B		
PFB1050w	MAL2: 913,244 - 914,457 (+)	rifin	gene	no	A		
PFC0010c	MAL3: 43,045 - 44,255 (-)	RIFIN	gene	no	A		
PFC0030c	MAL3: 52,066 - 53,260 (-)	RIFIN	gene	no	B		
PFC0035w	MAL3: 58,103 - 59,390 (+)	RIFIN	gene	no	A		
PFC0040w	MAL3: 61,248 - 62,459 (+)	RIFIN	gene	no	A		
PFC0045w	MAL3: 64,604 - 65,508 (+)	RIFIN-like protein	pseudo	no	?		
PFC1095w	MAL3: 1,012,465 - 1,013,612 (+)	RIFIN (3D7-rifT3-5)	gene	no	A		
PFC1100w	MAL3: 1,015,544 - 1,016,643 (+)	RIFIN	gene	no	B		
PFC1115w	MAL3: 1,024,241 - 1,025,599 (+)	RIFIN (3D7-rifT3-7)	gene	no	A		
PFD0015c	MAL4: 48,479 - 49,821 (-)	RIFIN	gene	no	A		
PFD0025w	MAL4: 66,083 - 67,386 (+)	RIFIN	gene	no	A		
PFD0030c	MAL4: 69,551 - 70,923 (-)	RIFIN	gene	no	A		
PFD0040c	MAL4: 76,408 - 77,560 (-)	RIFIN	gene	no	A		
PFD0045c	MAL4: 79,715 - 80,787 (-)	RIFIN	gene	no	B?		
PFD0050w	MAL4: 85,640 - 86,898 (+)	RIFIN	gene	no	A		
PFD0055w	MAL4: 88,694 - 90,022 (+)	RIFIN	gene	no	A		
PFD0060w	MAL4: 91,844 - 93,055 (+)	RIFIN	gene	no	A		
PFD0070c	MAL4: 99,023 - 100,256 (-)	RIFIN	gene	no	?		

PFD0120w	MAL4: 162,335 - 163,442 (+)	RIF pseudogene, RIFIN pseudogene	pseudo	no	A		
PFD0134c	MAL4: 168,969 - 169,472 (-)	RIF pseudogene, RIFIN pseudogene	pseudo	**yes**	A	169,969	170,182
PFD0135c	MAL4: 169,474 - 170,188 (-)	RIFIN, truncated	pseudo	**yes**	A	168,972	170,188
PFD0595c	MAL4: 566,507 - 567,535 (-)	RIFIN, truncated	pseudo	**yes**	A	566,285	567,535
PFD0640c	MAL4: 610,149 - 611,439 (-)	RIFIN	gene	no	A		
PFD0645w	MAL4: 616,138 - 617,416 (+)	RIFIN	gene	no	A		
PFD1010w	MAL4: 971,526 - 972,712 (+)	RIFIN	gene	no	B		
PFD1020c	MAL4: 986,508 - 987,434 (-)	RIFIN	gene	no	A		
PFD1200w	MAL4: 1,152,896 - 1,153,810 (+)	RIF pseudogene, RIFIN pseudogene	pseudo	no	A		
PFD1230c	MAL4: 1,156,126 - 1,157,255 (-)	RIFIN	gene	no	A		
PFD1240w	MAL4: 1,173,602 - 1,174,806 (+)	RIFIN	gene	no	A		
PFE0015c	MAL5: 29,923 - 30,963 (-)	RIF pseudogene, RIFIN pseudogene	pseudo	**yes**	B	29,779	30,963
PFE0020c	MAL5: 33,056 - 34,378 (-)	RIFIN	gene	no	A		
PFE0025c	MAL5: 36,464 - 37,576 (-)	RIFIN	gene	no	B?		
PFE0035c	MAL5: 41,129 - 41,403 (-)	RIF pseudogene, RIFIN pseudogene	pseudo rif??	no	?		
PFE1630w	MAL5: 1,326,240 - 1,327,424 (+)	RIFIN	gene	no	B		
PFE1635w	MAL5: 1,329,844 - 1,330,623 (+)	RIF pseudogene, RIFIN pseudogene	pseudo	**yes**	A	1,329,667	1,330,623
PFF0015c	MAL6: 15,065 - 16,410 (-)	RIFIN	gene	no	A		
PFF0025w	MAL6: 26,557 - 27,830 (+)	RIFIN	gene	no	A		
PFF0035c	MAL6: 31,965 - 33,244 (-)	RIFIN	gene	no	A		
PFF0040c	MAL6: 35,355 - 36,613 (-)	RIFIN pseudogene	**gene**	no	B		
PFF0045c	MAL6: 38,721 - 39,781 (-)	RIFIN pseudogene	pseudo	no	B		
PFF0855c	MAL6: 741,266 - 742,403 (-)	RIFIN	gene	no	A		
PFF1540w	MAL6: 1,326,982 - 1,327,947 (+)	RIFIN pseudogene	pseudo	**yes**	A	1,326,625	1,327,011
PFF1545w	MAL6: 1,329,498 - 1,330,966 (+)	RIFIN	gene	no	B		
PFF1555w	MAL6: 1,336,149 - 1,337,476 (+)	RIFIN	gene	no	A		

PFF1560c	MAL6: 1,338,221 - 1,339,420 (-)	RIFIN	gene	no	A		
PFF1565c	MAL6: 1,341,310 - 1,342,598 (-)	RIFIN	gene	no	A		
PFF1570w	MAL6: 1,347,344 - 1,348,574 (+)	RIFIN	gene	no	B		
PFF1575w	MAL6: 1,350,727 - 1,352,090 (+)	RIFIN	gene	no	A		
PFF1585w	MAL6: 1,367,913 - 1,369,105 (+)	RIFIN pseudogene	pseudo	no	B		
PFF1590w	MAL6: 1,371,502 - 1,372,862 (+)	RIFIN	gene	no	A		
MAL7P1.213	MAL7: 40,190 - 41,426 (-)	RIFIN	gene	no	A		
MAL7P1.215	MAL7: 45,987 - 47,238 (-)	RIFIN	gene	no	B		
MAL7P1.216	MAL7: 52,046 - 53,305 (+)	RIFIN	gene	no	A		
MAL7P1.217	MAL7: 55,331 - 56,518 (-)	RIFIN	gene	no	A		
MAL7P1.219	MAL7: 61,826 - 62,909 (-)	RIFIN	gene	no	B		
MAL7P1.222	MAL7: 70,256 - 71,400 (+)	RIFIN	gene	no	A		
MAL7P1.226	MAL7: 86,390 - 87,344 (+)	RIFIN, pseudogene	pseudo	**yes**	A (?)	86,084	87,359
MAL7P1.200	MAL7: 117,721 - 118,781 (-)	RIFIN	**pseudo**	no	B		
PF07_0003	MAL7: 131,296 - 132,433 (-)	RIFIN	gene	no	A		
MAL7P1.43	MAL7: 580,492 - 581,700 (-)	RIF pseudogene, RIFIN pseudogene	pseudo	**yes**	A	580,434	581,700
MAL7P1.47	MAL7: 595,723 - 596,949 (-)	RIF pseudogene, RIFIN pseudogene	pseudo	**yes**	A	596,949	596,921
MAL7P1.52	MAL7: 618,286 - 619,540 (-)	RIF pseudogene, RIFIN pseudogene	pseudo	no	A		
MAL7P1.57	MAL7: 657,521 - 658,761 (+)	RIFIN	gene	no	A		
PF07_0132	MAL7: 1,446,089 - 1,447,421 (+)	RIFIN	gene	no	A		
MAL7P1.184	MAL7: 1,451,815 - 1,453,017 (-)	RIFIN	gene	no	A		
PF07_0134	MAL7: 1,454,830 - 1,456,060 (-)	RIFIN	gene	no	A		
MAL7P1.185	MAL7: 1,458,001 - 1,459,356 (-)	RIFIN	gene	no	A		
PF07_0136	MAL7: 1,464,159 - 1,465,352 (+)	RIFIN	gene	no	B		
PF07_0138	MAL7: 1,469,812 - 1,471,061 (+)	RIFIN	gene	no	A		
PF08_0139	MAL8: 53,767 - 55,102 (-)	RIFIN	gene	no	A		
PF08_0138	MAL8: 57,476 - 58,827 (-)	RIFIN	gene	no	A		
PF08_0105	MAL8: 451,736 - 453,020 (+)	RIFIN	gene	no	A		

PF08_0104	MAL8: 454,924 - 456,040 (+)	RIFIN	gene	no	A		
MAL8P1.208	MAL8: 1,362,683 - 1,364,025 (+)	RIFIN	gene	no	A		
MAL8P1.218	MAL8: 1,384,737 - 1,385,956 (+)	RIFIN	gene	no	A		
MAL8P1.219	MAL8: 1,388,272 - 1,389,444 (-)	RIFIN	gene	no	A		
PFI0010c	MAL9: 29,797 - 31,157 (-)	RIFIN	gene	no	A		
PFI0015c	MAL9: 33,553 - 34,795 (-)	RIFIN	gene	no	B		
PFI0020w	MAL9: 39,554 - 40,740 (+)	RIFIN	gene	no	A		
PFI0025c	MAL9: 42,909 - 44,045 (-)	RIFIN	gene	no	B		
PFI0030c	MAL9: 45,902 - 47,236 (-)	RIFIN	gene	no	A		
PFI0035c	MAL9: 49,612 - 50,971 (-)	RIFIN	gene	no	A		
PFI0050c	MAL9: 58,162 - 59,240 (-)	RIFIN	gene	no	B?		
PFI0055c	MAL9: 61,342 - 62,553 (-)	RIFIN	**pseudo**	**yes**	A	61,285	62,553
PFI0065w	MAL9: 67,334 - 68,625 (+)	RIFIN	gene	no	A		
PFI0070w	MAL9: 70,521 - 71,738 (+)	RIFIN	gene	no	A		
PFI0075w	MAL9: 74,409 - 75,746 (+)	RIFIN	gene	no	A		
PFI1805w	MAL9: 1,474,419 - 1,475,692 (+)	RIFIN	**pseudo**	**yes**	A	1,474,479	1,475,692
PFI1810w	MAL9: 1,477,514 - 1,478,724 (+)	RIFIN	gene	no	B		
PFI1815c	MAL9: 1,480,935 - 1,482,199 (-)	RIFIN	gene	no	A		
PFI1825w	MAL9: 1,492,361 - 1,493,696 (+)	RIFIN	gene	no	A		
MAL8P1.216	MAL8: 1,378,088 - 1,379,253 (+)	hypothetical protein	gene	no	A		
NEW_3D7Rif_p_MAL7_3	MAL7 (+)		pseudo	new gene!	B	1437788	1438898
NEW_3D7Rif_p_MAL12_3	MAL12 (+)		pseudo, truncated	new gene!	?	764.441	765,145

8.2.2.2 HB3 Rifin sequences

Gene ID - Start - End - Length - E-value	Gene ID - Start – End – Length - E-value
HB3Rif_1.8_6 3013 3365 353 1.6e-184	HB3Rif_1.177_5c 544 858 315 6.5e-178
HB3Rif_1.47_2 23928 24235 308 5e-155	HB3Rif_1.177_5d 2643 2931 289 2.8e-160
HB3Rif_1.54_2a 6665 7015 351 1.1e-211	HB3Rif_1.177_6a 11664 11983 320 1.1e-176
HB3Rif_1.54_2b 12595 12947 353 1.5e-186	HB3Rif_1.177_6b 4741 5049 309 1.3e-174
HB3Rif_1.54_2c 22114 22461 348 1e-174	HB3Rif_1.189_2 2487 2839 353 4.8e-213
HB3Rif_1.54_3 23179 23491 313 2.5e-169	HB3Rif_1.193_4a 4021 4370 350 3.3e-222
HB3Rif_1.88_1 18672 19021 350 4.4e-206	HB3Rif_1.193_4b 1211 1538 328 5.3e-178
HB3Rif_1.88_4a 13489 13810 322 2e-193	HB3Rif_1.193_5 5113 5440 328 1.3e-195
HB3Rif_1.88_4b 5489 5778 292 1.7e-147	HB3Rif_1.195_4 5477 5768 292 7.4e-149
HB3Rif_1.88_6 6585 6943 359 3.5e-220	HB3Rif_1.195_5 7750 8098 349 5.3e-208
HB3Rif_1.96_1 19918 20267 350 1e-217	HB3Rif_1.195_6a 6509 6858 350 7.5e-206
HB3Rif_1.96_2 15796 16114 319 3.2e-186	HB3Rif_1.195_6b 9105 9422 318 4.1e-196
HB3Rif_1.96_5a 11043 11372 330 3.2e-202	HB3Rif_1.203_1 5152 5443 292 6.5e-149
HB3Rif_1.96_5b 9848 10133 288 1.3e-150	HB3Rif_1.203_3 7261 7569 309 2.8e-179
HB3Rif_1.96_5c 5717 6001 285 5.2e-150	HB3Rif_1.203_4 9279 9584 306 2.4e-155
HB3Rif_1.100_1 7733 8082 350 6.5e-211	HB3Rif_1.205_1 8711 9060 350 7e-217
HB3Rif_1.105_5 6949 7299 353 8.8e-215	HB3Rif_1.205_3a 6566 6899 334 3.3e-190
HB3Rif_1.105_6a 10376 10705 330 1e-185	HB3Rif_1.205_3b 9769 10060 292 3.1e-151
HB3Rif_1.105_6b 8042 8371 330 2.4e-178	HB3Rif_1.205_4 252 576 325 2e-193
HB3Rif_1.105_6c 9237 9562 326 7.3e-172	HB3Rif_1.218_1 4877 5199 323 9e-165
HB3Rif_1.114_1a 4255 4608 354 3.9e-205	HB3Rif_1.218_2a 3808 4162 355 8.5e-197
HB3Rif_1.114_1b 3169 3458 290 2.4e-123	HB3Rif_1.218_2b 1674 2001 328 1.1e-189
HB3Rif_1.114_2a 6525 6875 351 5.9e-215	HB3Rif_1.218_3 2700 3011 312 1.6e-171
HB3Rif_1.114_2b 5297 5630 336 2.3e-187	HB3Rif_1.218_4a 3711 4037 327 1.9e-183
HB3Rif_1.115_4 20109 20437 329 2.9e-11	HB3Rif_1.218_4b 1617 1907 291 2.3e-133
HB3Rif_1.118_2 16684 17045 362 1.9e-215	HB3Rif_1.218_6 4775 5087 313 6.5e-173
HB3Rif_1.118_3a 15663 15988 326 2e-185	HB3Rif_1.223_2 6401 6754 354 1.4e-222
HB3Rif_1.118_3b 17739 18054 316 23e-166	HB3Rif_1.245_1a 4277 4620 344 1.1e-207
HB3Rif_1.118_4a 6606 6958 353 4.9e-210	HB3Rif_1.249_3 6038 6327 290 2e-146
HB3Rif_1.118_4b 1296 1621 326 6.5e-193	HB3Rif_1.265_3 2332 2687 356 5.4e-207
HB3Rif_1.118_4c 7841 8160 320 3.9e-181	HB3Rif_1.265_6 4010 4325 316 1.2e-165
HB3Rif_1.125_1a 11067 11370 304 8e-177	HB3Rif_1.270_1a 1203 1548 346 9.1e-190
HB3Rif_1.130_2 6499 6792 294 1.9e-146	HB3Rif_1.270_1b 2281 2600 320 4.1e-184
HB3Rif_1.130_3 5427 5716 290 5.3e-152	HB3Rif_1.270_4 2468 2788 321 4.2e-166
HB3Rif_1.130_4 11373 11676 304 7.6e-160	HB3Rif_1.274_4a 3983 4339 357 2.8e-217
HB3Rif_1.130_5 10324 10648 325 1.9e-188	HB3Rif_1.274_4b 1502 1856 355 8.9e-205
HB3Rif_1.138_2 4322 4673 352 6.4e-211	HB3Rif_1.274_5a 2762 3081 320 7.4e-186
HB3Rif_1.142_1 11683 11998 316 8.1e-175	HB3Rif_1.274_5b 413 706 294 2.2e-156
HB3Rif_1.144_1a 1466 1793 328 2.1e-207	HB3Rif_1.285_4 3387 3715 329 1.1e-191
HB3Rif_1.144_1b 286 578 293 1.1e-157	HB3Rif_1.285_5 1284 1620 337 8.4e-188
HB3Rif_1.153_1 1849 2198 350 8e-198	HB3Rif_1.285_6a 194 544 351 5.5e-216
HB3Rif_1.168_2a 2501 2849 349 2.2e-215	HB3Rif_1.285_6b 2311 2602 292 9.9e-147
HB3Rif_1.168_2b 7385 7724 340 3.4e-183	HB3Rif_1.308_5a 1308 1657 350 3.9e-208
HB3Rif_1.168_3 1411 1726 316 2.5e-163	HB3Rif_1.316_3 2003 2352 350 1.7e-206
HB3Rif_1.168_4 11707 12042 336 9.6e-192	HB3Rif_1.338_1 1157 1462 306 9.3e-151
HB3Rif_1.170_5 13570 13885 316 1.4e-169	HB3Rif_1.353_2a 657 977 321 6.8e-165
HB3Rif_1.177_4a 9040 9387 348 6.7e-205	HB3Rif_1.353_2b 1688 1969 282 9.2e-144
HB3Rif_1.177_4b 6842 7134 293 4.2e-153	HB3Rif_1.360_5 844 1180 337 1.3e-112
HB3Rif_1.177_5a 5768 6088 325 6.1e-190	HB3Rif_1.366_1 1589 1891 303 3.1e-154
HB3Rif_1.177_5b 1567 1888 322 1.4e-178	HB3Rif_1.382_1 537 898 362 5.3e-216
HB3Rif_1.11_46 78558 78861	HB3Rif_1.177_4c 7997 8276 280 2e-91
HB3Rif_1.11_1 867 1139 273 2e-103	HB3Rif_1.183_5 1964 2258 295 1e-134
HB3Rif_1.100_2 12020 12289 270 5e-51	HB3Rif_1.223_32 3613 3904
HB3Rif_1.100_3 17143 17413 271 2e-50	HB3Rif_1.245_1b 1452 1801 350 4 e-188
HB3Rif_1.105_13 17168 17514	HB3Rif_1.249_1 7131 7447 317 4e-105
HB3Rif_1.125_1c 12091 12417 327 1.6e-89	HB3Rif_1.268_5 2358 2669 312 7e-160
HB3Rif_1.125_64 3898 4253	HB3Rif_1.295_2 4932 5264 333 3e-166

HB3Rif_1.125_1b	13249	13525	27	2e-102	HB3Rif_1.308_45b	2421	2747		
HB3Rif_1.138_4	15884	16166	285	7e-127	HB3Rif_1.381_6	519	707	189	8.7e-75
HB3Rif_1.153_3	753	1075	323	3e-153	HB3Rif_1.409_4	643	918	276	1.5e-90
					HB3Rif_1.512_4_2	0	351	352	1e-192

8.2.2.3 Dd2 Rifin sequences

Gene ID - Start - End - Length - E-value					Gene ID - Start – End – Length - E-value				
Dd2Rif_1.5_1	19619	19979	361	3.4e-213	Dd2Rif_1.64_1	6746	7069	324	1.9e-184
Dd2Rif_1.5_3	18556	18847	292	4.6e-163	Dd2Rif_1.64_2	7780	8093	315	6.1e-167
Dd2Rif_1.5_4	13847	14200	354	2.5e-206	Dd2Rif_1.64_4	2139	2430	292	1.3e-152
Dd2Rif_1.5_5a	16955	17304	350	9.8e-216	Dd2Rif_1.64_6a	889	1243	355	4.4e-203
Dd2Rif_1.5_5b	8717	9077	361	4.9e-207	Dd2Rif_1.64_6b	4305	4636	332	2.1e-193
Dd2Rif_1.5_5c	14882	15176	295	9.1e-162	Dd2Rif_1.64_6c	3194	3518	325	1.9e-164
Dd2Rif_1.5_6a	12756	13109	354	3.3e-204	Dd2Rif_1.76_1	2404	2729	326	1.4e-133
Dd2Rif_1.5_6b	9787	10078	292	3.8e-135	Dd2Rif_1.76_4	5506	5798	293	2.3e-137
Dd2Rif_1.6_1a	4683	5036	354	3.1e-208	Dd2Rif_1.76_6	7575	7885	311	4e-185
Dd2Rif_1.6_1b	5858	6147	290	1.9e-157	Dd2Rif_1.80_1	2404	2696	293	3.2e-154
Dd2Rif_1.6_5	16428	16776	349	1.7e-207	Dd2Rif_1.80_3a	5181	5535	355	4.2e-216
Dd2Rif_1.6_6a	17461	17790	330	1.9e-178	Dd2Rif_1.80_3b	1184	1534	351	8.4e-163
Dd2Rif_1.6_6b	23057	23393	337	2.3e-157	Dd2Rif_1.80_6	5291	5653	363	1.2e-206
Dd2Rif_1.9_5	2047	2375	329	1.9e-197	Dd2Rif_1.101_4a	7631	7985	355	3e-214
Dd2Rif_1.9_6	1002	1287	286	1.8e-150	Dd2Rif_1.101_5	9913	10267	355	5.6e-213
Dd2Rif_1.13_1a	12399	12754	356	2.2e-227	Dd2Rif_1.101_6a	4691	5042	352	6.7e-203
Dd2Rif_1.13_1b	13494	13812	319	7.3e-190	Dd2Rif_1.101_6b	8848	9180	333	3.2e-201
Dd2Rif_1.13_4a	3957	4315	359	5.1e-211	Dd2Rif_1.113_1a	3763	4109	347	1.8e-214
Dd2Rif_1.13_4b	5164	5450	287	6.3e-132	Dd2Rif_1.113_1b	925	1243	319	2.8e-169
Dd2Rif_1.13_6	1068	1365	298	1.7e-151	Dd2Rif_1.283_1a	2522	2867	346	5.2e-208
Dd2Rif_1.14_1	15817	16140	324	9.1e-196	Dd2Rif_1.283_1b	3584	3876	293	4.7e-156
Dd2Rif_1.14_2	9549	9873	325	7.4e-191	Dd2Rif_1.283_1c	5706	6041	336	5.6e-154
Dd2Rif_1.14_3a	14742	15093	352	1e-210	Dd2Rif_1.283_1d	1266	1596	331	4.8e-153
Dd2Rif_1.14_3b	10586	10904	319	4.2e-177	Dd2Rif_1.283_1e	4692	4997	306	2.5e-151
Dd2Rif_1.14_5	7875	8166	292	4e-157	Dd2Rif_1.303_1	2192	2544	353	4.6e-201
Dd2Rif_1.19_4	4930	5241	312	7.7e-205	Dd2Rif_1.303_3	3269	3593	325	9.8e-171
Dd2Rif_1.19_6b	1757	2078	322	3.5e-178	Dd2Rif_1.303_6	3388	3700	313	7e-186
Dd2Rif_1.19_6c	2833	3125	293	2.3e-167	Dd2Rif_1.317_3a	3330	3681	352	7.7e-217
Dd2Rif_1.25_2a	1134	1490	357	2.9e-207	Dd2Rif_1.317_6	2661	2983	323	1.4e-166
Dd2Rif_1.25_2b	31	322	292	2.9e-164	Dd2Rif_1.343_1a	1220	1570	351	5.7e-206
Dd2Rif_1.37_2	7405	7757	353	2.5e-208	Dd2Rif_1.343_1b	4162	4492	331	7.7e-201
Dd2Rif_1.37_4	6020	6354	335	4e-173	Dd2Rif_1.366_6	2370	2700	331	3.9e-198
Dd2Rif_1.37_5a	13258	13605	348	1.4e-207	Dd2Rif_1.436_1	2088	2424	337	1.4e-157
Dd2Rif_1.37_5b	2695	3055	361	5.5e-194	Dd2Rif_1.436_2	3137	3426	290	3.8e-166
Dd2Rif_1.37_5c	4929	5233	305	2.8e-169	Dd2Rif_1.481_2	571	924	354	7.6e-208
Dd2Rif_1.45_1a	4186	4541	356	2.7e-196	Dd2Rif_1.525_4a	1305	1594	290	2.4e-174
Dd2Rif_1.45_1b	6368	6659	292	7.2e-164	Dd2Rif_1.525_4b	3446	3736	291	6.9e-152
Dd2Rif_1.45_2	3069	3346	278	5.4e-131	Dd2Rif_1.525_6	2382	2730	349	8.1e-194
Dd2Rif_1.45_3a	7461	7780	320	1e-159	Dd2Rif_1.605_5	484	804	321	7.5e-176
Dd2Rif_1.45_3b	5317	5602	286	3.5e-139	Dd2Rif_1.696_2	2442	2778	315	3.9e-160
Dd2Rif_1.45_4a	943	1268	326	1.5e-188	Dd2Rif_1.696_3	1339	1666	328	3e-172
Dd2Rif_1.45_6a	4316	4630	315	1.3e-178	Dd2Rif_1.926_2b	594	941	348	3.4e-214
Dd2Rif_1.54_1	7057	7410	354	4.9e-190	Dd2Rif_1.960_3a	1265	1577	313	3.1e-185
Dd2Rif_1.54_4	4832	5156	325	1.1e-173	Dd2Rif_1.1020_2	1179	1494	316	2.3e-162
Dd2Rif_1.54_6	11853	12214	362	1.1e-212	Dd2Rif_1.1100_4a	1219	1573	355	6.2e-216
Dd2Rif_1.58_2a	2493	2851	359	1.8e-221	Dd2Rif_1.1100_4b	123	415	293	8.3e-154
Dd2Rif_1.58_2b	1273	1608	336	5.2e-179	Dd2Rif_1.1151_2	72	424	353	9.1e-211
					Dd2Rif_1.1169_5	328	662	335	8.4e-168
					Dd2Rif_1.1373_4	90	379	290	4.8e-142

8.2.2.4 IT Rifin sequences

Gene ID - Start - End - Length - E-value	Gene ID - Start – End – Length - E-value
ITRifA_0002180_6 391 740 350 3.6e-208	ITRifA_0001562_1 931 1258
ITRifA_0002177_1a 4686 5042 357 9e-213	ITRifA_0001466_6 335 691 357 3.1e-220
ITRifB_0002177_1b 5731 6048 318 2e-186	ITRifA_p_0000714_5 279 572
ITRifA_0002177_1c 7867 8227	ITRifA_0000647_3 656 992 337 2.3e-112
ITRifA_0002177_5 18872 19177 306 1.4e-155	ITRifA_0000640_3a 783 1110 328 6.3e-189
ITRifA_0002172_6 508 859 352 5.9e-209	ITRifA_p_0000640_31 1827 2122
ITRifA_0002164_1 6537 6893 357 2.9e-221	ITRifA_0000615_1 484 841 358 2.9e-202
ITRifB_0002164_2a 9638 9963 328 1.8e-177	ITRifB_0000615_3 1613 1907 295 4.6e-163
ITRifB_0002164_2b 7585 7882 298 2.1e-145	ITRifB_0000491_3 1134 1436 303 5.6e-149
ITRifA_0002164_3 8607 8917 311 1.4e-172	ITRifA_0000425_5 205 535 331 2.9e-204
ITRifA_p_0002159_5 4103 4443 341 1.1e-177	ITRifA_0000402_2 4696 5045 350 1.6e-208
ITRifA_p_0002157_2 335 669 335 9.7e-167	ITRifB_0000402_4a 6138 6422 285 6.9e-141
ITRifA_0002157_3a 3638 3953 316 1.7e-185	ITRifA_p_0000402_4b6 5092 5444
ITRifA_0002157_3b 1402 1723 322 2.3e-167	ITRifB_0000402_5 4043 4334 292 1.1e-142
ITRifA_0002157_6 12953 13315 363 3.1e-215	ITRifB_0000361_3 565 856 292 2.4e-145
ITRifA_0002155_2a 15207 15528 322 8e-185	ITRifA_p_0000356_23 837 1189
ITRifB_0002155_2b 13988 14315 328 2e-178	ITRifA_0000276_3 713 1031 319 8.7e-147
ITRifB_0002155_2c 2797 3109 313 9.3e-143	ITRifB_p_0000276_4 1742 1991 250 5.8e-77
ITRifA_p_0002155_2d 3890 4191 302 8.2e-109	ITRifA_0000276_6 4465 4778 314 2.4e-180
ITRifA_0002155_3 1755 2087 333 2.4e-155	ITRifB_0000262_2 6544 6834 291 3.7e-153
ITRifA_0002155_4a 13547 13877 331 3e-175	ITRifB_0000262_1 5463 5752
ITRifA_p_0002155_4b 15724 16054 331 9e-170	ITRifA_0000262_4 3923 4272 350 5.7e-202
ITRifA_p_0002155_4c 14610 14876 267 7e-109	ITRifB_0000246_2a 898 1231 334 7.1e-181
ITRifA_0002086_5a 570 921 352 2.1e-211	ITRifA_p_0000246_1 2060 2274 215 1.7e-77
ITRifA_0002086_5b 1636 1954 319 1.3e-186	ITRifB_p_0000246_32b 3280 3608
ITRifA_0002034_1 866 1179 314 8.8e-155	ITRifA_p_0000244_1 647 1001 355 1.4e-201
ITRifB_0002034_5 6351 6648 298 5.3e-138	ITRifB_p_0000244_2 2973 3182 210 4.3e-72
ITRifA_0002034_6 7391 7691 301 2.1e-149	ITRifA_0000244_3 1778 2134 357 6.4e-205
ITRifA_0002029_1 452 766 315 1.2e-177	ITRifA_0000242_1 387 734 348 3.9e-203
ITRifB_0002029_2a 1478 1799 322 2.5e-178	ITRifB_0000242_3 1450 1772 323 3.7e-169
ITRifB_0002029_2b 2552 2846 295 4e-157	ITRifA_0000238_1 677 996 320 2.4e-182
ITRifA_0002029_3 4661 4971 311 3.7e-195	ITRifA_0000211_1 901 1253 353 4.1e-184
ITRifA_0002013_2 7922 8239 318 1.3e-162	ITRifA_0000204_1 743 1069 327 1.5e-191
ITRifA_p_0002012_3 3495 3812	ITRifA_p_0000177_6a 225 451 227 5.7e-106
ITRifA_0002011_2 2063 2357 295 3.6e-134	ITRifB_0000177_6b 5539 5830
ITRifA_p_0002011_3 7010 7305	ITRifA_0000164_1 1277 1577 301 1.7e-167
ITRifA_0002009_3 1247 1555 309 9e-166	ITRifA_0000164_6 116 468 353 4.8e-204
ITRifA_0002009_4 7026 7381 356 2e-211	ITRifA_0000156_2 293 644 352 1.6e-217
ITRifB_0002009_6 8145 8430 286 9.1e-153	ITRifA_0000156_5a 598 945 348 2e-222
ITRifA_0002008_2 11482 11803 322 6e-168	ITRifB_0000156_5b 1816 2151 336 3.5e-185
ITRifA_0002007_4a 10218 10569 352 3e-218	ITRifor_0000095_3 4871 5204 334 2.5e-16
ITRifB_0002007_4b 7930 8221 292 1.7e-151	ITRifA_0000095_6a 1548 1898 351 4.1e-219
ITRifA_p_0002007_5 9029 9280 252 3e-109	ITRifA_p_0000095_6b 462 711 250 2e-94
ITRifA_0002007_6 6851 7165 315 1.3e-188	ITRifA_0000068_1a 1345 1694 350 1.6e-197
ITRifB_0002006_1 7386 7706 321 7.4e-154	ITRifA_0000068_1b 4617 4926 310 1.7e-159
ITRifA_0002006_2a 3960 4315 356 1.2e-192	ITRifB_0000068_1c 265 556 292 6.9e-146
ITRifB_0002006_2b 6148 6439 292 2.5e-157	ITRifA_0000068_3 2405 2708 304 2.1e-143
ITRifB_0002006_2c 5099 5383 285 6.7e-143	ITRifA_0000068_5 3189 3497 309 1.5e-168
ITRifB_0002006_2d 2845 3121 277 1.2e-102	ITRifA_0000065_1a 9685 10040 356 4e-210
ITRifA_0002006_4a 6040 6364 325 1.5e-196	ITRifA_0000065_1b 7367 7729 363 1.4e-196
ITRifA_0002006_4b 7061 7367 307 2e-169	ITRifB_0000065_2 5148 5439 292 4.5e-151
ITRifA_0002006_5 9239 9591 353 1.6e-210	ITRifB_0000065_3a 6226 6547 322 1.7e-171
ITRifA_0002006_6a 8210 8530 321 8.2e-193	ITRifB_0000065_3b 8598 8883 286 8.3e-138
ITRifA_0002006_6b 11607 11920 314 8e-166	ITRifA_0000045_1 570 873 304 3.4e-147
ITRifA_0002004_3 17916 18267 352 5.1e-207	ITRifA_p_0000045_5 9480 9774 295 2.8e-138
ITRifA_0002004_4a 7376 7684 309 2.8e-169	ITRifA_0000033_4 577 906 330 2.8e-194
ITRifA_0002004_4b 2071 2377 307 4.2e-156	ITRifB_0000019_2a 4568 4892 325 2.2e-174
ITRifB_0002004_5a 8396 8731 336 2.2e-182	ITRifB_0000019_2b 2488 2813 326 3.5e-165
ITRifB_0002004_5b 3097 3389 293 3e-143	ITRifA_0000019_3 3607 3925 319 2.1e-176

ITRifA_0002004_6	5182	5488	307	6.3e-175	ITRifA_0000014_1	5697	6020	324	3.9e-199
ITRifA_0001747_5	296	600	305	2.6e-162	ITRifA_0000000_4a	689	1001	313	4.8e-162
ITRifA_0000000_6a	15009	15323	315	2.-169	ITRifA_0000000_4b	13952	14254	303	2e-127
ITRifA_p_0000000_6b	8906	9195	290	3.8e-25					

8.2.3 Stevor sequences

8.2.3.1 3D7 re-annotated Stevor sequences

I re-annotated the Stevor family as part of the PlasmoDB reannotation effort, using the same HMMer approach described in this manuscript.

For the *stevor* family, the boundaries of 9 genes were redefined, 4 genes (PF11_0013, PFF0847w, MAL7P1.310 and MAL8P1.214) previously annotated as "STEVOR pseudogene putative" were not Stevor.

Gene ID	Current PlasmoDB annotation	Gene/pseudo	Sequence modified?	Comment
PFA0090c	STEVOR	gene	no	
PFA0105w	STEVOR	pseudo	**yes**	No exon1
PFA0705c	STEVOR pseudogene putative	pseudo	**yes**	90bp added at the end (were missing due to framesfhit)
PFA0750w	STEVOR	gene	no	
PF10_0009	pseudogene, stevor, putative	pseudo		
PF10_0395	stevor, putative	gene	no	
PF11_0013*	stevor, putative, degenerate			*NOT Stevor!*
PF11_0516	stevor, putative	gene	no	
PFL2610w	STEVOR	gene	no	
PFL2620w	stevor	gene	no	
PFL2635w	stevor	gene	no	
MAL13P1.7	stevor	gene	no	
MAL13P1.490	StevoR	Pseudo	**yes**	Was annotated as 4 exons. Now 3 exons with 1 frameshift and 182bp longer.
MAL13P1.505	STEVOR	gene	no	
PF14_0007	stevor, putative	gene	No	
PF14_0767	stevor, putative	gene	No	

PF14_0771	stevor, putative	gene	No	
PFB0025c	stevor, putative	gene	no	
PFB0050c	stevor isoform gam beta	pseudo	**yes**	Total of 318bp added at the start and at the end. Intron does not start with stop codon.
PFB0065w	stevor, putative	gene	**yes**	21bp added at start of exon1
PFB0955w	stevor, degenerate, putative	gene	**yes**	Exon1 changed.
PFB1020w	stevor, putative	gene	no	
PFC0025c	STEVOR	gene	no	
PFC1105w	stevor (3D7-stevorT3-2)	gene	no	
PFD0035c	STEVOR	gene	no	
PFD0065w	STEVOR pseudogene	pseudo	**yes**	Exon1 was wrong. Now intron does not start with a stop codon.
PFD0125c	STEVOR	gene	no	
PFD1220c	STEVOR	gene	no	
PFE0030c	STEVOR pseudogene	pseudo	**yes**	I removed the intron (sequence now 125bp shorter)
PFF0847w*	Stevor, pseudogene			*NOT Stevor!*
PFF0850c	STEVOR	gene	no	
PFF1550w	STEVOR	gene	no	
MAL7P1.218	STEVOR	gene	no	
MAL7P1.310*	Stevor, putative, degenerate			*NOT Stevor!*
MAL7P1.223	STEVOR, putative		**yes**	Exon1 was wrong.
MAL7P1.227	STEVOR	gene	no	
PF07_0130	STEVOR	gene	no	
MAL8P1.217	STEVOR		no	
PFI0045c	stevor	gene	no	
PFI0080w	stevor	gene	no	
MAL8P1.214*	Stever pseudogene, putative			Typo! It's *NOT Stevor!*

8.2.3.2 HB3 Stevor sequences

Gene ID - Start - End - Length - E-value					Gene ID - Start – End – Length - E-value				
HB3Ste_1.96_2	21189	21472	284	8e-165	HB3Ste_1.203_2	6200	6484	285	1e-165
HB3Ste_1.96_4	6773	7049	277	4e-170	HB3Ste_1.205_2	7641	7912	272	2e-171
HB3Ste_1.125_4	4993	5265	273	1e-163	HB3Ste_1.218_5	2651	2927	277	6e-177
HB3Ste_1.130_3	7538	7810	273	4e-168	HB3Ste_1.223_3	4666	4940	275	3e-182
HB3Ste_1.130_5	12424	12708	285	1e-161	HB3Ste_1.245_2	2530	2814	285	4e-174
HB3Ste_1.138_4	16939	17206	268	7e-155	HB3Ste_1.270_5	3655	3939	285	7e-171
HB3Ste_1.168_6	12824	13106	283	2e-158	HB3Ste_p_1.308_5	3655	3941	287	1e-165
HB3Ste_1.177_5	3709	3984	276	9e-172	HB3Ste_1.316_1	293	569	277	1e-172
HB3Ste_1.193_6	2290	2565	276	6e-170	HB3Ste_1.362_4	337	615	279	5e-175
HB3Ste_1.195_6	10136	10416	281	5e-166					

8.2.3.3 Dd2 Stevor sequences

Gene ID - Start - End - Length - E-value					Gene ID - Start – End – Length - E-value				
Dd2Ste_1.5_5a	15919	16203	285	2e-170	Dd2Ste_1.113_2	2036	2316	281	3e-169
Dd2Ste_1.5_5b	10836	11117	282	6e-159	Dd2Ste_1.261_6	4720	5003	284	4.9e-88
Dd2Ste_1.6_2	6903	7183	281	2e-172	Dd2Ste_1.303_4	2302	2580	279	1e-172
Dd2Ste_1.6_4	24160	24437	278	1e-159	Dd2Ste_1.317_2	2244	2523	280	5e-170
Dd2Ste_1.13_4a	61	329	269	2e-164	Dd2Ste_1.343_1	2412	2690	279	3e-170
Dd2Ste_1.13_4b	2225	2500	276	1e-160	Dd2Ste_1.366_3	2128	2410	283	1e-165
Dd2Ste_1.13_5	6194	6471	278	1e-158	Dd2Ste_1.723_3	1997	2287	291	2e-108
Dd2Ste_1.14_6a	8941	9217	277	3e-169	Dd2Ste_1.926_2	1839	2122	284	1.-164
Dd2Ste_1.14_6b	3708	3994	287	9e-156	Dd2Ste_1.37_6	3802	4083	282	
Dd2Ste_1.19_4	3903	4168	266	9e-165	Dd2Ste_1.45_5	11772	12056	285	
Dd2Ste_1.45_3	8580	8852	273	8e-169	Dd2Ste_1.54_1	9745	10027	283	
Dd2Ste_1.45_5a	3253	3531	279	2e-161	Dd2Ste_1.76_5	4506	4788	283	
Dd2Ste_1.76_4a	8760	9040	281	7e-170	Dd2Ste_1.101_1	9509	9787	280	
Dd2Ste_1.76_5a	6532	6816	285	6e-168	Dd2Ste_1.317_5	1573	1858	285	
Dd2Ste_1.80_2	3448	3724	277	4e-157	Dd2Ste_1.792_4	2392	2677	299	
Dd2Ste_1.101_4	5887	6167	281	2e-178					

8.2.3.4 IT Stevor sequences

Gene ID - Start - End - Length - E-value					Gene ID - Start – End – Length - E-value				
ITSte_0002177_3	6819	7091	273	4.5e-174	ITSte_0000402_1	5923	6203	281	3.7e-165
ITSte_p_0002164_32	10680	10964			ITSte_0000361_1	1586	1860	275	1.2e-159
ITSte_0002157_1	2558	2841	284	2.1e-166	ITSte_0000276_5	2720	3005	286	1.9e-164
ITSte_0002029_3	3623	3898	276	1.6e-170	ITSte_0000262_4	4995	5272	278	1.3e-159
ITSte_0002013_2	8984	9266	283	2.4e-165	ITSte_0000244_3	3950	4235	286	1.8e-166
ITSte_0002009_5	9162	9438	277	1.3e-166	ITSte_0000242_3	2409	2691	283	5.1e-171
ITSte_0002006_3	8446	8718	273	6.3e-169	ITSte_0000204_2	4375	4658	284	2.9e-162
ITSte_0002006_5a	10543	10821	279	1.7e-161	ITSte_p_0000204_13	1961	2242		
ITSte_p_0002006_45	19118	19407			ITSte_0000177_4	4553	4826	274	4.8e-178
ITSte_0002004_4a	6342	6621	280	7.4e-174	ITSte_0000177_6	6575	6852	278	9e-169
ITSte_0002004_4b	4122	4408	287	3.5e-169	ITSte_p_0000164_3	2327	2606	280	1.6e-146
ITSte_0001562_2	2069	2363	295	5.4e-62	ITSte_0000095_5a	2801	3087	287	2.5e-167
ITSte_0001455_2	684	942	259	2.2e-49	ITSte_0000095_5b	4906	5180	275	6.9e-166
ITSte_p_0001346_5	621	901	281	2.3e-90	ITSte_0000068_2	3549	3818	270	1.8e-160
ITSte_0000801_4	590	872	283	2.6e-73	ITSte_p_0000065_2	4176	4443	268	1.6e-31
ITSte_p_0000716_64	651	936	286		ITSte_0000045_4	10548	10831	284	1.1e-94
ITSte_p_0000491_123	2224	2510	287						

8.2.4 Pfmc-2TM sequences

8.2.4.1 HB3 Pfmc-2TM sequences

Gene ID - Start - End - Length - E-value	Gene ID - Start – End – Length - E-value
HB3Pfmc-2TM1.81_5 375 580 206 1e-147	HB3Pfmc-2TM1.316_5 157 362 206 3e-140
HB3Pfmc-2TM1.142_2 12840 13047 4e-138	HB3Pfmc-2TM1.326_5 145 351 211 8e-140
HB3Pfmc-2TM1.223_6 1129 1334 206 3e-143	HB3Pfmc-2TM1.327_3 0 194 195 4e-130
HB3Pfmc-2TM1.291_4 677 879 206 8e-136	HB3Pfmc-2TM1.330_4 2126 2336 211 3e-141
HB3Pfmc-2TM1.540_3 146 350 206 7e-144	

8.2.4.2 Dd2 Pfmc-2TM sequences

Gene ID - Start - End - Length - E-value	Gene ID - Start – End – Length - E-value
Dd2Pfmc-2TM _1.705_5 463 672 210 1.6e-149	Dd2Pfmc-2TM_1.1109_4 130 339 210 2.4e-124
Dd2Pfmc-2TM _1.442_5 136 341 210 7.3e-137	

8.2.4.3 IT Pfmc-2TM sequences

Pfmc-2TM sequences were not extracted for the IT strain because the hypervariable loop in these genes is too short for designing specific oligos (see main text of the manuscript).

8.2.5 Surfin sequences

8.2.5.1 HB3 Surfin sequences

Gene ID - Start - End - Length - E-value	Gene ID - Start – End – Length - E-value
HB3Surf_1.36_2 38585 40209 1625 0	HB3Surf_1.301_1 2396 4044 1649 0
HB3Surf_1.81_2 11793 13180 1388 0	HB3Surf_1.339_65 1287 3367 2080
HB3Surf_1.115_6 6976 8488 1513 3e-189	HB3Surf_1.348_64 905 2532 1627
HB3Surf_1.205_2 2174 3791 1618 0	HB3Surf_1.356_5 1323 2804 1482 0
HB3Surf_1.212_3a 7990 9589 1600 0	HB3Surf_1.212_3b 3285 4801 1517 0

8.2.5.2 Dd2 Surfin sequences

Gene ID - Start - End - Length - E-value	Gene ID - Start – End – Length - E-value
Dd2Surf_1.547_3 1590 3229 1639 0	Dd2Surf_1.224_1 1225 2649 1424 0
Dd2Surf_1.82_3 8124 9762 1638 0	Dd2Surf_1.576_5 1787 3201 1414 9.4e-73
Dd2Surf_1.694_5 1438 3068 1630 0	Dd2Surf_1.224_3 1262 2781 1519 2.3e-59
Dd2Surf_1.556_3 1607 3117 1510 0	Dd2Surf_1.693_2 1865 2956 1091 3.3e-25
Dd2Surf_1.387_3 999 2380 1381 0	

8.2.5.3 IT Surfin sequences

Surfin sequences were not extracted for the IT strain because it was realised that *surfin* genes are conserved in all strains (see main text of the manuscript).

8.3 VSA oligo sequences for microarray

Dr Hu Guangan selected the majority of VSA oligos using OligoRankPick (see the methods section of chapter 3). The oligos for the 8 "new" IT var genes were designed by myself.

All oligos specific to HB3/IT/Dd2 VSA can be found in the file "Oligo sequences for microarray.doc" on the attached CD.

8.4 Microarray data

All microarray data used in this thesis can be found in the following files on the attached CD (last page of the thesis):

- HB3-HBEC1_vs_HB3-Uns1.xls
- HB3-HBEC2_vs_HB3-Uns2.xls
- HB3-HBEC-TNF_vs_HB3-Uns2.xls
- 3D7-HBEC_vs_3D7-Uns.xls
- IT-HBEC_vs_IT-Uns.xls

In each file, the first column indicates the unique oligo ID, the second column is the gene name and PlasmoDB annotation. All following columns are the expression ratios.

8.5 Publication

The following paper was published during the course of this thesis:

Smargiasso†, N., Gabelica, V., Damblon, C., Rosu, F., De Pauw, E., Teulade-Fichou, M. P., Rowe, J. A., and Claessens†, A., 2009. Putative DNA G-quadruplex formation within the promoters of Plasmodium falciparum var genes. BMC Genomics 10, 362.

†Equal contributors

The paper is attached at the end of the thesis.

References

Abdel-Latif, M. S., Cabrera, G., Kohler, C., Kremsner, P. G., and Luty, A. J., 2004. Antibodies to rifin: a component of naturally acquired responses to Plasmodium falciparum variant surface antigens on infected erythrocytes. Am J Trop Med Hyg 71**,** 179-186.

Abdel-Latif, M. S., Dietz, K., Issifou, S., Kremsner, P. G., and Klinkert, M. Q., 2003. Antibodies to Plasmodium falciparum rifin proteins are associated with rapid parasite clearance and asymptomatic infections. Infect Immun 71**,** 6229-6233.

Abdel-Latif, M. S., Khattab, A., Lindenthal, C., Kremsner, P. G., and Klinkert, M. Q., 2002. Recognition of variant Rifin antigens by human antibodies induced during natural Plasmodium falciparum infections. Infect Immun 70**,** 7013-7021.

Adams, S., Turner, G. D., Nash, G. B., Micklem, K., Newbold, C. I., and Craig, A. G., 2000. Differential binding of clonal variants of Plasmodium falciparum to allelic forms of intracellular adhesion molecule 1 determined by flow adhesion assay. Infect Immun 68**,** 264-269.

Ades, E. W., Candal, F. J., Swerlick, R. A., George, V. G., Summers, S., Bosse, D. C., and Lawley, T. J., 1992. HMEC-1: establishment of an immortalized human microvascular endothelial cell line. J Invest Dermatol 99**,** 683-690.

Afonso Nogueira, P., Wunderlich, G., Shugiro Tada, M., d'Arc Neves Costa, J., Jose Menezes, M., Scherf, A., and Pereira-da-Silva, L. H., 2002. Plasmodium falciparum: analysis of transcribed var gene sequences in natural isolates from the Brazilian Amazon region. Exp Parasitol 101**,** 111-120.

Aird, W. C., 2007. Phenotypic heterogeneity of the endothelium: I. Structure, function, and mechanisms. Circ Res 100**,** 158-173.

Al-Khedery, B., and Allred, D. R., 2006. Antigenic variation in Babesia bovis occurs through segmental gene conversion of the ves multigene family, within a bidirectional locus of active transcription. Mol Microbiol 59**,** 402-414.

Alon, R., Hammer, D. A., and Springer, T. A., 1995. Lifetime of the P-selectin-carbohydrate bond and its response to tensile force in hydrodynamic flow. Nature 374**,** 539-542.

Alter, S. C., Metcalfe, D. D., Bradford, T. R., and Schwartz, L. B., 1987. Regulation of human mast cell tryptase. Effects of enzyme concentration, ionic strength and the structure and negative charge density of polysaccharides. Biochem J 248**,** 821-827.

Amodu, O. K., Gbadegesin, R. A., Ralph, S. A., Adeyemo, A. A., Brenchley, P. E., Ayoola, O. O., Orimadegun, A. E., Akinsola, A. K., Olumese, P. E., and Omotade, O. O., 2005. Plasmodium falciparum malaria in south-west Nigerian children: is the polymorphism of ICAM-1 and E-selectin genes contributing to the clinical severity of malaria? Acta Trop 95**,** 248-255.

Andres, O., Obojes, K., Kim, K. S., ter Meulen, V., and Schneider-Schaulies, J., 2003. CD46- and CD150-independent endothelial cell infection with wild-type measles viruses. J Gen Virol 84**,** 1189-1197.

Andrews, K. T., Adams, Y., Viebig, N. K., Lanzer, M., and Schwartz-Albiez, R., 2005. Adherence of Plasmodium falciparum infected erythrocytes to CHO-745 cells and inhibition of binding by protein A in the presence of human serum. Int J Parasitol 35**,** 1127-1134.

Andrews, K. T., Viebig, N. K., Wissing, F., Klatt, N., Oster, N., Wickert, H., Knolle, P., and Lanzer, M., 2003. A human schwannoma cell line supports the in vitro adhesion of Plasmodium falciparum infected erythrocytes to chondroitin-4-sulfate. Parasitol Res 89**,** 188-193.

Anstey, N. M., Russell, B., Yeo, T. W., and Price, R. N., 2009. The pathophysiology of vivax malaria. Trends Parasitol 25**,** 220-227.

Arman, M., Raza, A., Tempest, L. J., Lyke, K. E., Thera, M. A., Kone, A., Plowe, C. V., Doumbo, O. K., and Rowe, J. A., 2007. Platelet-mediated clumping of Plasmodium falciparum infected erythrocytes is associated with high parasitemia but not severe clinical manifestations of malaria in African children. Am J Trop Med Hyg 77**,** 943-946.

Arman, M., and Rowe, J. A., 2008. Experimental conditions affect the outcome of Plasmodium falciparum platelet-mediated clumping assays. Malar J 7**,** 243.

Aryee, M. J., Gutierrez-Pabello, J. A., Kramnik, I., Maiti, T., and Quackenbush, J., 2009. An improved empirical bayes approach to estimating differential gene expression in microarray time-course data: BETR (Bayesian Estimation of Temporal Regulation). BMC Bioinformatics 10**,** 409.

Avril, M., Kulasekara, B. R., Gose, S. O., Rowe, C., Dahlback, M., Duffy, P. E., Fried, M., Salanti, A., Misher, L., Narum, D. L., and Smith, J. D., 2008. Evidence for globally shared, cross-reacting polymorphic epitopes in the pregnancy-associated malaria vaccine candidate VAR2CSA. Infect Immun 76**,** 1791-1800.

Bailey, T. L., and Elkan, C., 1994. Fitting a mixture model by expectation maximization to discover motifs in biopolymers. Proc Int Conf Intell Syst Mol Biol 2**,** 28-36.

Barnwell, J. W., Asch, A. S., Nachman, R. L., Yamaya, M., Aikawa, M., and Ingravallo, P., 1989. A human 88-kD membrane glycoprotein (CD36) functions in vitro as a receptor for a cytoadherence ligand on Plasmodium falciparum-infected erythrocytes. J Clin Invest 84**,** 765-772.

Barragan, A., Fernandez, V., Chen, Q., von Euler, A., Wahlgren, M., and Spillmann, D., 2000. The duffy-binding-like domain 1 of Plasmodium falciparum erythrocyte membrane protein 1 (PfEMP1) is a heparan sulfate ligand that requires 12 mers for binding. Blood 95**,** 3594-3599.

Barry, A. E., Leliwa-Sytek, A., Tavul, L., Imrie, H., Migot-Nabias, F., Brown, S. M., McVean, G. A., and Day, K. P., 2007. Population genomics of the immune evasion (var) genes of Plasmodium falciparum. PLoS Pathog 3**,** e34.

Bartlett, A. H., and Park, P. W., 2010. Proteoglycans in host-pathogen interactions: molecular mechanisms and therapeutic implications. Expert Rev Mol Med 12**,** e5.

Baruch, D. I., Gamain, B., Barnwell, J. W., Sullivan, J. S., Stowers, A., Galland, G. G., Miller, L. H., and Collins, W. E., 2002. Immunization of Aotus monkeys with a functional domain of the Plasmodium falciparum variant antigen

induces protection against a lethal parasite line. Proc Natl Acad Sci U S A 99, 3860-3865.

Baruch, D. I., Gormely, J. A., Ma, C., Howard, R. J., and Pasloske, B. L., 1996. Plasmodium falciparum erythrocyte membrane protein 1 is a parasitized erythrocyte receptor for adherence to CD36, thrombospondin, and intercellular adhesion molecule 1. Proc Natl Acad Sci U S A 93, 3497-3502.

Baum, J., Richard, D., Healer, J., Rug, M., Krnajski, Z., Gilberger, T. W., Green, J. L., Holder, A. A., and Cowman, A. F., 2006. A conserved molecular motor drives cell invasion and gliding motility across malaria life cycle stages and other apicomplexan parasites. J Biol Chem 281, 5197-5208.

Beare, N. A., Southern, C., Chalira, C., Taylor, T. E., Molyneux, M. E., and Harding, S. P., 2004. Prognostic significance and course of retinopathy in children with severe malaria. Arch Ophthalmol 122, 1141-1147.

Beare, N. A., Taylor, T. E., Harding, S. P., Lewallen, S., and Molyneux, M. E., 2006. Malarial retinopathy: a newly established diagnostic sign in severe malaria. Am J Trop Med Hyg 75, 790-797.

Beckmann, C., Waggoner, J. D., Harris, T. O., Tamura, G. S., and Rubens, C. E., 2002. Identification of novel adhesins from Group B streptococci by use of phage display reveals that C5a peptidase mediates fibronectin binding. Infect Immun 70, 2869-2876.

Bellamy, R., Kwiatkowski, D., and Hill, A. V., 1998. Absence of an association between intercellular adhesion molecule 1, complement receptor 1 and interleukin 1 receptor antagonist gene polymorphisms and severe malaria in a West African population. Trans R Soc Trop Med Hyg 92, 312-316.

Belnoue, E., Kayibanda, M., Deschemin, J. C., Viguier, M., Mack, M., Kuziel, W. A., and Renia, L., 2003. CCR5 deficiency decreases susceptibility to experimental cerebral malaria. Blood 101, 4253-4259.

Benjamini, Y., and Hochberg, Y., 1995. Controlling the False Discovery Rate - a Practical and Powerful Approach to Multiple Testing. Journal of the Royal Statistical Society Series B-Methodological 57, 289-300.

Berendt, A. R., Simmons, D. L., Tansey, J., Newbold, C. I., and Marsh, K., 1989. Intercellular adhesion molecule-1 is an endothelial cell adhesion receptor for Plasmodium falciparum. Nature 341, 57-59.

Berteau, O., and Mulloy, B., 2003. Sulfated fucans, fresh perspectives: structures, functions, and biological properties of sulfated fucans and an overview of enzymes active toward this class of polysaccharide. Glycobiology 13, 29R-40R.

Berzins, K., Perlmann, H., Wahlin, B., Carlsson, J., Wahlgren, M., Udomsangpetch, R., Bjorkman, A., Patarroyo, M. E., and Perlmann, P., 1986. Rabbit and human antibodies to a repeated amino acid sequence of a Plasmodium falciparum antigen, Pf 155, react with the native protein and inhibit merozoite invasion. Proc Natl Acad Sci U S A 83, 1065-1069.

Biswas, A. K., Hafiz, A., Banerjee, B., Kim, K. S., Datta, K., and Chitnis, C. E., 2007. Plasmodium falciparum uses gC1qR/HABP1/p32 as a receptor to bind to

vascular endothelium and for platelet-mediated clumping. PLoS Pathog 3**,** 1271-1280.

Blomqvist, K., Normark, J., Nilsson, D., Ribacke, U., Orikiriza, J., Trillkott, P., Byarugaba, J., Egwang, T. G., Kironde, F., Andersson, B., and Wahlgren, M., 2009. var gene transcription dynamics in Plasmodium falciparum patient isolates. Mol Biochem Parasitol.

Blythe, J. E., Niang, M., Marsh, K., Holder, A. A., Langhorne, J., and Preiser, P. R., 2009. Characterization of the repertoire diversity of the Plasmodium falciparum stevor multigene family in laboratory and field isolates. Malar J 8**,** 140.

Blythe, J. E., Yam, X. Y., Kuss, C., Bozdech, Z., Holder, A. A., Marsh, K., Langhorne, J., and Preiser, P. R., 2008. Plasmodium falciparum STEVOR proteins are highly expressed in patient isolates and located in the surface membranes of infected red blood cells and the apical tips of merozoites. Infect Immun 76**,** 3329-3336.

Bozdech, Z., Llinas, M., Pulliam, B. L., Wong, E. D., Zhu, J., and DeRisi, J. L., 2003. The transcriptome of the intraerythrocytic developmental cycle of Plasmodium falciparum. PLoS Biol 1**,** E5.

Brown, G. V., Culvenor, J. G., Crewther, P. E., Bianco, A. E., Coppel, R. L., Saint, R. B., Stahl, H. D., Kemp, D. J., and Anders, R. F., 1985. Localization of the ring-infected erythrocyte surface antigen (RESA) of Plasmodium falciparum in merozoites and ring-infected erythrocytes. J Exp Med 162**,** 774-779.

Brown, H., Hien, T. T., Day, N., Mai, N. T., Chuong, L. V., Chau, T. T., Loc, P. P., Phu, N. H., Bethell, D., Farrar, J., Gatter, K., White, N., and Turner, G., 1999. Evidence of blood-brain barrier dysfunction in human cerebral malaria. Neuropathol Appl Neurobiol 25**,** 331-340.

Buffet, P. A., Safeukui, I., Milon, G., Mercereau-Puijalon, O., and David, P. H., 2009. Retention of erythrocytes in the spleen: a double-edged process in human malaria. Curr Opin Hematol 16**,** 157-164.

Bull, P. C., Berriman, M., Kyes, S., Quail, M. A., Hall, N., Kortok, M. M., Marsh, K., and Newbold, C. I., 2005. Plasmodium falciparum variant surface antigen expression patterns during malaria. PLoS Pathog 1**,** e26.

Bull, P. C., Buckee, C. O., Kyes, S., Kortok, M. M., Thathy, V., Guyah, B., Stoute, J. A., Newbold, C. I., and Marsh, K., 2008. Plasmodium falciparum antigenic variation. Mapping mosaic var gene sequences onto a network of shared, highly polymorphic sequence blocks. Mol Microbiol 68**,** 1519-1534.

Bull, P. C., Kortok, M., Kai, O., Ndungu, F., Ross, A., Lowe, B. S., Newbold, C. I., and Marsh, K., 2000. Plasmodium falciparum-infected erythrocytes: agglutination by diverse Kenyan plasma is associated with severe disease and young host age. J Infect Dis 182**,** 252-259.

Bull, P. C., Kyes, S., Buckee, C. O., Montgomery, J., Kortok, M. M., Newbold, C. I., and Marsh, K., 2007. An approach to classifying sequence tags sampled from Plasmodium falciparum var genes. Mol Biochem Parasitol 154**,** 98-102.

Bull, P. C., Lowe, B. S., Kortok, M., Molyneux, C. S., Newbold, C. I., and Marsh, K., 1998. Parasite antigens on the infected red cell surface are targets for naturally acquired immunity to malaria. Nat Med 4**,** 358-360.

Bultrini, E., Brick, K., Mukherjee, S., Zhang, Y., Silvestrini, F., Alano, P., and Pizzi, E., 2009. Revisiting the Plasmodium falciparum RIFIN family: from comparative genomics to 3D-model prediction. BMC Genomics 10**,** 445.

Cabral, F. J., and Wunderlich, G., 2009. Transcriptional memory and switching in the Plasmodium falciparumrif gene family. Mol Biochem Parasitol 168**,** 186-190.

Calis, J. C., Phiri, K. S., Faragher, E. B., Brabin, B. J., Bates, I., Cuevas, L. E., de Haan, R. J., Phiri, A. I., Malange, P., Khoka, M., Hulshof, P. J., van Lieshout, L., Beld, M. G., Teo, Y. Y., Rockett, K. A., Richardson, A., Kwiatkowski, D. P., Molyneux, M. E., and van Hensbroek, M. B., 2008. Severe anemia in Malawian children. N Engl J Med 358**,** 888-899.

Carlson, J., Ekre, H. P., Helmby, H., Gysin, J., Greenwood, B. M., and Wahlgren, M., 1992. Disruption of Plasmodium falciparum erythrocyte rosettes by standard heparin and heparin devoid of anticoagulant activity. Am J Trop Med Hyg 46**,** 595-602.

Carlson, J., Helmby, H., Hill, A. V., Brewster, D., Greenwood, B. M., and Wahlgren, M., 1990. Human cerebral malaria: association with erythrocyte rosetting and lack of anti-rosetting antibodies. Lancet 336**,** 1457-1460.

Carvalho, L. J., 2010. Murine cerebral malaria: how far from human cerebral malaria? Trends Parasitol 26**,** 271-272.

Casals-Pascual, C., Allen, S., Allen, A., Kai, O., Lowe, B., Pain, A., and Roberts, D. J., 2001. Short report: codon 125 polymorphism of CD31 and susceptibility to malaria. Am J Trop Med Hyg 65**,** 736-737.

Chakravorty, S. J., and Craig, A., 2005. The role of ICAM-1 in Plasmodium falciparum cytoadherence. Eur J Cell Biol 84**,** 15-27.

Chakravorty, S. J., Hughes, K. R., and Craig, A. G., 2008. Host response to cytoadherence in Plasmodium falciparum. Biochem Soc Trans 36**,** 221-228.

Cham, G. K., Turner, L., Lusingu, J., Vestergaard, L., Mmbando, B. P., Kurtis, J. D., Jensen, A. T., Salanti, A., Lavstsen, T., and Theander, T., 2009. Sequential, ordered acquisition of antibodies to Plasmodium falciparum erythrocyte membrane protein 1 domains. J Immunol 183**,** 3356-3363.

Chattopadhyay, R., Taneja, T., Chakrabarti, K., Pillai, C. R., and Chitnis, C. E., 2004. Molecular analysis of the cytoadherence phenotype of a Plasmodium falciparum field isolate that binds intercellular adhesion molecule-1. Mol Biochem Parasitol 133**,** 255-265.

Chen, Q., Barragan, A., Fernandez, V., Sundstrom, A., Schlichtherle, M., Sahlen, A., Carlson, J., Datta, S., and Wahlgren, M., 1998a. Identification of Plasmodium falciparum erythrocyte membrane protein 1 (PfEMP1) as the rosetting ligand of the malaria parasite P. falciparum. J Exp Med 187**,** 15-23.

Chen, Q., Fernandez, V., Sundstrom, A., Schlichtherle, M., Datta, S., Hagblom, P., and Wahlgren, M., 1998b. Developmental selection of var gene expression in Plasmodium falciparum. Nature 394**,** 392-395.

Chen, Q., Heddini, A., Barragan, A., Fernandez, V., Pearce, S. F., and Wahlgren, M., 2000. The semiconserved head structure of Plasmodium falciparum erythrocyte membrane protein 1 mediates binding to multiple independent host receptors. J Exp Med 192**,** 1-10.

Chen, Q., Pettersson, F., Vogt, A. M., Schmidt, B., Ahuja, S., Liljeström, P., and Wahlgren, M., 2004. Immunization with PfEMP1-DBL1alpha generates antibodies that disrupt rosettes and protect against the sequestration of Plasmodium falciparum-infected erythrocytes. Vaccine 22**,** 2701-2712.

Chotivanich, K., Sritabal, J., Udomsangpetch, R., Newton, P., Stepniewska, K. A., Ruangveerayuth, R., Looareesuwan, S., Roberts, D. J., and White, N. J., 2004. Platelet-induced autoagglutination of Plasmodium falciparum-infected red blood cells and disease severity in Thailand. J Infect Dis 189**,** 1052-1055.

Chou, S., Jensen, B. C., Parsons, M., Alber, T., and Grundner, C., 2010. The Trypanosoma brucei life cycle switch TbPTP1 is structurally conserved and dephosphorylates the nucleolar protein, NOPP44/46. J Biol Chem.

Cohuet, A., Harris, C., Robert, V., and Fontenille, D., 2010. Evolutionary forces on Anopheles: what makes a malaria vector? Trends Parasitol 26**,** 130-136.

Combes, V., Coltel, N., Faille, D., Wassmer, S. C., and Grau, G. E., 2006. Cerebral malaria: role of microparticles and platelets in alterations of the blood-brain barrier. Int J Parasitol 36**,** 541-546.

Combes, V., El-Assaad, F., Faille, D., Jambou, R., Hunt, N. H., and Grau, G. E., 2010. Microvesiculation and cell interactions at the brain-endothelial interface in cerebral malaria pathogenesis. Prog Neurobiol 91**,** 140-151.

Combes, V., Rosenkranz, A. R., Redard, M., Pizzolato, G., Lepidi, H., Vestweber, D., Mayadas, T. N., and Grau, G. E., 2004. Pathogenic role of P-selectin in experimental cerebral malaria: importance of the endothelial compartment. Am J Pathol 164**,** 781-786.

Cooke, B. M., Buckingham, D. W., Glenister, F. K., Fernandez, K. M., Bannister, L. H., Marti, M., Mohandas, N., and Coppel, R. L., 2006. A Maurer's cleft-associated protein is essential for expression of the major malaria virulence antigen on the surface of infected red blood cells. J Cell Biol 172**,** 899-908.

Cox, F. E., 2002. History of human parasitology. Clin Microbiol Rev 15**,** 595-612.

Coyne, C. B., Kim, K. S., and Bergelson, J. M., 2007. Poliovirus entry into human brain microvascular cells requires receptor-induced activation of SHP-2. EMBO J 26**,** 4016-4028.

Craig, A., Fernandez-Reyes, D., Mesri, M., McDowall, A., Altieri, D. C., Hogg, N., and Newbold, C., 2000. A functional analysis of a natural variant of intercellular adhesion molecule-1 (ICAM-1Kilifi). Hum Mol Genet 9**,** 525-530.

Crawley, J., Chu, C., Mtove, G., and Nosten, F., 2010. Malaria in children. Lancet 375**,** 1468-1481.

Cui, X., and Churchill, G. A., 2003. Statistical tests for differential expression in cDNA microarray experiments. Genome Biol 4**,** 210.

Curtidor, H., Garcia, J., Vanegas, M., Puentes, F., Forero, M., and Patarroyo, M. E., 2008. Identification of peptides with high red blood cell and hepatocyte

binding activity in the Plasmodium falciparum multi-stage invasion proteins: PfSPATR and MCP-1. Biochimie 90, 1750-1759.

Dahlback, M., Nielsen, M. A., and Salanti, A., Can any lessons be learned from the ambiguous glycan binding of PfEMP1 domains? Trends Parasitol 26, 230-235.

Daily, J. P., Le Roch, K. G., Sarr, O., Ndiaye, D., Lukens, A., Zhou, Y., Ndir, O., Mboup, S., Sultan, A., Winzeler, E. A., and Wirth, D. F., 2005. In vivo transcriptome of Plasmodium falciparum reveals overexpression of transcripts that encode surface proteins. J Infect Dis 191, 1196-1203.

David, P. H., Hommel, M., Miller, L. H., Udeinya, I. J., and Oligino, L. D., 1983. Parasite sequestration in Plasmodium falciparum malaria: spleen and antibody modulation of cytoadherence of infected erythrocytes. Proc Natl Acad Sci U S A 80, 5075-5079.

Day, N. P., Hien, T. T., Schollaardt, T., Loc, P. P., Chuong, L. V., Chau, T. T., Mai, N. T., Phu, N. H., Sinh, D. X., White, N. J., and Ho, M., 1999. The prognostic and pathophysiologic role of pro- and antiinflammatory cytokines in severe malaria. J Infect Dis 180, 1288-1297.

Day, N. P., Phu, N. H., Mai, N. T., Chau, T. T., Loc, P. P., Chuong, L. V., Sinh, D. X., Holloway, P., Hien, T. T., and White, N. J., 2000. The pathophysiologic and prognostic significance of acidosis in severe adult malaria. Crit Care Med 28, 1833-1840.

de Koning-Ward, T. F., Gilson, P. R., Boddey, J. A., Rug, M., Smith, B. J., Papenfuss, A. T., Sanders, P. R., Lundie, R. J., Maier, A. G., Cowman, A. F., and Crabb, B. S., 2009. A newly discovered protein export machine in malaria parasites. Nature 459, 945-949.

Delehedde, M., Lyon, M., Sergeant, N., Rahmoune, H., and Fernig, D. G., 2001. Proteoglycans: pericellular and cell surface multireceptors that integrate external stimuli in the mammary gland. J Mammary Gland Biol Neoplasia 6, 253-273.

Dobson, M. J., 1994. Malaria in England: a geographical and historical perspective. Parassitologia 36, 35-60.

Dondorp, A. M., Ince, C., Charunwatthana, P., Hanson, J., van Kuijen, A., Faiz, M. A., Rahman, M. R., Hasan, M., Bin Yunus, E., Ghose, A., Ruangveerayut, R., Limmathurotsakul, D., Mathura, K., White, N. J., and Day, N. P., 2008a. Direct in vivo assessment of microcirculatory dysfunction in severe falciparum malaria. J Infect Dis 197, 79-84.

Dondorp, A. M., Kager, P. A., Vreeken, J., and White, N. J., 2000. Abnormal blood flow and red blood cell deformability in severe malaria. Parasitol Today (Regul Ed) 16, 228-232.

Dondorp, A. M., Lee, S. J., Faiz, M. A., Mishra, S., Price, R., Tjitra, E., Than, M., Htut, Y., Mohanty, S., Yunus, E. B., Rahman, R., Nosten, F., Anstey, N. M., Day, N. P., and White, N. J., 2008b. The relationship between age and the manifestations of and mortality associated with severe malaria. CLIN INFECT DIS 47, 151-157.

Dorovini-Zis, K., Prameya, R., and Bowman, P. D., 1991. Culture and characterization of microvascular endothelial cells derived from human brain. Lab Invest 64, 425-436.

Doumbo, O. K., Thera, M. A., Kone, A. K., Raza, A., Tempest, L. J., Lyke, K. E., Plowe, C. V., and Rowe, J. A., 2009. High levels of Plasmodium falciparum rosetting in all clinical forms of severe malaria in African children. Am J Trop Med Hyg 81**,** 987-993.

Duffy, M. F., Brown, G. V., Basuki, W., Krejany, E. O., Noviyanti, R., Cowman, A. F., and Reeder, J. C., 2002. Transcription of multiple var genes by individual, trophozoite-stage Plasmodium falciparum cells expressing a chondroitin sulphate A binding phenotype. Mol Microbiol 43**,** 1285-1293.

Duraisingh, M. T., Voss, T. S., Marty, A. J., Duffy, M. F., Good, R. T., Thompson, J. K., Freitas-Junior, L. H., Scherf, A., Crabb, B. S., and Cowman, A. F., 2005. Heterochromatin silencing and locus repositioning linked to regulation of virulence genes in Plasmodium falciparum, Cell, pp. 13-24.

Durr, E., Yu, J., Krasinska, K. M., Carver, L. A., Yates, J. R., Testa, J. E., Oh, P., and Schnitzer, J. E., 2004. Direct proteomic mapping of the lung microvascular endothelial cell surface in vivo and in cell culture. Nat Biotechnol 22**,** 985-992.

Dzikowski, R., Frank, M., and Deitsch, K., 2006a. Mutually exclusive expression of virulence genes by malaria parasites is regulated independently of antigen production, PLoS Pathog, pp. e22.

Dzikowski, R., Frank, M., and Deitsch, K., 2006b. Mutually exclusive expression of virulence genes by malaria parasites is regulated independently of antigen production. PLoS Pathog 2**,** e22.

Dzikowski, R., Li, F., Amulic, B., Eisberg, A., Frank, M., Patel, S., Wellems, T. E., and Deitsch, K. W., 2007. Mechanisms underlying mutually exclusive expression of virulence genes by malaria parasites, EMBO Rep, pp. 959-965.

Eda, S., Lawler, J., and Sherman, I. W., 1999. Plasmodium falciparum-infected erythrocyte adhesion to the type 3 repeat domain of thrombospondin-1 is mediated by a modified band 3 protein. Mol Biochem Parasitol 100**,** 195-205.

Eda, S., and Sherman, I. W., 2002. Cytoadherence of malaria-infected red blood cells involves exposure of phosphatidylserine. Cell Physiol Biochem 12**,** 373-384.

Eda, S., and Sherman, I. W., 2004. Plasmodium falciparum-infected erythrocytes bind to the RGD motif of fibronectin via the band 3-related adhesin. Experimental Parasitology 107**,** 157-162.

Eddy, S. R., 1995. Multiple alignment using hidden Markov models. Proc Int Conf Intell Syst Mol Biol 3**,** 114-120.

Egan, T. J., 2002. Physico-chemical aspects of hemozoin (malaria pigment) structure and formation. J Inorg Biochem 91**,** 19-26.

Eksi, S., Haile, Y., Furuya, T., Ma, L., Su, X., and Williamson, K. C., 2005. Identification of a subtelomeric gene family expressed during the asexual-sexual stage transition in Plasmodium falciparum. Mol Biochem Parasitol 143**,** 90-99.

Essien, E. M., and Ebhota, M. I., 1983. Platelet secretory activities in acute malaria (Plasmodium falciparum) infection. Acta Haematol 70**,** 183-188.

Faille, D., Combes, V., Mitchell, A. J., Fontaine, A., Juhan-Vague, I., Alessi, M. C., Chimini, G., Fusaï, T., and Grau, G. E., 2009a. Platelet microparticles: a new player in malaria parasite cytoadherence to human brain endothelium. FASEB J.

Faille, D., El-Assaad, F., Alessi, M. C., Fusai, T., Combes, V., and Grau, G. E., 2009b. Platelet-endothelial cell interactions in cerebral malaria: the end of a cordial understanding. Thromb Haemost 102**,** 1093-1102.

Falk, N., Kaestli, M., Qi, W., Ott, M., Baea, K., Cortes, A., and Beck, H. P., 2009. Analysis of Plasmodium falciparum var genes expressed in children from Papua New Guinea. J Infect Dis 200**,** 347-356.

Fandeur, T., Vazeux, G., and Mercereau-Puijalon, O., 1993. The virulent Saimiri-adapted Palo Alto strain of Plasmodium falciparum does not express the ring-infected erythrocyte surface antigen. Mol Biochem Parasitol 60**,** 241-248.

Fernandez, V., Treutiger, C. J., Nash, G. B., and Wahlgren, M., 1998. Multiple adhesive phenotypes linked to rosetting binding of erythrocytes in Plasmodium falciparum malaria. Infect Immun 66**,** 2969-2975.

Fernandez-Reyes, D., Craig, A. G., Kyes, S. A., Peshu, N., Snow, R. W., Berendt, A. R., Marsh, K., and Newbold, C. I., 1997. A high frequency African coding polymorphism in the N-terminal domain of ICAM-1 predisposing to cerebral malaria in Kenya. Hum Mol Genet 6**,** 1357-1360.

Flueck, C., Bartfai, R., Volz, J., Niederwieser, I., Salcedo-Amaya, A. M., Alako, B. T., Ehlgen, F., Ralph, S. A., Cowman, A. F., Bozdech, Z., Stunnenberg, H. G., and Voss, T. S., 2009. Plasmodium falciparum heterochromatin protein 1 marks genomic loci linked to phenotypic variation of exported virulence factors. PLoS Pathog 5**,** e1000569.

Frank, M., Dzikowski, R., Amulic, B., and Deitsch, K., 2007. Variable switching rates of malaria virulence genes are associated with chromosomal position. Mol Microbiol 64**,** 1486-1498.

Frevert, U., Sinnis, P., Cerami, C., Shreffler, W., Takacs, B., and Nussenzweig, V., 1993. Malaria circumsporozoite protein binds to heparan sulfate proteoglycans associated with the surface membrane of hepatocytes. J Exp Med 177**,** 1287-1298.

Fry, A. E., Auburn, S., Diakite, M., Green, A., Richardson, A., Wilson, J., Jallow, M., Sisay-Joof, F., Pinder, M., Griffiths, M. J., Peshu, N., Williams, T. N., Marsh, K., Molyneux, M. E., Taylor, T. E., Rockett, K. A., and Kwiatkowski, D. P., 2008. Variation in the ICAM1 gene is not associated with severe malaria phenotypes. Genes Immun 9**,** 462-469.

Gamain, B., Smith, J. D., Miller, L. H., and Baruch, D. I., 2001. Modifications in the CD36 binding domain of the Plasmodium falciparum variant antigen are responsible for the inability of chondroitin sulfate A adherent parasites to bind CD36. Blood 97**,** 3268-3274.

Gardner, M. J., Hall, N., Fung, E., White, O., Berriman, M., Hyman, R. W., Carlton, J. M., Pain, A., Nelson, K. E., Bowman, S., Paulsen, I. T., James, K., Eisen, J. A., Rutherford, K., Salzberg, S. L., Craig, A., Kyes, S., Chan, M. S., Nene, V., Shallom, S. J., Suh, B., Peterson, J., Angiuoli, S., Pertea, M., Allen, J., Selengut, J., Haft, D., Mather, M. W., Vaidya, A. B., Martin, D. M., Fairlamb,

A. H., Fraunholz, M. J., Roos, D. S., Ralph, S. A., McFadden, G. I., Cummings, L. M., Subramanian, G. M., Mungall, C., Venter, J. C., Carucci, D. J., Hoffman, S. L., Newbold, C., Davis, R. W., Fraser, C. M., and Barrell, B., 2002. Genome sequence of the human malaria parasite Plasmodium falciparum. Nature 419, 498-511.

Gatton, M. L., Peters, J. M., Gresty, K., Fowler, E. V., Chen, N., and Cheng, Q., 2006. Detection Sensitivity And Quantitation Of Plasmodium Falciparum Var Gene Transcripts By Real-Time Rt-Pcr In Comparison With Conventional Rt-Pcr. Am J Trop Med Hyg 75, 212-218.

Gaur, D., Mayer, D. C., and Miller, L. H., 2004. Parasite ligand-host receptor interactions during invasion of erythrocytes by Plasmodium merozoites. Int J Parasitol 34, 1413-1429.

Gazzinelli, R. T., and Denkers, E. Y., 2006. Protozoan encounters with Toll-like receptor signalling pathways: implications for host parasitism. Nat Rev Immunol 6, 895-906.

Ge, Y., and Elghetany, M. T., 2005. CD36: a multiligand molecule. Lab Hematol 11, 31-37.

Genrich, G. L., Guarner, J., Paddock, C. D., Shieh, W. J., Greer, P. W., Barnwell, J. W., and Zaki, S. R., 2007. Fatal malaria infection in travelers: novel immunohistochemical assays for the detection of Plasmodium falciparum in tissues and implications for pathogenesis. Am J Trop Med Hyg 76, 251-259.

Gimenez, F., Barraud de Lagerie, S., Fernandez, C., Pino, P., and Mazier, D., 2003. Tumor necrosis factor alpha in the pathogenesis of cerebral malaria. Cell Mol Life Sci 60, 1623-1635.

Gingras, M. C., Roussel, E., Bruner, J. M., Branch, C. D., and Moser, R. P., 1995. Comparison of cell adhesion molecule expression between glioblastoma multiforme and autologous normal brain tissue. J Neuroimmunol 57, 143-153.

Glushakova, S., Yin, D., Li, T., and Zimmerberg, J., 2005. Membrane transformation during malaria parasite release from human red blood cells. Curr Biol 15, 1645-1650.

Goldring, J. D., Molyneux, M. E., Taylor, T., Wirima, J., and Hommel, M., 1992. Plasmodium falciparum: diversity of isolates from Malawi in their cytoadherence to melanoma cells and monocytes in vitro. Br J Haematol 81, 413-418.

Golnitz, U., Albrecht, L., and Wunderlich, G., 2008. Var transcription profiling of Plasmodium falciparum 3D7: assignment of cytoadherent phenotypes to dominant transcripts. Malar J 7, 14.

Gordon, M., Guralnik, M., Kaneko, Y., Mimura, T., Goodgame, J., and Lang, W., 1995. Further clinical studies of curdlan sulfate (CRDS)--an anti-HIV agent. J Med 26, 97-131.

Grau, G. E., Taylor, T. E., Molyneux, M. E., Wirima, J. J., Vassalli, P., Hommel, M., and Lambert, P. H., 1989. Tumor necrosis factor and disease severity in children with falciparum malaria. N Engl J Med 320, 1586-1591.

Gupta, K., Gupta, P., Wild, R., Ramakrishnan, S., and Hebbel, R. P., 1999a. Binding and displacement of vascular endothelial growth factor (VEGF) by

thrombospondin: effect on human microvascular endothelial cell proliferation and angiogenesis. Angiogenesis 3**,** 147-158.

Gupta, S., Snow, R. W., Donnelly, C., and Newbold, C., 1999b. Acquired immunity and postnatal clinical protection in childhood cerebral malaria. Proc Biol Sci 266**,** 33-38.

Haase, S., Cabrera, A., Langer, C., Treeck, M., Struck, N., Herrmann, S., Jansen, P. W., Bruchhaus, I., Bachmann, A., Dias, S., Cowman, A. F., Stunnenberg, H. G., Spielmann, T., and Gilberger, T. W., 2008. Characterization of a conserved rhoptry-associated leucine zipper-like protein in the malaria parasite Plasmodium falciparum. Infect Immun 76**,** 879-887.

Haldar, K., and Mohandas, N., 2009. Malaria, erythrocytic infection, and anemia. Hematology Am Soc Hematol Educ Program**,** 87-93.

Haldar, K., Murphy, S. C., Milner, D. A., and Taylor, T. E., 2007. Malaria: mechanisms of erythrocytic infection and pathological correlates of severe disease. Annu Rev Pathol 2**,** 217-249.

Hall, N., Karras, M., Raine, J. D., Carlton, J. M., Kooij, T. W., Berriman, M., Florens, L., Janssen, C. S., Pain, A., Christophides, G. K., James, K., Rutherford, K., Harris, B., Harris, D., Churcher, C., Quail, M. A., Ormond, D., Doggett, J., Trueman, H. E., Mendoza, J., Bidwell, S. L., Rajandream, M. A., Carucci, D. J., Yates, J. R., 3rd, Kafatos, F. C., Janse, C. J., Barrell, B., Turner, C. M., Waters, A. P., and Sinden, R. E., 2005. A comprehensive survey of the Plasmodium life cycle by genomic, transcriptomic, and proteomic analyses. Science 307**,** 82-86.

Hatabu, T., Kawazu, S., Aikawa, M., and Kano, S., 2003a. Binding of Plasmodium falciparum-infected erythrocytes to the membrane-bound form of Fractalkine/CX3CL1. Proc Natl Acad Sci U S A 100**,** 15942-15946.

Hatabu, T., Kawazu, S., Aikawa, M., and Kano, S., 2003b. Binding of Plasmodium falciparum-infected erythrocytes to the membrane-bound form of fractalkine/CX(3)CL1. Proceedings of the National Academy of Sciences of the United States of America 100**,** 15942-15946.

Havlik, I., Looareesuwan, S., Vannaphan, S., Wilairatana, P., Krudsood, S., Thuma, P. E., Kozbor, D., Watanabe, N., and Kaneko, Y., 2005. Curdlan sulphate in human severe/cerebral Plasmodium falciparum malaria. Trans R Soc Trop Med Hyg 99**,** 333-340.

Havlik, I., Rovelli, S., and Kaneko, Y., 1994. The effect of curdlan sulphate on in vitro growth of Plasmodium falciparum. Trans R Soc Trop Med Hyg 88**,** 686-687.

Hay, S. I., Okiro, E. A., Gething, P. W., Patil, A. P., Tatem, A. J., Guerra, C. A., and Snow, R. W., 2010. Estimating the global clinical burden of Plasmodium falciparum Malaria in 2007. PLoS Med 7**,** e1000290.

Heddini, A., Chen, Q. J., Obiero, J., Kai, O., Fernandez, V., Marsh, K., Muller, W. A., and Wahlgren, M., 2001a. Binding of Plasmodium falciparum-infected erythrocytes to soluble platelet endothelial cell adhesion molecule-1 (PECAM-1/CD31): Frequent recognition by clinical isolates. American Journal of Tropical Medicine and Hygiene 65**,** 47-51.

Heddini, A., Pettersson, F., Kai, O., Shafi, J., Obiero, J., Chen, Q., Barragan, A., Wahlgren, M., and Marsh, K., 2001b. Fresh isolates from children with

severe Plasmodium falciparum malaria bind to multiple receptors. Infect Immun 69, 5849-5856.

Heddini, A., Pettersson, F., Kai, O., Shafi, J., Obiero, J., Chen, Q. J., Barragan, A., Wahlgren, M., and Marsh, K., 2001c. Fresh isolates from children with severe Plasmodium falciparum malaria bind to multiple receptors. Infection and Immunity 69, 5849-5856.

Henn, V., Slupsky, J. R., Grafe, M., Anagnostopoulos, I., Forster, R., Muller-Berghaus, G., and Kroczek, R. A., 1998. CD40 ligand on activated platelets triggers an inflammatory reaction of endothelial cells. Nature 391, 591-594.

Herricks, T., Antia, M., and Rathod, P. K., 2009. Deformability limits of Plasmodium falciparum-infected red blood cells. Cell Microbiol.

Hiller, N. L., Bhattacharjee, S., van Ooij, C., Liolios, K., Harrison, T., Lopez-Estrano, C., and Haldar, K., 2004. A host-targeting signal in virulence proteins reveals a secretome in malarial infection. Science 306, 1934-1937.

Ho, M., Davis, T. M., Silamut, K., Bunnag, D., and White, N. J., 1991. Rosette formation of Plasmodium falciparum-infected erythrocytes from patients with acute malaria. Infect Immun 59, 2135-2139.

Ho, M., Schollaardt, T., Niu, X., Looareesuwan, S., Patel, K. D., and Kubes, P., 1998. Characterization of Plasmodium falciparum-infected erythrocyte and P-selectin interaction under flow conditions. Blood 91, 4803-4809.

Ho, M., and White, N. J., 1999. Molecular mechanisms of cytoadherence in malaria. Am J Physiol 276, C1231-1242.

Horrocks, P., Pinches, R., Christodoulou, Z., Kyes, S. A., and Newbold, C. I., 2004. Variable var transition rates underlie antigenic variation in malaria. Proc Natl Acad Sci U S A 101, 11129-11134.

Howell, D. P., Levin, E. A., Springer, A. L., Kraemer, S. M., Phippard, D. J., Schief, W. R., and Smith, J. D., 2008. Mapping a common interaction site used by Plasmodium falciparum Duffy binding-like domains to bind diverse host receptors. Mol Microbiol 67, 78-87.

Howitt, C. A., Wilinski, D., Llinas, M., Templeton, T. J., Dzikowski, R., and Deitsch, K. W., 2009. Clonally variant gene families in Plasmodium falciparum share a common activation factor. Mol Microbiol 73, 1171-1185.

Hu, G., Cabrera, A., Kono, M., Mok, S., Chaal, B. K., Haase, S., Engelberg, K., Cheemadan, S., Spielmann, T., Preiser, P. R., Gilberger, T. W., and Bozdech, Z., 2009. Transcriptional profiling of growth perturbations of the human malaria parasite Plasmodium falciparum. Nat Biotechnol.

Hu, G., Llinas, M., Li, J., Preiser, P. R., and Bozdech, Z., 2007. Selection of long oligonucleotides for gene expression microarrays using weighted rank-sum strategy. BMC Bioinformatics 8, 350.

Huang, S. H., Chen, Y. H., Fu, Q., Stins, M., Wang, Y., Wass, C., and Kim, K. S., 1999. Identification and characterization of an Escherichia coli invasion gene locus, ibeB, required for penetration of brain microvascular endothelial cells. Infect Immun 67, 2103-2109.

Huang, S. H., Wan, Z. S., Chen, Y. H., Jong, A. Y., and Kim, K. S., 2001. Further characterization of Escherichia coli brain microvascular endothelial cell

invasion gene ibeA by deletion, complementation, and protein expression. J Infect Dis 183**,** 1071-1078.

Hviid, L., 2010. The role of Plasmodium falciparum variant surface antigens in protective immunity and vaccine development. Human vaccines 6.

Hviid, L., and Staalsoe, T., 2004. Malaria immunity in infants: a special case of a general phenomenon? Trends Parasitol 20**,** 66-72.

Idro, R., Jenkins, N. E., and Newton, C. R., 2005. Pathogenesis, clinical features, and neurological outcome of cerebral malaria. Lancet Neurol 4**,** 827-840.

Ikenoue, N., Kawazu, S., Hatabu, T., Villacorte, E. A., Rivera, P. T., and Kano, S., 2002. PCR-amplification, sequencing, and comparison of the var/PfEMP-1 gene from the blood of patients with falciparum malaria in the Philippines. Southeast Asian J Trop Med Public Health 33 Suppl 3**,** 8-13.

Iuvone, T., D'Acquisto, F., Carnuccio, R., and Di Rosa, M., 1996. Nitric oxide inhibits LPS-induced tumor necrosis factor synthesis in vitro and in vivo. Life Sci 59**,** PL207-211.

Jemmely, N. Y., Niang, M., and Preiser, P. R., 2010. Small variant surface antigens and Plasmodium evasion of immunity. Future Microbiol 5**,** 663-682.

Jensen, A. T., Magistrado, P., Sharp, S., Joergensen, L., Lavstsen, T., Chiucchiuini, A., Salanti, A., Vestergaard, L. S., Lusingu, J. P., Hermsen, R., Sauerwein, R., Christensen, J., Nielsen, M., Hviid, L., Sutherland, C., Staalsoe, T., and Theander, T., 2004a. Plasmodium falciparum associated with severe childhood malaria preferentially expresses PfEMP1 encoded by group A var genes. J Exp Med 199**,** 1179-1190.

Jensen, A. T., Magistrado, P., Sharp, S., Joergensen, L., Lavstsen, T., Chiucchiuini, A., Salanti, A., Vestergaard, L. S., Lusingu, J. P., Hermsen, R., Sauerwein, R., Christensen, J., Nielsen, M. A., Hviid, L., Sutherland, C., Staalsoe, T., and Theander, T. G., 2004b. Plasmodium falciparum associated with severe childhood malaria preferentially expresses PfEMP1 encoded by group A var genes. J Exp Med 199**,** 1179-1190.

Jimenez, B., Volpert, O. V., Crawford, S. E., Febbraio, M., Silverstein, R. L., and Bouck, N., 2000. Signals leading to apoptosis-dependent inhibition of neovascularization by thrombospondin-1. Nat Med 6**,** 41-48.

Joannin, N., Abhiman, S., Sonnhammer, E. L., and Wahlgren, M., 2008. Sub-grouping and sub-functionalization of the RIFIN multi-copy protein family. BMC Genomics 9**,** 19.

Joergensen, L., Vestergaard, L. S., Turner, L., Magistrado, P., Lusingu, J. P., Lemnge, M., Theander, T. G., and Jensen, A. T., 2007. 3D7-Derived Plasmodium falciparum erythrocyte membrane protein 1 is a frequent target of naturally acquired antibodies recognizing protein domains in a particular pattern independent of malaria transmission intensity. J Immunol 178**,** 428-435.

Jong, A., Wu, C. H., Shackleford, G. M., Kwon-Chung, K. J., Chang, Y. C., Chen, H. M., Ouyang, Y., and Huang, S. H., 2008. Involvement of human CD44 during Cryptococcus neoformans infection of brain microvascular endothelial cells. Cell Microbiol 10**,** 1313-1326.

Kaestli, M., Cockburn, I. A., Cortes, A., Baea, K., Rowe, J. A., and Beck, H. P., 2006. Virulence of malaria is associated with differential expression of

Plasmodium falciparum var gene subgroups in a case-control study. J Infect Dis 193, 1567-1574.

Kaestli, M., Cortes, A., Lagog, M., Ott, M., and Beck, H. P., 2004. Longitudinal assessment of Plasmodium falciparum var gene transcription in naturally infected asymptomatic children in Papua New Guinea. J Infect Dis 189, 1942-1951.

Kalmbach, Y., Rottmann, M., Kombila, M., Kremsner, P. G., Beck, H. P., and Kun, J. F., 2010. Differential var gene expression in children with malaria and antidromic effects on host gene expression. J Infect Dis 202, 313-317.

Kaneko, Y., Yoshida, O., Nakagawa, R., Yoshida, T., Date, M., Ogihara, S., Shioya, S., Matsuzawa, Y., Nagashima, N., Irie, Y., and et al., 1990. Inhibition of HIV-1 infectivity with curdlan sulfate in vitro. Biochem Pharmacol 39, 793-797.

Kato, K., Sudo, A., Kobayashi, K., Tohya, Y., and Akashi, H., 2008. Characterization of Plasmodium falciparum protein kinase 2. Mol Biochem Parasitol 162, 87-95.

Kaul, D. K., Roth, E. F., Nagel, R. L., Howard, R. J., and Handunnetti, S. M., 1991. Rosetting of Plasmodium falciparum-infected red blood cells with uninfected red blood cells enhances microvascular obstruction under flow conditions. Blood 78, 812-819.

Kaviratne, M., Khan, S. M., Jarra, W., and Preiser, P. R., 2002. Small variant STEVOR antigen is uniquely located within Maurer's clefts in Plasmodium falciparum-infected red blood cells. Eukaryot Cell 1, 926-935.

Khan, N. A., Kim, Y., Shin, S., and Kim, K. S., 2007. FimH-mediated Escherichia coli K1 invasion of human brain microvascular endothelial cells. Cell Microbiol 9, 169-178.

Kidgell, C., Volkman, S. K., Daily, J., Borevitz, J. O., Plouffe, D., Zhou, Y., Johnson, J. R., Le Roch, K., Sarr, O., Ndir, O., Mboup, S., Batalov, S., Wirth, D. F., and Winzeler, E. A., 2006. A systematic map of genetic variation in Plasmodium falciparum. PLoS Pathog 2, e57.

Kikuchi, M., Looareesuwan, S., Ubalee, R., Tasanor, O., Suzuki, F., Wattanagoon, Y., Na-Bangchang, K., Kimura, A., Aikawa, M., and Hirayama, K., 2001. Association of adhesion molecule PECAM-1/CD31 polymorphism with susceptibility to cerebral malaria in Thais. Parasitol Int 50, 235-239.

Kim, K. J., Chung, J. W., and Kim, K. S., 2005. 67-kDa laminin receptor promotes internalization of cytotoxic necrotizing factor 1-expressing Escherichia coli K1 into human brain microvascular endothelial cells. J Biol Chem 280, 1360-1368.

Kirchgatter, K., and Portillo Hdel, A., 2002. Association of severe noncerebral Plasmodium falciparum malaria in Brazil with expressed PfEMP1 DBL1 alpha sequences lacking cysteine residues. Mol Med 8, 16-23.

Klein, M. M., Gittis, A. G., Su, H. P., Makobongo, M. O., Moore, J. M., Singh, S., Miller, L. H., and Garboczi, D. N., 2008. The cysteine-rich interdomain region from the highly variable plasmodium falciparum erythrocyte membrane protein-1 exhibits a conserved structure. PLoS Pathog 4, e1000147.

Klein, N. J., Shennan, G. I., Heyderman, R. S., and Levin, M., 1992. Alteration in glycosaminoglycan metabolism and surface charge on human umbilical

vein endothelial cells induced by cytokines, endotoxin and neutrophils. J Cell Sci 102 (Pt 4), 821-832.

Kraemer, S. M., Kyes, S. A., Aggarwal, G., Springer, A. L., Nelson, S. O., Christodoulou, Z., Smith, L. M., Wang, W., Levin, E., Newbold, C. I., Myler, P. J., and Smith, J. D., 2007. Patterns of gene recombination shape var gene repertoires in Plasmodium falciparum: comparisons of geographically diverse isolates. BMC Genomics 8, 45.

Kraling, B. M., and Bischoff, J., 1998. A simplified method for growth of human microvascular endothelial cells results in decreased senescence and continued responsiveness to cytokines and growth factors. In Vitro Cell Dev Biol Anim 34, 308-315.

Krump-Konvalinkova, V., Bittinger, F., Unger, R. E., Peters, K., Lehr, H. A., and Kirkpatrick, C. J., 2001. Generation of human pulmonary microvascular endothelial cell lines. Lab Invest 81, 1717-1727.

Kuehn, A., and Pradel, G., 2010. The coming-out of malaria gametocytes. J Biomed Biotechnol 2010, 976827.

Kyes, S., Christodoulou, Z., Pinches, R., Kriek, N., Horrocks, P., and Newbold, C., 2007. Plasmodium falciparum var gene expression is developmentally controlled at the level of RNA polymerase II-mediated transcription initiation, Mol Microbiol, pp. 1237-1247.

Kyes, S., Pinches, R., and Newbold, C., 2000. A simple RNA analysis method shows var and rif multigene family expression patterns in Plasmodium falciparum. Mol Biochem Parasitol 105, 311-315.

Kyes, S. A., Christodoulou, Z., Raza, A., Horrocks, P., Pinches, R., Rowe, J. A., and Newbold, C. I., 2003. A well-conserved Plasmodium falciparum var gene shows an unusual stage-specific transcript pattern. Mol Microbiol 48, 1339-1348.

Kyes, S. A., Rowe, J. A., Kriek, N., and Newbold, C. I., 1999. Rifins: a second family of clonally variant proteins expressed on the surface of red cells infected with Plasmodium falciparum. Proc Natl Acad Sci U S A 96, 9333-9338.

Kyriacou, H. M., Steen, K. E., Raza, A., Arman, M., Warimwe, G., Bull, P. C., Havlik, I., and Rowe, J. A., 2007. In vitro inhibition of Plasmodium falciparum rosette formation by Curdlan sulfate. Antimicrobial Agents and Chemotherapy 51, 1321-1326.

Kyriacou, H. M., Stone, G. N., Challis, R. J., Raza, A., Lyke, K. E., Thera, M. A., Kone, A. K., Doumbo, O. K., Plowe, C. V., and Rowe, J. A., 2006. Differential var gene transcription in Plasmodium falciparum isolates from patients with cerebral malaria compared to hyperparasitaemia. Mol Biochem Parasitol 150, 211-218.

Lambros, C., and Vanderberg, J. P., 1979. Synchronization of Plasmodium falciparum erythrocytic stages in culture. J Parasitol 65, 418-420.

Larkin, D., de Laat, B., Jenkins, P. V., Bunn, J., Craig, A. G., Terraube, V., Preston, R. J., Donkor, C., Grau, G. E., van Mourik, J. A., and O'Donnell, J. S., 2009. Severe Plasmodium falciparum malaria is associated with circulating ultra-large von Willebrand multimers and ADAMTS13 inhibition. PLoS Pathog 5, e1000349.

Lavazec, C., Sanyal, S., and Templeton, T. J., 2006. Hypervariability within the Rifin, Stevor and Pfmc-2TM superfamilies in Plasmodium falciparum. Nucleic Acids Res 34, 6696-6707.

Lavstsen, T., Salanti, A., Jensen, A. T., Arnot, D. E., and Theander, T., 2003a. Sub-grouping of Plasmodium falciparum 3D7 var genes based on sequence analysis of coding and non-coding regions. Malar J 2, 27.

Lavstsen, T., Salanti, A., Jensen, A. T., Arnot, D. E., and Theander, T. G., 2003b. Sub-grouping of Plasmodium falciparum 3D7 var genes based on sequence analysis of coding and non-coding regions. Malar J 2, 27.

Law, P. J., Claudel-Renard, C., Joubert, F., Louw, A. I., and Berger, D. K., 2008. MADIBA: a web server toolkit for biological interpretation of Plasmodium and plant gene clusters. BMC Genomics 9, 105.

Le Roch, K. G., Johnson, J. R., Florens, L., Zhou, Y., Santrosyan, A., Grainger, M., Yan, S. F., Williamson, K. C., Holder, A. A., Carucci, D. J., Yates, J. R., 3rd, and Winzeler, E. A., 2004. Global analysis of transcript and protein levels across the Plasmodium falciparum life cycle. Genome Res 14, 2308-2318.

Leung, Y. F., and Cavalieri, D., 2003. Fundamentals of cDNA microarray data analysis. Trends in Genetics 19, 649-659.

Lin, H., Lee, E., Hestir, K., Leo, C., Huang, M., Bosch, E., Halenbeck, R., Wu, G., Zhou, A., Behrens, D., Hollenbaugh, D., Linnemann, T., Qin, M., Wong, J., Chu, K., Doberstein, S. K., and Williams, L. T., 2008. Discovery of a cytokine and its receptor by functional screening of the extracellular proteome. Science 320, 807-811.

Lindsay, S. W., and Gibson, M. E., 1988. Bednets revisited- old idea, new angle. Parasitol Today 4, 270-272.

Llinas, M., Bozdech, Z., Wong, E. D., Adai, A. T., and DeRisi, J. L., 2006. Comparative whole genome transcriptome analysis of three Plasmodium falciparum strains. Nucleic Acids Res 34, 1166-1173.

Lopez-Rubio, J. J., Gontijo, A. M., Nunes, M. C., Issar, N., Hernandez Rivas, R., and Scherf, A., 2007. 5' flanking region of var genes nucleate histone modification patterns linked to phenotypic inheritance of virulence traits in malaria parasites, Mol Microbiol, pp. 1296-1305.

Luo, J., Kato, M., Wang, H., Bernfield, M., and Bischoff, J., 2001. Heparan sulfate and chondroitin sulfate proteoglycans inhibit E-selectin binding to endothelial cells. J Cell Biochem 80, 522-531.

Lyke, K. E., Burges, R., Cissoko, Y., Sangare, L., Dao, M., Diarra, I., Kone, A., Harley, R., Plowe, C. V., Doumbo, O. K., and Sztein, M. B., 2004. Serum levels of the proinflammatory cytokines interleukin-1 beta (IL-1beta), IL-6, IL-8, IL-10, tumor necrosis factor alpha, and IL-12(p70) in Malian children with severe Plasmodium falciparum malaria and matched uncomplicated malaria or healthy controls. Infect Immun 72, 5630-5637.

Mackinnon, M. J., Li, J., Mok, S., Kortok, M. M., Marsh, K., Preiser, P. R., and Bozdech, Z., 2009. Comparative transcriptional and genomic analysis of Plasmodium falciparum field isolates. PLoS Pathog 5, e1000644.

MacPherson, G. G., Warrell, M. J., White, N. J., Looareesuwan, S., and Warrell, D. A., 1985. Human cerebral malaria. A quantitative ultrastructural analysis of parasitized erythrocyte sequestration. Am J Pathol 119, 385-401.

Maier, A. G., Cooke, B. M., Cowman, A. F., and Tilley, L., 2009. Malaria parasite proteins that remodel the host erythrocyte. Nat Rev Microbiol 7, 341-354.

Maier, A. G., Rug, M., O'Neill, M. T., Brown, M., Chakravorty, S., Szestak, T., Chesson, J., Wu, Y., Hughes, K., Coppel, R. L., Newbold, C., Beeson, J. G., Craig, A., Crabb, B. S., and Cowman, A. F., 2008. Exported proteins required for virulence and rigidity of Plasmodium falciparum-infected human erythrocytes. Cell 134, 48-61.

Maitland, K., 2006. Severe malaria: lessons learned from the management of critical illness in children. Trends Parasitol 22, 457-462.

Maitland, K., and Newton, C. R., 2005. Acidosis of severe falciparum malaria: heading for a shock? Trends Parasitol 21, 11-16.

Marchiafava, E. a. B., A., 1894. On Summer-Autumnal Fever. The New Sydenham Society, London.

Marsh, K., Forster, D., Waruiru, C., Mwangi, I., Winstanley, M., Marsh, V., Newton, C. R., Winstanley, P., Warn, P., and Peshu, N., 1995. Indicators of life-threatening malaria in African children. N Engl J Med 332, 1399-1404.

Marsh, K., Marsh, V. M., Brown, J., Whittle, H. C., and Greenwood, B. M., 1988. Plasmodium falciparum: the behavior of clinical isolates in an in vitro model of infected red blood cell sequestration. Exp Parasitol 65, 202-208.

Marti, M., Good, R. T., Rug, M., Knuepfer, E., and Cowman, A. F., 2004. Targeting malaria virulence and remodeling proteins to the host erythrocyte. Science 306, 1930-1933.

Martins, Y. C., Carvalho, L. J., and Daniel-Ribeiro, C. T., 2009. Challenges in the determination of early predictors of cerebral malaria: lessons from the human disease and the experimental murine models. Neuroimmunomodulation 16, 134-145.

Matin, A., Siddiqui, R., Jung, S. Y., Kim, K. S., Stins, M., and Khan, N. A., 2007. Balamuthia mandrillaris interactions with human brain microvascular endothelial cells in vitro. J Med Microbiol 56, 1110-1115.

Mayor, A., Bir, N., Sawhney, R., Singh, S., Pattnaik, P., Singh, S. K., Sharma, A., and Chitnis, C. E., 2005. Receptor-binding residues lie in central regions of Duffy-binding-like domains involved in red cell invasion and cytoadherence by malaria parasites. Blood 105, 2557-2563.

McCormick, C. J., Craig, A., Roberts, D., Newbold, C. I., and Berendt, A. R., 1997. Intercellular adhesion molecule-1 and CD36 synergize to mediate adherence of Plasmodium falciparum-infected erythrocytes to cultured human microvascular endothelial cells. J Clin Invest 100, 2521-2529.

McGilvray, I. D., Serghides, L., Kapus, A., Rotstein, O. D., and Kain, K. C., 2000. Nonopsonic monocyte/macrophage phagocytosis of Plasmodium falciparum-parasitized erythrocytes: a role for CD36 in malarial clearance. Blood 96, 3231-3240.

McRobert, L., Preiser, P., Sharp, S., Jarra, W., Kaviratne, M., Taylor, M. C., Renia, L., and Sutherland, C. J., 2004. Distinct trafficking and localization of STEVOR proteins in three stages of the Plasmodium falciparum life cycle. Infect Immun 72, 6597-6602.

Medana, I. M., Mai, N. T., Day, N. P., Hien, T. T., Bethell, D., Phu, N. H., Farrar, J., White, N. J., and Turner, G. D., 2001. Cellular stress and injury responses in the brains of adult Vietnamese patients with fatal Plasmodium falciparum malaria. Neuropathol Appl Neurobiol 27**,** 421-433.

Medana, I. M., and Turner, G. D., 2006. Human cerebral malaria and the blood-brain barrier. International Journal for Parasitology 36**,** 555-568.

Mendu, D. R., Katinger, H., Sodroski, J., and Kim, K. S., 2007. HIV-1 envelope protein gp140 binding studies to human brain microvascular endothelial cells. Biochem Biophys Res Commun 363**,** 466-471.

Mercereau-Puijalon, O., Guillotte, M., and Vigan-Womas, I., 2008. Rosetting in Plasmodium falciparum: a cytoadherence phenotype with multiple actors. Transfusion clinique et biologique : journal de la Société française de transfusion sanguine 15**,** 62-71.

Miller, L. H., Hudson-Taylor, D., Gamain, B., and Saul, A. J., 2002. Definition of the minimal domain of CIDR1alpha of Plasmodium falciparum PfEMP1 for binding CD36. Mol Biochem Parasitol 120**,** 321-323.

Mills, J. P., Diez-Silva, M., Quinn, D. J., Dao, M., Lang, M. J., Tan, K. S., Lim, C. T., Milon, G., David, P. H., Mercereau-Puijalon, O., Bonnefoy, S., and Suresh, S., 2007. Effect of plasmodial RESA protein on deformability of human red blood cells harboring Plasmodium falciparum. Proc Natl Acad Sci U S A 104**,** 9213-9217.

Mishra, S. K., and Wiese, L., 2009. Advances in the management of cerebral malaria in adults. Curr Opin Neurol 22**,** 302-307.

Mok, B. W., Ribacke, U., Winter, G., Yip, B. H., Tan, C. S., Fernandez, V., Chen, Q., Nilsson, P., and Wahlgren, M., 2007. Comparative transcriptomal analysis of isogenic Plasmodium falciparum clones of distinct antigenic and adhesive phenotypes. Mol Biochem Parasitol 151**,** 184-192.

Moll, K., Pettersson, F., Vogt, A. M., Jonsson, C., Rasti, N., Ahuja, S., Spangberg, M., Mercereau-Puijalon, O., Arnot, D. E., Wahlgren, M., and Chen, Q., 2007. Generation of cross-protective antibodies against Plasmodium falciparum sequestration by immunization with an erythrocyte membrane protein 1-duffy binding-like 1 alpha domain. Infect Immun 75**,** 211-219.

Montgomery, J., Milner, D. A., Jr., Tse, M. T., Njobvu, A., Kayira, K., Dzamalala, C. P., Taylor, T. E., Rogerson, S. J., Craig, A. G., and Molyneux, M. E., 2006. Genetic analysis of circulating and sequestered populations of Plasmodium falciparum in fatal pediatric malaria. J Infect Dis 194**,** 115-122.

Montgomery, J., Mphande, F. A., Berriman, M., Pain, A., Rogerson, S. J., Taylor, T. E., Molyneux, M. E., and Craig, A., 2007. Differential var gene expression in the organs of patients dying of falciparum malaria. Mol Microbiol.

Muanza, K., Gay, F., Behr, C., and Scherf, A., 1996. Primary culture of human lung microvessel endothelial cells: a useful in vitro model for studying Plasmodium falciparum-infected erythrocyte cytoadherence. Res Immunol 147**,** 149-163.

Nair, M. K., Venkitanarayanan, K., Silbart, L. K., and Kim, K. S., 2009. Outer membrane protein A (OmpA) of Cronobacter sakazakii binds fibronectin

and contributes to invasion of human brain microvascular endothelial cells. Foodborne Pathog Dis 6, 495-501.

Nakamura, K., Hasler, T., Morehead, K., Howard, R. J., and Aikawa, M., 1992. Plasmodium falciparum-infected erythrocyte receptor(s) for CD36 and thrombospondin are restricted to knobs on the erythrocyte surface. J Histochem Cytochem 40, 1419-1422.

Nakano, Y., Fujioka, H., Luc, K. D., Rabbege, J. R., Todd, G. D., Collins, W. E., and Aikawa, M., 1996. A correlation of the sequestration rate of Plasmodium coatneyi-infected erythrocytes in cerebral and subcutaneous tissues of a rhesus monkey. Am J Trop Med Hyg 55, 311-314.

Nakazawa, S., Looareesuwan, S., Fujioka, H., Pongponratn, E., Luc, K. D., Rabbege, J., and Aikawa, M., 1995. A correlation between sequestered parasitized erythrocytes in subcutaneous tissue and cerebral malaria. Am J Trop Med Hyg 53, 544-546.

Narizhneva, N. V., Razorenova, O. V., Podrez, E. A., Chen, J., Chandrasekharan, U. M., DiCorleto, P. E., Plow, E. F., Topol, E. J., and Byzova, T. V., 2005. Thrombospondin-1 up-regulates expression of cell adhesion molecules and promotes monocyte binding to endothelium. FASEB J 19, 1158-1160.

Ndiaye, R., Sakuntabhai, A., Casademont, I., Rogier, C., Tall, A., Trape, J. F., Spiegel, A., Dieye, A., and Julier, C., 2005. Genetic study of ICAM1 in clinical malaria in Senegal. Tissue Antigens 65, 474-480.

Newbold, C., Warn, P., Black, G., Berendt, A., Craig, A., Snow, B., Msobo, M., Peshu, N., and Marsh, K., 1997. Receptor-specific adhesion and clinical disease in Plasmodium falciparum. Am J Trop Med Hyg 57, 389-398.

Newton, C. R., and Krishna, S., 1998. Severe falciparum malaria in children: current understanding of pathophysiology and supportive treatment. Pharmacol Ther 79, 1-53.

Newton, C. R., and Warrell, D. A., 1998. Neurological manifestations of falciparum malaria. Ann Neurol 43, 695-702.

Niang, M., Yan Yam, X., and Preiser, P. R., 2009. The Plasmodium falciparum STEVOR multigene family mediates antigenic variation of the infected erythrocyte. PLoS Pathog 5, e1000307.

Nielsen, M. A., Staalsoe, T., Kurtzhals, J. A., Goka, B. Q., Dodoo, D., Alifrangis, M., Theander, T. G., Akanmori, B. D., and Hviid, L., 2002. Plasmodium falciparum variant surface antigen expression varies between isolates causing severe and nonsevere malaria and is modified by acquired immunity. J Immunol 168, 3444-3450.

Normark, J., Nilsson, D., Ribacke, U., Winter, G., Moll, K., Wheelock, C. E., Bayarugaba, J., Kironde, F., Egwang, T. G., Chen, Q., Andersson, B., and Wahlgren, M., 2007. PfEMP1-DBL1alpha amino acid motifs in severe disease states of Plasmodium falciparum malaria. Proc Natl Acad Sci U S A 104, 15835-15840.

Noviyanti, R., Brown, G. V., Wickham, M. E., Duffy, M. F., Cowman, A. F., and Reeder, J. C., 2001. Multiple var gene transcripts are expressed in Plasmodium falciparum infected erythrocytes selected for adhesion. Mol Biochem Parasitol 114, 227-237.

O'Meara, W. P., Bejon, P., Mwangi, T. W., Okiro, E. A., Peshu, N., Snow, R. W., Newton, C. R., and Marsh, K., 2008. Effect of a fall in malaria transmission on morbidity and mortality in Kilifi, Kenya. Lancet 372**,** 1555-1562.

Ocana-Macchi, M., Bel, M., Guzylack-Piriou, L., Ruggli, N., Liniger, M., McCullough, K. C., Sakoda, Y., Isoda, N., Matrosovich, M., and Summerfield, A., 2009. Hemagglutinin-dependent tropism of H5N1 avian influenza virus for human endothelial cells. J Virol 83**,** 12947-12955.

Ockenhouse, C. F., Betageri, R., Springer, T. A., and Staunton, D. E., 1992. Plasmodium falciparum-infected erythrocytes bind ICAM-1 at a site distinct from LFA-1, Mac-1, and human rhinovirus. Cell 68**,** 63-69.

Ohnishi, K., and Kimura, K., 2001. Serum levels of vascular cell adhesion molecule 1 in the early post-treatment defervescent phase of falciparum malaria. Parasitology Research 87**,** 67-69.

Omer, F. M., and Riley, E. M., 1998. Transforming growth factor beta production is inversely correlated with severity of murine malaria infection. J Exp Med 188**,** 39-48.

Oquendo, P., Hundt, E., Lawler, J., and Seed, B., 1989. CD36 directly mediates cytoadherence of Plasmodium falciparum parasitized erythrocytes. Cell 58**,** 95-101.

Otto, T. D., Wilinski, D., Assefa, S., Keane, T. M., Sarry, L. R., Bohme, U., Lemieux, J., Barrell, B., Pain, A., Berriman, M., Newbold, C., and Llinas, M., 2010. New insights into the blood-stage transcriptome of Plasmodium falciparum using RNA-Seq. Mol Microbiol.

Paccaud, J. P., Carpentier, J. L., and Schifferli, J. A., 1988. Direct evidence for the clustered nature of complement receptors type 1 on the erythrocyte membrane. J Immunol 141**,** 3889-3894.

Pain, A., Ferguson, D. J., Kai, O., Urban, B. C., Lowe, B., Marsh, K., and Roberts, D. J., 2001. Platelet-mediated clumping of Plasmodium falciparum-infected erythrocytes is a common adhesive phenotype and is associated with severe malaria. Proc Natl Acad Sci U S A 98**,** 1805-1810.

Pasloske, B. L., Baruch, D. I., van Schravendijk, M. R., Handunnetti, S. M., Aikawa, M., Fujioka, H., Taraschi, T. F., Gormley, J. A., and Howard, R. J., 1993. Cloning and characterization of a Plasmodium falciparum gene encoding a novel high-molecular weight host membrane-associated protein, PfEMP3. Mol Biochem Parasitol 59**,** 59-72.

Patel, S. N., Serghides, L., Smith, T. G., Febbraio, M., Silverstein, R. L., Kurtz, T. W., Pravenec, M., and Kain, K. C., 2004. CD36 mediates the phagocytosis of Plasmodium falciparum-infected erythrocytes by rodent macrophages. J Infect Dis 189**,** 204-213.

Pearce, J. A., Mills, K., Triglia, T., Cowman, A. F., and Anders, R. F., 2005. Characterisation of two novel proteins from the asexual stage of Plasmodium falciparum, H101 and H103. Mol Biochem Parasitol 139**,** 141-151.

Pei, X., Guo, X., Coppel, R., Mohandas, N., and An, X., 2007. Plasmodium falciparum erythrocyte membrane protein 3 (PfEMP3) destabilizes erythrocyte membrane skeleton. J Biol Chem 282**,** 26754-26758.

Persson, K. E., 2010. Erythrocyte invasion and functionally inhibitory antibodies in Plasmodium falciparum malaria. Acta Trop 114, 138-143.

Peters, J., Fowler, E., Gatton, M., Chen, N., Saul, A., and Cheng, Q., 2002. High diversity and rapid changeover of expressed var genes during the acute phase of Plasmodium falciparum infections in human volunteers. Proc Natl Acad Sci U S A 99, 10689-10694.

Petter, M., Bonow, I., and Klinkert, M. Q., 2008. Diverse expression patterns of subgroups of the rif multigene family during Plasmodium falciparum gametocytogenesis. PLoS ONE 3, e3779.

Petter, M., Haeggstrom, M., Khattab, A., Fernandez, V., Klinkert, M. Q., and Wahlgren, M., 2007. Variant proteins of the Plasmodium falciparum RIFIN family show distinct subcellular localization and developmental expression patterns. Mol Biochem Parasitol 156, 51-61.

Piper, R., Lebras, J., Wentworth, L., Hunt-Cooke, A., Houze, S., Chiodini, P., and Makler, M., 1999. Immunocapture diagnostic assays for malaria using Plasmodium lactate dehydrogenase (pLDH). Am J Trop Med Hyg 60, 109-118.

Pongponratn, E., Riganti, M., Punpoowong, B., and Aikawa, M., 1991. Microvascular sequestration of parasitized erythrocytes in human falciparum malaria: a pathological study. Am J Trop Med Hyg 44, 168-175.

Pongponratn, E., Turner, G. D., Day, N. P., Phu, N. H., Simpson, J. A., Stepniewska, K., Mai, N. T., Viriyavejakul, P., Looareesuwan, S., Hien, T. T., Ferguson, D. J., and White, N. J., 2003. An ultrastructural study of the brain in fatal Plasmodium falciparum malaria. Am J Trop Med Hyg 69, 345-359.

Porta, J., Carota, A., Pizzolato, G. P., Wildi, E., Widmer, M. C., Margairaz, C., and Grau, G. E., 1993. Immunopathological changes in human cerebral malaria. Clin Neuropathol 12, 142-146.

Pouvelle, B., Matarazzo, V., Jurzynski, C., Nemeth, J., Ramharter, M., Rougon, G., and Gysin, J., 2007. Neural cell adhesion molecule, a new cytoadhesion receptor for Plasmodium falciparum-infected erythrocytes capable of aggregation. Infect Immun 75, 3516-3522.

Prakash, D., Fesel, C., Jain, R., Cazenave, P. A., Mishra, G. C., and Pied, S., 2006. Clusters of cytokines determine malaria severity in Plasmodium falciparum-infected patients from endemic areas of Central India. J Infect Dis 194, 198-207.

Prudencio, M., Rodriguez, A., and Mota, M. M., 2006. The silent path to thousands of merozoites: the Plasmodium liver stage. Nat Rev Microbiol 4, 849-856.

Reiff, S. B., and Striepen, B., 2009. Malaria: The gatekeeper revealed. Nature 459, 918-919.

Reitsma, S., Slaaf, D. W., Vink, H., van Zandvoort, M. A., and oude Egbrink, M. G., 2007. The endothelial glycocalyx: composition, functions, and visualization. Pflugers Arch 454, 345-359.

Renia, L., Gruner, A. C., and Snounou, G., 2010. Cerebral malaria: in praise of epistemes. Trends Parasitol 26, 275-277.

Ribaut, C., Berry, A., Chevalley, S., Reybier, K., Morlais, I., Parzy, D., Nepveu, F., Benoit-Vical, F., and Valentin, A., 2008. Concentration and purification by

magnetic separation of the erythrocytic stages of all human Plasmodium species. Malar J 7, 45.

Roberts, D. D., Sherwood, J. A., Spitalnik, S. L., Panton, L. J., Howard, R. J., Dixit, V. M., Frazier, W. A., Miller, L. H., and Ginsburg, V., 1985. Thrombospondin binds falciparum malaria parasitized erythrocytes and may mediate cytoadherence. Nature 318, 64-66.

Robinson, B. A., Welch, T. L., and Smith, J. D., 2003. Widespread functional specialization of Plasmodium falciparum erythrocyte membrane protein 1 family members to bind CD36 analysed across a parasite genome. Mol Microbiol 47, 1265-1278.

Rock, E. P., Roth, E. F., Rojascorona, R. R., Sherwood, J. A., Nagel, R. L., Howard, R. J., and Kaul, D. K., 1988. Thrombospondin Mediates the Cytoadherence of Plasmodium-Falciparum Infected Red-Cells to Vascular Endothelium in Shear-Flow Conditions. Blood 71, 71-75.

Rogerson, S. J., and Carter, R., 2008. Severe vivax malaria: newly recognised or rediscovered. PLoS Med 5, e136.

Rogerson, S. J., Tembenu, R., Dobano, C., Plitt, S., Taylor, T. E., and Molyneux, M. E., 1999. Cytoadherence characteristics of Plasmodium falciparum-infected erythrocytes from Malawian children with severe and uncomplicated malaria. Am J Trop Med Hyg 61, 467-472.

Rothwell, N. J., and Luheshi, G. N., 2000. Interleukin 1 in the brain: biology, pathology and therapeutic target. Trends Neurosci 23, 618-625.

Rottmann, M., Lavstsen, T., Mugasa, J. P., Kaestli, M., Jensen, A. T., Muller, D., Theander, T., and Beck, H. P., 2006. Differential expression of var gene groups is associated with morbidity caused by Plasmodium falciparum infection in Tanzanian children. Infect Immun 74, 3904-3911.

Rowe, A., Berendt, A. R., Marsh, K., and Newbold, C. I., 1994. Plasmodium falciparum: a family of sulphated glycoconjugates disrupts erythrocyte rosettes. Exp Parasitol 79, 506-516.

Rowe, A., Obeiro, J., Newbold, C. I., and Marsh, K., 1995. Plasmodium falciparum rosetting is associated with malaria severity in Kenya. Infect Immun 63, 2323-2326.

Rowe, A. K., Rowe, S. Y., Snow, R. W., Korenromp, E. L., Schellenberg, J. R., Stein, C., Nahlen, B. L., Bryce, J., Black, R. E., and Steketee, R. W., 2006. The burden of malaria mortality among African children in the year 2000. Int J Epidemiol 35, 691-704.

Rowe, J. A., Claessens, A., Corrigan, R. A., and Arman, M., 2009a. Adhesion of Plasmodium falciparum-infected erythrocytes to human cells: molecular mechanisms and therapeutic implications. Expert reviews in molecular medicine 11, e16.

Rowe, J. A., Handel, I. G., Thera, M. A., Deans, A. M., Lyke, K. E., Koné, A., Diallo, D. A., Raza, A., Kai, O., Marsh, K., Plowe, C. V., Doumbo, O. K., and Moulds, J. M., 2007. Blood group O protects against severe Plasmodium falciparum malaria through the mechanism of reduced rosetting. Proc Natl Acad Sci USA 104, 17471-17476.

Rowe, J. A., Moulds, J. M., Newbold, C. I., and Miller, L. H., 1997. P. falciparum rosetting mediated by a parasite-variant erythrocyte membrane protein and complement-receptor 1. Nature 388, 292-295.

Rowe, J. A., Opi, D. H., and Williams, T. N., 2009b. Blood groups and malaria: fresh insights into pathogenesis and identification of targets for intervention. Curr Opin Hematol 16, 480-487.

Rowe, J. A., Rogerson, S. J., Raza, A., Moulds, J. M., Kazatchkine, M. D., Marsh, K., Newbold, C. I., Atkinson, J. P., and Miller, L. H., 2000. Mapping of the region of complement receptor (CR) 1 required for Plasmodium falciparum rosetting and demonstration of the importance of CR1 in rosetting in field isolates. J Immunol 165, 6341-6346.

Rug, M., Prescott, S. W., Fernandez, K. M., Cooke, B. M., and Cowman, A. F., 2006. The role of KAHRP domains in knob formation and cytoadherence of P falciparum-infected human erythrocytes. Blood 108, 370-378.

Rug, M., Wickham, M. E., Foley, M., Cowman, A. F., and Tilley, L., 2004. Correct promoter control is needed for trafficking of the ring-infected erythrocyte surface antigen to the host cytosol in transfected malaria parasites. Infect Immun 72, 6095-6105.

Saeed, A. I., Bhagabati, N. K., Braisted, J. C., Liang, W., Sharov, V., Howe, E. A., Li, J., Thiagarajan, M., White, J. A., and Quackenbush, J., 2006. TM4 microarray software suite. Methods Enzymol 411, 134-193.

Saeed, A. I., Sharov, V., White, J., Li, J., Liang, W., Bhagabati, N., Braisted, J., Klapa, M., Currier, T., Thiagarajan, M., Sturn, A., Snuffin, M., Rezantsev, A., Popov, D., Ryltsov, A., Kostukovich, E., Borisovsky, I., Liu, Z., Vinsavich, A., Trush, V., and Quackenbush, J., 2003. TM4: a free, open-source system for microarray data management and analysis. Biotechniques 34, 374-378.

Sallares, R., Bouwman, A., and Anderung, C., 2004. The spread of malaria to Southern Europe in antiquity: new approaches to old problems. Med Hist 48, 311-328.

Sam-Yellowe, T. Y., 2009. The role of the Maurer's clefts in protein transport in Plasmodium falciparum. Trends Parasitol 25, 277-284.

Sam-Yellowe, T. Y., Florens, L., Johnson, J. R., Wang, T., Drazba, J. A., Le Roch, K. G., Zhou, Y., Batalov, S., Carucci, D. J., Winzeler, E. A., and Yates, J. R., 3rd, 2004. A Plasmodium gene family encoding Maurer's cleft membrane proteins: structural properties and expression profiling. Genome Res 14, 1052-1059.

Sargeant, T. J., Marti, M., Caler, E., Carlton, J. M., Simpson, K., Speed, T. P., and Cowman, A. F., 2006. Lineage-specific expansion of proteins exported to erythrocytes in malaria parasites. Genome Biol 7, R12.

Saridaki, T., Frohlich, K. S., Braun-Breton, C., and Lanzer, M., 2009. Export of PfSBP1 to the Plasmodium falciparum Maurer's clefts. Traffic 10, 137-152.

Schreiber, N., Khattab, A., Petter, M., Marks, F., Adjei, S., Kobbe, R., May, J., and Klinkert, M. Q., 2008. Expression of Plasmodium falciparum 3D7 STEVOR proteins for evaluation of antibody responses following malaria infections in naive infants. Parasitology 135, 155-167.

Senczuk, A. M., Reeder, J. C., Kosmala, M. M., and Ho, M., 2001. Plasmodium falciparum erythrocyte membrane protein 1 functions as a ligand for P-selectin. Blood 98**,** 3132-3135.

Serghides, L., and Kain, K. C., 2001. Peroxisome proliferator-activated receptor gamma-retinoid X receptor agonists increase CD36-dependent phagocytosis of Plasmodium falciparum-parasitized erythrocytes and decrease malaria-induced TNF-alpha secretion by monocytes/macrophages. J Immunol 166**,** 6742-6748.

Serghides, L., Smith, T. G., Patel, S. N., and Kain, K. C., 2003. CD36 and malaria: friends or foes? Trends Parasitol 19**,** 461-469.

Serirom, S., Raharjo, W. H., Chotivanich, K., Loareesuwan, S., Kubes, P., and Ho, M., 2003. Anti-adhesive effect of nitric oxide on Plasmodium falciparum cytoadherence under flow. Am J Pathol 162**,** 1651-1660.

Seydel, K. B., Milner, D. A., Kamiza, S. B., Molyneux, M. E., and Taylor, T. E., 2006. The distribution and intensity of parasite sequestration in comatose Malawian children. J Infect Dis 194**,** 208-205.

Sharling, L., 2004. Novel approaches for the characterisation of Plasmodium variant surface antigens, Edinburgh.

Sharling, L., Enevold, A., Sowa, K. M., Staalsoe, T., and Arnot, D. E., 2004. Antibodies from malaria-exposed pregnant women recognize trypsin resistant epitopes on the surface of Plasmodium falciparum-infected erythrocytes selected for adhesion to chondroitin sulphate A. Malar J 3**,** 31.

Shen, J., Ham, R. G., and Karmiol, S., 1995. Expression of adhesion molecules in cultured human pulmonary microvascular endothelial cells. Microvasc Res 50**,** 360-372.

Shin, S., Lu, G., Cai, M., and Kim, K. S., 2005. Escherichia coli outer membrane protein A adheres to human brain microvascular endothelial cells. Biochem Biophys Res Commun 330**,** 1199-1204.

Shock, J. L., Fischer, K. F., and DeRisi, J. L., 2007. Whole-genome analysis of mRNA decay in Plasmodium falciparum reveals a global lengthening of mRNA half-life during the intra-erythrocytic development cycle. Genome Biol 8**,** R134.

Siano, J. P., Grady, K. K., Millet, P., Swerlick, R. A., and Wick, T. M., 1997. Plasmodium falciparum: soluble thrombospondin increases cytoadherence of parasitized erythrocytes to human microvascular endothelium under shear flow conditions. Exp Parasitol 87**,** 69-72.

Siano, J. P., Grady, K. K., Millet, P., and Wick, T. M., 1998. Short report: Plasmodium falciparum: Cytoadherence to alpha(v)beta(3) on human microvascular endothelial cells. American Journal of Tropical Medicine and Hygiene 59**,** 77-79.

Silamut, K., Phu, N. H., Whitty, C., Turner, G. D., Louwrier, K., Mai, N. T., Simpson, J. A., Hien, T. T., and White, N. J., 1999. A quantitative analysis of the microvascular sequestration of malaria parasites in the human brain. Am J Pathol 155**,** 395-410.

Silva, M. D., Cooke, B. M., Guillotte, M., Buckingham, D. W., Sauzet, J. P., Le Scanf, C., Contamin, H., David, P., Mercereau-Puijalon, O., and Bonnefoy, S., 2005.

A role for the Plasmodium falciparum RESA protein in resistance against heat shock demonstrated using gene disruption. Mol Microbiol 56, 990-1003.

Singh, B., Ho, M., Looareesuwan, S., Mathai, E., Warrell, D. A., and Hommel, M., 1988. Plasmodium falciparum: inhibition/reversal of cytoadherence of Thai isolates to melanoma cells by local immune sera. Clin Exp Immunol 72, 145-150.

Slupsky, J. R., Kalbas, M., Willuweit, A., Henn, V., Kroczek, R. A., and Muller-Berghaus, G., 1998. Activated platelets induce tissue factor expression on human umbilical vein endothelial cells by ligation of CD40. Thromb Haemost 80, 1008-1014.

Smargiasso, N., Gabelica, V., Damblon, C., Rosu, F., De Pauw, E., Teulade-Fichou, M. P., Rowe, J. A., and Claessens, A., 2009. Putative DNA G-quadruplex formation within the promoters of Plasmodium falciparum var genes. BMC Genomics 10, 362.

Smith, J. D., Craig, A. G., Kriek, N., Hudson-Taylor, D., Kyes, S., Fagan, T., Fagen, T., Pinches, R., Baruch, D. I., Newbold, C. I., and Miller, L. H., 2000a. Identification of a Plasmodium falciparum intercellular adhesion molecule-1 binding domain: a parasite adhesion trait implicated in cerebral malaria. Proc Natl Acad Sci USA 97, 1766-1771.

Smith, J. D., Subramanian, G., Gamain, B., Baruch, D. I., and Miller, L. H., 2000b. Classification of adhesive domains in the Plasmodium falciparum erythrocyte membrane protein 1 family. Mol Biochem Parasitol 110, 293-310.

Snow, R. W., Schellenberg, J. R., Peshu, N., Forster, D., Newton, C. R., Winstanley, P. A., Mwangi, I., Waruiru, C., Warn, P. A., Newbold, C., and et al., 1993. Periodicity and space-time clustering of severe childhood malaria on the coast of Kenya. Trans R Soc Trop Med Hyg 87, 386-390.

Snowden, F. M., 2006. The Conquest of Malaria: Italy, 1900-1962. Yale University Press.

Spielmann, T., Hawthorne, P. L., Dixon, M. W., Hannemann, M., Klotz, K., Kemp, D. J., Klonis, N., Tilley, L., Trenholme, K. R., and Gardiner, D. L., 2006. A cluster of ring stage-specific genes linked to a locus implicated in cytoadherence in Plasmodium falciparum codes for PEXEL-negative and PEXEL-positive proteins exported into the host cell. Mol Biol Cell 17, 3613-3624.

Springer, A. L., Smith, L. M., Mackay, D. Q., Nelson, S. O., and Smith, J. D., 2004. Functional interdependence of the DBLbeta domain and c2 region for binding of the Plasmodium falciparum variant antigen to ICAM-1. Mol Biochem Parasitol 137, 55-64.

Spycher, C., Klonis, N., Spielmann, T., Kump, E., Steiger, S., Tilley, L., and Beck, H. P., 2003. MAHRP-1, a novel Plasmodium falciparum histidine-rich protein, binds ferriprotoporphyrin IX and localizes to the Maurer's clefts. Journal of Biological Chemistry 278, 35373-35383.

Spycher, C., Rug, M., Klonis, N., Ferguson, D. J. P., Cowman, A. F., Beck, H. P., and Tilley, L., 2006. Genesis of and trafficking to the Maurer's clefts of

Plasmodium falciparum-infected erythrocytes. Molecular and Cellular Biology 26, 4074-4085.

Spycher, C., Rug, M., Pachlatko, E., Hanssen, E., Ferguson, D., Cowman, A. F., Tilley, L., and Beck, H. P., 2008. The Maurer's cleft protein MAHRP1 is essential for trafficking of PfEMP1 to the surface of Plasmodium falciparum-infected erythrocytes. Molecular Microbiology 68, 1300-1314.

Srivastava, K., Cockburn, I. A., Swaim, A., Thompson, L. E., Tripathi, A., Fletcher, C. A., Shirk, E. M., Sun, H., Kowalska, M. A., Fox-Talbot, K., Sullivan, D., Zavala, F., and Morrell, C. N., 2008. Platelet factor 4 mediates inflammation in experimental cerebral malaria. Cell Host Microbe 4, 179-187.

Staalsoe, T., Nielsen, M. A., Vestergaard, L. S., Jensen, A. T., Theander, T. G., and Hviid, L., 2003. In vitro selection of Plasmodium falciparum 3D7 for expression of variant surface antigens associated with severe malaria in African children. Parasite Immunol 25, 421-427.

Steer, A. C., Batzloff, M. R., Mulholland, K., and Carapetis, J. R., 2009. Group A streptococcal vaccines: facts versus fantasy. Curr Opin Infect Dis 22, 544-552.

Stevenson, M. M., Gros, P., Olivier, M., Fortin, A., and Serghides, L., 2010. Cerebral malaria: human versus mouse studies. Trends Parasitol 26, 274-275.

Stins, M. F., Gilles, F., and Kim, K. S., 1997. Selective expression of adhesion molecules on human brain microvascular endothelial cells. J Neuroimmunol 76, 81-90.

Sutherland, C. J., Tanomsing, N., Nolder, D., Oguike, M., Jennison, C., Pukrittayakamee, S., Dolecek, C., Hien, T. T., do Rosario, V. E., Arez, A. P., Pinto, J., Michon, P., Escalante, A. A., Nosten, F., Burke, M., Lee, R., Blaze, M., Otto, T. D., Barnwell, J. W., Pain, A., Williams, J., White, N. J., Day, N. P., Snounou, G., Lockhart, P. J., Chiodini, P. L., Imwong, M., and Polley, S. D., 2010. Two nonrecombining sympatric forms of the human malaria parasite Plasmodium ovale occur globally. J Infect Dis 201, 1544-1550.

Suwanarusk, R., Cooke, B. M., Dondorp, A. M., Silamut, K., Sattabongkot, J., White, N. J., and Udomsangpetch, R., 2004. The deformability of red blood cells parasitized by Plasmodium falciparum and P. vivax. J Infect Dis 189, 190-194.

Swerlick, R. A., Brown, E. J., Xu, Y., Lee, K. H., Manos, S., and Lawley, T. J., 1992a. Expression and modulation of the vitronectin receptor on human dermal microvascular endothelial cells. J Invest Dermatol 99, 715-722.

Swerlick, R. A., Lee, K. H., Wick, T. M., and Lawley, T. J., 1992b. Human dermal microvascular endothelial but not human umbilical vein endothelial cells express CD36 in vivo and in vitro. J Immunol 148, 78-83.

Taylor, H. M., Kyes, S. A., Harris, D., Kriek, N., and Newbold, C. I., 2000a. A study of var gene transcription in vitro using universal var gene primers. Mol Biochem Parasitol 105, 13-23.

Taylor, H. M., Kyes, S. A., and Newbold, C. I., 2000b. Var gene diversity in Plasmodium falciparum is generated by frequent recombination events. Mol Biochem Parasitol 110, 391-397.

Taylor, K. R., and Gallo, R. L., 2006. Glycosaminoglycans and their proteoglycans: host-associated molecular patterns for initiation and modulation of inflammation. FASEB J 20, 9-22.

Taylor, T. E., Fu, W. J., Carr, R. A., Whitten, R. O., Mueller, J. S., Fosiko, N. G., Lewallen, S., Liomba, N. G., and Molyneux, M. E., 2004. Differentiating the pathologies of cerebral malaria by postmortem parasite counts. Nat Med 10, 143-145.

Tembo, D., and Montgomery, J., 2010. Var gene expression and human Plasmodium pathogenesis. Future Microbiol 5, 801-815.

Templeton, T. J., 2009. The varieties of gene amplification, diversification and hypervariability in the human malaria parasite, Plasmodium falciparum. Mol Biochem Parasitol.

Tenenbaum, T., Bloier, C., Adam, R., Reinscheid, D. J., and Schroten, H., 2005. Adherence to and invasion of human brain microvascular endothelial cells are promoted by fibrinogen-binding protein FbsA of Streptococcus agalactiae. Infect Immun 73, 4404-4409.

Tenenbaum, T., Spellerberg, B., Adam, R., Vogel, M., Kim, K. S., and Schroten, H., 2007. Streptococcus agalactiae invasion of human brain microvascular endothelial cells is promoted by the laminin-binding protein Lmb. Microbes Infect 9, 714-720.

Tham, W. H., Payne, P. D., Brown, G. V., and Rogerson, S. J., 2007. Identification of basic transcriptional elements required for rif gene transcription. Int J Parasitol 37, 605-615.

Trager, W., 1993. FCR-3, chloroquine resistance and cross-contamination of culture lines of Plasmodium falciparum. Parasitol Today 9, 127; author reply 127.

Traore, B., Muanza, K., Looareesuwan, S., Supavej, S., Khusmith, S., Danis, M., Viriyavejakul, P., and Gay, F., 2000. Cytoadherence characteristics of Plasmodium falciparum isolates in Thailand using an in vitro human lung endothelial cells model. American Journal of Tropical Medicine and Hygiene 62, 38-44.

Tripathi, A. K., Sullivan, D. J., and Stins, M. F., 2006. Plasmodium falciparum-infected erythrocytes increase intercellular adhesion molecule 1 expression on brain endothelium through NF-kappaB. Infect Immun 74, 3262-3270.

Tripathi, A. K., Sullivan, D. J., and Stins, M. F., 2007. Plasmodium falciparum-infected erythrocytes decrease the integrity of human blood-brain barrier endothelial cell monolayers. J Infect Dis 195, 942-950.

Tse, M. T., Chakrabarti, K., Gray, C., Chitnis, C. E., and Craig, A., 2004. Divergent binding sites on intercellular adhesion molecule-1 (ICAM-1) for variant Plasmodium falciparum isolates. Mol Microbiol 51, 1039-1049.

Tuikue Ndam, N., Bischoff, E., Proux, C., Lavstsen, T., Salanti, A., Guitard, J., Nielsen, M. A., Coppee, J. Y., Gaye, A., Theander, T., David, P. H., and Deloron, P., 2008. Plasmodium falciparum transcriptome analysis reveals pregnancy malaria associated gene expression. PLoS ONE 3, e1855.

Tuikue Ndam, N., and Deloron, P., 2008. Towards a vaccine against pregnancy-associated malaria. Parasite 15, 515-521.

Turner, D. P., Marietou, A. G., Johnston, L., Ho, K. K., Rogers, A. J., Wooldridge, K. G., and Ala'Aldeen, D. A., 2006. Characterization of MspA, an immunogenic autotransporter protein that mediates adhesion to epithelial and endothelial cells in Neisseria meningitidis. Infect Immun 74**,** 2957-2964.

Turner, G. D., Morrison, H., Jones, M., Davis, T. M., Looareesuwan, S., Buley, I. D., Gatter, K. C., Newbold, C. I., Pukritayakamee, S., Nagachinta, B., and et al., 1994. An immunohistochemical study of the pathology of fatal malaria. Evidence for widespread endothelial activation and a potential role for intercellular adhesion molecule-1 in cerebral sequestration. Am J Pathol 145**,** 1057-1069.

Tusher, V. G., Tibshirani, R., and Chu, G., 2001. Significance analysis of microarrays applied to the ionizing radiation response. Proc Natl Acad Sci U S A 98**,** 5116-5121.

Udomsangpetch, R., Pipitaporn, B., Krishna, S., Angus, B., Pukrittayakamee, S., Bates, I., Suputtamongkol, Y., Kyle, D. E., and White, N. J., 1996a. Antimalarial drugs reduce cytoadherence and resetting of Plasmodium falciparum. Journal of Infectious Diseases 173**,** 691-698.

Udomsangpetch, R., Reinhardt, P. H., Schollaardt, T., Elliott, J. F., Kubes, P., and Ho, M., 1997. Promiscuity of clinical Plasmodium falciparum isolates for multiple adhesion molecules under flow conditions. Journal of Immunology 158**,** 4358-4364.

Udomsangpetch, R., Taylor, B. J., Looareesuwan, S., White, N. J., Elliott, J. F., and Ho, M., 1996b. Receptor specificity of clinical Plasmodium falciparum isolates: Nonadherence to cell-bound E-selectin and vascular cell adhesion molecule-1. Blood 88**,** 2754-2760.

Unkmeir, A., Latsch, K., Dietrich, G., Wintermeyer, E., Schinke, B., Schwender, S., Kim, K. S., Eigenthaler, M., and Frosch, M., 2002. Fibronectin mediates Opc-dependent internalization of Neisseria meningitidis in human brain microvascular endothelial cells. Mol Microbiol 46**,** 933-946.

van der Heyde, H. C., Nolan, J., Combes, V., Gramaglia, I., and Grau, G. E., 2006. A unified hypothesis for the genesis of cerebral malaria: sequestration, inflammation and hemostasis leading to microcirculatory dysfunction. Trends Parasitol 22**,** 503-508.

van Hensbroek, M. B., Palmer, A., Onyiorah, E., Schneider, G., Jaffar, S., Dolan, G., Memming, H., Frenkel, J., Enwere, G., Bennett, S., Kwiatkowski, D., and Greenwood, B., 1996. The effect of a monoclonal antibody to tumor necrosis factor on survival from childhood cerebral malaria. J Infect Dis 174**,** 1091-1097.

van Ooij, C., Tamez, P., Bhattacharjee, S., Hiller, N. L., Harrison, T., Liolios, K., Kooij, T., Ramesar, J., Balu, B., Adams, J., Waters, A. P., Janse, C. J., and Haldar, K., 2008. The malaria secretome: from algorithms to essential function in blood stage infection. PLoS Pathog 4**,** e1000084.

Verducci, J. S., Melfi, V. F., Lin, S. L., Wang, Z., Roy, S., and Sen, C. K., 2006. Microarray analysis of gene expression: considerations in data mining and statistical treatment. Physiological Genomics 25**,** 355-363.

Viebig, N. K., Wulbrand, U., Forster, R., Andrews, K. T., Lanzer, M., and Knolle, P. A., 2005. Direct activation of human endothelial cells by Plasmodium falciparum-infected erythrocytes. Infect Immun 73**,** 3271-3277.

Vigan-Womas, I., Guillotte, M., Le Scanf, C., Igonet, S., Petres, S., Juillerat, A., Badaut, C., Nato, F., Schneider, A., Lavergne, A., Contamin, H., Tall, A., Baril, L., Bentley, G. A., and Mercereau-Puijalon, O., 2008. An in vivo and in vitro model of Plasmodium falciparum rosetting and autoagglutination mediated by varO, a group A var gene encoding a frequent serotype. Infect Immun 76**,** 5565-5580.

Vignali, M., McKinlay, A., LaCount, D. J., Chettier, R., Bell, R., Sahasrabudhe, S., Hughes, R. E., and Fields, S., 2008. Interaction of an atypical Plasmodium falciparum ETRAMP with human apolipoproteins. Malar J 7**,** 211.

Vlachou, D., Schlegelmilch, T., Runn, E., Mendes, A., and Kafatos, F. C., 2006. The developmental migration of Plasmodium in mosquitoes. Curr Opin Genet Dev 16**,** 384-391.

Vogt, A. M., Barragan, A., Chen, Q., Kironde, F., Spillmann, D., and Wahlgren, M., 2003. Heparan sulfate on endothelial cells mediates the binding of Plasmodium falciparum-infected erythrocytes via the DBL1alpha domain of PfEMP1. Blood 101**,** 2405-2411.

Voss, T. S., Kaestli, M., Vogel, D., Bopp, S., and Beck, H. P., 2003. Identification of nuclear proteins that interact differentially with Plasmodium falciparum var gene promoters, Mol Microbiol, pp. 1593-1607.

Voss, T. S., Tonkin, C. J., Marty, A. J., Thompson, J. K., Healer, J., Crabb, B. S., and Cowman, A. F., 2007. Alterations in local chromatin environment are involved in silencing and activation of subtelomeric var genes in Plasmodium falciparum, Mol Microbiol, pp. 139-150.

Waller, K. L., Stubberfield, L. M., Dubljevic, V., Nunomura, W., An, X., Mason, A. J., Mohandas, N., Cooke, B. M., and Coppel, R. L., 2007. Interactions of Plasmodium falciparum erythrocyte membrane protein 3 with the red blood cell membrane skeleton. Biochim Biophys Acta 1768**,** 2145-2156.

Walliker, D., Quakyi, I. A., Wellems, T. E., McCutchan, T. F., Szarfman, A., London, W. T., Corcoran, L. M., Burkot, T. R., and Carter, R., 1987. Genetic analysis of the human malaria parasite Plasmodium falciparum. Science 236**,** 1661-1666.

Wang, C., Magistrado, P., Nielsen, M., Theander, T., and Lavstsen, T., 2009a. Preferential transcription of conserved rif genes in two phenotypically distinct Plasmodium falciparum parasite lines. International Journal for Parasitology 39**,** 655-664.

Wang, C. W., Magistrado, P. A., Nielsen, M. A., Theander, T. G., and Lavstsen, T., 2009b. Preferential transcription of conserved rif genes in two phenotypically distinct Plasmodium falciparum parasite lines. Int J Parasitol 39**,** 655-664.

Wang, H., Wang, Q., Pape, U. J., Shen, B., Huang, J., Wu, B., and Li, X., 2010. Systematic investigation of global coordination among mRNA and protein in cellular society. BMC Genomics 11**,** 364.

Warimwe, G. M., Keane, T. M., Fegan, G., Musyoki, J. N., Newton, C. R., Pain, A., Berriman, M., Marsh, K., and Bull, P. C., 2009. Plasmodium falciparum var gene expression is modified by host immunity. Proc Natl Acad Sci U S A.

Wassmer, S. C., Cianciolo, G. J., Combes, V., and Grau, G. E., 2005. Inhibition of endothelial activation: a new way to treat cerebral malaria? PLoS Med 2**,** e245.

Wassmer, S. C., Cianciolo, G. J., Combes, V., and Grau, G. E., 2006a. [LMP-420, a new therapeutic approach for cerebral malaria?]. Med Sci (Paris) 22**,** 343-345.

Wassmer, S. C., Combes, V., Candal, F. J., Juhan-Vague, I., and Grau, G. E., 2006b. Platelets potentiate brain endothelial alterations induced by Plasmodium falciparum. Infect Immun 74**,** 645-653.

Wassmer, S. C., de Souza, J. B., Frere, C., Candal, F. J., Juhan-Vague, I., and Grau, G. E., 2006c. TGF-beta1 released from activated platelets can induce TNF-stimulated human brain endothelium apoptosis: a new mechanism for microvascular lesion during cerebral malaria. J Immunol 176**,** 1180-1184.

Wassmer, S. C., Lepolard, C., Traore, B., Pouvelle, B., Gysin, J., and Grau, G. E., 2004. Platelets reorient Plasmodium falciparum-infected erythrocyte cytoadhesion to activated endothelial cells. J Infect Dis 189**,** 180-189.

Wassmer, S. C., Taylor, T., Maclennan, C. A., Kanjala, M., Mukaka, M., Molyneux, M. E., and Grau, G. E., 2008. Platelet-induced clumping of Plasmodium falciparum-infected erythrocytes from Malawian patients with cerebral malaria-possible modulation in vivo by thrombocytopenia. J Infect Dis 197**,** 72-78.

Waterkeyn, J. G., Wickham, M. E., Davern, K. M., Cooke, B. M., Coppel, R. L., Reeder, J. C., Culvenor, J. G., Waller, R. F., and Cowman, A. F., 2000. Targeted mutagenesis of Plasmodium falciparum erythrocyte membrane protein 3 (PfEMP3) disrupts cytoadherence of malaria-infected red blood cells. EMBO J 19**,** 2813-2823.

Weinberg, J. B., Lopansri, B. K., Mwaikambo, E., and Granger, D. L., 2008. Arginine, nitric oxide, carbon monoxide, and endothelial function in severe malaria. Curr Opin Infect Dis 21**,** 468-475.

White, N. J., Turner, G. D., Medana, I. M., Dondorp, A. M., and Day, N. P., 2010. The murine cerebral malaria phenomenon. Trends Parasitol 26**,** 11-15.

WHO, 2000. Severe falciparum malaria. World Health Organization, Communicable Diseases Cluster. Trans R Soc Trop Med Hyg 94 Suppl 1**,** S1-90.

WHO, 2009. World malaria report 2009.

Wilairatana, P., Riganti, M., Puchadapirom, P., Punpoowong, B., Vannaphan, S., Udomsangpetch, R., Krudsood, S., Brittenham, G. M., and Looareesuwan, S., 2000. Prognostic significance of skin and subcutaneous fat sequestration of parasites in severe falciparum malaria. Southeast Asian J Trop Med Public Health 31**,** 203-212.

Wilson, N. O., Huang, M. B., Anderson, W., Bond, V., Powell, M., Thompson, W. E., Armah, H. B., Adjei, A. A., Gyasi, R., Tettey, Y., and Stiles, J. K., 2008. Soluble factors from Plasmodium falciparum-infected erythrocytes

induce apoptosis in human brain vascular endothelial and neuroglia cells. Mol Biochem Parasitol 162**,** 172-176.

Winter, G., Kawai, S., Haeggstrom, M., Kaneko, O., von Euler, A., Kawazu, S., Palm, D., Fernandez, V., and Wahlgren, M., 2005. SURFIN is a polymorphic antigen expressed on Plasmodium falciparum merozoites and infected erythrocytes. J Exp Med 201**,** 1853-1863.

Xiao, L., Yang, C., Dorovini-Zis, K., Tandon, N. N., Ades, E. W., Lal, A. A., and Udhayakumar, V., 1996. Plasmodium falciparum: involvement of additional receptors in the cytoadherence of infected erythrocytes to microvascular endothelial cells. Exp Parasitol 84**,** 42-55.

Xu, Y., Swerlick, R. A., Sepp, N., Bosse, D., Ades, E. W., and Lawley, T. J., 1994. Characterization of expression and modulation of cell adhesion molecules on an immortalized human dermal microvascular endothelial cell line (HMEC-1). J Invest Dermatol 102**,** 833-837.

Yipp, B. G., Hickey, M. J., Andonegui, G., Murray, A. G., Looareesuwan, S., Kubes, P., and Ho, M., 2007. Differential roles of CD36, ICAM-1, and P-selectin in Plasmodium falciparum cytoadherence in vivo. Microcirculation 14**,** 593-602.

Zou, Y., He, L., Chi, F., Jong, A., and Huang, S. H., 2008. Involvement of Escherichia coli K1 ibeT in bacterial adhesion that is associated with the entry into human brain microvascular endothelial cells. Med Microbiol Immunol 197**,** 337-344.

Zou, Y., He, L., and Huang, S. H., 2006. Identification of a surface protein on human brain microvascular endothelial cells as vimentin interacting with Escherichia coli invasion protein IbeA. Biochem Biophys Res Commun 351**,** 625-630.

Zougbede, S., Miller, F., Ravassard, P., Rebollo, A., Ciceron, L., Couraud, P. O., Mazier, D., and Moreno, A., 2010. Metabolic acidosis induced by Plasmodium falciparum intraerythrocytic stages alters blood-brain barrier integrity. J Cereb Blood Flow Metab.